THE SCIENCE AND CULTURE SERIES — PHYSICS

Series Editor: A. Zichichi

Proceedings of the 43rd Course of the
International School of Solid State Physics

EPIOPTICS-10

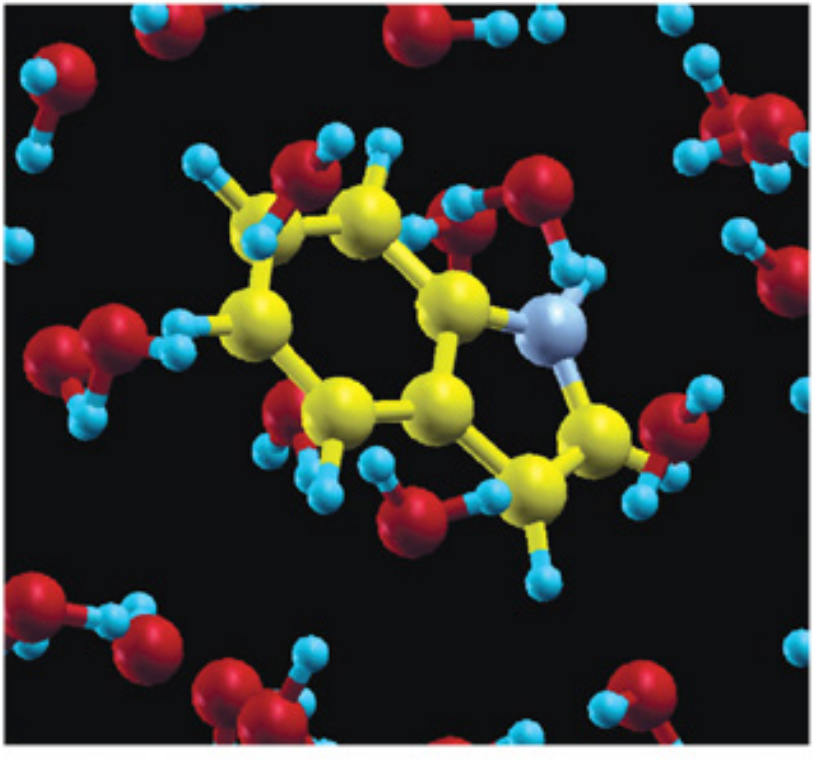

Editor
Antonio Cricenti

EPIOPTICS-10

This page intentionally left blank

THE SCIENCE AND CULTURE SERIES — PHYSICS

EPIOPTICS-10

Proceedings of the 43rd Course of the
International School of Solid State Physics

Erice, Italy 19 — 26 July 2008

Editors
Antonio Cricenti

Series Editor
A. Zichichi

World Scientific

NEW JERSEY • LONDON • SINGAPORE • BEIJING • SHANGHAI • HONG KONG • TAIPEI • CHENNAI

Published by

World Scientific Publishing Co. Pte. Ltd.

5 Toh Tuck Link, Singapore 596224

USA office: 27 Warren Street, Suite 401-402, Hackensack, NJ 07601

UK office: 57 Shelton Street, Covent Garden, London WC2H 9HE

British Library Cataloguing-in-Publication Data
A catalogue record for this book is available from the British Library.

NON-EQUILIBRIUM THERMODYNAMICS FOR ENGINEERS

ISBN-13 978-981-4322-15-7
ISBN-10 981-4322-15-6

Printed in Singapore.

PREFACE

This special volume contains the Proceedings of the 10th Epioptics Workshop, held at the Ettore Majorana Foundation and Centre for Scientific Culture, Erice, Sicily, from June 19 to 26, 2008. This was the 10th Workshop in the Epioptics series and the 43rd of the International School of Solid State Physics. Antonio Cricenti from CNR Istituto di Struttura della Materia and Theo Rasing from the University of Njimegen, were the Directors of the Workshop. The Advisory Committee of the Workshop included Y. Borensztein from U. Paris VII (F), R. Del Sole from U. Roma II Tor Vergata (I), D. Aspnes from NCSU (USA), O. Hunderi from U. Trondheim (N), J. McGilp from Trinity College Dublin (Eire), W. Richter from TU Berlin (D), N. Tolk from Vanderbilt University (USA), and P. Weightman from Liverpool University (UK). Fifty scientists from sixteen countries attended the Workshop.

The Workshop brought together researchers from universities and research institutes who work in the fields of (semiconductor) surface science, epitaxial growth, materials deposition and optical diagnostics relevant to (semiconductor) materials and structures of interest for present and anticipated (spin) electronic devices. The Workshop was aimed at assessing the capabilities of state-of-the-art optical techniques in elucidating the fundamental electronic and structural properties of semiconductor and metal surfaces, interfaces, thin layers, and layer structures, and assessing the usefulness of these techniques for optimization of high quality multilayer samples through feedback control during materials growth and processing. Particular emphasis was dedicated to the theory of non-linear optics and to dynamical processes through the use of pump-probe techniques together with the search for new optical sources. Some new applications of Scanning Probe Microscopy to Material science and biological samples, dried and in vivo, with the use of different laser sources were also presented. Materials of particular interest were silicon, semiconductor-metal interfaces, semiconductor and magnetic multi-layers and III-V compound semiconductors. As well as the notes collected in this Volume, the Workshop

combined tutorial aspects proper to a School with some of the most advanced topics in the field, which better characterized the Workshop.

I wish to thank Prof. A. Zichichi, President of the Ettore Majorana Foundation and Centre for Scientific Culture (EMFCSC), the Italian National Research Council (CNR) and the Sicilian Regional Government. I wish to thank Prof. G. Benedek, Director of the International School of Solid State Physics of the EMFCSC. Our thanks are also due to the Director for Administration and Organizational Affairs, Ms. F. Ruggiu and all the staff of the Centre for their excellent work.

Antonio Cricenti

Preface

To meet the entropy challenge, is probably more central than the issue of provision of sufficient power to the world. The entropy production, not the energy used, can measure our wastes and the efficiency of work, or the limit of our activity. This book introduces non-equilibrium thermodynamics to engineers, and discusses how the theory can be useful for typical engineering problems.

The book has been written on the basis of many years of teaching at the Norwegian University of Science and Technology, Trondheim, Norway, and the Technical University of Delft, Delft, The Netherlands. Early versions of the book have been used at short courses at the International Center of Thermodynamics, Istanbul, Chalmers Technical University, Gothenburg, Helsinki Technical University and Pennsylvania State University.

It can be used in the Bachelor or Master study programs after a basic course in thermodynamics, or for self study in the industry. The book requires knowledge of basic thermodynamics corresponding to that given by Smith, van Ness and Abbott, Introduction to chemical engineering, or Moran and Shapiro, Fundamentals of Engineering Thermodynamics.

To facilitate learning, exercises for the topics of the book and

solutions to these, are available on the NTNU homepage.[1] Eight DVD lectures are likewise available there or from The Technical University of Delft.[2]

Financial support from the Research Council of Norway is acknowledged. The authors are grateful to Statoil ASA for the cover picture from Mongstad.

The authors welcome comments and suggestions that can improve future editions.

Trondheim and Stuttgart, March 2010

Signe Kjelstrup
signe.kjelstrup@chem.ntnu.no

Dick Bedeaux
dick.bedeaux@chem.ntnu.no

Eivind Johannessen
eijoh@statoil.com

Joachim Gross
gross@itt.uni-stuttgart.de

[1] http://www.chem.ntnu.no/nonequilibrium-thermodynamics/

[2] http://collegerama.tudelft.nl/mediasite/Catalog/?cid=0cbe1b45-06c6-4d03-a692-92a6dad4711d

Contents

Chapter 1

Scope

The aim of this book is to present the essence of non-equilibrium thermodynamics for engineers. The field was established in 1931 and developed during the forties and fifties for transport in homogeneous phases. Applications of the theory are now increasing. Some perspectives on the applications are given after a brief introduction.

Non-equilibrium thermodynamics describes transport processes in systems that are not in global equilibrium. The field resulted from efforts of many scientists to find a more explicit formulation of the second law of thermodynamics. This started already in 1856 with Thomson's studies of thermoelectricity, see [1]. Onsager is, however, counted as the founder of the field with his papers from 1931 [2, 3], see also [4], because these put earlier research by Thomson, Boltzmann, Nernst, Duhem, Jauman and Einstein into a systematic framework. Onsager was given the Nobel prize in chemistry in 1968 for this work.

The second law is reformulated in terms of the entropy production σ. In Onsager's formulation, the entropy production is

given by the product sum of so-called conjugate fluxes, J_i, and forces, X_i, in the system. The second law then becomes

$$\sigma = \sum_i J_i X_i \geq 0 \tag{1.1}$$

where σ is larger than or equal to zero. Each flux is taken to be a linear combination of all forces,

$$J_i = \sum_j L_{ij} X_j \tag{1.2}$$

and the reciprocal relations

$$L_{ji} = L_{ij} \tag{1.3}$$

apply. They now bear Onsager's name.

In order to use the theory, one first has to identify a complete set of extensive *independent* variables, α_i. The resulting conjugate fluxes and forces are $J_i = d\alpha_i/dt$ and $X_i = (\partial S/\partial \alpha_i)_{\alpha_{j\neq i}}$, respectively. Here t is the time and S is the entropy of the system. The three equations above contain then all information on the non-equilibrium behavior of the system.

Following Onsager, a consistent theory of non-equilibrium processes in continuous systems was set up in the forties by Meixner [5–8] and Prigogine [9]. They calculated the entropy production for a number of physical problems. Prigogine received the Nobel price for his work on dissipative structures in systems that are not in equilibrium in 1977, and Mitchell the year after for his application of the driving force concept to transport processes in biology [10].

The most general description of non-equilibrium thermodynamics is still the 1962 monograph of de Groot and Mazur [11] reprinted in 1985 [12]. Haase's book [13] also reprinted [14], contains many results for electrochemical systems and systems

with temperature gradients. Katchalsky and Curran developed the theory for biophysical systems [15]. Their analysis was carried further by Caplan and Essig [16]. Førland and coworkers gave various applications in electrochemistry and biology, and they treated frost heave [17,18]. Their book presented the theory in a way suitable for chemists. Newer books on equilibrium thermodynamics or statistical thermodynamics often include chapters on non-equilibrium thermodynamics, see e.g. [19]. In 1998, Kondepudi and Prigogine [20] presented an integrated approach of basic equilibrium and non-equilibrium thermodynamics. Jou et al. [21] published the second edition of their book on extended non-equilibrium thermodynamics and Öttinger gave a non-equilibrium description of the nonlinear regime [22].

Non-equilibrium thermodynamics is constantly being applied in new contexts. Fitts gave an early presentation of viscous phenomena [23]. Kuiken [24] has written the most general treatment of multicomponent diffusion and rheology of colloidal systems. Rubi and coworkers [25–27] used the internal molecular degrees of freedom to explore the development within a system. We are now able to deal with chemical reactions within the framework of non-equilibrium thermodynamics [12] and shall do so in Chapter 7. Bedeaux and Mazur [28] extended the theory to quantum mechanical systems. Kjelstrup and Bedeaux [29] wrote a book dealing with transports into and across surfaces. All these efforts broaden the scope of the theory.

Chemical and mechanical engineering needs theories of transport in systems with gradients in pressure, concentration, and temperature, see Denbigh [30, 31]. In isotropic systems there is no coupling between tensorial (viscous) and vectorial (diffusional) phenomena, so the two classes can usually be dealt with separately [12]. We concentrate on isotropic systems here.

Simple vectorial transport laws have long worked well in engineering, but there is now an increased effort to be more precise. The need for more accurate flux equations in modeling [32] increases the need for non-equilibrium thermodynamics. The books by Taylor and Krishna [32], Cussler [33] and Demirel [34], which present Maxwell-Stefan's formulation of the flux equations, are important books in this context. Krishna and Wesselingh [35] and Kuiken [24] have shown that the coefficients in the Maxwell-Stefan equations are relatively well-behaved, by analyzing an impressive amount of experimental data.

Non-equilibrium thermodynamics is necessary for a precise description of all systems that exchange heat, mass and charge. There is a need in mechanical and chemical engineering to design systems that waste less work [36–38]. Fossil energy sources, as long as they last, lead to waste that may harm the environment. Better and more efficient use of energy resources is therefore central. It is then not good enough to only optimize the first law efficiency. The second law has to be taken into account. The entropy production σ can be seen as a measure for the non-sustainability of a technical process. Through non-equilibrium thermodynamics, one can develop methods to improve the second law efficiency. One purpose of the book is to present such methods.

The process industry may, in a not too distant future, have to give annual reports not only on the products that they produce, but also on their annual lost exergy or entropy production. Some energy companies are making an effort in this direction already. The public sector can enhance this development, by giving benefits to those who limit their entropy production, or increase their energy efficiency. And the engineering community can develop tools to accomplish the task. The present book should be seen in this context. Efforts in other fields, like control theory [39], are also made. This book as well as the references cited above,

gives instruments that are needed to understand the nature of the entropy production and can therefore help to avoid it.

We give in Chapter 2 the *characteristics of non-equilibrium thermodynamics* and explain why it is an important field. In Chapter 3, we show how to derive *the entropy production* for systems with diffusion and conduction. The derivations follow de Groot and Mazur [12] and Førland, Førland and Kjelstrup [18]. Chapter 4 presents examples of *flux equations* for coupled transport of heat, mass and charge. Chapter 6 deals with shear flow and 7 with chemical reactions. Examples are used to show how the different processes are coupled. In Chapter 8 we estimate the lost work in an industrial process, the Hall-Heroult process for aluminum electrolysis. The entropy production by charge transfer and by heat transfer are both large. In Chapter 9, we describe a method to minimize the entropy production in process equipment. The method is described in detail for ideal gas expansion and energy efficient heat exchange in this Chapter. Its application to chemical reactors and distillation columns is illustrated in Chapter 10.

This page intentionally left blank

Chapter 2

Why non-equilibrium thermodynamics?

This chapter explains in more detail what non-equilibrium thermodynamics is, and how it adds to engineering fields.

The most common industrial and living systems are those that transport heat, mass, charge, and volume, in the presence or absence of a chemical reaction. The process industry, the electrochemical industry, biological systems, as well as laboratory experiments; all are systems that are out of equilibrium. Equilibrium thermodynamics is then not sufficient. There are six main reasons why non-equilibrium thermodynamics theory [12, 13, 18, 29] is needed. The theory

- gives an accurate description of coupled transport processes.
- gives the same systematic basis to all transport processes.
- can be used to define experiments.

- quantifies produced entropy, lost work or lost exergy.
- gives an entropy balance to use in thermodynamic modeling.
- can be used to optimize the energy efficiency.

These statements will be illustrated briefly in this Chapter, and more in-depth in the rest of the book.

The design of systems which waste less energy, is becoming increasingly more important [37]. We show in the end of this Chapter how entropy production of an industrial plant is related to the lost work in the plant. Non-equilibrium thermodynamics is the only theory that can be used to assess in detail the second law efficiency, or how valuable (energy) resources are exploited. It is the aim of this book to contribute especially to this issue. Chapter 10 develops rules for energy efficient designs in engineering practice.

2.1 Simple flux equations

Accurate expressions for the fluxes are required in engineering. In order to see immediately what non-equilibrium thermodynamics can add to the modeling of real systems, we compare simple flux equations to flux equations given by non-equilibrium thermodynamics in the following two sections.

The simplest descriptions of heat-, mass-, charge- and volume transport are the equations of Fourier, Fick, Ohm, Darcy and Newton. Fourier's law expresses the measurable heat flux in terms of the temperature gradient by:

$$J'_q = -\lambda \frac{dT}{dx} \tag{2.1}$$

where λ is the thermal conductivity, T is the absolute temperature, and x is the direction of transport. Fick's law gives the

mass flux of one of the components in terms of the gradient of its molar concentration c:

$$J = -D\frac{dc}{dx} \tag{2.2}$$

where D is the diffusion coefficient. Ohm's law gives the electric current in terms of the gradient of the electric potential:

$$j = -\kappa\frac{d\phi}{dx} \tag{2.3}$$

where κ is the electrical conductivity, and ϕ is the electric potential. Darcy's law says that the volume flow J_v in a tube is proportional to the pressure gradient dp/dx via the coefficient L_p:

$$J_v = -L_p\frac{dp}{dx} \tag{2.4}$$

And, a laminar flow in the x-direction with velocity $\mathbf{v} = (v_x, 0, 0)$ and velocity component $v_x = v_x(y)$ obeys Newton's law of friction:

$$\Pi_{xy} = -\eta\frac{\partial v_x}{\partial y} \tag{2.5}$$

where Π_{xy} is the viscous pressure tensor, and the proportionality constant, η, is the shear viscosity.

The fluxes in Eqs. (2.1)-(2.5) are all caused by one gradient, or one driving force (see next Section). Fick's law, for instance, says that there is no mass flux if there is no concentration gradient. We know from experiments that a temperature gradient and an electric potential gradient also can give rise to a mass flux. To neglect such effects can have severe consequences. When used at interfaces, such assumptions can even be in conflict with the laws of thermodynamics [29, 40].

Non-equilibrium thermodynamics generalizes equations (2.1)-(2.5) by taking all driving forces into account. The theory gives

a common basis to all simple transport equations, and show how they are connected. The basis is the second law of thermodynamics as expressed through (1.1)-(1.3). This means that the hydrodynamics of viscous fluids, the theory of diffusion, heat conduction, and chemical reaction, all have a common systematic basis [12]. One purpose of the book is to give this.

Exercise 2.1.1 *In a stationary state there is no accumulation of internal energy, mass or charge. This means that the heat, molar, and electric fluxes are independent of position. The derivative of the above equations with respect to x are then zero. For the first equation, we have:*

$$\frac{d}{dx}\lambda\frac{dT}{dx} = 0 \tag{2.6}$$

Equations like these can be used to calculate the temperature, concentration, electric potential and pressure as a function of the position, when their values on the boundaries of the system and λ, D, κ, L_p and η are known.

Calculate the temperature as a function of position between two walls separated by 10 cm. The walls are kept at constant temperature, 5 and 25 ^oC, respectively. Assume that the thermal conductivity is constant.

- **Solution:** According to Eq. (2.6) $d^2T/dx^2 = 0$. The general solution of this equation is $T(x) = a + bx$. The constants a and b follow from the boundary condition. We have $T(0) = 278$ K and $T(10) = 298$ K. It follows that $T(x) = (278 + 2x/\text{cm})$ K.

2.2 Flux equations in non-equilibrium thermodynamics

Many natural and man-made processes are not adequately described by the simple flux equations given above. There are, for instance, always large fluxes of mass and heat that accompany charge transport in batteries and electrolysis cells. The resulting local cooling in electrolysis cells may lead to unwanted freezing of electrolyte. Electrical energy is frequently used to transport mass in biological systems. Large temperature gradients across space ships have been used to supply electric power to the ships. Salt concentration differences between river water and sea water can be used to generate electric power. Pure water can be generated from salt water by application of pressure gradients. In all these more or less randomly chosen examples, one needs transport equations that describe coupling between various fluxes. The flux equations (2.1)-(2.5) become then too simple.

Non-equilibrium thermodynamics prescribes coupling among fluxes. Coupling means that transport of mass will take place in a system, not only when the gradient in the chemical potential is different from zero, but also when there are gradients in temperature or electric potential. Coupling between fluxes describes precisely the phenomena mentioned above.

For example, in a bulk system with transport of heat, mass, and electric charge, we shall learn in Chapters 3 and 4 that the linear relations for the fluxes (2.1)-(2.3) take the form

$$J'_q = L_{qq}\frac{d}{dx}\left(\frac{1}{T}\right) + L_{q\mu}\left(-\frac{1}{T}\frac{d\mu_T}{dx}\right) + L_{q\phi}\left(-\frac{1}{T}\frac{d\phi}{dx}\right) \quad (2.7)$$

$$J = L_{\mu q}\frac{d}{dx}\left(\frac{1}{T}\right) + L_{\mu\mu}\left(-\frac{1}{T}\frac{d\mu_T}{dx}\right) + L_{\mu\phi}\left(-\frac{1}{T}\frac{d\phi}{dx}\right) \quad (2.8)$$

$$j = L_{\phi q}\frac{d}{dx}\left(\frac{1}{T}\right) + L_{\phi\mu}\left(-\frac{1}{T}\frac{d\mu_T}{dx}\right) + L_{\phi\phi}\left(-\frac{1}{T}\frac{d\phi}{dx}\right) \qquad (2.9)$$

The forces of transport conjugate to the fluxes J'_q, J and j are the thermal force $d\left(1/T\right)/dx$, the chemical force $[-\left(1/T\right)\left(d\mu_T/dx\right)]$, and the electrical force $[-\left(1/T\right)\left(d\phi/dx\right)]$, respectively. The subscript T of the chemical potential, μ_T, indicates that the derivative should be taken keeping the temperature constant. We return to this point in Section 3.2.

The L-coefficients are so-called phenomenological coefficients, or Onsager coefficients, as we shall call them. They must be measured. The Onsager coefficients on the diagonal of the matrix can be related to λ, D, and κ. They are called *main coefficients*. The off-diagonal L-coefficients describe the coupling between the fluxes. They are called *coupling coefficients*. Another common name is cross coefficients. According to Onsager, we have here three reciprocal relations or *Onsager relations* for the coupling coefficients:

$$L_{\mu q} = L_{\mu q}, \qquad L_{q\phi} = L_{\phi q}, \qquad L_{\phi\mu} = L_{\mu\phi} \qquad (2.10)$$

The Onsager relations simplify the system. They reduce the number of independent coefficients from nine to six. Coupling coefficients are small in some cases but large in others. We shall see that large coupling coefficients lead to a small entropy production. If it is difficult to measure L_{ij}, we can rather measure L_{ji}. To measure both, gives a good control.

We shall see in Chapters 3, 6 and 7 how the conjugate forces can be found in a systematic manner. In Chapter 4 we shall learn how to write equations like the ones above. The importance of some coupling coefficients will be discussed. The exercise below show that knowledge of non-equilibrium thermodynamics is useful for interpretating experiments.

Exercise 2.2.1 *Find the electric current in terms of the electric field* $E = -d\phi/dx$*, using Eqs.* (2.7)-(2.9)*, in a system where there is no transport of heat and mass,* $J'_q = 0, J = 0$.

Solution: It follows from Eqs. (2.7) and (2.8) that

$$\frac{L_{qq}}{T}\frac{dT}{dx} + L_{q\mu}\frac{d\mu_T}{dx} = L_{q\phi}E \quad \text{and} \quad \frac{L_{\mu q}}{T}\frac{dT}{dx} + L_{\mu\mu}\frac{d\mu_T}{dx} = L_{\mu\phi}E$$

Solving these equations, using the Onsager relations, one finds

$$\frac{1}{T}\frac{dT}{dx} = \frac{L_{q\phi}L_{\mu\mu} - L_{\mu\phi}L_{q\mu}}{L_{qq}L_{\mu\mu} - L_{q\mu}^2}E \quad \text{and} \quad \frac{d\mu_T}{dx} = \frac{L_{qq}L_{\mu\phi} - L_{\mu q}L_{q\phi}}{L_{qq}L_{\mu\mu} - L_{q\mu}^2}E$$

Substitution into Eq. (2.9) then gives

$$j = \frac{E}{T}\left[L_{\phi\phi} - L_{\phi q}\frac{L_{q\phi}L_{\mu\mu} - L_{\mu\phi}L_{q\mu}}{L_{qq}L_{\mu\mu} - L_{q\mu}^2} - L_{\phi\mu}\frac{L_{qq}L_{\mu\phi} - L_{\mu q}L_{q\phi}}{L_{qq}L_{\mu\mu} - L_{q\mu}^2}\right]$$

The exercise shows that the electric conductivity that is normally measured, as the ratio of measured values of j and E, is not given by $L_{\phi\phi}/T$ as one might have thought considering Eq. (2.9). The coupling coefficients lead to temperature and chemical potential gradients, which affect the electric current. The measured electric conductivity is the combination of the conductivity of a pure homogeneous conductor, found at zero chemical potential gradient and temperature gradients, minus additional terms. The combination of coefficients is an *effective* conductivity, or stationary state conductivity.

2.3 The lost work of an industrial plant

We shall see here why a second law analysis is important for the process industry. The industrial plant is a system, in which the materials undergo transformations. Materials are taken in and

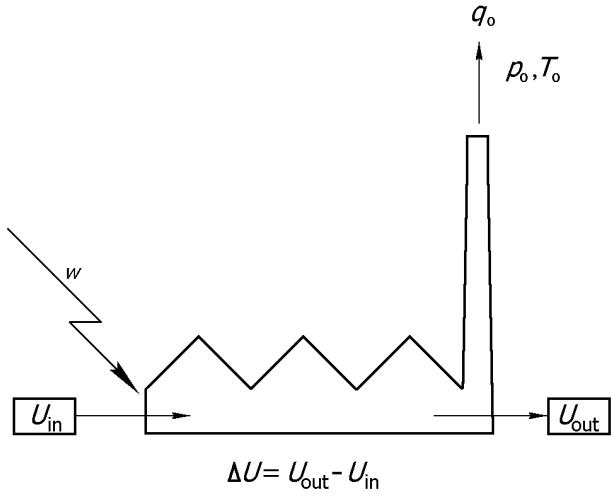

Figure 2.1: A schematic illustration of thermodynamic variables that are essential for the lost work in an industrial plant.

are leaving the plant at the conditions of the environment, see Fig. 2.1.

The environment is therefore the reference state for the thermodynamic analysis. It has constant pressure, p_0 (1 bar) and constant temperature, T_0 (for instance 298 K). We consider changes that take place during the time interval Δt. The first law of thermodynamics gives the change in internal energy of the process $\Delta U = U_{\text{out}} - U_{\text{in}}$:

$$\Delta U = q - p_0 \Delta V + w \tag{2.11}$$

Here q is the heat delivered to the materials. The total work delivered to the system is decomposed in two parts; with $-p_0 \Delta V$ as the work done on the system by volume expansion, ΔV, against the pressure of the environment, p_0, and w as the additional work done on the materials.

We consider first processes for which work is needed, so that $w > 0$. The minimum work needed to perform a process, was defined as the least amount of energy that must be supplied, when at the conclusion of the process, the only parts which have undergone any change are the process materials and the environment [30]. To see that this is so, we first replace q by the heat delivered to the environment, $q_0 = -q$:

$$\Delta U = -q_0 - p_0 \Delta V + w \tag{2.12}$$

In the classical formulation of the second law, we have

$$\Delta S + \Delta S_0 \geq 0 \tag{2.13}$$

where ΔS is the entropy change of the process materials and ΔS_0 is the entropy change in the environment. The total entropy change is positive. For a completely reversible process the sum of the entropy changes is zero. For an irreversible process, the sum can be used to define the average total entropy production, dS_{irr}/dt, in the time interval Δt of a stationary process, as

$$\left(\frac{dS_{\text{irr}}}{dt}\right) \Delta t \equiv \Delta S + \Delta S_0 \tag{2.14}$$

Assuming always that the environment behaves reversibly, the entropy change in the surroundings is $\Delta S_0 = q_0/T_0$. By introducing q_0 into the expression for the entropy production, and combining the result with the first law, we obtain

$$w = T_0 \left(\frac{dS_{\text{irr}}}{dt}\right) \Delta t + \Delta U + p_0 \Delta V - T_0 \Delta S \tag{2.15}$$

The left hand side of this equation is the work that is needed to accomplish the process with a particular value of the entropy production, (dS_{irr}/dt). Since $(dS_{\text{irr}}/dt) \geq 0$, the *least* work requirement is

$$w_{\text{ideal}} = \Delta U + p_0 \Delta V - T_0 \Delta S \equiv E \tag{2.16}$$

This is the work requirement for a completely reversible process. The equation defines the *exergy*, E, of the material [37,41]. The exergy of the environment at p_0, T_0 (the reference state) is set to zero. We see that exergy analysis uses the classical formulation of the second law. It calculates the ideal work and the lost work (see below) from values at the system boundaries. Another word for exergy is availability [42]. It is an important supplement to non-equilibrium thermodynamics.

For processes that produce work, w and w_{ideal} are negative as defined above. Correspondingly, the signs of $\Delta U, \Delta V$, and ΔS are such that the system can perform work. The ideal work w_{ideal} is minus the maximum work that can be obtained in the time interval Δt. This is the work performed by the system if the process is completely reversible. By comparing Eqs. (2.15) and (2.16), we see that $T_0\,(dS_{\text{irr}}/dt)\,\Delta t$ is the additional quantity of work that must be used in the actual process, compared to the work in an ideal reversible process. Thus $T_0\,(dS_{\text{irr}}/dt)\,\Delta t$ is the so-called non-compensated heat of Clausius. By comparing Eqs. (2.15) and (2.16), we see that $T_0\,(dS_{\text{irr}}/dt)\,\Delta t$ is the work that is lost in the actual process, compared to the available work produced in an ideal (reversible) process. So, the lost work relative to the surroundings is:

$$w_{\text{lost}} = w - w_{\text{ideal}} = T_0(\frac{dS_{\text{irr}}}{dt})\Delta t \tag{2.17}$$

This is the Gouy-Stodola theorem [43]. Equations (2.16, 2.17) are central in the field that bears the name exergy analysis. In exergy analysis, the lost work is calculated from knowledge of w and w_{ideal} in Eq. (2.17).

In non-equilibrium thermodynamics we calculate the lost work from the entropy production. The entropy production is be found by integrating the local entropy production, σ, over the

volume of the system

$$\frac{dS_{\text{irr}}}{dt} = \int \sigma dV \tag{2.18}$$

Non-equilibrium thermodynamics provide an explicit expression for σ of Eq. (1.1) from Eq. (1.2). The local resolution of dS_{irr}/dt in terms of σ is beyond the scope of exergy analysis, where only a balance around the outside of a process (unit) is conducted. The explicit expression of σ can be used to understand the origin of the entropy production or the lost work. At stationary state, the entropy production in a volume element is equal to the entropy flow into the surroundings of the element, see Section 2.5, and Chapter 3, Eq. (3.1). In Chapters 9 and 10 we show how the local resolution of irreversibilities can be used to optimize process units, by minimization of the entropy production.

Exercise 2.3.1 *A cylinder of a combustion engine contains 600 cm^3 of air at a pressure of 10 bar and a temperature of 1200 K, just before the exhaust valve opens (before the expansion starts). Determine the maximum available work (the exergy) of the air. Assume that air consists of ideal gases. The molar weight of air is $M_{air} = 28$ g/mol. The temperature and pressure of the surroundings are $T_0 = 300$ K, $p_0 = 1$ bar.*

- **Solution:** The maximum available work per kg of gas is

$$\begin{aligned} |w_{\text{ideal}}| = {} & u(T,p) - u(T_0,p_0) + p_0 [v(T,p) - v(T_0,p_0)] \\ & - T_0 [s(T,p) - s(T_0,p_0)] \end{aligned}$$

  where the subscript 0 refers to values of the internal energy, the specific volume and the entropy of the air in the engine at the temperature and pressure of the surroundings. The thermodynamic functions were tabulated, see for instance

Moran and Shapiro [44]

$$\begin{aligned} u\left(T,p\right)-u\left(T_0,p_0\right) &= 719.3 \text{ kJ/kg} \\ T_0\left[s\left(T,p\right)-s\left(T_0,p_0\right)\right] &= \\ T_0\left[s(T,p_0)-s(T_0,p_0)+\frac{R}{M_{\text{air}}}\ln\frac{p_0}{p}\right] &= 237.9 \text{ kJ/kg} \\ p_0\left[v\left(T,p\right)-v\left(T_0,p_0\right)\right] = \frac{R}{M_{\text{air}}}\left(\frac{T}{p}-\frac{T_0}{p_0}\right) &= -\,53.5 \text{ kJ/kg} \end{aligned}$$

This results in

$$|w_{\text{ideal}}| = 427.9 \text{ kJ/kg}$$

for the maximum available work. Most of this work is normally not converted into useful work. The lost work is often significant in processes with chemical reactions, cf. Chapter 7.

Exercise 2.3.2 *A heat reservoir has a temperature-independent heat capacity at constant volume C_V. The temperature of the environment is $T_0 = 300$ K. Determine the maximum available work (the exergy) of the heat reservoir when it has temperatures $T = 400$, 4000 and 40000 K. The volume of the reservoir is constant, $V = V_0$.*

- **Solution:** The maximum available work is

  $$|w_{\text{ideal}}| = U\left(T,V_0\right) - U\left(T_0,V_0\right) - T_0\left[S\left(T,V_0\right) - S\left(T_0,V_0\right)\right]$$

  We have:

  $$U\left(T,V_0\right) - U\left(T_0,V_0\right) = C_V\left(T-T_0\right)$$

  and

  $$S\left(T,V_0\right) - S\left(T_0,V_0\right) = C_V \ln\left(\frac{T}{T_0}\right)$$

This results in

$$|w_{\text{ideal}}| = C_V \left[(T - T_0) - T_0 \ln \left(\frac{T}{T_0} \right) \right]$$

for the maximum available work. By introducing $T = 400$, 4000 and 40000 K and $T_0 = 300$ K, $|w_{\text{ideal}}| = 13.7$ K C_V, 2923 K C_V and 38232 K C_V where C_V has unit J, respectively. The entropy contribution becomes negligible for $(T - T_0) \gg T_0$. The relative contribution of the entropy to the ideal work is larger, the lower is the temperature. We can thus expect larger losses of work at temperatures around T_0.

2.4 The second law efficiency

In a work consuming process $w > w_{\text{ideal}}$, see Section 2.3. The second law efficiency is then:

$$\eta_{II} \equiv \frac{w_{\text{ideal}}}{w} = 1 - \frac{w_{lost}}{w} \tag{2.19}$$

This efficiency is also called the thermodynamic efficiency or the exergy efficiency. It includes w_{lost}. In a work producing process $w < w_{\text{ideal}}$ and

$$\eta_{II} \equiv \frac{|w|}{|w_{\text{ideal}}|} = 1 - \frac{w_{\text{lost}}}{|w_{\text{ideal}}|} \tag{2.20}$$

The exergy destruction coefficient is $\xi \equiv 1 - \eta_{II}$. The definitions of η_{II} in work (exergy) consuming or producing processes have values that vary between zero and one. An ideal reversible machine has $\eta_{II} = 1$, while a real machine has normally an efficiency far from one. A fuel cell, which is considered to be rather efficient, has typically $\eta_{II} = 0.6$. The efficiency refers to an unattainable reversible limit. An alternative practical limit is therefore proposed in Section 9.2; the state of minimum entropy production [45].

The Carnot-process played an important role in the definition of the entropy by Clausius. The process starts with a volume of gas at pressure p_A and temperature T_h. The system, in contact with a hot thermal reservoir with temperature T_h, is expanded isothermally to a pressure p_B. Subsequently it is expanded adiabatically ($q_{BC} = 0$) until it has the temperature T_c of a cold thermal reservoir. The pressure has then been changed to p_C. The next step is to compress the system in contact with the cold reservoir at constant temperature to a pressure p_D. Finally, the system is compressed adiabatically ($q_{DA} = 0$) to the original pressure p_A and temperature T_h. The system has now returned to its original state, but an amount of heat q_{AB} has been taken from the hot bath and converted into work w_{ideal} and heat $|q_{CD}|$ added to the cold bath.

In the reversible cycle of the Carnot process, the entropy production is zero, and the second law efficiency is unity. Stirling machines are examples of nearly reversible machines.

The first law efficiency [46] of a process is defined as

$$\eta_I = \frac{w}{q} \tag{2.21}$$

where q is the heat added to the process. For the Carnot process, this efficiency depends only on the temperatures of the two reservoirs

$$\eta_I \equiv \frac{w_{\text{ideal}}}{q_{AB}} = \frac{q_{AB} + q_{CD}}{q_{AB}} = \frac{T_h - T_c}{T_h} \tag{2.22}$$

where T_h and T_c are the temperatures of the hot and cold reservoirs, respectively. The first law efficiency is only close to unity if $T_h \gg T_c$.

In a combustion process, the heat available for work is the enthalpy of reaction, giving $q = \Delta_r H$ and $w = \eta_I \Delta_r H$. This is no measure of how well the machine operates in terms of frictional

and other losses. Such information can only be obtained from the second law efficiency, which measures how far the system is from reversible operation.

Exercise 2.4.1 *A saline power plant produces electric power from the mixing of sea water and river water to brackish water, at one bar and temperature T_0= 300 K. One way to do this is by reverse electrodialysis, see Fig.4.3. Discuss the second law efficiency of this plant.*

- **Solution:** The ideal electric work obtainable from an electrochemical cell is given by Nernst's equation $w_{\text{ideal}} = FE = -\Delta G$ [46]. Here ΔG is the Gibbs energy difference of the mixing process, E is the ideal cell potential and F is Faraday's constant. We refer to one faraday of electrons transferred. The cell delivers in reality a smaller voltage, E', due to its resistance and the concentration gradients inside the cell. The difference between E and E' is the lost work. The second law efficiency is

$$\eta_{II} = \frac{E'}{E}$$

  The enthalpy of mixing ΔH is negligibly small for the mixing process. The ratio $-\Delta G/\Delta H$ obtained from η_I is therefore clearly not a good measure of the plant's performance.

2.5 Consistent thermodynamic models

We refer to a thermodynamic model as a set of thermodynamic and transport relations (equation of state, system variables etc., and flux-force equations) that are needed to solve the balance equations of the system. General balance equations are given in the Appendix A.1.

Non-equilibrium thermodynamics offers possibilities to test the model for consistency. We mentioned a first test in Section 2.2. Two independent experiments can be done to find the coefficients L_{ij} and L_{ji}. According to Onsager, these should be identical.

A second possibility is to use the entropy balance to evaluate the consistency of the thermodynamic model. The local entropy production can be calculated from Eq. (1.1) using the flux equations, Eq. (1.2), or alternatively, from the entropy balance 2.24. By integrating the local entropy production, σ, we obtain the total value:

$$\frac{dS_{\text{irr}}}{dt} = \int \sigma dV \tag{2.23}$$

At stationary state, we also have from Eq.(3.1):

$$\frac{dS_{\text{irr}}}{dt} = -\left(J_s^{\text{i}} - J_s^{\text{o}}\right)\Omega \tag{2.24}$$

where J_s^{i} is the entropy flux into the volume, J_s^{o} the entropy flux out of the volume and Ω is the surface area through which the fluxes enter or leave the volume. The entropy balance is a governing equation. Examples of entropy balances are given for heat exchangers, chemical reactors and distillation columns in Tables 9.1 and 10.3.

While dS_{irr}/dt depends on L_{ij} and the local values of the thermodynamic variables, the entropy fluxes J_s^{i} and J_s^{o} can be calculated without knowledge of L_{ij}. When the entropy production from Eq. (2.24) agrees with the one found from Eq. (2.23), the model is consistent with the second law of thermodynamics.

Through such analyses one may reveal inconsistencies in assumptions that are made, either in thermodynamic relations or in choice of parameters [47, 48]. Verification of assumptions is essential for model improvements. Examples of consistency controls are given in Chapter 9 and 10, Exercises 9.3.1 and 10.1.1.

Chapter 3

The entropy production of one-dimensional transport processes

We derive the entropy production for a volume element of a homogeneous phase where diffusion, conduction, and chemical reaction can take place along the x-axis. The system is in mechanical equilibrium. Equivalent pairs of conjugate fluxes and forces are derived.

The second law of thermodynamics, Eq. (2.13), says that the entropy change of a system plus its surroundings is positive for irreversible processes and zero for reversible processes. This formulation of the law gives the direction of a process; it does not give its rate. Non-equilibrium thermodynamics assumes that the Gibbs equation remains valid locally. We shall see that the second law, as expressed by Eq. (1.1), results from Gibbs equation. Rates of processes as introduced through Eq. (1.2) will then have a thermodynamic basis.

In this Chapter we shall consider systems where the transport processes are one-dimensional. They take place in the x-direction only. Such systems are essential in many industrial applications, where diffusion, conduction and chemical reaction take place.

The change in the entropy in a volume element is the result of a flow of entropy into and out of a volume element, and of the entropy production inside. The rate of change in the local entropy density is

$$\frac{\partial s}{\partial t} = -\frac{\partial}{\partial x} J_s + \sigma \tag{3.1}$$

where s is the entropy density per unit of volume, J_s is the entropy flux and σ the entropy production per unit of volume. By integrating Eq. (3.1) for stationary state conditions, we obtain Eq. (2.24). We shall now find an explicit expression for σ by combining:

- mass balances,
- the first law of thermodynamics,
- the local form of Gibbs' equation.

We shall see that σ can be written as the sum of the products of thermodynamic forces and fluxes in the system. These are the so-called *conjugate* fluxes and forces. The fluxes are used in subsequent Chapters to describe transports. The importance of σ for determination and minimization of lost work, see Eq. (2.17), shall be dealt with in Chapters 8, 9 and 10.

Consider a volume element between x and $x + dx$ of a container with an electroneutral homogeneous phase, see Fig. 3.1. The volume element does not move with respect to the walls of the container. It has a sufficient number of particles to give a statistical basis for thermodynamic calculations. We assume local equilibrium in the element. Its state is given by the temperature

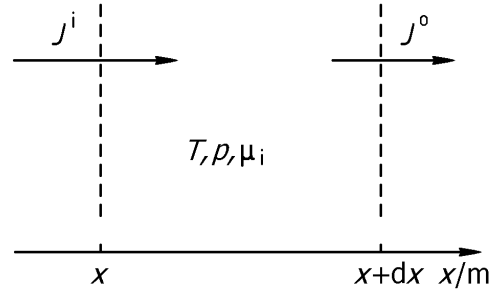

Figure 3.1: A volume element of a homogeneous phase with transport along the $x-$axis. J^{i} and J^{o} indicate fluxes that enter and leave the element. The element is in local equilibrium. indicates one of the fluxes.

$T(x)$, the pressure $p(x)$, and the chemical potentials $\mu_i(x)$. The system is in mechanical equilibrium. This means that the system has no acceleration. The pressure in a homogeneous phase is then constant.

The assumption of local equilibrium is basic to irreversible thermodynamics. It has been tested using non-equilibrium molecular dynamics and found valid for very large temperature gradients [49]. Our aim is to find σ in Eq. (3.1). The symbol list in the front of the book gives the dimensions in the equations that follow.

3.1 Balance equations

The balance equations for the components of the system in the volume element are

$$\frac{\partial c_j}{\partial t} = -\frac{\partial}{\partial x} J_j + \nu_j r \quad \text{for} \qquad j = 1, ..., n \tag{3.2}$$

where J_j are the component fluxes, all directed along the x-axis, ν_j are the stoichiometric constants in a chemical reaction, r is

its rate in the volume element. The reaction Gibbs energy[1] is

$$\Delta_r G = \sum_j \nu_j \mu_j \tag{3.3}$$

Exercise 3.1.1 *Derive Eq.* (3.1) *by considering changes in a fixed volume element.*

- **Solution:** The change of entropy is equal to the entropy flux into the volume element minus the flux out of the volume element, plus the increase in the entropy production. One has therefore

$$\frac{dS}{dt} = -\Omega[J_s(x+dx) - J_s(x)] + V\sigma$$

By using again that the cross section is equal to the volume divided by dx, we obtain in the limit of small dx

$$\frac{dS}{dt} = -V\frac{[J_s(x+dx) - J_s(x)]}{dx} + V\sigma = -V\frac{dJ_s(x)}{dx} + V\sigma$$

By dividing this equation left and right by the volume, one obtains Eq. (3.1).

The conservation equation for charge is

$$\frac{\partial z}{\partial t} = -\frac{\partial}{\partial x} j \tag{3.4}$$

where z is the charge density. The systems that we consider, can all be described as electroneutral. It follows that $\partial j/\partial x = 0$ so that the electric current, j, is constant throughout the system.

[1] The driving force of the chemical reaction was called the affinity, A, by De Donder, with $A = -\Delta_r G$, see e.g. [21].

According to the first law of thermodynamics, the change in internal energy is the net heat plus the work added to the system. For a change in the internal energy density $u = U/V$ per unit of time, we have for a volume element:

$$\frac{\partial u}{\partial t} = -\frac{\partial}{\partial x} J_q + Ej \tag{3.5}$$

where J_q is the energy flux. In most of the cases in the book we shall use the definition

$$J_q = J'_q + \sum_{j=1}^{n} H_j J_j \tag{3.6}$$

The energy flux is here the sum of the measurable heat flux $J'_q(x)$ and the enthalpy flux carried by the component fluxes, J_j, where H_j are the partial molar enthalpies. This definition has lead to the name "total heat flux" which we shall use for this quantity throughout the book. For other definitions, see Appendix A.1.

The product Ej in Eq. (3.5) is the electric power added to the volume element. The electric field is often replaced by minus the gradient of the electric potential:

$$E = -\frac{\partial \phi}{\partial x} \tag{3.7}$$

The first law is illustrated in Fig. 3.2. Appendix A.1 gives a discussion of the relation between Eq. (3.5), the first law and the definition of the total heat flux.

3.2 Entropy production

The balance equations shall be combined with the Gibbs equation

$$dU = TdS - pdV + \sum_{j=1}^{n} \mu_j dN_j \tag{3.8}$$

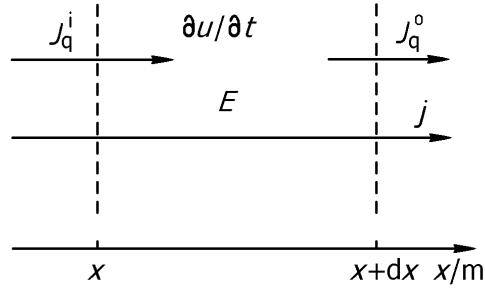

Figure 3.2: The internal energy change of a volume element with fluxes of total heat and charge across the boundaries.

in order to find σ. We replace the internal energy, U, entropy, S and the mole numbers, N_j, by densities of the same variables, $u = U/V$, $s = S/V$ and $c_j = N_j/V$. By using also the fundamental relation $U = TS - pV + \Sigma_j \mu_j N_j$, we obtain the local form of Gibbs' equation

$$du = Tds + \sum_{j=1}^{n} \mu_j dc_j \tag{3.9}$$

with μ_j as the chemical potential. The time derivative of the local entropy density is therefore

$$\frac{\partial s}{\partial t} = \frac{1}{T}\frac{\partial u}{\partial t} - \frac{1}{T}\sum_{j=1}^{n} \mu_j \frac{\partial c_j}{\partial t} \tag{3.10}$$

The use of partial derivatives indicates that the variables are also position dependent. By introducing the balance equations, Eqs. (3.2) and (3.5) into (3.10), using the rule for derivation of products, and solving for $\partial s/\partial t$, we obtain the balance equation

for the entropy

$$\frac{\partial s}{\partial t} = -\frac{\partial}{\partial x}\left[\frac{1}{T}\left(J_q - \sum_{j=1}^{n}\mu_j J_j\right)\right] + J_q\frac{\partial}{\partial x}(\frac{1}{T}) + \sum_{j=1}^{n} J_j\frac{\partial}{\partial x}(-\frac{\mu_j}{T}) + j(-\frac{1}{T}\frac{\partial\phi}{\partial x}) + r\left(-\frac{\Delta_r G}{T}\right) \tag{3.11}$$

By comparing the above equations with the original Eq. (3.1), we can identify the entropy flux in the system

$$J_s = \frac{1}{T}\left(J_q - \sum_{j=1}^{n}\mu_j J_j\right) = \frac{1}{T}J'_q + \sum_{j=1}^{n} S_j J_j \tag{3.12}$$

and the entropy production

$$\sigma = J_q\left(\frac{\partial}{\partial x}\frac{1}{T}\right) + \sum_{j=1}^{n} J_j\left(-\frac{\partial}{\partial x}\frac{\mu_j}{T}\right) + j\left(-\frac{1}{T}\frac{\partial\phi}{\partial x}\right) + r\left(-\frac{\Delta_r G}{T}\right) \tag{3.13}$$

By replacing the total heat flux, J_q, by the entropy flux, J_s, we obtain an alternative expression

$$\sigma = J_s\left(-\frac{1}{T}\frac{\partial T}{\partial x}\right) + \sum_{j=1}^{n} J_j\left(-\frac{1}{T}\frac{\partial\mu_j}{\partial x}\right) + j\left(-\frac{1}{T}\frac{\partial\phi}{\partial x}\right) + r\left(-\frac{\Delta_r G}{T}\right) \tag{3.14}$$

We finally replace the total heat flux, J_q, by the more practical measurable heat flux, J'_q, by introducing Eq. (3.6) into Eq. (3.13). The result is yet an alternative expression:

$$\sigma = J'_q\left(\frac{\partial}{\partial x}\frac{1}{T}\right) + \sum_{j=1}^{n} J_j(-\frac{1}{T}\frac{\partial\mu_{j,T}}{\partial x}) + j\left(-\frac{1}{T}\frac{\partial\phi}{\partial x}\right) + r\left(-\frac{\Delta_r G}{T}\right) \tag{3.15}$$

where $\partial\mu_{j,T}/\partial x = \partial H_i/\partial x - T\partial S_i/\partial x$. The result was derived for electroneutral, homogeneous phases, without any other assumption than that of local equilibrium. Local equilibrium does not imply local *chemical* equilibrium!

Remark 3.1 *Equation* (3.15) *shall be the starting point for further considerations in this book.*

Remark 3.2 *Equation* (3.15) *was derived from the Gibbs equation and the balance equations and is valid whenever these equations are valid.*

Remark 3.3 *The difference between the total heat flux and the measurable heat flux can be illustrated by an example. Consider a liquid and its vapor in a box. A constant heat flux,* $J_q'^l$*, is supplied to the liquid through the bottom of the box. A heat flux* $J_q'^g$ *is removed from the top of the vapor phase. From Eqs.* (3.6) *and (3.5) the energy flux is*

$$J_q = J_q'^{,l} + H_1^l J_1^l = J_q'^{,g} + H_1^g J_1^g$$

In the stationary state, $J_1^l = J_1^g = J$*, so*

$$J_q'^{,l} - J_q'^{,g} = (H_1^g - H_1^l)J$$

The measurable heat fluxes in the liquid and the gas differ because of the source term at the interface. The total heat flux is constant. It cannot be measured in either of the phases, however, because H_1^g *and* H_1^l *are not absolute.*

The entropy production contains pairs of fluxes and forces. We call the corresponding pairs *conjugate fluxes and forces.* In Eq. (3.15) the measurable heat flux J_q' has the conjugate force $\partial(1/T)/\partial x$, the mass flux J_j has the conjugate force $-\partial\mu_{j,T}/T\partial x$, the electric current density j has the conjugate force $-\partial\phi/T\partial x$) and the reaction rate r has the conjugate force $-\Delta_r G/T$. The conjugate flux-force pairs in Eqs. (3.13), (3.14) and (3.15) are different. All these different choices are equivalent, however, and describe the same physical phenomena.

All force-flux pairs, except the last one, have a direction and are thus vectors. The reaction has a scalar flux-force pair, r and $-\Delta_r G/T$. We are dealing with one-dimensional problems in this Chapter and all vectorial fluxes and forces are directed along the x-axis. A divergence of a flux reduces to the derivative of the x-component with respect to x. A gradient is similarly directed along the x-direction, and is given by the derivative of a potential or a temperature with respect to x. As it is known that, for instance a heat flux or an electric field, is vectorial, we do not complicate the notation further by making this distinction explicit.

Introduction of different fluxes, or changing the frame of reference, does not change the value or the physical interpretation of σ. The entropy production is an absolute quantity, as is the entropy. The preference for one of the expressions for a particular system, is always motivated by the system itself. We can illustrate this by an example: If the system is such that the chemical potentials of all components are constant, Eq. (3.14) is appropriate. In that expression the second term, containing the sum over j, is zero. One can of course also use the other two forms of the entropy production and simplify them using the constant nature of the chemical potentials. It is then easy to verify that the first and the second term combine and reduce to the first term in Eq. (3.14). Thus it is the properties of the system that determine which form of the entropy production is useful. We will use the last one, Eq. (3.15) when we describe experiments. The three alternative expressions are given as a help to find the appropriate form quickly.

The separate products do not necessarily represent pure losses of work (cf. Section 2.3). For instance, the electric power per unit of volume, $-(j\partial\phi/\partial x)$, does not necessarily give only an ohmic contribution to the entropy production, there may also be electric work included in the product, as we shall see in detail

in Section 4.4. Each of the separate products normally contains work terms, and energy storage terms, see [18]. It is *their combination* which gives the entropy production and the work that is lost locally, $T_0\,\sigma$. The temperature of the surroundings T_0 enter the formula for the lost work.

Dependent variables should be eliminated from σ. This simplifies the flux equations, and makes their solution easier. Such a simplification is one motivation for using electroneutral components in Eq. (3.2). Mass variables of this kind lead to straightforward reductions of Eq. (3.13). For instance, when the electric current density is zero, the electric power term disappears. The entropy production due to the chemical reaction disappears when the reaction rate vanishes, $r = 0$, or when the chemical reaction is in equilibrium, $\Delta_r G = 0$. Local chemical equilibrium introduces a relation between the remaining forces in the system. To see this, consider a reaction with $\Delta_r G = 0$. We can express the chemical potential μ_{D} of component D by the other chemical potentials contained in $\Delta_r G$. This can lead to a redefinition of the independent molar fluxes of the system. Gibbs-Duhem's equation (see also Exercise A.2.1 in Appendix A.2)

$$dp = s dT + \sum_{j=1}^{n} c_j d\mu_j \tag{3.16}$$

gives a further possibility for elimination of one of the chemical forces, $-(1/T)\partial\mu_j/\partial x$.

According to Prigogine's theorem [9] the expressions for σ, Eqs. (3.13)-(3.15), are valid in any frame of reference, which has a constant velocity v with respect to the laboratory frame of reference, provided that the system is in mechanical equilibrium. The mass fluxes change from J_j in the laboratory frame to $J_j - c_j v$ in a frame of reference with a constant velocity v, and the entropy flux changes from $J_s - sv$. The expression for the measurable heat flux remains the same. The transformation

formula for the energy and entropy fluxes follow from those of the mass and measurable heat fluxes. We consider only systems that are in mechanical equilibrium, so Prigogine's theorem is applicable. A discussion and proof of the theorem was given by de Groot and Mazur [12], see also Chapter 6.

Haase [14] defined the dissipation function in non-equilibrium thermodynamics, analogous to the Rayleigh dissipation function for hydrodynamic flow, by $\Psi = T\sigma$. The integral over this function may be called D. An integration with $T > T_0$, gives $w_{lost} < \mathsf{D}$. The lost work was defined unambiguously in Chapter 2. It follows for cases with $T > T_0$, that parts of D can be extracted to do work. This means that D is ambiguous and leads to potentially incorrect results, when it comes to analysis of efficiencies in industrial processes. We shall avoid using Ψ for this reason (see also [29] Section 4.2.1).

3.3 Examples

The exercises below illustrate in more detail how the contributions to the entropy production arise. The exercises 3.3.1-3.3.5 are meant to illustrate the theory. Exercises 3.3.6, 3.3.7 give numerical insight and 3.3.8, 3.3.9 give physical insight.

Exercise 3.3.1 *Consider the special case that only component number j is transported. The densities of the other components, the internal energy, the molar volume and the polarization densities are all constant. Show that the entropy production is given by*

$$\sigma = -J_j \frac{\partial}{\partial x}\left(\frac{\mu_j}{T}\right)$$

- **Solution:** In this case the Gibbs equation, Eq. (3.10), reduces to

$$T\frac{\partial s}{\partial t} + \mu_j \frac{\partial c_j}{\partial t} = 0$$

The rate of change of the entropy is therefore given by

$$\frac{\partial s}{\partial t} = -\frac{\mu_j}{T}\frac{\partial c_j}{\partial t}$$

We use the balance equation for component j, Eq. (3.2), and obtain

$$\frac{\partial s}{\partial t} = \frac{\mu_j}{T}\frac{\partial}{\partial x}J_j = \frac{\partial}{\partial x}\left(\frac{\mu_i}{T}J_j\right) - J_j\frac{\partial}{\partial x}\frac{\mu_j}{T}$$

By comparing this equation with the entropy balance, Eq. (3.1), we may identify the entropy flux and the entropy production as

$$J_s = -\frac{\mu_j}{T}J_j \text{ and } \sigma = -J_j\frac{\partial}{\partial x}\left(\frac{\mu_j}{T}\right)$$

Exercise 3.3.2 *Consider the case that only heat is transported. The molar densities, the molar volume and the polarization densities are all constant. Show that the entropy production is given by*

$$\sigma = J'_q\frac{\partial}{\partial x}\left(\frac{1}{T}\right)$$

- **Solution:**In this case the Gibbs equation, Eq. (3.10), reduces to

$$\frac{\partial u}{\partial t} = T\frac{\partial s}{\partial t}$$

The rate of change of the entropy is therefore given by

$$\frac{\partial s}{\partial t} = \frac{1}{T}\frac{\partial u}{\partial t}$$

The energy balance Eq. (3.5) reduces to

$$\frac{\partial u}{\partial t} = -\frac{\partial}{\partial x}J'_q$$

By substituting this into the equation above, we obtain

$$\frac{\partial s}{\partial t} = -\frac{1}{T}\frac{\partial}{\partial x}J'_q = -\frac{\partial}{\partial x}\left(\frac{1}{T}J'_q\right) + J'_q\frac{\partial}{\partial x}\left(\frac{1}{T}\right)$$

By comparing this equation with the entropy balance, Eq. (3.1), we can identify the entropy flux and the entropy production as

$$J_s = \frac{1}{T}J'_q \quad \text{and} \quad \sigma = J'_q\frac{\partial}{\partial x}\left(\frac{1}{T}\right)$$

Exercise 3.3.3 *Consider a system with two components ($n = 2$), having $dT = 0$ and $dp = 0$. Show, using Gibbs-Duhem's equation, that one may reduce the description in terms of two components to one with only one component.*

- **Solution:** Gibbs-Duhem's equation (3.16) gives

$$c_1 d\mu_{1,T} + c_2 d\mu_{2,T} = 0$$

The entropy production in Eq. (3.15) reduces for these conditions to

$$\sigma = -\frac{1}{T}(J_1 - \frac{c_1}{c_2}J_2)\frac{\partial \mu_{1,T}}{\partial x}$$

The equation contains only one (independent) force. Energy is lost by interdiffusion of the two components. We can also write this entropy production as

$$\sigma = J_V\left(-\frac{c_1}{T}\frac{\partial \mu_{1,T}}{\partial x}\right)$$

with $J_V \equiv J_1/c_1 - J_2/c_2$. This is the volumetric velocity flux of component 1 relative to the velocity, J_2/c_2, of component 2. Note that J_V is independent of the frame of reference.

Exercise 3.3.4 *Show how the chemical force in Eq.* (3.15) *can be derived from Eq.* (3.13).

- **Solution:** The chemical force in Eq. (3.15) can be rewritten as

$$\begin{aligned}\frac{\partial}{\partial x}\left(\frac{\mu_i}{T}\right) =& \frac{1}{T}\frac{\partial}{\partial x}\mu_{i,T} + TS_i\left(\frac{1}{T^2}\frac{\partial T}{\partial x}\right) + \mu_i\frac{\partial \frac{1}{T}}{\partial x} \\ =& \frac{1}{T}\frac{\partial \mu_{i,T}}{\partial x} + H_i\frac{\partial \frac{1}{T}}{\partial x}\end{aligned}$$

By substituting this result into Eq. (3.13), we obtain

$$\begin{aligned}\sigma = &\left[J_q - \sum_{i=1}^{n} H_i J_i\right]\frac{\partial}{\partial x}\left(\frac{1}{T}\right) + \sum_{i=1}^{n} J_i\left(-\frac{1}{T}\frac{\partial}{\partial x}\mu_{i,T}\right) \\ &+ j\left(-\frac{1}{T}\frac{\partial \phi}{\partial x}\right)\end{aligned}$$

By using $J_q = J_q' + \sum_{i=1}^{n} H_i J_i$, Eq. (3.15) follows. The new chemical force is related to the chemical potential by:

$$d\mu_{i,T} = d\mu_i - \left(\partial \mu_i/\partial T\right)_{p,\mu_j,j\neq i} dT = d\mu_i + S_i dT$$

Exercise 3.3.5 *Derive the entropy production for an isothermal two-component system that does not transport charge. The solvent is the frame of reference for the fluxes.*

- **Solution:** In an isothermal system $\partial(1/T)/\partial x = 0$. Furthermore there is no charge transport so that $j = 0$. Finally the solvent is the frame of reference, so $J_{solvent} = 0$. There remains only one force-flux pair, namely for transport of solute. Using Eq. (3.15) we then find

$$\sigma = -\frac{J}{T}\frac{\partial \mu_T}{\partial x}$$

for the entropy production. Knowing that $\sigma \geq 0$ it follows that the solute will move from a higher to a lower value of its chemical potential.

Exercise 3.3.6 *Find the average entropy production due to the heat flux through a sidewalk pavement by a hot plate placed d = 8 cm under the pavement. The plate has a temperature of 343 K. The surface is in contact with melting ice (273 K). The Fourier type thermal conductivity of the pavement is 0.7 W/Km.*

- Fourier's law for heat conduction is $J'_q = -\lambda(dT/dx)$. The entropy production per surface area is

$$\int_0^d \sigma dx = \int_0^d J'_q \frac{\partial}{\partial x}(\frac{1}{T})dx = -\lambda \frac{\Delta T}{d}\left(\frac{1}{T_2} - \frac{1}{T_1}\right)$$
$$= -0.7\frac{(-70)}{(0.08)}\left(\frac{1}{273} - \frac{1}{343}\right) = 0.46\frac{W}{Km^2}$$

The lost work $w_{lost} = T_0\Omega\int_0^d \sigma dx$ per surface area Ω is $w_{lost}/\Omega = 275\ \mathrm{K} \cdot 0.46\ \frac{W}{Km^2} = 125\ \frac{W}{m^2}$. It is typical for heat conduction around room temperature that the entropy production is large.

Exercise 3.3.7 *In order to produce drinking water, one filters water through a 1 m thick sand layer with grain diameters around 0.1 mm. The height of the water column above the sand is d = 1 m, and the clean water outlet is at the top of the filter. Evaluate the entropy production for a water flux of 10^{-6} kg/m^2 s^1 at 293 K. The density of water is ρ =1000 kg/m^3, and the process can be considered to be in mechanical equilibrium.*

- The contribution to the chemical potential gradient is from the hydrostatic pressure gradient of the water column. The

increase in the pressure of water at a distance x from the sand surface is given by $dp = \rho g dx$. This gives $-d\mu_{w,T}/dx = V_w \rho g$, and

$$\sigma = J_w \frac{1}{T} V_w \rho g = 3.2 \times 10^{-8} \text{W/K m}^3$$

This value is considerably smaller than the value for transport of heat to a pavement per m^2 surface (see exercise above).

Exercise 3.3.8 *What is the entropy production for systems that are described by Eqs.* (2.1)*,* (2.2) *and* (2.3)*?*

- **Solution:** Substitution of these equations into Eq. (3.15), setting the reaction rate zero, yields

$$\begin{aligned}\sigma &= \frac{\lambda}{T^2}\left(\frac{\partial T}{\partial x}\right)^2 + \frac{D}{T}\frac{\partial \mu_T}{\partial c}\left(\frac{\partial c}{\partial x}\right)^2 + \frac{\kappa}{T}\left(\frac{\partial \phi}{\partial x}\right)^2 \\ &\equiv \sigma_T + \sigma_\mu + \sigma_\phi\end{aligned}$$

Typical values in an electrolyte are: $\lambda = 2$ J/msK, $T = 300$ K, $dT/dx = 100$ K/m, $D = 10^{-9}$ m^2/s, $\partial \mu_T/\partial c = RT/c$, $c = 100$ kmol/m^3, $dc/dx = 10^{-5}$ mol/m^4, $\kappa = 400$ Si/m, $d\phi/dx = 10^{-2}$ V/m. The resulting entropy productions are: $\sigma_T = 0.2$ J/Ksm^3, $\sigma_\mu = 10^{-13}$ J/Ksm^3 and $\sigma_\phi = 10^{-4}$ J/Ksm^3. Heat conduction therefore clearly gives the largest contribution to the entropy production in electrolytes

Exercise 3.3.9 *The Carnot machine converts heat into work in a reversible way. The efficiency is defined as the work output divided by the heat input [44,46], see Section 2.4. This efficiency is* $(T_h - T_c)/T_h$*, where* T_h *and* T_c *are the temperatures of the hot and the cold reservoir, respectively. Compare this efficiency with the expression for the entropy production of a system that transports heat from a hot reservoir to the surroundings.*

- **Solution:** If we do not use the heat to produce work, but simply bring the hot and cold reservoirs in thermal contact with one another, there is a heat flow from the hot to the cold reservoir. The entropy production for the path, which has a cross section Ω is:

$$\frac{dS_{\text{irr}}}{dt} = \Omega \int \sigma(x) dx = \Omega \int J'_q(x) \frac{\partial}{\partial x} \left(\frac{1}{T(x)} \right) dx$$

As there is no other transport of thermal energy, the heat flux is constant. This results in

$$\begin{aligned} \frac{dS_{\text{irr}}}{dt} &= J'_q \Omega \int \frac{\partial}{\partial x} \left(\frac{1}{T(x)} \right) dx = J'_q \Omega \int_{T_h}^{T_c} \frac{\partial}{\partial T} \left(\frac{1}{T} \right) dT \\ &= J'_q \Omega \left(\frac{1}{T_c} - \frac{1}{T_h} \right) = J'_q \Omega \left(\frac{T_h - T_c}{T_h T_c} \right) = J'_q \Omega \frac{\eta_I}{T_c} \end{aligned}$$

The work lost per unit of time, $T_c dS_{\text{irr}}/dt$, is thus identical to the work that can be obtained by a Carnot cycle, $\eta_I J'_q \Omega$, per unit of time. This can be used as a derivation of the first law efficiency of the Carnot machine. This machine is reversible and has as a consequence no lost work.

Exercise 3.3.10 *Consider the reaction:*

$$B + C \rightleftarrows D$$

The reaction Gibbs energy is:

$$\Delta_r G = \mu_D - \mu_C - \mu_B$$

In the absence of chemical equilibrium, the three chemical potentials are independent. The contribution to σ from the reaction is:

$$\sigma_{chem} = r \left(-\frac{\Delta_r G}{T} \right)$$

Derive this expression for σ_{chem}, assuming that the reaction takes place in a reactor in which the internal energy is independent of the time.

- **Solution:** The three balance equations for components B, C and D have a source term from the reaction rate, cf. Eq. (3.2)

$$\begin{aligned}\frac{\partial c_{\mathrm{B}}}{\partial t} &= -\frac{\partial}{\partial x}J_{\mathrm{B}} - r\\ \frac{\partial c_{\mathrm{C}}}{\partial t} &= -\frac{\partial}{\partial x}J_{\mathrm{C}} - r\\ \frac{\partial c_{\mathrm{D}}}{\partial t} &= -\frac{\partial}{\partial x}J_{\mathrm{D}} + r\end{aligned}$$

When the internal energy is independent of the time, the Gibbs equation, Eq. (3.10), reduces to

$$T\frac{\partial s}{\partial t} + \sum_{i=1}^{3}\mu_i\frac{\partial c_i}{\partial t} = 0$$

The rate of change of entropy is therefore given by

$$\frac{\partial s}{\partial t} = -\sum_{i=1}^{3}\frac{\mu_i}{T}\frac{\partial c_i}{\partial t}$$

We introduce the balance equations in this expression and obtain

$$\begin{aligned}\frac{\partial s}{\partial t} &= \frac{\mu_{\mathrm{B}}}{T}(\frac{\partial}{\partial x}J_{\mathrm{B}} + r) + \frac{\mu_{\mathrm{C}}}{T}(\frac{\partial}{\partial x}J_{\mathrm{C}} + r) + \frac{\mu_{\mathrm{D}}}{T}(\frac{\partial}{\partial x}J_{\mathrm{D}} - r)\\ &= \frac{\partial}{\partial x}(\frac{\mu_{\mathrm{B}}}{T}J_{\mathrm{B}} + \frac{\mu_{\mathrm{C}}}{T}J_{\mathrm{C}} + \frac{\mu_D}{T}J_{\mathrm{D}}) - J_{\mathrm{B}}\frac{\partial}{\partial x}(\frac{\mu_{\mathrm{B}}}{T})\\ &- J_{\mathrm{C}}\frac{\partial}{\partial x}(\frac{\mu_{\mathrm{C}}}{T}) - J_{\mathrm{D}}\frac{\partial}{\partial x}(\frac{\mu_{\mathrm{D}}}{T}) + (\frac{\mu_{\mathrm{B}}}{T} + \frac{\mu_{\mathrm{C}}}{T} - \frac{\mu_{\mathrm{D}}}{T})r\end{aligned}$$

By comparing this equation with Eq. (3.1), we can identify the entropy flux as

$$J_s = -\left[\frac{\mu_{\mathrm{B}}}{T}J_{\mathrm{B}} + \frac{\mu_{\mathrm{C}}}{T}J_{\mathrm{C}} + \frac{\mu_{\mathrm{D}}}{T}J_{\mathrm{D}}\right]$$

and the entropy production as

$$\sigma = -J_{\mathrm{B}}\frac{\partial}{\partial x}(\frac{\mu_{\mathrm{B}}}{T}) - J_{\mathrm{C}}\frac{\partial}{\partial x}(\frac{\mu_{\mathrm{C}}}{T}) - J_{\mathrm{D}}\frac{\partial}{\partial x}(\frac{\mu_{\mathrm{D}}}{T}) + r(\frac{\mu_{\mathrm{B}}}{T} + \frac{\mu_{\mathrm{C}}}{T} - \frac{\mu_{\mathrm{D}}}{T})$$

By writing this entropy production as a sum of a scalar and a vectorial part, $\sigma = \sigma_{vect} + \sigma_{scal}$, we find

$$\sigma_{vect} = -J_{\mathrm{B}}\frac{\partial}{\partial x}(\frac{\mu_{\mathrm{B}}}{T}) - J_{\mathrm{C}}\frac{\partial}{\partial x}(\frac{\mu_{\mathrm{C}}}{T}) - J_{\mathrm{D}}\frac{\partial}{\partial x}(\frac{\mu_{\mathrm{D}}}{T})$$

$$\sigma_{scal} = (\frac{\mu_{\mathrm{B}}}{T} + \frac{\mu_{\mathrm{C}}}{T} - \frac{\mu_{\mathrm{D}}}{T})r = -\frac{r\Delta_r G}{T} = \sigma_{chem}$$

The vectorial contributions are due to diffusion while the scalar contribution is due to the reaction.

3.4 The frame of reference for fluxes

We need a frame of reference for the fluxes when we want to measure transport. In electroneutral systems, the electric current density, j, is constant throughout the system and independent of the frame of reference. Mass fluxes, on the other hand, depend on the velocity of the frame of reference. The solvent frame of reference is used when movement of solutes with respect to the solvent is of interest. In flow problems, the center of mass frame of reference is convenient, see Chapter 6 and Appendix A.1.

We do not treat transport across surfaces in this book. Transport across phase boundaries is technically important, and we mention that the frame of reference that gives a simple description of the surface, is the surface itself [29]. In this frame of reference the observer moves along with the surface. If the surface is at rest, so is the observer. This is then also the laboratory frame of reference.

Some frames of references are defined below, to show how descriptions can be converted into one another. In the conversion we take advantage of the fact that the entropy production is independent of the frame of reference. The notions, reversible and irreversible, are also independent of the frame of reference. They are in other words Galilei invariant. We may therefore convert all fluxes and conjugate forces from any frame of reference to another frame of reference and back without changing the entropy production, σ. According to Prigogine's theorem, any frame of reference that move with a constant velocity with respect to the laboratory frame of reference, can be used for mass fluxes.

The mass flux of a component A relative to a frame of reference can be written as

$$J_{\mathrm{A,ref}} = c_{\mathrm{A}}(v_{\mathrm{A}} - v_{\mathrm{ref}}) \tag{3.17}$$

where c_{A} is the concentration in mole/m^3, v_{A} is the velocity of A and v_{ref} is the velocity of the frame of reference relative to the laboratory frame of reference.

The laboratory frame of reference or the wall frame of reference. In this frame of reference

$$J_{\mathrm{A}} = c_{\mathrm{A}} v_{\mathrm{A}} \qquad \text{and} \qquad v_{\mathrm{ref}} = 0 \tag{3.18}$$

This is a convenient experimental frame of reference.

The solvent frame of reference. This frame of the reference is typically used when there is an excess of one component, the solvent. For transports of component A relative to the solvent one has:

$$J_{\mathrm{A,solv}} = c_{\mathrm{A}}\,(v_{\mathrm{A}} - v_{\mathrm{solv}}) \quad \text{and} \qquad v_{\mathrm{ref}} = v_{\mathrm{solv}} \tag{3.19}$$

The frame of reference moves with the velocity of the solvent, v_{solv}.

The average molar frame of reference. In a multicomponent mixture

when there is no excess of one component one can use the average molar velocity, which is defined by:

$$v_{\text{molar}} \equiv \frac{1}{c} \sum_i c_i v_i = \sum_i x_i v_i \tag{3.20}$$

where $x_i = c_i/c$ is the mole fraction of i. This gives

$$J_{\text{A,molar}} \equiv c_{\text{A}} \left(v_{\text{A}} - v_{\text{molar}} \right) \tag{3.21}$$

The average volume frame of reference has been used when transport occurs in a closed volume. The average volume velocity is

$$v_{\text{vol}} \equiv \sum_i c_i V_i v_i \tag{3.22}$$

The flux of A becomes

$$J_{\text{A,vol}} \equiv c_{\text{A}} \left(v_{\text{A}} - v_{\text{vol}} \right) \tag{3.23}$$

The barycentric (average center of mass) frame of reference. This frame of reference is used in Navier-Stokes equation, Eq. (6.6). The average mass velocity is

$$v_{\text{bar}} \equiv \frac{1}{\rho} \sum_i \rho_i v_i \tag{3.24}$$

where ρ is the mass density of the fluid, and ρ_i are the partial mass densities. The diffusion flux of A (in mol/s m^2) in a barycentric frame of reference is

$$J_{\text{A,bar}} \equiv c_{\text{A}} \left(v_{\text{A}} - v_{\text{bar}} \right) \tag{3.25}$$

The diffusion flux of A in kg/s m^2 is equal to $M_{\mathrm{A}} J_{\mathrm{A,bar}} \equiv \rho_{\mathrm{A}} (v_{\mathrm{A}} - v_{\mathrm{bar}})$, where M_{A} is the molar mass. The advantage of the barycentric frame of reference for fluid dynamics is illustrated in Chapter 6.

Chapter 4

Flux equations and transport coefficients

We present examples of flux equations that follow from the entropy production in Chapter 3. The determination of Onsager coefficients from experimental data, for instance, conductivities, diffusion coefficients and transport numbers, is discussed for simple homogeneous systems. We show that the coupling coefficients can be related to stored energy or work.

In Chapter 3, we derived the entropy production for systems in mechanical equilibrium, using the assumption of local equilibrium. The entropy production determines the conjugate thermodynamic forces and fluxes of the system. The next major assumption in non-equilibrium thermodynamics is the assumption of linear flux-force relations. From this assumption, and the assumption of microscopic reversibility, Onsager derived the symmetry relation (1.3) for the coupling coefficients. He also gave the fundamental relation between a flux and a force, and why they can be called conjugate [2, 3].

In this Chapter we give examples of flux equations in order to illustrate the meaning of a characteristic property of the theory; the coupling coefficient. The transport problems we are dealing with here can be well studied in one dimension. Shear flow which has more dimensions, is dealt with in Chapter 6. The general aspects discussed in Section 4.1, apply also to Chapter 6.

4.1 Linear flux-force relations

Irreversible thermodynamics assumes that all fluxes, J_i, are linear functions of all forces, X_j. In general:

$$J_i = \sum_{j=1}^{n} L_{ij} X_j \qquad \text{for} \qquad j = 1, 2, ..., n \tag{4.1}$$

where n is the number of *independent* fluxes. The coefficients must be determined from experiments. We assume that the linear relations are valid *locally*. All coefficients are functions of the local values of the state variables of the system. A global description of the system might thus give a nonlinear relation between J_i and integrated forces. Locally, the conductivities L_{ij} 's *do not depend on the* X_j's, however. The description is linear only in this sense. It means for instance that the thermal conductivity is allowed to depend on the temperature, but not on the gradient of the temperature.

Remark 4.1 *The theory is often called "linear non-equilibrium thermodynamics". Contrary to what is sometimes stated, the theory results in an extremely nonlinear description of the system. Phenomena like turbulence and the Rayleigh-Benard instability, as described with the Navier-Stokes equation, cf. Eq. (6.6), occur within the framework of linear non-equilibrium thermodynamics. The use of the adjective "linear" is therefore rather misleading.*

Alternatively the forces may be expressed as linear functions of all fluxes

$$X_k = \sum_{j=1}^{n} R_{kj} J_j \qquad k = 1, 2, ..., n \tag{4.2}$$

The resistivity matrix is the inverse of the conductivity matrix

$$\sum_{i=1}^{n} L_{ik} R_{kj} = \sum_{i=1}^{n} R_{ik} L_{kj} = \delta_{ij} \tag{4.3}$$

Here δ_{ij} is a Kronecker delta, which is one if the indices are equal and zero otherwise. Equations (4.1) and (4.2) are equivalent. It depends on the system which formulation is more convenient to use.

Onsager [2,3] proved that the matrix of coefficients for Eq. (4.1) is symmetric when the system is microscopically reversible[1].

$$L_{ik} = L_{ki} \quad \text{or equivalently} \quad R_{ik} = R_{ki} \tag{4.4}$$

We shall not repeat Onsager's derivation. Førland et al. [18] gave a simple presentation of the original work. The Onsager relations simplify the transport problem. When the *Onsager conductivity* coefficients L_{ik} are known, we know how the different processes are coupled to one another. "Being coupled" is here used solely in the sense that a force X_k leads to a flux J_i, and vice versa. A temperature gradient can, for instance, give rise to a mass flux and a chemical potential gradient can give rise to a heat flux.

[1]Microscopic reversibility is the following property: The probability that a fluctuation α_i in some property at time t, is followed by a fluctuation α_j in another property after a time lag τ is equal to the probability of the reverse situation, where the fluctuation α_j at time t, is followed by α_i after a time lag τ. This property is a consequence of the time reversal invariance of Newton's equations.

Before we study examples, we examine some general properties of the Onsager coefficients. By substituting the linear laws (4.1) into the entropy production, we have

$$\sigma = \sum_i X_i \sum_k L_{ik} X_k = \sum_{i,k} X_i L_{ik} X_k \geq 0 \tag{4.5}$$

Similarly, we find by introducing Eq. (4.2)

$$\sigma = \sum_{i,k} J_i R_{ik} J_k \geq 0 \tag{4.6}$$

The inequalities follow from the second law of thermodynamics. By taking all the forces, except one, equal to zero, it follows immediately that main coefficients are always positive

$$L_{ii} \geq 0 \quad \text{and} \quad R_{ii} \geq 0 \tag{4.7}$$

It follows for two pairs of fluxes and forces that:

$$L_{ii}L_{kk} - L_{ik}L_{ki} \geq 0 \quad \text{and} \quad R_{ii}R_{kk} - R_{ik}R_{ki} \geq 0 \tag{4.8}$$

Transport is thus dominated by the main coefficients. The inequalities (4.8) can be found by taking all except two forces zero, and subsequently eliminating one of the two forces in terms of the corresponding flux. For the conductivities, we obtain

$$\begin{aligned} J_1 &= L_{11}X_1 + L_{12}X_2 \\ J_2 &= L_{21}X_1 + L_{22}X_2 \end{aligned} \tag{4.9}$$

By expressing X_2 by the second equation and introducing it into the first, we obtain

$$J_1 = (L_{11} - \frac{L_{12}L_{21}}{L_{22}})X_1 + \frac{L_{12}}{L_{22}}J_2 \tag{4.10}$$

When this is introduced into the entropy production, we find:

$$\begin{aligned} \sigma &= (L_{11} - \frac{L_{12}L_{21}}{L_{22}})X_1^2 + \frac{L_{12}}{L_{22}}J_2X_1 - \frac{L_{21}}{L_{22}}J_2X_1 + \frac{J_2^2}{L_{22}} \\ &= (L_{11} - \frac{L_{12}L_{21}}{L_{22}})X_1^2 + \frac{J_2^2}{L_{22}} \end{aligned} \tag{4.11}$$

We must have $\sigma \geq 0$, also for the special case that $J_2 = 0$. Equation (4.8) for the conductivities follows from this and the last equality. The inequalities for the resistivities can be derived analogously. Two terms in the first equality cancel because of the Onsager relations. We shall see in Sections 4.3 and 4.4 that the terms can be allocated to work performed and internal energy converted.

Remark 4.2 *When $X_1 = 0$, a finite flux J_2 gives rise to a flux $J_1 = (L_{12}/L_{22})J_2$ in Eq. (4.10). The expression for the entropy production (4.11) shows, however, that a contribution to J_1 due to J_2 does not contribute to the entropy production. This transport along with J_2 is therefore reversible. The coupling coefficients describe reversible contributions to σ.*

An equality sign in Eq. (4.8) implies that two fluxes are proportional to one another. In the remark $J_1 = (L_{12}/L_{22})J_2$. A consequence is that the number of fluxes, and therefore the number of variables, can be reduced in the entropy production. By keeping the flux, J_2, rather than the force, X_2, equal to zero, the entropy production is reduced from $L_{11}X_1^2$ to $(L_{11} - L_{12}L_{21}/L_{22})X_1^2$. The combination of coefficients is an effective conductivity, see exercise 2.2.1 in Section 2.2.

All cases studied in this Chapter can be cast into the general pattern above. We shall see how we can recognize the general pattern in the particular processes below.

4.2 Transport of heat and mass

Mass is transported, not only by a gradient in chemical potential. A gradient in temperature, can also lead to mass transport. This is called thermal diffusion or the Soret effect. Likewise, the gradient in chemical potential, leads to a heat flux; the so called Dufour effect.

Consider a two-component system with heat and mass transfer. The second component has a concentration much larger than the first. It is then convenient to use the velocity of this component as the frame of reference for the velocity of the first component. This is the solvent frame of reference, cf. Section 3.4. Assume that the heat- and mass transport take place in the x-direction only. The entropy production is, see Eq. (3.15),

$$\sigma = J'_q \frac{\partial}{\partial x}(\frac{1}{T}) + J_1 \left(-\frac{1}{T} \frac{\partial \mu_{1,T}}{\partial x} \right) \tag{4.12}$$

The linear flux-force relations for the measurable heat flux and the mass flux are

$$\begin{aligned} J'_q &= l_{qq} \frac{\partial}{\partial x} \left(\frac{1}{T} \right) + l_{q\mu} \left(-\frac{1}{T} \frac{\partial}{\partial x} \mu_{1,T} \right) \\ J_1 &= l_{\mu q} \frac{\partial}{\partial x} \left(\frac{1}{T} \right) + l_{\mu\mu} \left(-\frac{1}{T} \frac{\partial}{\partial x} \mu_{1,T} \right) \end{aligned} \tag{4.13}$$

where according to the Onsager relations $l_{q\mu} = l_{\mu q}$. Lower case l's are used to describe diffusive transport of heat and mass. The chemical potential for a non-electrolyte is:

$$\mu_1 = \mu_1^\circ + RT \ln \gamma_1 c_1 \tag{4.14}$$

where c_1 is the concentration, γ_1 is the activity coefficient of component 1, and μ_1° is the standard chemical potential, see Appendix A.3. When the temperature is constant, the equation for the mass flux (in mol/m^{2}s) is

$$J_1 = -l_{\mu\mu} \frac{1}{T} \frac{\partial \mu_{1,T}}{\partial x}$$

The expression can the be related to Fick's law by

$$J_1 = -l_{\mu\mu} \frac{1}{T} \frac{\partial \mu_{1,T}}{\partial x} = -l_{\mu\mu} \frac{1}{T} \frac{\partial \mu_{1,T}}{\partial c_1} \frac{\partial c_1}{\partial x} = -D_{1,2} \frac{\partial c_1}{\partial x} \tag{4.15}$$

Table 4.1: Some interdiffusion coefficients at 300 K.

System	$D_{1,2}/\mathrm{m^2 s^{-1}}$
CH_4 in nitrogen	5×10^{-5}
NaCl in water	1.3×10^{-9}
Sucrose in water	4.5×10^{-10}
C in steel	1×10^{-20}

where the *interdiffusion coefficient* of the first component $D_{1,2}$ can be identified with

$$D_{1,2} = \frac{l_{\mu\mu}}{T}\left[\frac{\partial \mu_{1,T}}{\partial c_1}\right] = \frac{l_{\mu\mu}R}{c_1}\left[1 + \frac{\partial\ \ln\gamma_1}{\partial\ \ln c_1}\right] \tag{4.16}$$

For ideal mixtures the parenthesis is unity. Interdiffusion coefficients vary by orders of magnitude when one compares gas, liquid, or solid phases, see Table 4.1 and ref. [35]. Even within the same phase, Fick's diffusion coefficient can vary by orders of magnitude. The variation of the Maxwell-Stefan diffusion coefficients (see Chapter 5) is less pronounced. Diffusion is often a rate-limiting process, not only in chemical reactors.

Remark 4.3 *Interdiffusion coefficients are measured by spectroscopic and analytical techniques. When the coefficient is not known, one can obtain an estimate from the self diffusion coefficient, D_s, which is measured using NMR. The self diffusion coefficient is also given for pure components. It describes the Brownian motion of a single particle. Einstein gave the self diffusion coefficient as $D_s =< x^2 > /2t$, in terms of the mean square displacement $< x^2 >$ during the time t. The self diffusion coefficient of liquid water (in water) is $2.3\times10^{-9} m^2\ s^{-1}$ at 300 K. For gases, kinetic theory gives $D_s = \ell v/3$, where ℓ is the mean free path of the molecule and v is the mean thermal velocity. With a typical value ℓ = 30 nm, and v =300 m s^{-1}, $D_s = 3\times10^{-6}\ m^2 s^{-1}$. These estimates can be compared to the inter-*

diffusion coefficients in Table 4.1. For low density gas mixtures the interdiffusion and the self diffusion coefficient are the same.

Exercise 4.2.1 *How do you think the interdiffusion coefficient varies with increasing concentration of component 1 in a mixture?*

- **Solution:** From the expression for the interdiffusion coefficient given above we know that $D_{1,2} = l_{\mu\mu}\partial\mu_{1,T}/T\partial c_1$ For low densities this reduces to $D_{1,2} = l_{\mu\mu}R/c_1$. For higher densities this becomes

$$D_{1,2} = \frac{l_{\mu\mu}R}{c_1}\left[1 + \partial \ln \gamma_1/\partial \ln c_1\right]$$

  The concentration dependence of $l_{\mu\mu}$ must be measured.

When the chemical potential at constant temperature, $\mu_{1,T}$, is constant, the equation for the heat flux reduces to Fourier's law for a homogeneous system

$$J'_q = l_{qq}\frac{\partial}{\partial x}\left(\frac{1}{T}\right) = -\lambda_\mu \frac{\partial T}{\partial x} \tag{4.17}$$

This gives the following relation between l_{qq} and the thermal conductivity of a homogeneous material:

$$\lambda_\mu = -\left(\frac{J'_q}{\partial T/\partial x}\right)_{\partial\mu/\partial x=0} = \frac{1}{T^2}l_{qq} \tag{4.18}$$

This is not the conductivity measured in a two-component system at stationary state, see Eq. (4.27) below. In the stationary state, internal energy and mass densities are independent of time. As a consequence, their fluxes are not only independent of time, but also independent of position. In the present example the total heat flux, J_q, and the mass flux, J_1, are constant

both with respect to time and position. The measurable heat flux $J'_q = J_q - H_1 J_1$ is not necessarily constant as a function of position, however, due to the variation of the enthalpy density with local temperature and molar densities.

The Soret effect is mass transport that takes place due to dT/dx. For a constant chemical potential the mass flux in the solvent frame of reference is given by Eq. (4.13) or

$$J_1 = l_{\mu q} \frac{\partial}{\partial x} \left(\frac{1}{T} \right) = -c_1 D_T \frac{\partial T}{\partial x} \tag{4.19}$$

where the *thermal diffusion coefficient*, D_T, is defined by[2]

$$D_T = \frac{l_{\mu q}}{c_1 (T)^2} \tag{4.20}$$

The ratio of the thermal diffusion coefficient and the interdiffusion coefficient is called the Soret coefficient, s_T. For the system in a stationary state such that $J_1 = 0$, the Soret coefficient can be expressed as the ratio of the concentration and the temperature gradients:

$$s_T \equiv -\left(\frac{\partial c_1 / \partial x}{c_1 \partial T / \partial x} \right)_{J=0} = \frac{D_T}{D_{1,2}} \tag{4.21}$$

By measuring the gradients in temperature and concentration, and the interdiffusion coefficient, one can calculate the thermal diffusion coefficient.

Heat transport due to a concentration gradient is called the *Dufour effect*. This effect is expressed by $l_{q\mu}$, and is the *reciprocal* of the Soret effect. The coefficient ratio

$$q^* = \left(\frac{J'_q}{J_1} \right)_{dT=0} = \frac{l_{q\mu}}{l_{\mu\mu}} \tag{4.22}$$

[2]Kuiken [24] used a different definition of the thermal diffusion coefficient, which is more appropriate in a multicomponent system where none of the components is present are excess.

is the *heat of transfer*. By using Eqs. (4.20) and (4.16), we can express the heat of transfer by the ratio of the thermal diffusion coefficient and the interdiffusion coefficient:

$$\begin{aligned} q^* &= \frac{c_1 D_T T}{D_{1,2}} \left(\frac{d\mu_{1,T}}{dc_1} \right) \\ &= s_T c_1 T \left(\frac{d\mu_{1,T}}{dc_1} \right) = s_T R T^2 \left[1 + \frac{\partial \ln \gamma_1}{\partial \ln c_1} \right] \end{aligned} \tag{4.23}$$

An experiment that gives the Soret coefficient, s_T, also gives the heat of transfer, q^*.

The Soret effect is known to damage materials that have their strength defined by small additives. For instance, depletion of chromium, molybdenum as well as of carbon, will weaken steels. A familiar example of the Soret effect can be observed at hot radiators in houses. There is convection, but also thermal diffusion. We see dust particles accumulate near the cold window, but not at the hot radiator. The Soret coefficient is normally positive for the light component and negative for the heavy component in a mixture. This explains that heavy components accumulate on cold sides, and light ones on the warm side. Holt et al. [50] studied the distribution of methane and decane under oil reservoir conditions using this. The Soret effect is larger in liquids than in gases. Some values are given in Table 4.2 [51].

The Soret coefficient in gases is usually small. Nevertheless, it has been used to separate isotopes, a difficult separation. Isotopes differ by their masses only (m_2 and m_1). Furry et al. [52] used the formula

$$s_T = \frac{0.35(m_2 - m_1)}{T(m_2 + m_1)}$$

to design separation columns for radioactive isotopes. Kempers formula [53] for the thermal diffusion factor is now well estab-

Table 4.2: Soret coefficients at 300 K for some binary mixtures. The mole fraction, $x_1 = c_1/c$, refers to the first-mentioned component.

System	x_1	T/K	p/bar	s_T/K^{-1}
Methane in propane	0.34	346	60800	0.042
Methane in cyclopentane	.0026	293	1	-0.016
i-butane in methylcyclopentane	0.5	293	1	-0.0096
Cyclohexane in benzene	0.5	293	1	-0.0063
Carbon dioxide in hydrogen	0.51	223	15	.00046

lished:

$$\alpha_T \equiv s_T T = \frac{V_1 V_2}{x_1 V_1 + x_2 V_2} \frac{\frac{H_2 - H_2^0}{V_2} - \frac{H_1 - H_1^0}{V_1}}{x_1 \left(\frac{\partial \mu_1}{\partial x_1}\right)_{p,T}} + \frac{RT\alpha^0}{x_1 \left(\frac{\partial \mu_1}{\partial x_1}\right)_{p,T}} \quad (4.24)$$

The first identity defines the thermal diffusion factor. The value α^0 can be calculated from kinetic theory. The partial molar enthalpies of the mixture (H_i) and of pure components (H_i^0), the partial molar volumes and the composition, and the thermodynamic factor (the derivative of the chemical potential with respect to composition) can all be determined from an equation of state of the fluid.

The heat transport due to mass transport is:

$$J_q' = -\frac{1}{T^2}\left(l_{qq} - \frac{l_{q\mu} l_{\mu q}}{l_{\mu\mu}}\right)\frac{\partial T}{\partial x} + q^* J \quad (4.25)$$

The part of the heat flux that contains q^*, changes direction with J, compare Eq. (4.10). The heat transport due to the Dufour effect is reversible in this sense.

Fourier's law

$$J_q' = -\lambda \frac{\partial T}{\partial x} \quad (4.26)$$

can also be used to identify the effective thermal conductivity for zero mass flux, λ. We obtain the heat flux for these conditions from Eq. (4.25) as

$$\lambda = -\left[\frac{J_q'}{(dT/dx)}\right]_{J=0} = \frac{1}{T^2}\left(l_{qq} - \frac{l_{q\mu}l_{\mu q}}{l_{\mu\mu}}\right) \tag{4.27}$$

The thermal conductivity λ can be found from plots like shown

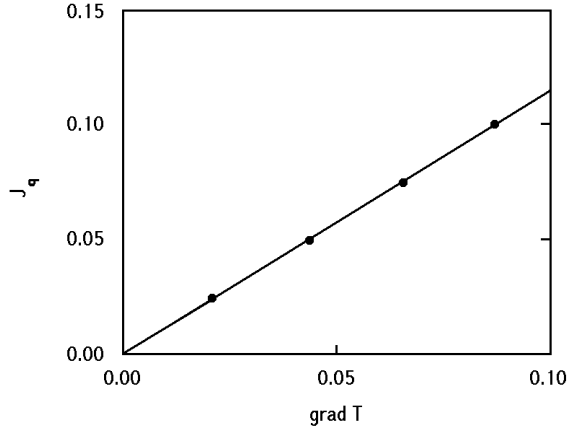

Figure 4.1: The dimensionless stationary state heat flux as a function of the dimensionless temperature gradient of a binary mixture obtained by molecular dynamics simulations [49]. The temperature gradient is of the order 10^8 K/m.

in Fig. 4.1. It is generally found that λ rather than $(l_{qq} - l_{q\mu}l_{\mu q}/l_{\mu\mu})$ is constant over a wide range of temperatures. By comparing Eq. (4.18) to Eq. (4.27), we find that λ is smaller than λ_μ. A temperature difference across a homogeneous system, leads initially to a heat flux and thus a particle flux. The entropy production is initially proportional to λ_μ, when $\partial T/\partial x$ is constant and $\partial\mu_{1,T}/\partial x = 0$. The particle flux changes the chemical potential gradient until, in the resulting stationary

state, the particle flux becomes zero. The entropy production becomes then proportional to λ. The entropy production in the stationary state is therefore smaller than in the initial state, cf. Eq. (4.11).

From the positive nature of the entropy production, it follows that the diffusion coefficient and the thermal conductivity are positive, cf. Eqs. (4.7)), (4.16) and (4.27). The thermal diffusion coefficient and the heat of transfer can be positive or negative. From Eq. (4.8) we have an upper bound on the absolute value of the thermal diffusion coefficient.

$$(D_T)^2 \leqslant D_1 \lambda_\mu \left((c_1)^2 \, T \frac{d\mu_{1T}}{dc_1} \right)^{-1} \tag{4.28}$$

Exercise 4.2.2 *Express* $-\frac{1}{T^2}\left(\partial T/\partial x\right)$ *and* $-\frac{1}{T}\partial\mu_{1,T}/\partial x$ *in terms of* J'_q *and* J.

- **Solution:** By inverting Eqs. (4.13) we have:

$$-\frac{1}{T^2}\frac{\partial T}{\partial x} = r_{qq} J'_q + r_{q\mu} J \quad \text{and} \quad -\frac{1}{T}\frac{\partial \mu_{1,T}}{\partial x} = r_{\mu q} J'_q + r_{\mu\mu} J$$

with

$$r_{qq} = \frac{l_{\mu\mu}}{l_{qq} l_{\mu\mu} - l_{\mu q} l_{q\mu}}, \quad r_{\mu q} = r_{q\mu} = \frac{-l_{q\mu}}{l_{qq} l_{\mu\mu} - l_{\mu q} l_{q\mu}},$$
$$r_{\mu\mu} = \frac{l_{qq}}{l_{qq} l_{\mu\mu} - l_{\mu q} l_{q\mu}}$$

Exercise 4.2.3 *Consider a room with air and a trace (10ppm) of perfume. Near the wall, the temperature is* $20^o C$ *(*$x = 0$*). Near the window at a distance of 4 m, the temperature is* $10^o C$*. The heat of transfer of perfume in air is* $q^* = 700$ *J/mol. The*

thermal conductivity is constant. The room has heat leakage only to wall with the window and there is no convection in the room. Calculate the concentration difference of perfume between the window and the wall in the stationary state.

- **Solution:** In the stationary state there is no perfume flux. This implies that, cf. Eqs. (4.25)) and (4.27)), $J'_q = -\lambda dT/dx$. Furthermore it follows from Eqs. (4.13)) and (4.22) that $d\mu_T/dx = -(q^*/T)dT/dx$. Because of the absence of perfume flux, the heat current is constant so that $T(x) = 20 - 2.5x$. This results in $d\mu_T/dx = (RT/c)dc/dx = 2.5q^*/T$, where the temperature is in K. The concentration gradient $dc/dx = cq^*/RT^2(dT/dx) \simeq 0.025$. This gives a concentration of 0.1 ppm higher at the window than close to the wall. Perfume concentrates at the cold side, it is heavier than air.

4.3 Transport of heat and charge

Coupled transports of heat and charge take place in semiconducting devices. To illustrate the coupling between fluxes of heat and charge, consider a piece of lead, which is connected to a potentiometer via molybdenum wires

$$\text{Mo} \mid \text{Pb} \mid \text{Mo} \tag{4.29}$$

The joints are kept at different temperatures. The temperature changes continuously in the homogeneous phases and jumps at the surfaces. The electric current is defined as positive when positive charges are moving from left to right in the system. Such a system can be used to generate electric power from a waste heat source (the Seebeck effect). It can also be used for cooling purposes (the Peltier effect).

The entropy production for the homogeneous phases is obtained from Eq. (3.15). In this case, it reduces to

$$\sigma = -J'_q \frac{1}{T^2}\frac{\partial T}{\partial x} - j\frac{1}{T}\frac{\partial \phi}{\partial x} \tag{4.30}$$

The flux equations are

$$\begin{aligned} J'_q &= -L_{qq}\frac{1}{T^2}\frac{\partial T}{\partial x} - L_{q\phi}\frac{1}{T}\frac{\partial \phi}{\partial x} \\ j &= -L_{\phi q}\frac{1}{T^2}\frac{\partial T}{\partial x} - L_{\phi\phi}\frac{1}{T}\frac{\partial \phi}{\partial x} \end{aligned} \tag{4.31}$$

The first flux equation says that heat can be transported by means of an electric field. According to the last equation we can use a temperature gradient to generate a potential difference and an electric current.

In order to define the coefficients, consider first isothermal conditions. The electric current density is:

$$j = -L_{\phi\phi}\frac{1}{T}\frac{\partial \phi}{\partial x} \tag{4.32}$$

By equating this to Ohm's law $j = -\kappa \partial\phi/\partial x$, we identify the electric conductivity

$$\kappa = \frac{L_{\phi\phi}}{T} \tag{4.33}$$

The *Peltier coefficient*, π, is defined as the heat transferred *reversibly* with the electric current (cf. Remark 4.2) at constant temperature:

$$\pi \equiv F\left(\frac{J'_q}{j}\right)_{dT=0} = F\frac{L_{q\phi}}{L_{\phi\phi}} \tag{4.34}$$

The coupling between heat and charge transport gives rise to a potential gradient, when there is a temperature gradient. From Eq. (4.31), we obtain

$$\frac{\partial \phi}{\partial x} = -\frac{L_{\phi q}}{L_{\phi\phi}}\frac{1}{T}\frac{\partial T}{\partial x} - j\frac{T}{L_{\phi\phi}} \tag{4.35}$$

The ratio $d\phi/dT$ is called the Seebeck coefficient. The Peltier and Seebeck coefficients are related by the Onsager relations:

$$F\left(\frac{d\phi}{dT}\right)_{j=0} = -\frac{\pi}{T} \tag{4.36}$$

The Peltier coefficient can be interpreted as entropy that is *transported* by the charge carrier. For the molybdenum and lead phases, we have

$$\pi_{\mathrm{i}} \equiv F\left(\frac{J_q'^{\mathrm{i}}}{j}\right)_{dT=0} = TS^*_{\mathrm{e}^-,\mathrm{i}} \tag{4.37}$$

where i stands for Mo or Pb, respectively, and $S^*_{\mathrm{e}^-,\mathrm{i}}$ is the transported entropy.

The transported entropy is positive when entropy is transported along with positive charges. In metals, charge is mostly carried by electrons. Electronic conductors have transported entropies between -1 and -20 J/K mol [54]. Some transition metals like Mo, Cr and W have negative transported entropies, while Pb has a positive value. The maximum value for Mo is $S^*_{\mathrm{e}^-,\mathrm{Mo}} = -17$ J/K mol at 900 K [54]. At the same temperature, $S^*_{\mathrm{e}^-,\mathrm{Pb}} = 5$ J/K mol. The transported entropy in Eq. (4.37) can therefore be positive or negative. Transported entropies are kinetic, not thermodynamic properties.

Remark 4.4 *While the thermodynamic entropy is an absolute quantity, the transported entropy of a charge carrier is not. It depends on a choice of a reference compound, since only the combination of transported entropies enter the expression for the electromotive force. The transported entropy of electrons in lead is the commonly used reference value. This means that the entropy flux for a material depends on this reference. The net heat effect at the surface is absolute, however.*

By eliminating the potential gradient in Eq. (4.31), we can write the heat flux on the form given by Eq. (4.10):

$$J'_q = -\lambda \frac{\partial T}{\partial x} + \frac{\pi}{F} j \tag{4.38}$$

where

$$\lambda \equiv -\left(\frac{J'_q}{\partial T / \partial x} \right)_{j=0} = \frac{1}{T^2} \left(L_{qq} - \frac{L_{\phi q} L_{q\phi}}{L_{\phi\phi}} \right) \tag{4.39}$$

The factor λ is the thermal conductivity when the electric current is zero, compare Eq. (4.27). Equation (4.38) expresses that a heat flux may arise due to not only a temperature gradient but also due to an electric current. This effect has been used to construct thermoelectric cooling devices. Cooling occurs particularly at junctions, when the transported entropy changes more than in the homogeneous conductor. In the example above, there is a Peltier effect at 900 K of - 10.8 kJ/mol. In the presence of an electric current of 1 A/m^{2}s, the cooling effect is 0.11 J/m^2 s.

The heat flux due to the electric current reverses direction by reversing the current. In this manner we can turn a cooling device into a heating device.

Exercise 4.3.1 *Consider the example described in this subsection. When we let an electric current of 10^4 A/m^2 run through the lead, entropy will be transported. If the system is thermally insulated, a temperature gradient will build up. Calculate the stationary temperature difference over a distance of 2 m for an insulated system. Use a stationary thermal conductivity of 5 J/K m s and an average temperature of 300 K. The transported entropy is 5 J/K mol.*

- **Solution:** Eq. (4.38) gives the heat flux in terms of the

temperature gradient and the electric current

$$J'_q = -\lambda_{\mathrm{Pb}} \frac{\partial T}{\partial x} + \frac{\pi_{\mathrm{Pb}}}{F} j$$

In the stationary state, the heat flux is zero and it follows that $dT/dx = \pi_{\mathrm{Pb}} j / F\lambda_{\mathrm{Pb}}$. Substituting the values of all the coefficients gives $dT/dx = 3$ K/m. Over a distance of 2 m this gives a temperature increase of 6 K.

The ends of the left (l) and right (r) molybdenum wires have the temperature of the potentiometer, $T^{\mathrm{l,o}} = T^{\mathrm{r,o}} = T^{\mathrm{o}}$. We neglect the temperature dependence of the transported entropies and calculate the contributions to the electromotive force. The lead conductor gives

$$(\Delta_{\mathrm{m}}\phi)_{j=0} = \frac{1}{F} S^*_{\mathrm{e^-,Pb}} \left(T^{\mathrm{m,r}} - T^{\mathrm{m,l}}\right) \tag{4.40}$$

where m denoted the homogeneous lead phase. The left and right molybdenum wires give

$$\begin{aligned}(\Delta_{\mathrm{l}}\phi)_{j=0} &= \frac{1}{F} S^*_{\mathrm{e^-,Mo}} \left(T^{\mathrm{l,m}} - T^{\mathrm{o}}\right) \\ (\Delta_{\mathrm{r}}\phi)_{j=0} &= \frac{1}{F} S^*_{\mathrm{e^-,Mo}} \left(T^{\mathrm{o}} - T^{\mathrm{r,m}}\right)\end{aligned} \tag{4.41}$$

With $T^{\mathrm{l,m}} = T^{\mathrm{m,l}}$ and $T^{\mathrm{m,r}} = T^{\mathrm{r,m}}$, the sum is:

$$(\Delta\phi)_{j=0} = \frac{1}{F}(S^*_{\mathrm{e^-,Pb}} - S^*_{\mathrm{e^-,Mo}}) \left(T^{\mathrm{m,r}} - T^{\mathrm{m,l}}\right) \tag{4.42}$$

This sum is the electromotive force of the system. The Seebeck coefficient becomes:

$$\left(\frac{\Delta\phi}{T^{\mathrm{m,r}} - T^{\mathrm{m,l}}}\right)_{j=o} = \frac{1}{F}(S^*_{\mathrm{e^-,Pb}} - S^*_{\mathrm{e^-,Mo}}) \tag{4.43}$$

The Seebeck coefficient is frequently used to determine transported entropies. With a typical value for the Seebeck coefficient

of 20 J/K mol, a temperature difference of 100 K will generate a potential difference of 20 mV. This is a small effect, but it can be enlarged by coupling single elements in series. In this manner one can make use of industrial waste heat.

4.4 Transport of mass and charge

Coupled transports of mass and charge take place in all kinds of electrochemical cells, including in biological systems. Batteries and fuel cells generate electric potentials with order of magnitude 1 V, by invoking chemical reactions between the components of the cell. The coupled transports of mass and charge in concentration cells are simpler. In such cells, there is no spontaneous chemical reaction, and the electric potential is generated by changes in the electrolyte. To illustrate the principles, take the isothermal concentration cell:

$$\mathrm{Ag(s)} \mid \mathrm{AgNO_3}(c_1) \parallel \mathrm{AgNO_3}(c_2) \mid \mathrm{Ag(s)}$$

The electrodes are made of pure silver. The electrolyte is $\mathrm{AgNO_3}$ in water, and there is a varying concentration of salt across the cell, see Fig. 4.2.

Consider the electrolyte. The entropy production Eq. (3.15) is

$$\sigma = J_{\mathrm{AgNO_3}} \left(-\frac{1}{T} \frac{\partial \mu_{\mathrm{AgNO_3}}}{\partial x} \right) + j \left(-\frac{1}{T} \frac{\partial \phi}{\partial x} \right) \tag{4.44}$$

The temperature is constant throughout the system, and we have dropped subscript T in $\mu_{\mathrm{AgNO_3}}$. The flux equations are:

$$\begin{aligned} J_{\mathrm{AgNO_3}} &= -L_{\mu\mu} \frac{1}{T} \frac{\partial}{\partial x} \mu_{\mathrm{AgNO_3}} - L_{\mu\phi} \frac{1}{T} \frac{\partial \phi}{\partial x} \\ j &= -L_{\phi\mu} \frac{1}{T} \frac{\partial}{\partial x} \mu_{\mathrm{AgNO_3}} - L_{\phi\phi} \frac{1}{T} \frac{\partial \phi}{\partial x} \end{aligned} \tag{4.45}$$

The frame of reference for the mass flux is the electrode surface. In this frame of reference, water is at rest. The solution is

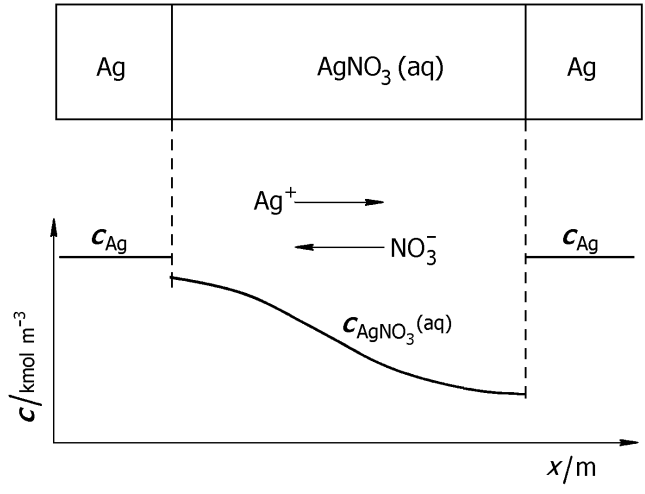

Figure 4.2: An isothermal electrochemical cell with a concentration gradient.

electroneutral, so that

$$c_{\mathrm{AgNO_3}} = c_{\mathrm{Ag^+}} = c_{\mathrm{NO_3^-}} \tag{4.46}$$

The chemical potential of $\mathrm{AgNO_3}$ is

$$\mu_{\mathrm{AgNO_3}} = \mu_{\mathrm{Ag^+}} + \mu_{\mathrm{NO_3^-}} = \mu^{\circ}_{\mathrm{AgNO_3}} + 2RT \ln\left(c_{\mathrm{AgNO_3}}\gamma_{\pm}\right) \tag{4.47}$$

where $\mu_{\mathrm{Ag^+}}$ and $\mu_{\mathrm{NO_3^-}}$ are the chemical potentials of the ions, $\gamma_{\pm}$ is the mean activity coefficient of the ions, equal for both ions, and $\mu^0_{\mathrm{AgNO_3}}$ is the chemical potential of the salt in the standard state, see Appendix A.2. The electric conductivity for a uniform distribution of salt is

$$\kappa \equiv \frac{L_{\phi\phi}}{T} \tag{4.48}$$

The coefficient $L_{\mu\mu}$ describes transport of $\mathrm{AgNO_3}$ when the cell is short-circuited ($\Delta\phi = 0$). By eliminating the electric potential

gradient with the help of Eq. (4.45), we obtain the salt flux

$$J_{\mathrm{AgNO_3}} = -\frac{1}{T}\left(L_{\mu\mu} - \frac{L_{\phi\mu}L_{\mu\phi}}{L_{\phi\phi}}\right)\frac{\partial}{\partial x}\mu_{\mathrm{AgNO_3}} + \frac{L_{\mu\phi}}{L_{\phi\phi}}j \qquad (4.49)$$

The diffusion coefficient from Fick's law, for zero electric current, is given by:

$$\begin{aligned} D_{\mathrm{AgNO_3}} &\equiv -\left(\frac{J_{\mathrm{AgNO_3}}}{\partial c_{\mathrm{AgNO_3}}/\partial x}\right)_{j=0} = \frac{1}{T}\left(L_{\mu\mu} - \frac{L_{\phi\mu}L_{\mu\phi}}{L_{\phi\phi}}\right)\frac{d\mu_{\mathrm{AgNO_3}}}{dc_{\mathrm{AgNO_3}}} \\ &= \left(L_{\mu\mu} - \frac{L_{\phi\mu}L_{\mu\phi}}{L_{\phi\phi}}\right)\frac{2R}{c_{\mathrm{AgNO_3}}}\left[1 + \frac{d\ln\gamma_{\pm}}{d\ln c_{\mathrm{AgNO_3}}}\right]^{-1} \end{aligned} \qquad (4.50)$$

The *transference coefficient* is defined as the ratio of the flux of salt and the electric current density at uniform composition:

$$t_{\mathrm{AgNO_3}} = F\left(\frac{J_{\mathrm{AgNO_3}}}{j}\right)_{d\mu_{\mathrm{AgNO_3}}=0} = F\frac{L_{\mu\phi}}{L_{\phi\phi}} \qquad (4.51)$$

Using these coefficients, the salt flux of Eq. (4.49) can be written as

$$J_{\mathrm{AgNO_3}} = -D_{\mathrm{AgNO_3}}\frac{\partial}{\partial x}c_{\mathrm{AgNO_3}} + \frac{t_{\mathrm{AgNO_3}}}{F}j \qquad (4.52)$$

Equation (4.52) expresses that diffusion and charge transfer are superimposed on one another. We described determination of diffusion coefficients in Section 4.2. We give a method to estimate D of electrolytes in Section 4.4.1.

The transference coefficient can be found in a *Hittorf* experiment, see e.g. [46]. In this experiment, an electric current is passing a cell of a uniform composition. A differential amount of salt will accumulate on one of the sides, and can be taken

for analysis to determine the number of moles transported per moles of electric charge that is passing. The anode produces one mole of silver, and the cathode consumes one mole, per Faraday electrons passing the outer circuit. These changes plus the transport in the electrolyte, lead to a change in composition on both sides. The total flux of silver nitrate is given by Eq. (4.52). The equation says that in order to find $t_{\mathrm{AgNO_3}}$ one must correct for the first term; diffusion. This can be done by measuring the concentration for small values of j for a decreasing period of time and extrapolating to a zero period of time. The transference coefficient can be related to the transport number of one of the ions. The transport number is defined as the fraction of the electric current carried by the ion:

$$\begin{aligned} t_{\mathrm{Ag^+}} &= F\left(\frac{J_{\mathrm{Ag^+}}}{j}\right)_{d\mu_{\mathrm{AgNO_3}}=0} \\ t_{\mathrm{NO_3^-}} &= -F\left(\frac{J_{\mathrm{NO_3^-}}}{j}\right)_{d\mu_{\mathrm{AgNO_3}}=0} \end{aligned} \tag{4.53}$$

The two ions move in opposite directions, but together they are responsible for the total electric current, so that:

$$t_{\mathrm{Ag^+}} + t_{\mathrm{NO_3^-}} = 1 \tag{4.54}$$

The electrodes of the present system are both reversible to $\mathrm{Ag^+}$. The $\mathrm{NO_3^-}$-ions do not leave the electrolyte, so the flux of the $\mathrm{Ag^+}$ ions is therefore equal to j/F plus the salt flux, while the flux of $\mathrm{NO_3^-}$- ions is equal to minus the salt flux. The flux of $\mathrm{AgNO_3}$ can therefore be defined by the flux of $\mathrm{NO_3^-}$ ions [29]. As a consequence,

$$t_{\mathrm{AgNO_3}} = -t_{\mathrm{NO_3^-}} = -1 + t_{\mathrm{Ag^+}} \tag{4.55}$$

Remark 4.5 *The transference coefficient for the salt in the electrolyte are determined by the ions for which the reactions at the*

electrode surfaces are reversible. They are therefore not a material property of the electrolyte alone.

The contribution from the electrolyte to the cell *potential* is obtained by solving Eq. (4.45), using $L_{\phi\mu} = L_{\mu\phi}$

$$\Delta\phi = -\frac{L_{\phi\mu}}{L_{\phi\phi}} \int_1^2 d\mu_{\mathrm{AgNO_3}} - \frac{jd}{\kappa} = \frac{2t_{\mathrm{NO_3^-}}}{F} \int_1^2 RTd \ln c_{\mathrm{AgNO_3}} - \frac{jd}{\kappa} \tag{4.56}$$

where d is the electrolyte thickness. This is the cell potential of a concentration cell (a cell with identical electrodes). Again, we see that the coupling coefficient provides the electric work. The potential at $j = 0$ is the reversible chemical work done by the system on expense of a lowering of its internal energy, cf. Eq. (4.11). This can be seen by introducing Eq. (4.45) into Eq. (4.44) and comparing compensating terms.[3]

The expression can be used to find $t_{\mathrm{AgNO_3}}$ when $j = 0$ and the chemical potential in the two electrode compartments are known. This gives probably a more accurate determination than that obtainable from the Hittorf experiment, since the electric potential can be measured with a higher accuracy than concentration changes can.

A power plant that uses an electrolyte concentration difference to give electric current from Eq. (4.56) is illustrated in Fig. 4.3. The plant, called a saline power plant, operates by reverse electrodialysis. Sea water and fresh water are fed into alternating compartments which are separated by ion-exchange membranes. The membranes alternate between anion- and cation-exchange membranes. One unit cell consists of a salt water compartment, an anion-exchange membrane, a fresh water compartment, a

[3]The electromotive force of the concentration cell is related to reversible phenomena only, and the common name of this potential, the "diffusion potential", is thus misleading.

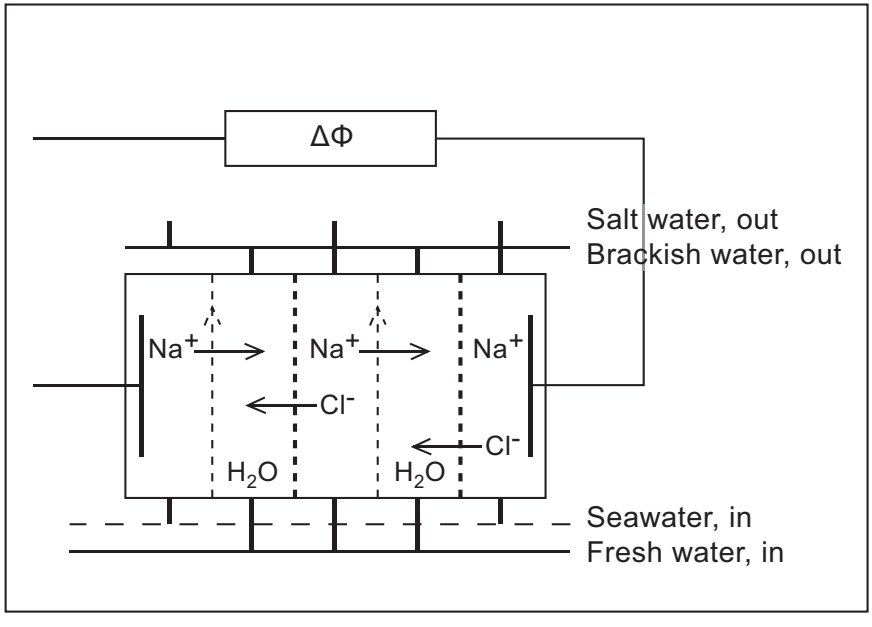

Figure 4.3: The principle of a salt power plant that uses reverse electro-dialysis. The figure shows two unit cells in series. The concentration difference of sodium chloride, between sea water and the fresh water, drives an electric current and creates an electric power.

cation-exchange membrane and a salt water compartment. The gradient in chemical potential of salt drives chloride ions through the anion-exchange membrane and sodium ions through the cation-exchange membrane. The transport numbers for the ions are near unity in these membranes. The electric field that arises, causes an electric current in the external circuit.

Diffusion of salt is prevented by the ion-exchange membranes. Salt may leak into the fresh water compartment and reduce the potential difference. But some salt is required also there to give an acceptable ohmic resistance in this compartment.

By introducing a transport number equal to one into Eq. (4.56), we obtain the electromotive force across a cation exchange membrane

$$(\Delta\phi)_{j=0} = -\frac{2RT}{F}\ln\frac{c_{\mathrm{NaCl}(2)}}{c_{\mathrm{NaCl}(1)}} \tag{4.57}$$

A salt concentration ratio of 10:1 at 300 K gives −230 mV from this formula, when the electrodes are reversible to chloride ion. The low value gives a reason to stack unit cells like indicated in the figure. The electric potential of the plant is proportional to the number of unit cells. The figure shows two units. Power densities around 4 W/m^2 can be expected.

4.4.1 The mobility model

A common model for the Onsager coefficients of an electrolytic solution uses the mobilities of the ions. In the example above the mobilities are $u_{\mathrm{Ag^+}}$ and $u_{\mathrm{NO_3^-}}$. The assumption is now that the chemical potential gradient is equally effective as a force for transport as the electric potential gradient (Nernst-Einstein's assumption). In terms of symbols used here, this gives $FL_{\mu\mu} = -L_{\mu\phi}$. The mobility of an ion is defined as the ratio between the stationary velocity of the ion in a constant electric field, divided by the electric field [46]. For the present example, we find

$$\begin{aligned} L_{\mu\mu} &= \frac{T}{F}c_{\mathrm{NO_3^-}}u_{\mathrm{NO_3^-}}, \qquad L_{\phi\mu} = L^{\mathrm{e}}_{\mu\phi} = -Tc_{\mathrm{NO_3^-}}u_{\mathrm{NO_3^-}} \\ L_{\phi\phi} &= FT\left(c^{\mathrm{e}}_{\mathrm{NO_3^-}}u_{\mathrm{NO_3^-}} + c_{\mathrm{Ag^+}}u_{\mathrm{Ag^+}}\right) \end{aligned} \tag{4.58}$$

Together with Eq. (4.46), the electric conductivity becomes

$$\kappa = Fc_{\mathrm{AgNO_3}}\left(u_{\mathrm{NO_3^-}} + u_{\mathrm{Ag^+}}\right) \tag{4.59}$$

and the transference coefficient for the salt is, cf. Eq. (4.51),

$$t_{\mathrm{AgNO_3}} = -\frac{u_{\mathrm{NO_3^-}}}{u_{\mathrm{NO_3^-}} + u_{\mathrm{Ag^+}}} \tag{4.60}$$

Table 4.3: Transference numbers and conductivities at infinite dilution at 298 K according to [55].

Salt, MX	t_{M^+}	(κ_{MX}/c_{MX}) $/10^2 \text{ohm}^{-1}\text{mol}^{-1}\text{m}^2$	u_{M^+} $/10^8 \text{m}^2\text{s}^{-1}\text{V}^{-1}$
HCl	0.8209	426.16	36.23
LiCl	0.3360	114.99	73.52
NaCl	0.3870	126.50	5.19
KCl	0.4905	149.85	7.62
KBr	0.4846	151.67	not available

The diffusion coefficient for the salt becomes

$$D_{AgNO_3} = \frac{2RTu_{Ag^+}u_{NO_3^-}}{F(u_{Ag^+} + u_{NO_3^-})} \tag{4.61}$$

Experimental data show that the diffusion coefficient is weakly dependent on the concentration. This can be explained by the mobility ratio being weakly dependent on the concentration of the salt. Some numbers from Ref. [55] are given in Table 4.3. The above equations in terms of the ionic mobilities, even though derived for an ideal mixture, have a rather large range of validity.

4.5 Transport of volume and charge

A membrane can sustain a pressure difference. Also this transport can lead to charge transport and work generation, when a driving force for volume transport is available. Consider therefore the transport of water across a cation exchange membrane by a pressure difference Δp, in the cell

$$(\text{Pt})\,\text{H}_2(g),\ \text{HCl}(c_1)|\text{HM}|\text{HCl}(c_2),\ \text{H}_2(g)\,(\text{Pt}) \tag{4.62}$$

The membrane HM is a proton conductor, for instance the Nafion membrane that is used in fuel cells. Pt serves as electron car-

rier. Hydrogen gas disproportionates on the left hand side giving protons in the membrane and electrons in the metal. The membrane needs water to conduct electricity well. Protons react on the right hand side to form hydrogen gas. The entropy production of the membrane is:

$$\sigma = J_{\mathrm{w}} \left(-\frac{1}{T} \frac{\partial \mu_{\mathrm{w}}}{\partial x} \right) + j \left(-\frac{1}{T} \frac{\partial \phi}{\partial x} \right) \tag{4.63}$$

The proton concentration in the membrane is everywhere fixed by the cation sites of the membrane, but the water chemical potential can vary in a pressure gradient. The flux of protons is identical to the electric current j and is no independent flux. The temperature is assumed constant so again we drop subscript T in μ_{w}. The flux equations are:

$$\begin{aligned} J_{\mathrm{w}} &= -L_{\mu\mu} \frac{1}{T} \frac{\partial}{\partial x} \mu_{\mathrm{w}} - L_{\mu\phi} \frac{1}{T} \frac{\partial \phi}{\partial x} \\ j &= -L_{\phi\mu} \frac{1}{T} \frac{\partial}{\partial x} \mu_{\mathrm{w}} - L_{\phi\phi} \frac{1}{T} \frac{\partial \phi}{\partial x} \end{aligned} \tag{4.64}$$

The frame of reference for water transport is the membrane. The electric conductivity of the membrane is

$$\kappa \equiv \frac{L_{\phi\phi}}{T} \tag{4.65}$$

The coefficient $L_{\mu\mu}$ describes transport of water when the cell is short-circuited ($\Delta\phi = 0$). Following the same procedure as in the preceding Section, Eq. (4.52), we arrive at an expression for the water flux

$$J_{\mathrm{w}} = -D_{\mathrm{w}} \frac{\partial}{\partial x} c_{\mathrm{w}} + \frac{t_{\mathrm{w}}}{F} j \tag{4.66}$$

where D_{w} is the diffusion coefficient of water in the membrane, and the transference coefficient of water is defined as:

$$t_{\mathrm{w}} = F \left(\frac{J_{\mathrm{w}}}{j} \right)_{d\mu_{\mathrm{w}}=0} = F \frac{L_{\mu\phi}}{L_{\phi\phi}} \tag{4.67}$$

The transference coefficient can be found by measuring the water flux or the volume flow caused by electric current through the membrane, or by measuring the electric potential difference with different water pressures on the two sides [56]. The relation between two experiments is given by the Onsager relation, leading to

$$\left(\frac{J_{\mathrm{w}}}{j}\right)_{d\mu_{\mathrm{w}}=0} = -\left(\frac{\Delta\phi}{\Delta P}\right)_{j=0} \tag{4.68}$$

This is known as the Saxén relation. Volume flow by electric current is called electro-osmosis, while an electric potential generated by pressure difference is called a streaming potential.

When the water concentration is the same on the two sides, but a hydrostatic pressure difference exists, $d\mu_{\mathrm{w}} = V_{\mathrm{w}}dp$, where V_{w} is the partial molar volume of water. We solve Eq. (4.64) for $j = 0$, using $L_{\phi\mu} = L_{\mu\phi}$ and obtain:

$$\Delta\phi = -\int_1^2 \frac{L_{\phi\mu}}{L_{\phi\phi}} d\mu_{\mathrm{w}} = -\frac{t_{\mathrm{w}}}{F}\int_1^2 d\mu_{\mathrm{w}} = -\frac{t_{\mathrm{w}}}{F}V_{\mathrm{w}}\Delta p \tag{4.69}$$

The pressure driven flow is able to generate an electric potential through the coupling coefficient t_{w}. With liquid water on the sides of the membrane, $t_{\mathrm{w}} = 2.6$ [56]. A pressure difference of 1 bar then generates an electromotive force of -9 mV at 300 K. This potential is much smaller than for a unit cell of a saline power plant. A pressure difference is less effective than a concentration difference.

Membrane transport phenomena were described at large by Katchalsky and Curran, and Førland and coworkers [15, 18]. In the example above, we did not consider membrane surface effects. If these are important, for instance when the absorption and desorption enthalpies are large, one can consider the surface regions as additional thermodynamic systems. The theory for this was given by Kjelstrup and Bedeaux [29].

4.6 Concluding remarks

In this Chapter we have studied the coupling between pairs of processes, in total four examples. We have seen that the entropy production becomes smaller in the presence of coupling, and that coupling coefficients are central for extraction of work. Real systems have more than a pair of coupled transport processes. In polymer electrolyte fuel cells, for instance, there is coupled transport of water, electric charge (protons) and heat. The same systematic procedure can still be used to to describe these processes, see [57].

The available work, which was examined here for coupled transports of heat and charge, mass and charge and volume and charge, is smaller than work obtained in combustion engines, batteries and fuel cells. Work generated in the absence of chemical reactions is generally smaller. It may nevertheless become important, in a systematic effort to reduce excess entropy production beyond state-of-the art today. Better systems than those presented here should be looked for.

The efficiency of energy converting processes is central in engineering and in Chapter 9 we study how the excess entropy production can be reduced by changing the way some process units are operated. The coupling effects presented in this Chapter, could be used in combination with the procedure outlined in Chapter 9.

This page intentionally left blank

Chapter 5

Non-isothermal multi-component diffusion

Maxwell-Stefan equations were derived before Onsager established non-equilibrium thermodynamics. The equations are important, because they place all components on the same footing, and contain a diffusion coefficient which for homogeneous fluids is relatively constant. We show how the equations are compatible with non-equilibrium thermodynamics and give rules of transformations between alternatives frames of reference for transport.

Diffusion takes place in all chemical mixtures. Diffusion is often rate-limiting for processes that occur in nature and in industry, and it is therefore of interest to have a good description of diffusion, in isothermal as well as in nonisothermal systems. The simplest equation that describes diffusion is Fick's law, cf. Eq. (2.2). Very often there is an effect on the diffusion of one component due to concentration gradients of other components. There is, in other words, coupling of the diffusion fluxes. Such coupling effects are most efficiently described using the Maxwell-Stefan

equations. In this Chapter we will explain how the Maxwell-Stefan equations are obtained in the context of non-equilibrium thermodynamics and also how they are related to alternative descriptions of multi-component diffusion.

5.1 Isothermal diffusion

Consider an isothermal and isobaric three-component bulk mixture. For an elegant discussion of the more general case when the system is neither isothermal nor isobaric, and when the system contains an arbitrary number of components, we refer to the monograph by Kuiken [24] and to the review by Krishna and Wesselingh [35]. The entropy production in the present simple case is

$$\begin{aligned}\sigma &= J_{\mathrm{A}}\left(-\frac{1}{T}\frac{d\mu_{\mathrm{A}}}{dx}\right) + J_{\mathrm{B}}\left(-\frac{1}{T}\frac{d\mu_{\mathrm{B}}}{dx}\right) + J_{\mathrm{C}}\left(-\frac{1}{T}\frac{d\mu_{\mathrm{C}}}{dx}\right)\\ &= \mathrm{v}_{\mathrm{A}}\left(-\frac{c_{\mathrm{A}}}{T}\frac{d\mu_{\mathrm{A}}}{dx}\right) + \mathrm{v}_{\mathrm{B}}\left(-\frac{c_{\mathrm{B}}}{T}\frac{d\mu_{\mathrm{B}}}{dx}\right) + \mathrm{v}_{\mathrm{C}}\left(-\frac{c_{\mathrm{C}}}{T}\frac{d\mu_{\mathrm{C}}}{dx}\right) \quad (5.1)\end{aligned}$$

where the volumetric velocity of component i is defined by $\mathrm{v}_i \equiv J_i/c_i$. The phenomenological equations for the thermodynamic forces can now be written as

$$\begin{aligned}-\frac{c_{\mathrm{A}}}{T}\frac{d\mu_{\mathrm{A}}}{dx} &= r_{\mathrm{AA}}c_{\mathrm{A}}c_{\mathrm{A}}\mathrm{v}_{\mathrm{A}} + r_{\mathrm{AB}}c_{\mathrm{A}}c_{\mathrm{B}}\mathrm{v}_{\mathrm{B}} + r_{\mathrm{AC}}c_{\mathrm{A}}c_{\mathrm{C}}\mathrm{v}_{\mathrm{C}}\\ -\frac{c_{\mathrm{B}}}{T}\frac{d\mu_{\mathrm{B}}}{dx} &= r_{\mathrm{BA}}c_{\mathrm{B}}c_{\mathrm{A}}\mathrm{v}_{\mathrm{A}} + r_{\mathrm{BB}}c_{\mathrm{B}}c_{\mathrm{B}}\mathrm{v}_{\mathrm{B}} + r_{\mathrm{BC}}c_{\mathrm{B}}c_{\mathrm{C}}\mathrm{v}_{\mathrm{C}}\\ -\frac{c_{\mathrm{C}}}{T}\frac{d\mu_{\mathrm{C}}}{dx} &= r_{\mathrm{CA}}c_{\mathrm{C}}c_{\mathrm{A}}\mathrm{v}_{\mathrm{A}} + r_{\mathrm{CB}}c_{\mathrm{C}}c_{\mathrm{B}}\mathrm{v}_{\mathrm{B}} + r_{\mathrm{CC}}c_{\mathrm{C}}c_{\mathrm{C}}\mathrm{v}_{\mathrm{C}} \quad (5.2)\end{aligned}$$

The Onsager relations apply

$$r_{\mathrm{AB}} = r_{\mathrm{BA}}, \quad r_{\mathrm{AC}} = r_{\mathrm{CA}}, \quad r_{\mathrm{BC}} = r_{\mathrm{CB}} \quad (5.3)$$

According to Gibbs-Duhem's equation, the sum of the terms on the left hand side of these equations is zero

$$c_{\mathrm{A}}\frac{d\mu_{\mathrm{A}}}{dx}+c_{\mathrm{B}}\frac{d\mu_{\mathrm{B}}}{dx}+c_{\mathrm{C}}\frac{d\mu_{\mathrm{C}}}{dx}=0 \tag{5.4}$$

Only two of the forces are therefore independent. As this is true for arbitrary velocities of the components, it follows that the resistivities in the matrix are dependent, and satisfy

$$\begin{aligned}
r_{\mathrm{AA}}c_{\mathrm{A}}c_{\mathrm{A}}+r_{\mathrm{BA}}c_{\mathrm{B}}c_{\mathrm{A}}+r_{\mathrm{CA}}c_{\mathrm{C}}c_{\mathrm{A}}&=0\\
r_{\mathrm{AB}}c_{\mathrm{A}}c_{\mathrm{B}}+r_{\mathrm{BB}}c_{\mathrm{B}}c_{\mathrm{B}}+r_{\mathrm{CB}}c_{\mathrm{C}}c_{\mathrm{B}}&=0\\
r_{\mathrm{AC}}c_{\mathrm{A}}c_{\mathrm{C}}+r_{\mathrm{BC}}c_{\mathrm{B}}c_{\mathrm{C}}+r_{\mathrm{CC}}c_{\mathrm{C}}c_{\mathrm{C}}&=0
\end{aligned} \tag{5.5}$$

Using the Onsager relations it follows that also

$$\begin{aligned}
r_{\mathrm{AA}}c_{\mathrm{A}}c_{\mathrm{A}}+r_{\mathrm{AB}}c_{\mathrm{A}}c_{\mathrm{B}}+r_{\mathrm{AC}}c_{\mathrm{A}}c_{\mathrm{C}}&=0\\
r_{\mathrm{BA}}c_{\mathrm{B}}c_{\mathrm{A}}+r_{\mathrm{BB}}c_{\mathrm{B}}c_{\mathrm{B}}+r_{\mathrm{BC}}c_{\mathrm{B}}c_{\mathrm{C}}&=0\\
r_{\mathrm{CA}}c_{\mathrm{C}}c_{\mathrm{A}}+r_{\mathrm{CB}}c_{\mathrm{C}}c_{\mathrm{B}}+r_{\mathrm{CC}}c_{\mathrm{C}}c_{\mathrm{C}}&=0
\end{aligned} \tag{5.6}$$

Onsager relations apply here also when the forces are dependent [12]. The resistivity matrix has an eigenvalue equal to zero, and thus a zero determinant. It can therefore not be inverted into a conductivity matrix. It follows from the above relations that there are only three independent resistivities. Once these have been obtained from experiments, the others can be calculated using the above relations. Similarly, one of the equations in (5.2) is minus the sum of the other two, and can be disregarded.

5.1.1 Prigogine's theorem applied

In writing the linear laws, Eq. (5.2), we used the laboratory frame of reference. Other choices for the frame of reference are often used. Possible choices of a reference velocity, $\mathrm{v}_{\mathrm{ref}}$, are the center of mass, the average volume, the average molar or the solvent velocity, see Section 3.4.

According to Prigogine's theorem we can use an arbitrary frame of reference for the transports when the system is in mechanical equilibrium, see ref. [12]. This gives

$$\begin{aligned}
-\frac{c_{\mathrm{A}}}{T}\frac{d\mu_{\mathrm{A}}}{dx} &= r_{\mathrm{AA}}c_{\mathrm{A}}c_{\mathrm{A}}\left(\mathrm{v_A}-\mathrm{v_{ref}}\right)+r_{\mathrm{AB}}c_{\mathrm{A}}c_{\mathrm{B}}\left(\mathrm{v_B}-\mathrm{v_{ref}}\right)\\
&\quad + r_{\mathrm{AC}}c_{\mathrm{A}}c_{\mathrm{C}}\left(\mathrm{v_C}-\mathrm{v_{ref}}\right)\\
-\frac{c_{\mathrm{B}}}{T}\frac{d\mu_{\mathrm{B}}}{dx} &= r_{\mathrm{BA}}c_{\mathrm{B}}c_{\mathrm{A}}\left(\mathrm{v_A}-\mathrm{v_{ref}}\right)+r_{\mathrm{BB}}c_{\mathrm{B}}c_{\mathrm{B}}\left(\mathrm{v_B}-\mathrm{v_{ref}}\right)\\
&\quad + r_{\mathrm{BC}}c_{\mathrm{B}}c_{\mathrm{C}}\left(\mathrm{v_C}-\mathrm{v_{ref}}\right)\\
-\frac{c_{\mathrm{C}}}{T}\frac{d\mu_{\mathrm{C}}}{dx} &= r_{\mathrm{CA}}c_{\mathrm{C}}c_{\mathrm{A}}\left(\mathrm{v_A}-\mathrm{v_{ref}}\right)+r_{\mathrm{CB}}c_{\mathrm{C}}c_{\mathrm{B}}\left(\mathrm{v_B}-\mathrm{v_{ref}}\right)\\
&\quad + r_{\mathrm{CC}}c_{\mathrm{C}}c_{\mathrm{C}}\left(\mathrm{v_C}-\mathrm{v_{ref}}\right) \qquad (5.7)
\end{aligned}$$

These expressions follow from Eq. (5.2) using Eqs. (5.6). By introducing $J_{i,\mathrm{ref}} = c_i(\mathrm{v}_i - \mathrm{v_{ref}})$, the above equations become

$$\begin{aligned}
-\frac{1}{T}\frac{d\mu_{\mathrm{A}}}{dx} &= r_{\mathrm{AA}}J_{\mathrm{A,ref}}+r_{\mathrm{AB}}J_{\mathrm{B,ref}}+r_{\mathrm{AC}}J_{\mathrm{C,ref}}\\
-\frac{1}{T}\frac{d\mu_{\mathrm{B}}}{dx} &= r_{\mathrm{BA}}J_{\mathrm{A,ref}}+r_{\mathrm{BB}}J_{\mathrm{B,ref}}+r_{\mathrm{BC}}J_{\mathrm{C,ref}}\\
-\frac{1}{T}\frac{d\mu_{\mathrm{C}}}{dx} &= r_{\mathrm{CA}}J_{\mathrm{A,ref}}+r_{\mathrm{CB}}J_{\mathrm{B,ref}}+r_{\mathrm{CC}}J_{\mathrm{C,ref}} \qquad (5.8)
\end{aligned}$$

The same frame of reference, $\mathrm{v_{ref}}$, has been used. We can measure three independent resistivities in this frame of reference, and calculate the others using Eqs. (5.5) and (5.6), and subsequently use them in all other frames of reference. The procedure is explained in Section 5.1.2 using the solvent frame of reference as an example.

5.1.2 Diffusion in the solvent frame of reference

In this subsection we show how we can use one set of transport coefficients, determined in the solvent frame of reference, to calculate an equivalent set with a different frame of reference.

The solvent frame of reference is used when there is an excess of one component, say component C. The velocity of the frame of reference is then $\mathrm{v_{ref}} = \mathrm{v_{solv}} = \mathrm{v_C}$. The first two flux equations in Section 5.1.1 reduce to

$$\begin{aligned} -\frac{1}{T}\frac{d\mu_\mathrm{A}}{dx} &= r_{\mathrm{AA}}c_\mathrm{A}\left(\mathrm{v_A}-\mathrm{v_C}\right) + r_{\mathrm{AB}}c_\mathrm{B}\left(\mathrm{v_B}-\mathrm{v_C}\right) \\ &= r_{\mathrm{AA}}J_{\mathrm{A,solv}} + r_{\mathrm{AB}}J_{\mathrm{B,solv}} \\ -\frac{1}{T}\frac{d\mu_\mathrm{B}}{dx} &= r_{\mathrm{BA}}c_\mathrm{A}\left(\mathrm{v_A}-\mathrm{v_C}\right) + r_{\mathrm{BB}}c_\mathrm{B}\left(\mathrm{v_B}-\mathrm{v_C}\right) \\ &= r_{\mathrm{BA}}J_{\mathrm{A,solv}} + r_{\mathrm{BB}}J_{\mathrm{B,solv}} \end{aligned} \tag{5.9}$$

The resistivity matrix has been reduced to a symmetric two by two matrix which can be inverted. The fluxes relative to the solvent velocity become

$$\begin{aligned} J_{\mathrm{A,solv}} &= -l_{\mathrm{AA}}\frac{1}{T}\frac{d\mu_\mathrm{A}}{dx} - l_{\mathrm{AB}}\frac{1}{T}\frac{d\mu_\mathrm{B}}{dx} \\ J_{\mathrm{B,solv}} &= -l_{\mathrm{BA}}\frac{1}{T}\frac{d\mu_\mathrm{A}}{dx} - l_{\mathrm{BB}}\frac{1}{T}\frac{d\mu_\mathrm{B}}{dx} \end{aligned} \tag{5.10}$$

where

$$\begin{aligned} l_{\mathrm{AA}} &= \frac{r_{\mathrm{BB}}}{r_{\mathrm{AA}}r_{\mathrm{BB}} - r_{\mathrm{BA}}r_{\mathrm{AB}}}\,, \quad l_{\mathrm{AB}} = l_{\mathrm{BA}} = \frac{-r_{\mathrm{AB}}}{r_{\mathrm{AA}}r_{\mathrm{BB}} - r_{\mathrm{BA}}r_{\mathrm{AB}}}\,, \\ l_{\mathrm{BB}} &= \frac{r_{\mathrm{AA}}}{r_{\mathrm{AA}}r_{\mathrm{BB}} - r_{\mathrm{BA}}r_{\mathrm{AB}}} \end{aligned} \tag{5.11}$$

and vice-versa

$$\begin{aligned} r_{\mathrm{AA}} &= \frac{l_{\mathrm{BB}}}{l_{\mathrm{AA}}l_{\mathrm{BB}} - l_{\mathrm{BA}}l_{\mathrm{AB}}}\,, \quad r_{\mathrm{AB}} = r_{\mathrm{BA}} = \frac{-l_{\mathrm{AB}}}{l_{\mathrm{AA}}l_{\mathrm{BB}} - l_{\mathrm{BA}}l_{\mathrm{AB}}}\,, \\ r_{\mathrm{BB}} &= \frac{l_{\mathrm{AA}}}{l_{\mathrm{AA}}l_{\mathrm{BB}} - l_{\mathrm{BA}}l_{\mathrm{AB}}} \end{aligned} \tag{5.12}$$

The entropy production becomes:

$$\begin{aligned}\sigma &= J_{\mathrm{A,solv}}\left(-\frac{1}{T}\frac{d\mu_{\mathrm{A}}}{dx}\right) + J_{\mathrm{B,solv}}\left(-\frac{1}{T}\frac{d\mu_{\mathrm{B}}}{dx}\right)\\ &= l_{\mathrm{AA}}\left(\frac{1}{T}\frac{d\mu_{\mathrm{A}}}{dx}\right)^2 + 2l_{\mathrm{AB}}\left(\frac{1}{T}\frac{d\mu_{\mathrm{A}}}{dx}\right)\left(\frac{1}{T}\frac{d\mu_{\mathrm{B}}}{dx}\right) + l_{\mathrm{BB}}\left(\frac{1}{T}\frac{d\mu_{\mathrm{B}}}{dx}\right)^2\\ &= r_{\mathrm{AA}}J^2_{\mathrm{A,solv}} + 2r_{\mathrm{AB}}J_{\mathrm{A,solv}}J_{\mathrm{B,solv}} + r_{\mathrm{BB}}J^2_{\mathrm{B,solv}} \qquad (5.13)\end{aligned}$$

The fluxes have also been expressed in terms of the concentration gradients:

$$\begin{aligned}J_{\mathrm{A,solv}} &= -D_{\mathrm{AA,solv}}\frac{dc_{\mathrm{A}}}{dx} - D_{\mathrm{AB,solv}}\frac{dc_{\mathrm{B}}}{dx}\\ J_{\mathrm{B,solv}} &= -D_{\mathrm{BA,solv}}\frac{dc_{\mathrm{A}}}{dx} - D_{\mathrm{BB,solv}}\frac{dc_{\mathrm{B}}}{dx} \qquad (5.14)\end{aligned}$$

where the diffusion coefficients are given by

$$\begin{aligned}D_{\mathrm{AA,solv}} &= l_{\mathrm{AA}}\frac{1}{T}\frac{d\mu_{\mathrm{A}}}{dc_{\mathrm{A}}} = l_{\mathrm{AA}}\frac{R}{c_{\mathrm{A}}}\\ D_{\mathrm{AB,solv}} &= l_{\mathrm{AB}}\frac{1}{T}\frac{d\mu_{\mathrm{B}}}{dc_{\mathrm{B}}} = l_{\mathrm{AB}}\frac{R}{c_{\mathrm{A}}}\\ D_{\mathrm{BA,solv}} &= l_{\mathrm{BA}}\frac{1}{T}\frac{d\mu_{\mathrm{A}}}{dc_{\mathrm{A}}} = l_{\mathrm{BA}}\frac{R}{c_{\mathrm{B}}}\\ D_{\mathrm{BB,solv}} &= l_{\mathrm{BB}}\frac{1}{T}\frac{d\mu_{\mathrm{B}}}{dc_{\mathrm{B}}} = l_{\mathrm{BB}}\frac{R}{c_{\mathrm{B}}} \qquad (5.15)\end{aligned}$$

The matrix of diffusion coefficients in the solvent frame of reference is not symmetric. The second identity applies to the case of ideal solutions.

Once three of the four diffusion coefficients have been measured, we can determine the three conductivities l_{AA}, $l_{\mathrm{AB}} = l_{\mathrm{BA}}$ and l_{BB}. By using Eq. (5.12), we can next obtain the three independent resistivities. From the relations between the resistivities (5.5 and 5.6) we can next obtain a complete matrix of (dependent) resistivities in Eq. (5.2).

The procedure can be repeated with any other frame of reference. Alternatively, we can use the coefficients of Eq. (5.2) to calculate coefficients that belong to any frame of reference.

To summarize, Eq. (5.2) gives a common ground to transformations between different frames of reference. But a matrix with independent coefficients is needed to define experiments and determine the transport coefficients which are independent.

5.1.3 Maxwell-Stefan equations

Flux equations for isothermal mass transport were written already by Maxwell and Stefan in the nineteenth century, before Onsager established the theory of non-equilibrium thermodynamics, see [24] and [35]. The Maxwell-Stefan equations for multi-component diffusion have become popular for two reasons. The formulation uses velocity differences, which makes it independent of the choice of frame of reference, and the transport coefficients defined by these equations are relatively well-behaved if the fluid is homogeneous.

The Maxwell-Stefan equations can be derived from nonequilibrium thermodynamics by eliminating the main resistivities, r_{AA}, r_{BB} and r_{CC}, in Eq. (5.2), using the identities in Eq. (5.6) giving

$$\begin{aligned}
\frac{c_{\mathrm{A}}}{T}\frac{d\mu_{\mathrm{A}}}{dx} &= r_{\mathrm{AB}}c_{\mathrm{A}}c_{\mathrm{B}}\left(\mathrm{v}_{\mathrm{A}}-\mathrm{v}_{\mathrm{B}}\right)+r_{\mathrm{AC}}c_{\mathrm{A}}c_{\mathrm{C}}\left(\mathrm{v}_{\mathrm{A}}-\mathrm{v}_{\mathrm{C}}\right)\\
\frac{c_{\mathrm{B}}}{T}\frac{d\mu_{\mathrm{B}}}{dx} &= r_{\mathrm{BA}}c_{\mathrm{B}}c_{\mathrm{A}}\left(\mathrm{v}_{\mathrm{B}}-\mathrm{v}_{\mathrm{A}}\right)+r_{\mathrm{BC}}c_{\mathrm{B}}c_{\mathrm{C}}\left(\mathrm{v}_{\mathrm{B}}-\mathrm{v}_{\mathrm{C}}\right)\\
\frac{c_{\mathrm{C}}}{T}\frac{d\mu_{\mathrm{C}}}{dx} &= r_{\mathrm{CA}}c_{\mathrm{C}}c_{\mathrm{A}}\left(\mathrm{v}_{\mathrm{C}}-\mathrm{v}_{\mathrm{A}}\right)+r_{\mathrm{CB}}c_{\mathrm{C}}c_{\mathrm{B}}\left(\mathrm{v}_{\mathrm{C}}-\mathrm{v}_{\mathrm{B}}\right)
\end{aligned}\qquad(5.16)$$

These were the equations written by Maxwell and Stefan. Only velocity differences of the components appear, making the description independent of the frame of reference.

By using Gibbs-Duhem's equation and the Onsager symmetry

relations it follows that the third equation is minus the sum of the other two equations. The above set of equations is therefore equivalent to

$$\begin{aligned}\frac{c_{\rm A}}{T}\frac{d\mu_{\rm A}}{dx} &= r_{\rm AB}c_{\rm A}c_{\rm B}\left(\mathrm{v}_{\rm A}-\mathrm{v}_{\rm B}\right)+r_{\rm AC}c_{\rm A}c_{\rm C}\left(\mathrm{v}_{\rm A}-\mathrm{v}_{\rm C}\right)\\ \frac{c_{\rm B}}{T}\frac{d\mu_{\rm B}}{dx} &= r_{\rm AB}c_{\rm B}c_{\rm A}\left(\mathrm{v}_{\rm B}-\mathrm{v}_{\rm A}\right)+r_{\rm BC}c_{\rm B}c_{\rm C}\left(\mathrm{v}_{\rm B}-\mathrm{v}_{\rm C}\right)\end{aligned} \qquad (5.17)$$

These equations express two independent forces in two independent velocity differences. The Maxwell-Stefan diffusion coefficients are given in terms of the resistances by[1]

$$\mathcal{D}_{\rm AB}=-\frac{R}{cr_{\rm AB}} \qquad \mathcal{D}_{\rm AC}=-\frac{R}{cr_{\rm AC}} \qquad \mathcal{D}_{\rm BC}=-\frac{R}{cr_{\rm BC}} \qquad (5.18)$$

By using these diffusion coefficients, Eq.(5.17) becomes

$$\begin{aligned}-\frac{1}{RT}\frac{d\mu_{\rm A}}{dx} &= \frac{x_{\rm B}}{\mathcal{D}_{\rm AB}}\left(\mathrm{v}_{\rm A}-\mathrm{v}_{\rm B}\right)+\frac{x_{\rm C}}{\mathcal{D}_{\rm AC}}\left(\mathrm{v}_{\rm A}-\mathrm{v}_{\rm C}\right)\\ -\frac{1}{RT}\frac{d\mu_{\rm B}}{dx} &= \frac{x_{\rm A}}{\mathcal{D}_{\rm AB}}\left(\mathrm{v}_{\rm B}-\mathrm{v}_{\rm A}\right)+\frac{x_{\rm C}}{\mathcal{D}_{\rm BC}}\left(\mathrm{v}_{\rm B}-\mathrm{v}_{\rm C}\right)\end{aligned} \qquad (5.19)$$

where $x_i \equiv c_i/c$ is the mole fraction of component i. The chemical potential is defined by, see Section A.3,

$$\mu_i = \mu_i^{\circ}(T) + RT\ln\gamma_i x_i \qquad (5.20)$$

where $\mu_i^0(T)$ is the standard state value and γ_i is the activity coefficient. This gives

$$\begin{aligned}-\frac{dx_{\rm A}}{dx}\left(1+\frac{\partial\ln\gamma_{\rm A}}{\partial\ln x_{\rm A}}\right) &= \frac{x_{\rm B}}{\mathcal{D}_{\rm AB}}\left(\mathrm{v}_{\rm A}-\mathrm{v}_{\rm B}\right)+\frac{x_{\rm C}}{\mathcal{D}_{\rm AC}}\left(\mathrm{v}_{\rm A}-\mathrm{v}_{\rm C}\right)\\ -\frac{dx_{\rm B}}{dx}\left(1+\frac{\partial\ln\gamma_{\rm B}}{\partial\ln x_{\rm B}}\right) &= \frac{x_{\rm A}}{\mathcal{D}_{\rm AB}}\left(\mathrm{v}_{\rm B}-\mathrm{v}_{\rm A}\right)+\frac{x_{\rm C}}{\mathcal{D}_{\rm BC}}\left(\mathrm{v}_{\rm B}-\mathrm{v}_{\rm C}\right)\end{aligned} \qquad (5.21)$$

[1] We follow [35] in this definition rather than [24] who used the pressure p instead of cRT.

Experiments have shown that Maxwell-Stefan diffusion coefficients are well-behaved; although the diffusion coefficient D_{AB} is different for $x_{\mathrm{A}} \to 1$ and for $x_{\mathrm{B}} \to 1$, one can fairly reliably estimate D_{AB} for any composition of A and B according to the Vignes rule

$$D_{\mathrm{AB}} = \left[D_{\mathrm{AB}(x_{\mathrm{A}}\to 1)}\right]^{x_{\mathrm{A}}} \cdot \left[D_{\mathrm{AB}(x_{\mathrm{B}}\to 1)}\right]^{x_{\mathrm{B}}} \tag{5.22}$$

A linear interpolation of the logarithm of D_{AB} is used. The coefficient for two given components remain more or less the same if the third component is replaced by another one. Measured values in one mixture for two components give therefore a good approximation to values of other mixtures containing these components.

With experimental values of the Maxwell-Stefan diffusion coefficients, we can calculate the resistivities of Eq. (5.18), which gives

$$\begin{aligned} r_{\mathrm{AB}} = r_{\mathrm{BA}} &= -\frac{R}{c\mathcal{D}_{\mathrm{AB}}} \quad , \quad r_{\mathrm{AC}} = r_{\mathrm{CA}} = -\frac{R}{c\mathcal{D}_{\mathrm{AC}}} \quad , \\ r_{\mathrm{BC}} = r_{\mathrm{CB}} &= -\frac{R}{c\mathcal{D}_{\mathrm{BC}}} \end{aligned} \tag{5.23}$$

Equation (5.6) gives next the main resistivities.

A property of the Maxwell-Stefan equations is that they are symmetric for interchange of components, contrary to all choices relative to some frame of reference. Therefore, there are $n(n-1)/2$ Maxwell-Stefan diffusion coefficients, but $(n-1)^2$ coefficients of all other choices. The fact that the Maxwell-Stefan diffusion coefficients are rather independent of the concentrations gives a possibility to predict the concentration dependence in, for instance, the solvent frame of reference. By knowing the diffusion coefficients in the solvent frame of reference for low concentrations, we can, following the scheme explained above, calculate the Maxwell-Stefan diffusion coefficients for low concentrations.

Table 5.1: Coefficients for transformations between frames of reference.

	a_A	a_B	a_C
solvent	0	0	1
average molar	x_A	x_B	x_C
average volume	$c_\mathrm{A}V_\mathrm{A}$	$c_\mathrm{B}V_\mathrm{B}$	$c_\mathrm{C}V_\mathrm{C}$
barycentric	ρ_A/ρ	ρ_B/ρ	ρ_C/ρ

Assuming these values to be correct for all concentrations, we can next proceed to calculate back and obtain reasonable approximations for the diffusion coefficients in the solvent frame of reference for all concentrations.

5.1.4 Changing a frame of reference

While the volume or the solvent frame of reference are convenient in analyzing experiments, the barycentric frame of reference is needed to describe pipe flow, see Chapter 6. It is therefore important to be able to convert from one frame of reference to another.

Most of the reference velocities given in Section 3.4 are averages of the velocities of the components and can be written as

$$\mathrm{v}_\mathrm{ref} \equiv a_\mathrm{A}\mathrm{v}_\mathrm{A} + a_\mathrm{B}\mathrm{v}_\mathrm{B} + a_\mathrm{C}\mathrm{v}_\mathrm{C} \quad \text{with} \quad a_\mathrm{A} + a_\mathrm{B} + a_\mathrm{C} = 1 \tag{5.24}$$

Exceptions are the laboratory or the wall frame of reference, where $\mathrm{v}_\mathrm{ref} = 0$, and the surface frame of reference, which uses the velocity of the surface as a reference velocity. It follows from Eq. (5.24) that the mass fluxes satisfy

$$\frac{a_\mathrm{A}}{c_\mathrm{A}}J_\mathrm{A,ref} + \frac{a_\mathrm{B}}{c_\mathrm{B}}J_\mathrm{B,ref} + \frac{a_\mathrm{C}}{c_\mathrm{C}}J_\mathrm{C,ref} = 0 \tag{5.25}$$

They are therefore dependent in these frames of reference. For the various frames of reference the averaging coefficients are

given in Table 5.1. For any choice of the reference velocity, it is sufficient to use only two of the equations in Eq. (5.8). By using also Eq. (5.25), these two equations can be written as

$$\begin{aligned}
-\frac{1}{T}\frac{d\mu_{\mathrm{A}}}{dx} &= \left(r_{\mathrm{AA}} - \frac{a_{\mathrm{A}}}{a_{\mathrm{C}}}\frac{c_{\mathrm{C}}}{c_{\mathrm{A}}}r_{\mathrm{AC}}\right) J_{\mathrm{A,ref}} + \left(r_{\mathrm{AB}} - \frac{a_{\mathrm{B}}}{a_{\mathrm{C}}}\frac{c_{\mathrm{C}}}{c_{\mathrm{B}}}r_{\mathrm{AC}}\right) J_{\mathrm{B,ref}} \\
&\equiv r_{\mathrm{AA,ref}} J_{\mathrm{A,ref}} + r_{\mathrm{AB,ref}} J_{\mathrm{B,ref}} \\
-\frac{1}{T}\frac{d\mu_{\mathrm{B}}}{dx} &= \left(r_{\mathrm{BA}} - \frac{a_{\mathrm{A}}}{a_{\mathrm{C}}}\frac{c_{\mathrm{C}}}{c_{\mathrm{A}}}r_{\mathrm{BC}}\right) J_{\mathrm{A,ref}} + \left(r_{\mathrm{BB}} - \frac{a_{\mathrm{B}}}{a_{\mathrm{C}}}\frac{c_{\mathrm{C}}}{c_{\mathrm{B}}}r_{\mathrm{BC}}\right) J_{\mathrm{B,ref}} \\
&\equiv r_{\mathrm{BA,ref}} J_{\mathrm{A,ref}} + r_{\mathrm{BB,ref}} J_{\mathrm{B,ref}}
\end{aligned} \tag{5.26}$$

By inverting this equation, we obtain

$$\begin{aligned}
J_{\mathrm{A,ref}} &= -l_{\mathrm{AA,ref}}\left(\frac{1}{T}\frac{d\mu_{\mathrm{A}}}{dx}\right) - l_{\mathrm{AB,ref}}\left(\frac{1}{T}\frac{d\mu_{\mathrm{B}}}{dx}\right) \\
J_{\mathrm{B,ref}} &= -l_{\mathrm{BA,ref}}\left(\frac{1}{T}\frac{d\mu_{\mathrm{A}}}{dx}\right) - l_{\mathrm{BB,ref}}\left(\frac{1}{T}\frac{d\mu_{\mathrm{B}}}{dx}\right)
\end{aligned} \tag{5.27}$$

where

$$\begin{aligned}
l_{\mathrm{AA,ref}} &= \frac{r_{\mathrm{BB,ref}}}{r_{\mathrm{AA,ref}} r_{\mathrm{BB,ref}} - r_{\mathrm{BA,ref}} r_{\mathrm{AB,ref}}} \\
l_{\mathrm{AB,ref}} &= \frac{-r_{\mathrm{BA,ref}}}{r_{\mathrm{AA,ref}} r_{\mathrm{BB,ref}} - r_{\mathrm{BA,ref}} r_{\mathrm{AB,ref}}} \\
l_{\mathrm{BA,ref}} &= \frac{-r_{\mathrm{AB,ref}}}{r_{\mathrm{AA,ref}} r_{\mathrm{BB,ref}} - r_{\mathrm{BA,ref}} r_{\mathrm{AB,ref}}} \\
l_{\mathrm{BB,ref}} &= \frac{r_{\mathrm{AA,ref}}}{r_{\mathrm{AA,ref}} r_{\mathrm{BB,ref}} - r_{\mathrm{BA,ref}} r_{\mathrm{AB,ref}}}
\end{aligned} \tag{5.28}$$

and vice-versa

$$\begin{aligned}
r_{\mathrm{AA,ref}} &= \frac{l_{\mathrm{BB,ref}}}{l_{\mathrm{AA,ref}} l_{\mathrm{BB,ref}} - l_{\mathrm{BA,ref}} l_{\mathrm{AB,ref}}} \\
r_{\mathrm{AB,ref}} &= \frac{-l_{\mathrm{BA,ref}}}{l_{\mathrm{AA,ref}} l_{\mathrm{BB,ref}} - l_{\mathrm{BA,ref}} l_{\mathrm{AB,ref}}}
\end{aligned}$$

$$r_{\mathrm{BA,ref}} = \frac{-l_{\mathrm{AB,ref}}}{l_{\mathrm{AA,ref}}l_{\mathrm{BB,ref}} - l_{\mathrm{BA,ref}}l_{\mathrm{AB,ref}}}$$
$$r_{\mathrm{BB,ref}} = \frac{l_{\mathrm{AA,ref}}}{l_{\mathrm{AA,ref}}l_{\mathrm{BB,ref}} - l_{\mathrm{BA,ref}}l_{\mathrm{AB,ref}}} \tag{5.29}$$

We want to cast the diffusion equations in terms of concentration gradients, because these are often measured in diffusion experiments. By introducing the diffusion coefficients:

$$D_{\mathrm{AA,ref}} = l_{\mathrm{AA,ref}}\frac{1}{T}\frac{d\mu_{\mathrm{A}}}{dc_{\mathrm{A}}}$$
$$D_{\mathrm{AB,ref}} = l_{\mathrm{AB,ref}}\frac{1}{T}\frac{d\mu_{\mathrm{B}}}{dc_{\mathrm{B}}}$$
$$D_{\mathrm{BA,ref}} = l_{\mathrm{BA,ref}}\frac{1}{T}\frac{d\mu_{\mathrm{A}}}{dc_{\mathrm{A}}}$$
$$D_{\mathrm{BB,ref}} = l_{\mathrm{BB,ref}}\frac{1}{T}\frac{d\mu_{\mathrm{B}}}{dc_{\mathrm{B}}} \tag{5.30}$$

we can write Eq. (5.27) in the usual form

$$J_{\mathrm{A,ref}} = -D_{\mathrm{AA,ref}}\frac{dc_{\mathrm{A}}}{dx} - D_{\mathrm{AB,ref}}\frac{dc_{\mathrm{B}}}{dx}$$
$$J_{\mathrm{B,ref}} = -D_{\mathrm{BA,ref}}\frac{dc_{\mathrm{A}}}{dx} - D_{\mathrm{BB,ref}}\frac{dc_{\mathrm{B}}}{dx} \tag{5.31}$$

The conductivity, the diffusivity and the resistivity matrices are, however, now all asymmetric! Given the experimental values of these diffusion coefficients, we can calculate the conductivities l_{ij} using Eq. (5.30). The two by two matrix of resistivities follows using Eq. (5.29). In order to find the six dependent resistivities, we use again the identities in Eq. (5.6), and the definitions of the resistivities in Eq. (5.26). The result is:

$$r_{\mathrm{AA,ref}}c_{\mathrm{A}}c_{\mathrm{A}} + r_{\mathrm{AB,ref}}c_{\mathrm{A}}c_{\mathrm{B}} + \frac{1}{a_{\mathrm{C}}}r_{\mathrm{AC}}c_{\mathrm{A}}c_{\mathrm{C}} = 0$$
$$r_{\mathrm{BA,ref}}c_{\mathrm{B}}c_{\mathrm{A}} + r_{\mathrm{BB,ref}}c_{\mathrm{B}}c_{\mathrm{B}} + \frac{1}{a_{\mathrm{C}}}r_{\mathrm{BC}}c_{\mathrm{B}}c_{\mathrm{C}} = 0$$
$$r_{\mathrm{CA}}c_{\mathrm{C}}c_{\mathrm{A}} + r_{\mathrm{CB}}c_{\mathrm{C}}c_{\mathrm{B}} + r_{\mathrm{CC}}c_{\mathrm{C}}c_{\mathrm{C}} = 0 \tag{5.32}$$

After calculating $r_{\mathrm{AC}} = r_{\mathrm{CA}}$, $r_{\mathrm{BC}} = r_{\mathrm{CB}}$ and r_{CC} with these expressions we can find r_{AA}, $r_{\mathrm{AB}} = r_{\mathrm{BA}}$ and r_{BB} using the definitions of the resistivities in the frame of reference.

Exercise 5.1.1 *When we use the solvent frame of reference, Fick's law can be written* $J_{A,solv} = -D_{AA,solv} dc_A/dx$. *With the average volume frame of reference, we write* $J_{A,vol} = -D_{AA,vol} dc_A/dx$. *For what condition is* $D_{AA,vol} \simeq D_{AA,solv}$?

- **Solution:** When $D_{\mathrm{AA,vol}} \simeq D_{\mathrm{AA,solv}}$ it follows using Fick's law that $J_{\mathrm{A,solv}} \simeq J_{\mathrm{A,vol}}$. For the solvent and average volume frames of reference we write

$$J_{\mathrm{A,solv}} = c_{\mathrm{A}} \left(\mathrm{v_A} - \mathrm{v_{solv}} \right)$$
$$J_{\mathrm{A,vol}} = c_{\mathrm{A}} \left(\mathrm{v_A} - \mathrm{v_{vol}} \right)$$

  The fluxes and the diffusion constants are therefore approximately the same when

$$\mathrm{v_{solv}} \simeq \mathrm{v_{vol}}$$

  Consider a two-component mixture where component 2 is the solvent. We then have

$$\mathrm{v_{solv}} = \mathrm{v_2}$$
$$\mathrm{v_{vol}} = c_1 V_1 \mathrm{v_1} + c_2 V_2 \mathrm{v_2} = \mathrm{v_2} + c_1 V_1 \left(\mathrm{v_1} - \mathrm{v_2} \right)$$

  We see that $\mathrm{v_{solv}} \simeq \mathrm{v_{vol}}$, when $c_1 V_1 \ll c_2 V_2 \simeq 1$. This is often true for a dilute solution of component 1 in component 2.

5.2 Maxwell-Stefan equations generalized

It is interesting to generalize the Maxwell-Stefan form of the transport equations (cf. Section 5.1.3) to include also heat transport. Consider therefore again the coupled transport of three

components in a system without external forces, but now in the presence of a temperature gradient.

The entropy production is according to Eq. (3.15)

$$\sigma = J'_q \left(-\frac{1}{T^2} \frac{dT}{dx} \right) + \sum_j^n J_i \left(-\frac{1}{T} \frac{d\mu_{j,T}}{dx} \right) \tag{5.33}$$

The flux equations in the resistivity-form become

$$\begin{aligned}
-\frac{c_\mathrm{A}}{T} \frac{d\mu_{\mathrm{A},T}}{dx} &= r_{\mathrm{AA}} c_\mathrm{A} c_\mathrm{A} \mathrm{v}_\mathrm{A} + r_{\mathrm{AB}} c_\mathrm{A} c_\mathrm{B} \mathrm{v}_\mathrm{B} + r_{\mathrm{AC}} c_\mathrm{A} c_\mathrm{C} \mathrm{v}_\mathrm{C} + r_{\mathrm{A}q} c_\mathrm{A} J'_q \\
-\frac{c_\mathrm{B}}{T} \frac{d\mu_{\mathrm{B},T}}{dx} &= r_{\mathrm{BA}} c_\mathrm{B} c_\mathrm{A} \mathrm{v}_\mathrm{A} + r_{\mathrm{BB}} c_\mathrm{B} c_\mathrm{B} \mathrm{v}_\mathrm{B} + r_{\mathrm{BC}} c_\mathrm{B} c_\mathrm{C} \mathrm{v}_\mathrm{C} + r_{\mathrm{B}q} c_\mathrm{B} J'_q \\
-\frac{c_\mathrm{C}}{T} \frac{d\mu_{\mathrm{C},T}}{dx} &= r_{\mathrm{CA}} c_\mathrm{C} c_\mathrm{A} \mathrm{v}_\mathrm{A} + r_{\mathrm{CB}} c_\mathrm{C} c_\mathrm{B} \mathrm{v}_\mathrm{B} + r_{\mathrm{CC}} c_\mathrm{C} c_\mathrm{C} \mathrm{v}_\mathrm{C} + r_{\mathrm{C}q} c_\mathrm{C} J'_q \\
-\frac{1}{T^2} \frac{dT}{dx} &= r_{q\mathrm{A}} c_\mathrm{A} \mathrm{v}_\mathrm{A} + r_{q\mathrm{B}} c_\mathrm{B} \mathrm{v}_\mathrm{B} + r_{q\mathrm{C}} c_\mathrm{C} \mathrm{v}_\mathrm{C} + r_{qq} J'_q
\end{aligned} \tag{5.34}$$

The Gibbs-Duhem equation

$$0 = -v dp + S dT + \sum_i x_i d\mu_i \tag{5.35}$$

plays a central role in the derivation of the Maxwell-Stefan equations. We have constant pressure, giving

$$0 = \sum_i \frac{c_i}{T} \frac{d\mu_{i,T}}{dx} \tag{5.36}$$

Equation (5.36) does not assume that the temperature is constant in the system. The differential chemical potential $d\mu_{i,T} = d\mu_i + (d\mu_i/dT)_{p,x_j} dT = d\mu_i - S_i dT$ is the change of chemical potential in the direction of constant temperature. The term $-S_i dT$ accounts for the variation in temperature and this term, after summation over all components, cancels the term SdT of Eq. (5.35), compare also Appendix A.2.

By using the Gibbs-Duhem equation (5.36) the sum of the first three equations of (5.34) is zero. Since the component velocities $\mathrm{v_A}$, $\mathrm{v_B}$, $\mathrm{v_C}$, and the measurable heat flux J'_q are not generally zero, the coefficients (resistivities) have to be correlated and we obtain

$$\begin{aligned} r_{\mathrm{AA}}c_{\mathrm{A}}c_{\mathrm{A}} + r_{\mathrm{BA}}c_{\mathrm{B}}c_{\mathrm{A}} + r_{\mathrm{CA}}c_{\mathrm{C}}c_{\mathrm{A}} &= 0 \\ r_{\mathrm{AB}}c_{\mathrm{A}}c_{\mathrm{B}} + r_{\mathrm{BB}}c_{\mathrm{B}}c_{\mathrm{B}} + r_{\mathrm{CB}}c_{\mathrm{C}}c_{\mathrm{B}} &= 0 \\ r_{\mathrm{AC}}c_{\mathrm{A}}c_{\mathrm{C}} + r_{\mathrm{BC}}c_{\mathrm{B}}c_{\mathrm{C}} + r_{\mathrm{CC}}c_{\mathrm{C}}c_{\mathrm{C}} &= 0 \\ r_{\mathrm{A}q}c_{\mathrm{A}} + r_{\mathrm{B}q}c_{\mathrm{B}} + r_{\mathrm{C}q}c_{\mathrm{C}} &= 0 \end{aligned} \tag{5.37}$$

By using these relations and Gibbs-Duhem's equation, it follows that the third equation in Eq. (5.34) is minus the sum of the first two equations. The four equations are therefore equivalent to

$$\begin{aligned} -\frac{c_{\mathrm{A}}}{T}\frac{d\mu_{\mathrm{A},T}}{dx} &= r_{\mathrm{AA}}c_{\mathrm{A}}c_{\mathrm{A}}\mathrm{v_A} + r_{\mathrm{AB}}c_{\mathrm{A}}c_{\mathrm{B}}\mathrm{v_B} + r_{\mathrm{AC}}c_{\mathrm{A}}c_{\mathrm{C}}\mathrm{v_C} + r_{\mathrm{A}q}c_{\mathrm{A}}J'_q \\ -\frac{c_{\mathrm{B}}}{T}\frac{d\mu_{\mathrm{B},T}}{dx} &= r_{\mathrm{BA}}c_{\mathrm{B}}c_{\mathrm{A}}\mathrm{v_A} + r_{\mathrm{BB}}c_{\mathrm{B}}c_{\mathrm{B}}\mathrm{v_B} + r_{\mathrm{BC}}c_{\mathrm{B}}c_{\mathrm{C}}\mathrm{v_C} + r_{\mathrm{B}q}c_{\mathrm{B}}J'_q \\ -\frac{1}{T^2}\frac{dT}{dx} &= r_{q\mathrm{A}}c_{\mathrm{A}}\mathrm{v_A} + r_{q\mathrm{B}}c_{\mathrm{B}}\mathrm{v_B} + r_{q\mathrm{C}}c_{\mathrm{C}}\mathrm{v_C} + r_{qq}J'_q \end{aligned} \tag{5.38}$$

With the relations of Eq. (5.37) we can now eliminate the symmetric resistivities $r_{\mathrm{AA}}c_{\mathrm{A}}c_{\mathrm{A}}$, $r_{\mathrm{BB}}c_{\mathrm{B}}c_{\mathrm{B}}$, and $r_{q\mathrm{A}}c_{\mathrm{A}}$ from Eq. (5.38), and obtain

$$\begin{aligned} \frac{c_{\mathrm{A}}}{T}\frac{d\mu_{\mathrm{A},T}}{dx} &= r_{\mathrm{AB}}c_{\mathrm{A}}c_{\mathrm{B}}(\mathrm{v_A} - \mathrm{v_B}) + r_{\mathrm{AC}}c_{\mathrm{A}}c_{\mathrm{C}}(\mathrm{v_A} - \mathrm{v_C}) - r_{\mathrm{A}q}c_{\mathrm{A}}J'_q \\ \frac{c_{\mathrm{B}}}{T}\frac{d\mu_{\mathrm{B},T}}{dx} &= r_{\mathrm{AB}}c_{\mathrm{B}}c_{\mathrm{A}}(\mathrm{v_B} - \mathrm{v_A}) + r_{\mathrm{BC}}c_{\mathrm{B}}c_{\mathrm{C}}(\mathrm{v_B} - \mathrm{v_C}) - r_{\mathrm{B}q}c_{\mathrm{B}}J'_q \\ \frac{1}{T^2}\frac{dT}{dx} &= r_{\mathrm{B}q}c_{\mathrm{B}}(\mathrm{v_A} - \mathrm{v_B}) + r_{\mathrm{C}q}c_{\mathrm{C}}(\mathrm{v_A} - \mathrm{v_C}) - r_{qq}J'_q \end{aligned} \tag{5.39}$$

where we have made use of the Onsager relations, $r_{\mathrm{AB}} = r_{\mathrm{BA}}$, $r_{\mathrm{AC}} = r_{\mathrm{CA}}$, $r_{\mathrm{BC}} = r_{\mathrm{CB}}$, $r_{q\mathrm{A}} = r_{\mathrm{A}q}$, $r_{q\mathrm{B}} = r_{\mathrm{B}q}$, and $r_{q\mathrm{C}} = r_{\mathrm{C}q}$. The derivation of Eq. (5.39) was done for a three component mixture. A multi-component mixture of n components is similarly

described by

$$\frac{1}{T}\frac{d\mu_{i,T}}{dx} = \sum_{j\neq i}^{n} r_{ij}c_j(\mathrm{v}_i - \mathrm{v}_j) - r_{iq}J'_q \qquad \forall i = 1,\ldots,n-1 \quad (5.40)$$

$$\lambda\frac{dT}{dx} = \sum_{j\neq i}^{n} \frac{r_{jq}}{r_{qq}}c_j(\mathrm{v}_i - \mathrm{v}_j) - J'_q \quad (5.41)$$

The thermal conductivity $\lambda = (r_{qq}T^2)^{-1}$ was introduced. Equation (5.40) and (5.41) can be used to eliminate the heat flux J'_{q} and we obtain for all $i = 1,\ldots,n-1$

$$\begin{aligned}\frac{1}{T}\frac{d\mu_{i,T}}{dx} &= \sum_{j\neq i}^{n} r_{ij}c_j(\mathrm{v}_i - \mathrm{v}_j) - \sum_{j\neq i}^{n}\frac{r_{iq}r_{jq}}{r_{qq}}c_j(\mathrm{v}_i - \mathrm{v}_j) + \lambda r_{iq}\frac{dT}{dx} \\ &= \sum_{j\neq i}^{n}\left(r_{ij} - \frac{r_{iq}r_{jq}}{r_{qq}}\right)c_j(\mathrm{v}_i - \mathrm{v}_j) + \lambda r_{iq}\frac{dT}{dx} \quad (5.42)\end{aligned}$$

A symmetric set of Maxwell-Stefan diffusion coefficients can be defined analogous to earlier, see Section 5.1.3.

$$\left(r_{ij} - \frac{r_{iq}r_{jq}}{r_{qq}}\right) = -\frac{R}{c\mathcal{D}_{ij}} \quad (5.43)$$

so that the transport due to a chemical potential gradient and a temperature gradient is

$$-\frac{1}{RT}\frac{d\mu_{i,T}}{dx} = \sum_{j\neq i}^{n}\frac{x_j}{\mathcal{D}_{ij}}(\mathrm{v}_i - \mathrm{v}_j) - \lambda\frac{r_{iq}}{R}\frac{dT}{dx} \qquad \forall i = 1,\ldots,n-1 \quad (5.44)$$

Thermal diffusion is defined in the absence of chemical potential gradients. This motivates the relation

$$0 = \sum_{j\neq i}^{n}\frac{x_j}{\mathcal{D}_{ij}}(\mathrm{v}_i - \mathrm{v}_j) - \lambda\frac{r_{iq}}{R}\frac{dT}{dx} \qquad \forall i = 1,\ldots,n-1 \quad (5.45)$$

The velocity v_i is in this case solely due to thermal diffusion. From the definition $J_i = c_i \mathrm{v}_i$ and Eq. (4.19), we obtain the relation

$$\mathrm{v}_i = -D_i^T \frac{dT}{dx} \tag{5.46}$$

where D_i^T is the thermal diffusion coefficient, see Section 4.2. By introducing the thermal diffusion coefficient Eq. (5.46) in (5.45), we find for i and j

$$0 = \sum_{j \neq i}^{n} \frac{x_j}{\mathcal{D}_{ij}} \left(D_i^T - D_j^T \right) + \lambda \frac{r_{iq}}{R} \qquad \forall i = 1, \ldots, n-1 \tag{5.47}$$

and this can be reintroduced in Eq. (5.44) to finally give

$$-\frac{1}{RT} \frac{d\mu_{i,T}}{dx} = \sum_{j \neq i}^{n} \frac{x_j}{\mathcal{D}_{ij}} (\mathrm{v}_i - \mathrm{v}_j) + \sum_{j \neq i}^{n} \frac{x_j}{\mathcal{D}_{ij}} \left(D_i^T - D_j^T \right) \frac{dT}{dx} \tag{5.48}$$

for $i = 1, \ldots, n-1$. Equation (5.47) can be seen as an alternative definition for the thermal diffusion coefficient.

5.3 Concluding remarks

The Maxwell-Stefan equations were at the center of interest in this Chapter, and their relation to other formulations of multicomponent interdiffusion was shown. Their generalisation to nonisothermal systems was pointed out.

Also coupled transports of heat and mass can give work. Interdiffusion can for instance lead to work in biological systems. Thermal driving forces can lead to separation work, for example, in the presence of membranes.

This page intentionally left blank

Chapter 6

Systems with shear flow

We derive the entropy production for a system with chemical reactions, temperature gradients and shear flow. The momentum balance contributes to a change in the internal energy. The Navier-Stokes equation and other relations are given. The Navier-Stokes equation contains a mechanical force due to the gradient of the reaction Gibbs energy. The rate of the chemical reaction obtains for symmetry reasons a term due to expansion or contraction. We discuss stationary pipe- and plug flow.

Transport in pipes and other flow-equipment is central in chemical and mechanical engineering. Such flows exert viscous shear, which must be described by at least two coordinates. In Chapter 3 we assumed that the system was in mechanical equilibrium and that shear forces were absent. We now study viscous flow due to a pressure gradient. The second law of thermodynamics governs also this flow, and we shall see how the Navier-Stokes equation (the equation of motion) is related to the entropy production, and how the conjugate fluxes and forces can be defined in the presence of chemical reactions, temperature gradients and shear flow. These phenomena are typical in chemical reactors.

The purpose of the Chapter is to give the central equations for a simple chemical reactor, the stationary pipe- or plug flow reactor.

In order to find the entropy production, we again start with the time derivative of the Gibbs equation for a mixture of n components, see also Appendix A.1

$$\frac{\partial s}{\partial t} = \frac{1}{T}\frac{\partial u}{\partial t} - \frac{1}{T}\sum_{j=1}^{n} \mu_j \frac{\partial c_j}{\partial t} \tag{6.1}$$

Gibbs' equation is also valid for the spacial derivative and for the time derivative in a volume element that moves with the flow (the substantial time derivative).

When the balance equations for entropy, mass, and internal energy are introduced into Eq. (6.1), we find the entropy flux as well as the entropy production, like we did in Chapter 3. The momentum balance was not needed in Chapter 3. We shall now include the momentum balance, and see that also viscous systems follow the structure given by Eqs. (1.1)-(1.3). Viscous contributions enter the Gibbs equation via the balance equation for internal energy.

6.1 Balance equations

The entropy balance, Eq. (3.1), for three-dimensional flow is:

$$\frac{\partial s}{\partial t} = -\nabla\cdot\mathbf{J}_s + \sigma \tag{6.2}$$

where nabla (the $\nabla \equiv (\partial/\partial x, \partial/\partial y, \partial/\partial z)$-operator) is a derivative -vector for all coordinate directions. The balance equations for mass, momentum, internal energy are given below. More details on their derivations can be found in Appendix A.1.

6.1.1 Component balances

The mass balance for component j is

$$\frac{\partial c_j}{\partial t} = -\nabla\cdot\mathbf{J}_j + \nu_j r \tag{6.3}$$

where the molar flux vector is $\mathbf{J_j} = c_j\mathbf{v}_j$, compare Eq. (3.2) and c_j is given in mol/m^3.

6.1.2 Momentum balance

The momentum balance, or equation of motion, for three- dimensional flow is:

$$\frac{\partial \rho\mathbf{v}}{\partial t} = -\nabla\cdot(\rho\mathbf{v}\mathbf{v} + \mathbf{\Pi}) - \nabla p + \sum_{i=1}^{n} \rho_i\mathbf{f}_i \tag{6.4}$$

where $\mathbf{\Pi}$ is the viscous pressure tensor.

An example of a viscous pressure tensor element is Newton's law of friction, see Eq. (2.5). That equation describes laminar flow in the x-direction, with velocity $\mathbf{v} = (\mathrm{v}_x, 0, 0)$ and velocity component $\mathrm{v}_x = \mathrm{v}_x(y)$. The more general law of friction, or the law of Navier-Poisson, is

$$\mathbf{\Pi} = -\eta\left(\nabla\mathbf{v} + (\nabla\mathbf{v})^{\mathrm{T}} - \frac{2}{3}(\nabla\cdot\mathbf{v})\mathbf{1}\right) - \zeta(\nabla\cdot\mathbf{v})\mathbf{1} - \lambda_r\Delta_r G\ \mathbf{1} \tag{6.5}$$

where the coefficient η is the shear viscosity, ζ is the bulk viscosity (or second viscosity) and λ_r is the chemical viscosity. The viscosities can be functions of composition, densities and temperature. The shear and the bulk viscosities have dimension Pa s, and the chemical viscosity has dimension m^{-3}. Superscript T indicates the transpose of a matrix, $(\nabla\mathbf{v})^{\mathrm{T}}_{\alpha\beta} \equiv \nabla_\beta \mathrm{v}_\alpha$, The divergence of the velocity is $\nabla\cdot\mathbf{v} \equiv \partial\mathrm{v}_x/\partial x + \partial\mathrm{v}_y/\partial y + \partial\mathrm{v}_z/\partial z$. The second term on the right hand side in Eq. (6.5) captures

the viscous pressure contribution of an expanding or contracting fluid flow. The bulk viscosity is zero for ideal monoatomic gases. For incompressible fluids $\nabla\cdot\mathbf{v} = 0$. When the fluid is incompressible, the contribution from the second term is zero.

The third term describes the coupling of the tensor to a chemical reaction. Meixner [58] explained that the chemical viscosity is caused by a chemical reaction which progresses fast compared to the rate of exchange of momentum. The third term is usually not taken into account. Experiments show that the shear viscosity of non-Newtonian fluids is a function of the shear, $\nabla\mathbf{v}$. The structure of Eqs. (1.1)-(1.3) is then not preserved, as the viscosity should not depend on a thermodynamic force. It is possible to generalize non-equilibrium thermodynamic theory to include this case, by introducing the orientation of the molecules as internal variable [59–61], see Chapter 7.

By substituting the viscous pressure tensor in the equation of motion, and assuming η, ζ and λ_r to be constant, we obtain

$$\begin{aligned}\frac{\partial\rho\mathbf{v}}{\partial t} = &-\nabla\cdot\rho\mathbf{v}\mathbf{v} - \eta\Delta\mathbf{v} - \left(\zeta + \frac{1}{3}\eta\right)\nabla\nabla\cdot\mathbf{v} \\ &- \lambda_r\nabla\Delta_r G - \nabla p + \sum_{i=1}^{n}\rho_i\mathbf{f}_i \end{aligned} \tag{6.6}$$

where $\Delta \equiv \nabla\cdot\nabla$ is the Laplace operator. This is the Navier-Stokes equation.

6.1.3 Internal energy balance

The internal energy of a volume element changes with respect to time according to

$$\frac{\partial u}{\partial t} = -\nabla\cdot\left(\mathbf{J}'_q + \sum \mathbf{J}_i H_i\right) + \mathbf{v}\cdot\nabla p - \boldsymbol{\Pi} : \nabla\mathbf{v} \tag{6.7}$$

See also Appendix A.1. The first term on the right hand side is the divergence of the total heat flux in an electroneutral system,

see Chapter 3. The second term adds energy to the volume element from changes in pressure, while the last term adds internal energy because of shear. The last term is called the Rayleigh dissipation function, see e.g. [2]. Viscous flow gives heat production as we shall see in the exercise below, so one may speak of energy dissipated as heat. The cause of the dissipation is a positive entropy production.

Exercise 6.1.1 *Consider a fluid in stationary shear flow between two plates of infinite length positioned at $z = 0$ and $z = z_0$. The lower plate is fixed while the upper plate moves with velocity v_{x0} in the x-direction. The configuration can be used to measure a fluid's viscosity. The upper and lower temperatures are T_u and T_l, respectively. Assume that the viscosity, η, and thermal conductivity, λ are constant. Calculate the velocity profile and the temperature profile.*

- **Solution:** We want to calculate the two fields $\mathrm{v}_x = \mathrm{v}_x(z)$ and $T = T(z)$ with the four boundary conditions $\mathrm{v}_x(z = 0) = 0$, $\mathrm{v}_x(z = z_0) = \mathrm{v}_{x0}$, $T(z = 0) = T_l$, and $T(z = z_0) = T_u$. As there is no pressure difference along the plates the pressure p is everywhere constant. The momentum balance for the velocity field then is

$$\frac{d}{dz}\left(\Pi_{xz}\right) = 0 \quad \Rightarrow \quad -\eta\frac{\partial^2 \mathrm{v}_x}{\partial z^2} = 0$$
$$\Rightarrow \quad \mathrm{v}_x = c_1 z + c_2 \quad \Rightarrow \quad \mathrm{v}_x = \mathrm{v}_{x0}\frac{z}{z_0}$$

The internal energy balance for the temperature field gives

$$-\nabla\cdot\mathbf{J}'_q = \mathbf{\Pi} : \nabla\mathbf{v} \qquad \Rightarrow \qquad -\lambda\frac{\partial^2 T}{\partial z^2} = \eta\left(\frac{\partial \mathrm{v}_x}{\partial z}\right)^2$$
$$\Rightarrow \qquad -\lambda\frac{\partial^2 T}{\partial z^2} = \eta\left(\frac{\mathrm{v}_{x0}}{z_0}\right)^2$$

$$\Rightarrow \qquad T(z) = -\frac{\eta}{\lambda}\left(\frac{\mathrm{v}_{x0}}{z_0}\right)^2 z^2 + c_3 z + c_4$$

and

$$T(z) = -\frac{\eta}{\lambda}\mathrm{v}_{x0}\left(\frac{z}{z_0}\right)^2 + \left((T_u - T_l) + \frac{\eta}{\lambda}\mathrm{v}_{x0}\right)\left(\frac{z}{z_0}\right) + T_l$$

The four integration constants $c_1, \ldots c_4$ were determined from the four boundary conditions. The result is a velocity profile which is linear between the two plates, and a temperature profile which is parabolic, see Fig. 6.1. The viscous shear leads to a heat flux from the fluid in both directions to the plates.

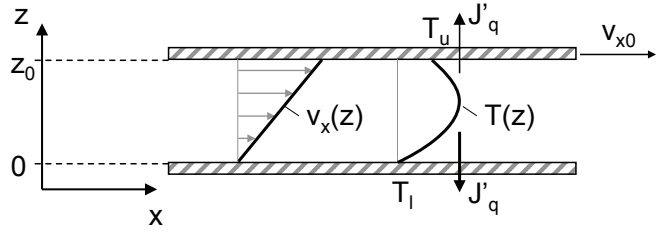

Figure 6.1: Velocity and temperature profile for a shear flow between two plates.

The exercise shows that a heat flux $-\lambda(\partial T/\partial z)$ is due to viscous flow. The heat flux is a sign of the irreversibility of the shear flow. The expression for the entropy production in systems with viscous flows contains therefore also a shear term, $\mathbf{\Pi} : \nabla\mathbf{v}$ as we shall see below. The entropy flux into the surroundings leads to lost work according to Section 2.3.

6.2 Entropy production

Consider a volume element moving with a flow. Its center-of-mass or barycentric velocity is $\mathbf{v}$. This velocity is defined by

$\mathbf{v} \equiv \frac{1}{\rho}\sum_{i=1}^{n}\mathbf{v}_i\rho_i = \sum_{i=1}^{n}\mathbf{v}_i w_i$ where w_i is the mass-fraction of component i. The diffusion of a component with respect to the barycentric frame of reference is

$$\mathbf{J}_{i,\mathrm{bar}} \equiv c_i(\mathbf{v}_i - \mathbf{v}) \tag{6.8}$$

while the flux of the same component with respect to the wall is

$$\mathbf{J}_i = c_i\mathbf{v}_i = c_i\mathbf{v} + \mathbf{J}_{i,\mathrm{bar}} \tag{6.9}$$

The second last term is called the convective and the last part the diffusive part of the total flux. Using the fact that $\rho_i = M_i c_i$ it follows from the definition of $\mathbf{J}_{i,\mathrm{bar}}$ that

$$\sum_{i=1}^{n} M_i\mathbf{J}_{i,\mathrm{bar}} = 0 \tag{6.10}$$

so the barycentric diffusion fluxes are not independent of one another. The entropy balance is

$$\begin{aligned}\frac{\partial s}{\partial t} &= -\nabla\cdot\mathbf{J}_s + \sigma \\ &= -\nabla\cdot(s\mathbf{v} + \mathbf{J}_{s,\mathrm{bar}}) + \sigma\end{aligned} \tag{6.11}$$

The entropy flux, $\mathbf{J}_s$, has also a convective and a diffusive term. The second line distinguishes between the entropy carried by the flow and by diffusion with respect to the center of mass, $\mathbf{J}_{s,\mathrm{bar}}$. The entropy production in the volume element, σ, is positive according to the second law of thermodynamics. In order to obtain explicit expressions for the entropy production and flux, we introduce the component balance (Eq. (6.3)) and the balance for internal energy (Eq. (6.7)) in the Gibbs equation Eq. (6.1). This gives

$$\begin{aligned}\frac{\partial s}{\partial t} =& -\frac{1}{T}\nabla\cdot\left(\mathbf{J}'_q + \sum_{i=1}^{n}\mathbf{J}_i H_i\right) + \frac{1}{T}\mathbf{v}\cdot\nabla p - \frac{1}{T}\boldsymbol{\Pi} : \nabla\mathbf{v} \\ &+ \sum_{i=1}^{n}\frac{\mu_i}{T}\nabla\cdot\mathbf{J}_i - r\,\frac{\Delta_r G}{T}\end{aligned} \tag{6.12}$$

This equation can rewritten by

$$\frac{\partial s}{\partial t} = -\nabla\cdot\left(\frac{\sum_{i=1}^{n}\mathbf{J}_i(H_i-\mu_i)+\mathbf{J}'_q}{T}\right)+\mathbf{J}'_q\cdot\nabla\frac{1}{T}+\sum_{i=1}^{n}\mathbf{J}_i H_i\cdot\nabla\frac{1}{T}$$
$$-\sum_{i=1}^{n}\mathbf{J}_i\cdot\nabla\frac{\mu_i}{T}+\frac{1}{T}\mathbf{v}\cdot\nabla p-\frac{1}{T}\,\mathbf{\Pi}:\nabla\mathbf{v}-r\,\frac{\Delta_r G}{T} \qquad (6.13)$$

By comparing Eq. (6.13) to Eq. (6.11), we can identify the total entropy flux and the entropy production. The entropy flux is

$$\begin{aligned}\mathbf{J}_s &= \frac{\mathbf{J}'_q}{T}+\sum_{i=1}^{n}\mathbf{J}_i S_i\\ &= \frac{\mathbf{J}'_q}{T}+s\mathbf{v}+\sum_{i=1}^{n}\mathbf{J}_{i,\mathrm{bar}}\,S_i\end{aligned} \qquad (6.14)$$

In the second line we decomposed $\sum_{i=1}^{n}(c_i\mathbf{v}_i)S_i$ into a convective entropy flux $\mathbf{v}\ \sum_{i=1}^{n}c_i S_i = \mathbf{v}\ s$ and a diffusive flux $\sum_{i=1}^{n}\mathbf{J}_{i,\mathrm{bar}}S_i$ making use of Eq. (6.9). The entropy flux is due to the heat flux over the temperature, $\mathbf{J}'_q/T$, and the entropy carried by mass with velocity $\mathbf{v}$ and by diffusion. If another velocity than the barycentric velocity is chosen as a frame of reference, the above equations will be modified, see Eqs. (6.23) and (6.24) below.

By comparing Eq. (6.13) to Eq. (6.11), we identify the entropy production as

$$\begin{aligned}\sigma &= \mathbf{J}'_q\cdot\nabla\frac{1}{T}+\sum_{i=1}^{n}\mathbf{J}_i H_i\cdot\nabla\frac{1}{T}-\sum_{i=1}^{n}\mathbf{J}_i\cdot\nabla\frac{\mu_i}{T}+\frac{1}{T}\mathbf{v}\cdot\nabla p\\ &\quad -\frac{1}{T}\,\mathbf{\Pi}:\nabla\mathbf{v}-r\,\frac{\Delta_r G}{T}\\ &= \mathbf{J}'_q\cdot\nabla\frac{1}{T}-\frac{1}{T}\sum_{i=1}^{n}\mathbf{J}_i\cdot(S_i\nabla T+\nabla\mu_i)+\frac{1}{T}\mathbf{v}\cdot\nabla p\\ &\quad -\frac{1}{T}\,\mathbf{\Pi}:\nabla\mathbf{v}-r\,\frac{\Delta_r G}{T}\end{aligned} \qquad (6.15)$$

We use Gibbs-Duhem's equation to eliminate terms proportional to $\mathbf{v}$, Eq. (A.66), and the definition of the gradient of the chemical potential in the direction of constant temperature $\nabla\mu_{i,T} = \nabla\mu_i + S_i\nabla T$ (see Eq. (A.66)). The entropy production obtains then a convenient form

$$\sigma = \mathbf{J}'_q \cdot \nabla\frac{1}{T} - \sum_{i=1}^{n} \mathbf{J}_{i,\mathrm{bar}} \cdot \frac{1}{T}\nabla\mu_{i,T} - \frac{1}{T}\mathbf{\Pi} : \nabla\mathbf{v} - r\frac{\Delta_r G}{T} \quad (6.16)$$

The expression has a set of products and can be compared to Eq. (1.1). The fluxes are the measurable heat flux, the diffusional fluxes, the shear pressure tensor and the rate of the chemical reaction. The forces conjugate to these are the gradient in the inverse temperature, minus the gradient in the chemical potential in the direction of constant temperature over the temperature, minus the gradient in the velocity over the temperature and minus the reaction Gibbs energy over the temperature. All flux-force pairs contribute to the entropy production and to dissipation of energy as heat. The fluxes and forces are, however, defined by Eq. (6.16) only, and not by the Rayleigh dissipation function [29]. The lost work in the flow is likewise connected to Eq. (6.16).

The first two contributions to σ are vectorial. The third term is the product of two symmetric tensors. They can both be written as the sum of a symmetric traceless tensor with rank two and the trace which is a scalar. The last term contains scalars (tensors of rank zero). For the viscous pressure tensor we can therefore write

$$\mathbf{\Pi} = \overline{\mathbf{\Pi}} + \frac{1}{3}\mathbf{1}\mathrm{Tr}\mathbf{\Pi} \quad (6.17)$$

where the bar above the tensor indicates the symmetric traceless part, and Tr stands for trace. The entropy production can now be written as

$$\sigma = \sigma_{vect} + \sigma_{tens} + \sigma_{scal} \quad (6.18)$$

where

$$\begin{aligned}
\sigma_{vect} &= \mathbf{J}'_q \cdot \nabla \frac{1}{T} - \sum_{i=1}^{n} \mathbf{J}_{i,\mathrm{bar}} \cdot \frac{1}{T} \nabla \mu_{i,T} = \mathbf{J}'_q \cdot \nabla \frac{1}{T} \\
&\quad - \sum_{i=1}^{n-1} \mathbf{J}_{i,\mathrm{bar}} \cdot \frac{1}{T} \nabla \left(\mu_{i,T} - \frac{M_i}{M_n} \mu_{n,T} \right) \\
\sigma_{tens} &= -\frac{1}{2T} \overline{\mathbf{\Pi}} : \left(\nabla \mathbf{v} + (\nabla \mathbf{v})^{\mathrm{T}} - \frac{2}{3} (\nabla \cdot \mathbf{v}) \mathbf{1} \right) \\
\sigma_{scal} &= -\frac{1}{3T} (\mathrm{Tr} \mathbf{\Pi}) \nabla \cdot \mathbf{v} - r \frac{\Delta_r G}{T}
\end{aligned} \tag{6.19}$$

We used $\mathbf{\Pi} : \mathbf{1} = \mathrm{Tr}\mathbf{\Pi}$. Coupling takes only place between tensors of the same order (the Curie principle). The vectorial contribution leads to linear force-flux relations that have already be discussed extensively in the previous Chapter, where we started with expressions for the forces in terms of the fluxes. Using Gibbs-Duhem it was then possible to show that the equation for $\nabla \mu_{n,T}$ followed from the equations for $\nabla \mu_{i,T}$, $i = \overline{1, n-1}$. In these equations all velocities could be replaced by velocity differences. The diffusion fluxes contain velocity differences with the barycentric velocity. As a consequence $\mathbf{J}_{n,\mathrm{bar}}$ is a function of the other diffusion fluxes. In Eq. (6.19a) we have used Eq. (6.10) to eliminate $\mathbf{J}_{n,\mathrm{bar}}$. This procedure is an alternative to the one used in Chapter 5.

In the tensorial contribution there is only one force-flux pair and the resulting linear law is

$$\mathbf{\Pi} = -\eta \left(\nabla \mathbf{v} + (\nabla \mathbf{v})^{\mathrm{T}} - \frac{2}{3} (\nabla \cdot \mathbf{v}) \mathbf{1} \right) \tag{6.20}$$

In the scalar contribution there are two force-flux pairs, and the resulting linear equations are

$$\begin{aligned}
\frac{1}{3} (\mathrm{Tr} \mathbf{\Pi}) &= -\zeta \nabla \cdot \mathbf{v} - \lambda_r \Delta_r G \\
r &= -\lambda_r \nabla \cdot \mathbf{v} - L_r \Delta_r G
\end{aligned} \tag{6.21}$$

A factor $1/T$ was absorbed in the coefficients in Eqs. (6.20) and (6.21). Navier-Stokes equation, Eq. (6.6), is obtained by substituting Eqs. (6.17), (6.20) and (6.21) into Eq. (6.5), keeping η, ζ and λ_r constant. A force term appears in the Navier-Stokes equation due to a gradient of the reaction Gibbs energy. By substituting Eq. (6.21) for the reaction rate into the component balance equation, Eq. (6.3), we obtain

$$\frac{\partial c_j}{\partial t} = -\nabla\cdot\mathbf{J}_j - \nu_j\lambda_r\nabla\cdot\mathbf{v} - \nu_j L_r\Delta_r G \tag{6.22}$$

This shows that expansion and compression gives a contribution to the reaction rate and a corresponding change of the concentrations. As we discussed above, the contribution containing λ_r is usually neglected.

The vectorial fluxes, tensors of rank one, can couple to one another, but not to the tensors of rank zero or two. No other terms can couple to the shear viscosity. But the bulk viscosity term may couple to the chemical reaction rate. This effect has so far not been investigated in detail.

The entropy production is independent of the frame of reference, but several fluxes are not. The flux, $\mathbf{J}_{i,\mathrm{bar}}$, of component i relative to the barycentric velocity was introduced in the reformulation of Eq. (6.15) into Eq. (6.16). If a different velocity field, $\mathbf{v}_{\mathrm{ref}}(\mathbf{r},t)$, is chosen as the frame of reference, the component fluxes become

$$\mathbf{J}_i = c_i\mathbf{v}_{\mathrm{ref}} + \mathbf{J}_{i,\mathrm{ref}} \tag{6.23}$$

$$\mathbf{J}_s = s\mathbf{v}_{\mathrm{ref}} + \mathbf{J}_{s,\mathrm{ref}} \quad \text{and} \quad \mathbf{J}_{s,\mathrm{ref}} = \frac{\mathbf{J}'_q}{T} + \sum_{i=1}^{n}\mathbf{J}_{i,\mathrm{ref}}\,S_i$$

The corresponding entropy production is:

$$\sigma = \mathbf{J}'_q \cdot \nabla \frac{1}{T} - \sum_{i=1}^{n} \mathbf{J}_{i,\mathrm{ref}} \cdot \frac{1}{T} \nabla \mu_{i,T} + (\mathbf{v} - \mathbf{v}_{\mathrm{ref}}) \cdot \frac{1}{T} \nabla p - \frac{1}{T} \mathbf{\Pi} : \nabla \mathbf{v} - r \frac{\Delta_r G}{T} \tag{6.24}$$

where $(\mathbf{v} - \mathbf{v}_{\mathrm{ref}}) \cdot (\nabla p)/T$ appears as an additional vectorial flux-force pair. From the discussion in the previous Section it is clear that two of the vectorial flux-force pairs depend on the others. This makes the use of an arbitrary reference velocity impractical when $\nabla p \neq 0$. The term disappears when the barycentric velocity is chosen as the frame of reference, $\mathbf{v}_{\mathrm{ref}} = \mathbf{v}$. This is the case discussed in the previous Section.

6.3 Stationary pipe flow

Material is flowing along a pipe because a pressure difference is applied. It is often a practical aim to obtain stationary flow conditions. Consider therefore stationary Poisseuille flow. The flow is characterized by a parabolic velocity profile with a shearing force equal to minus the gradient of the pressure down the pipe. When the density is constant, there are no other mechanical forces.

The mechanical forces are balanced in the stationary state. It follows from Eqs. (A.14) that

$$0 = \nabla \cdot (\rho \mathbf{v}\mathbf{v} + \mathbf{\Pi} + p\mathbf{1}) \tag{6.25}$$

We restrict ourselves to incompressible laminar flow. The velocity has the direction of the pressure gradient and changes only in the direction normal to this gradient. It follows that $\nabla \cdot (\rho \mathbf{v}\mathbf{v}) = 0$. Eq. (6.25) then simplifies to

$$\nabla \cdot \mathbf{\Pi} = -\nabla p \tag{6.26}$$

From Eqs. (A.38) we obtain the entropy balance in the stationary state

$$\nabla\cdot\mathbf{J}_s = \nabla\cdot(s\mathbf{v} + \mathbf{J}_{s,\mathrm{bar}}) = \sigma \tag{6.27}$$

where $\mathbf{J}_{s,\mathrm{bar}}$ and σ are given by Eqs. (A.51) and (A.52):

$$\mathbf{J}_{s,\mathrm{bar}} = \frac{\mathbf{J}_q - \sum_{k=1}^{n}\mu_k\mathbf{J}_{k,\mathrm{bar}}}{T} \tag{6.28}$$

$$\sigma = \mathbf{J}_q\cdot\nabla\frac{1}{T} - \sum_{k=1}^{n}\mathbf{J}_{k,\mathrm{bar}}\cdot\nabla\frac{\mu_k}{T} - \frac{1}{T}\boldsymbol{\Pi} : \nabla\mathbf{v} - r\frac{\Delta_r G}{T} \tag{6.29}$$

As the viscous pressure is now controlled by the pressure gradient, rather than being an independent response to the velocity gradient, we should rewrite the last two equations to reflect this. We have

$$\begin{aligned}\frac{1}{T}\boldsymbol{\Pi} : \nabla\mathbf{v} &= \nabla\cdot\frac{\boldsymbol{\Pi}\cdot\mathbf{v}}{T} - (\nabla\cdot\boldsymbol{\Pi})\cdot\frac{\mathbf{v}}{T} - \mathbf{v}\cdot\boldsymbol{\Pi}\cdot\nabla\frac{1}{T}\\ &= \nabla\cdot\frac{\boldsymbol{\Pi}\cdot\mathbf{v}}{T} + \frac{\mathbf{v}}{T}\cdot\nabla p - \mathbf{v}\cdot\boldsymbol{\Pi}\cdot\nabla\frac{1}{T}\end{aligned} \tag{6.30}$$

where we used the symmetric nature of the viscous pressure tensor, and Eq. (6.26). Substituting this equality we can write the entropy balance in Eq. (6.27) in the form

$$\nabla\cdot(s\mathbf{v} + \mathbf{J}_{s,\mathrm{pipe}}) = \sigma_{\mathrm{pipe}} \tag{6.31}$$

where

$$\mathbf{J}_{s,\mathrm{pipe}} = \frac{\mathbf{J}_{q,\mathrm{pipe}} - \sum_{k=1}^{n}\mu_k\mathbf{J}_{k,\mathrm{bar}}}{T} \tag{6.32}$$

$$\sigma_{\mathrm{pipe}} = \mathbf{J}_{q,\mathrm{pipe}}\cdot\nabla\frac{1}{T} - \sum_{k=1}^{n}\mathbf{J}_{k,\mathrm{bar}}\cdot\nabla\frac{\mu_k}{T} - \frac{\mathbf{v}}{T}\cdot\nabla p - r\frac{\Delta_r G}{T} \tag{6.33}$$

A new total heat flux appears

$$\mathbf{J}_{q,\mathrm{pipe}} = \mathbf{J}_q + \mathbf{v}\cdot\boldsymbol{\Pi} \tag{6.34}$$

Here the name energy flux, may be more appropriate. The condition of mechanical equilibrium in the pipe flow has lead to two important changes in the equations. The first is that the viscous force-flux pair in the entropy is replaced by a velocity $(\nabla p)/T$ flux-force pair. This flux-force pair gives Darcy's law for pipe flow. The second change is an additional $\mathbf{v}\cdot\mathbf{\Pi}$ contribution in the energy flux. Experimental or theoretical studies of pipe flow should take this into account. The additional contribution to the energy flux, appears in the energy balance.

6.3.1 The measurable heat flux

The measurable heat flux can be directly connected to experiments:

$$\mathbf{J}'_{q,\text{pipe}} = \mathbf{J}_{q,\text{pipe}} - \sum_{k=1}^{n} H_k \mathbf{J}_{k,\text{bar}} \tag{6.35}$$

If we substitute this relation into Eq. (6.32), we find

$$\mathbf{J}_{s,\text{pipe}} = \frac{\mathbf{J}'_{q,\text{pipe}} + \sum_{k=1}^{n} S_k \mathbf{J}_{k,\text{bar}}}{T} \tag{6.36}$$

By using the measurable heat flux in the entropy production, (6.33), we obtain

$$\begin{aligned}\sigma &= \mathbf{J}'_{q,\text{pipe}} \cdot \nabla \frac{1}{T} - \sum_{k=1}^{n} \mathbf{J}_{k,\text{bar}} \cdot \frac{\nabla \mu_{k,T}}{T} - \frac{\mathbf{v}}{T} \cdot \nabla p - r\frac{\Delta_r G}{T} \\ &= \mathbf{J}'_{q,\text{pipe}} \cdot \nabla \frac{1}{T} - \sum_{k=1}^{n-1} \mathbf{J}_{k,\text{bar}} \cdot \frac{1}{T}\left(\nabla \mu_{k,T} - \frac{M_k}{M_n}\nabla \mu_{n,T}\right) \\ &\quad - \frac{\mathbf{v}}{T}\cdot\nabla p - r\frac{\Delta_r G}{T}\end{aligned} \tag{6.37}$$

where the subscript T of the chemical potential indicates that the gradient is taken keeping the temperature constant.

The resulting flux-force relations for the vectorial fluxes are

$$\begin{aligned}
\mathbf{J}'_{q,\text{pipe}} &= L_{qq}\nabla\frac{1}{T} - \frac{1}{T}\sum_{k=1}^{n-1} L_{qk}\left(\nabla\mu_{k,T} - \frac{M_k}{M_n}\nabla\mu_{n,T}\right) \\
&\quad - L_{qp}\frac{1}{T}\nabla p \\
\mathbf{J}_{j,\text{bar}} &= L_{jq}\nabla\frac{1}{T} - \frac{1}{T}\sum_{k=1}^{n-1} L_{jk}\left(\nabla\mu_{k,T} - \frac{M_k}{M_n}\nabla\mu_{n,T}\right) \\
&\quad - L_{jp}\frac{1}{T}\nabla p \\
\mathbf{v} &= L_{pq}\nabla\frac{1}{T} - \frac{1}{T}\sum_{k=1}^{n-1} L_{pk}\left(\nabla\mu_{k,T} - \frac{M_k}{M_n}\nabla\mu_{n,T}\right) \\
&\quad - L_{pp}\frac{1}{T}\ \nabla p
\end{aligned} \tag{6.38}$$

The matrix of conductivities is symmetric. For the scalar flux-force pair one obtains

$$r = -L_r\Delta_r G \tag{6.39}$$

where we absorbed the factor $1/T$ in L_r.

6.4 The plug flow reactor

The plug flow model for chemical reactions gives a first order approximation to phenomena that take place in a chemical reactor. Equation (6.37) is used as a starting point. Thermal conduction is frequently neglected in the axial direction. Diffusion relative to the barycentric frame of reference is also neglected, and a pressure gradient is assumed only along the reactor, in the z-direction, not in the radial direction. The local entropy production becomes

$$\sigma = \mathbf{J}'_{q,\text{pipe}}\frac{d}{dr}\frac{1}{T} - \frac{\mathbf{v}}{T}\cdot\frac{dp}{dz} - r\frac{\Delta_r G}{T} \tag{6.40}$$

The tube has diameter D. We integrate over the cross-sectional area, Ω, and obtain the entropy production on a unit length basis

$$\sigma' = \Omega\,\rho_{\mathrm{B}}\,\sum_j \left[\, r_j\,\left(-\frac{\Delta_{\mathrm{r}}G_j}{T}\right)\,\right] + \pi\,D\,J'_q\,\Delta\frac{1}{T} + \Omega\,v\,\left(-\frac{1}{T}\,\frac{dp}{dz}\right) \tag{6.41}$$

This equation is the starting point of the studies of energy efficient reactor design in Section 10.1.2, see Eq. (10.3).

6.5 Concluding remarks

We have seen that the systematic treatment prescribed by non-equilibrium thermodynamics helps to define and relate fluxes and forces in systems with viscous flow. The Navier-Stokes equation fits well into the format of the theory. The entropy production is the origin of viscous heating or Rayleigh dissipation. Coupling of the reaction to compressional shearing is little studied.

Our analysis allows a systematic evaluation of the shear- contribution to the entropy production and the equations of motion. This has a bearing on optimal design of process equipment. The optimal state may arise from a trade-off between shear contributions (viscous dissipation) and losses due to heat and mass transport, see Chapter 10.

Chapter 7

Chemical reactions

Chemical reactions have rates which normally are non-linear in their driving force. In order to describe this and derive the law of mass action using non-equilibrium thermodynamics, we shall introduce as internal variable, the probability that the reaction is in a state γ on the path between the reactant and product states. The processes along this path occur on an intermediate (mesoscopic) level, and the extended theory is called mesoscopic non-equilibrium thermodynamics. A linear force-flux relation along the mesoscopic reaction path leads to a non-linear macroscopic law of an Arrhenius-type. This theory captures the nature of the chemical reaction, and gives it a thermodynamic basis.

Spontaneous chemical reactions have high rates of energy dissipation. The contribution to the entropy production from the chemical reaction was given in Chapter 3

$$\sigma = r\left(-\frac{\Delta_r G}{T}\right) \tag{7.1}$$

We shall learn in Chapter 10 how this entropy production can

be minimized in chemical reactors. The expression (7.1) is valid, whenever the Gibbs equation is valid, cf. remark 3.2.

A problem is that the relation between the reaction rate r and $\Delta_r G$ is normally non-linear. In the theory of non-equilibrium thermodynamics discussed in Chapters 1-6, the fluxes (rates) are linear functions of the driving forces. For chemical reactions we then have

$$r = -l\frac{\Delta_r G}{T} \tag{7.2}$$

For a numerical example, see [62]. But such relations do not normally apply to chemical reactions that occur in the industry. Take as an example the elementary reaction

$$\mathrm{A} + \mathrm{B} \rightleftharpoons \mathrm{C} + \mathrm{D}$$

In standard chemical reaction kinetics [63], the rate of such a reaction is described as

$$r = k_f c_A c_B - k_r c_C c_D \tag{7.3}$$

where k_f and k_r are kinetic constants for the forward and the reverse reaction, and c_i is the concentration of i. This follows by applying the law of mass action.

A rate like (7.3) can be used with Eq. (7.1), but a thermodynamic expression for r which contains the explicit limit that $r = 0$ for $\Delta_r G = 0$, is preferable for optimization studies. The purpose of this Chapter is to present such an expression. We shall also see that the thermodynamic form contains a generalized version of the law of mass action. The thermodynamic expression for the reaction rate is useful for engineers who want to consider a chemical reactor, not only as a producer of chemicals, but also as a work-producing or work consuming apparatus. This viewpoint is essential for designing an optimal reactor with minimal entropy production, where fluxes of heat, mass, and reaction rate have to be balanced, cf. Chapters 9 and 10.

The variables of the reaction Gibbs energy, $\Delta_r G(T, p, N_1, ...N_n)$ of Eqs. (7.1 and 7.2) are macroscopic variables, meaning that they can be controlled from the outside of the system. The Gibbs energy of reaction is determined by two states: the reactant state and the product state. We need to describe the transition from reactants to products on a more detailed level. For this purpose we introduce the reaction path along which the reacting complex passes on its way from reactants to products. This reaction path, which is a well known concept in reaction kinetics, will be called the internal coordinate γ for the chemical reaction. The coordinate is continuous and varies between 0 (for reactants) and 1 (for products). The end points can be chosen without any loss of generality. The internal variable is now the probability, $c(\gamma)$, that the reaction is in the state γ. It is not possible to independently control an internal variable from the outside.

The use of internal variables was first proposed by Prigogine and Mazur, see ref. [12]. It was recently used by Rubi and coworkers [27, 64, 65] to describe nucleation, evaporation, and molecular pumps.

The extension of the theory to the mesoscopic level is called *mesocopic* non-equilibrium thermodynamics. In this Chapter, we shall see how mesocopic non-equilibrium thermodynamics can be used to give rate equations that are useful in thermodynamic applications as well as in reaction kinetics.

We recapitulate first the procedure to calculate the chemical driving force $-\Delta_r G/T$ in Section 7.1 before we proceed to the mesoscopic description in Section 7.2. The temperature shall be taken constant in the analysis in this Chapter.

7.1 The Gibbs energy change of a chemical reaction

The variation in the Gibbs energy with the composition, at constant p, T is, for the above reaction is

$$dG = \mu_A dN_A + \mu_B dN_B + \mu_C dN_C + \mu_D dN_D \tag{7.4}$$

The Gibbs energy of a mixture is given in the Appendix A.2. The reaction relates the changes in mole numbers, leading to the definition of the extent of the reaction, $d\xi$

$$d\xi \equiv dN_C = dN_D = -dN_A = -dN_B \tag{7.5}$$

In general, we have

$$\mathrm{d}\xi = \frac{\mathrm{d}N_i}{\nu_i} \tag{7.6}$$

where ν_i is a stoichiometric coefficient, negative for reactants and positive for products.

The Gibbs energy is plotted in Fig. 7.1. The reacton Gibbs energy, $\Delta_r G$, is obtained as the derivative of the mixture Gibbs energy with respect to the extent of reaction, illustrated for one composition by the tangent to the curve in Fig. 7.1.

$$\Delta_r G \equiv \left(\frac{\partial G}{\partial \xi}\right)_{T,p} = \sum_{i=1}^{n} \nu_i \mu_i \tag{7.7}$$

This is the reaction Gibbs energy used in Eq. (3.3).

A reaction that spontaneously converts reactants to products has a negative slope. A positive slope means that the backwards reaction occurs spontaneously. At equilibrium $\Delta_r G = 0$. This state is represented by the minimum of the curve in Fig. 7.1 at $\xi = \xi^{equilibrium}$.

We are concerned with reactions in incompressible liquid phases. Appendix A.3 describes how to calculate the chemical potential

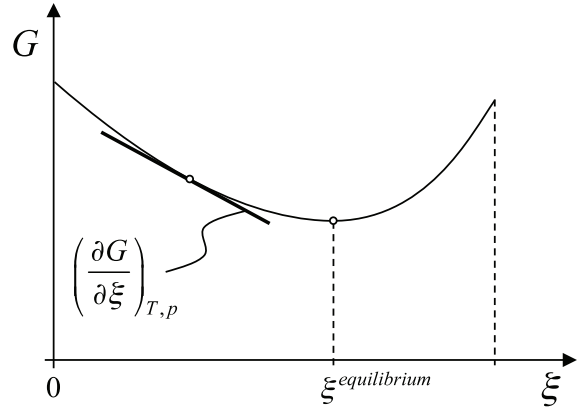

Figure 7.1: Gibbs energy of a reacting mixture as a function of the extent of reaction. The reaction Gibbs energy is the tangent to the curve.

and the driving force for a chemical reaction. We use Eqs. (A.79) and (A.80) in this Appendix, and find the chemical potential as a function of fugacity f_i for the components A, B, C and D in the mixture

$$\Delta_r G = \mu_C^{\ominus} + \mu_D^{\ominus} - \mu_A^{\ominus} - \mu_B^{\ominus} + RT \ln \frac{f_C f_D}{f_A f_B} \tag{7.8}$$

where the standard pressure $p^{\ominus} = 1$ bar, and $\mu_i^{\ominus}$ is the chemical potential of component i in the standard state. At equilibrium, when $\Delta_r G = 0$,

$$\begin{aligned} \Delta_r G^{\ominus} &= -RT \ln K \\ K &= \left(\frac{f_C f_D}{f_A f_B}\right)_{eq} = \left(\frac{x_C x_D}{x_A x_B}\frac{\gamma_C \gamma_D}{\gamma_A \gamma_B}\right)_{eq} \end{aligned} \tag{7.9}$$

where K is the dimensionless thermodynamic equilibrium constant. The general form of Eq. (7.8) is

$$\Delta_r G = \sum_{i=1}^{n} \nu_i \mu_i^{\ominus} + RT \ln \left(\prod_i^n f_i^{\nu_i}\right) \tag{7.10}$$

For the equilibrium constant this gives

$$K = \prod_i^n f_{i,eq}^{\nu_i} = \prod_i^n x_{i,eq}^{\nu_i} \gamma_{i,eq}^{\nu_i} \tag{7.11}$$

where x_i and γ_i are the mole fraction and the activity coefficient of component i, respectively. The equilibrium constant, K, is used to replace $\Delta_r G^{\ominus}$ in Eq. (7.8). This gives

$$\Delta_r G = RT \ln \left(\prod_i^n \left(\frac{f_i}{f_{i,eq}} \right)^{\nu_i} \right) = RT \ln \left(\prod_i^n \left(\frac{x_i}{x_{i,eq}} \right)^{\nu_i} \left(\frac{\gamma_i}{\gamma_{i,eq}} \right)^{\nu_i} \right) \tag{7.12}$$

In an ideal mixture all γ_i are equal to one.

The Gibbs-Helmholtz equation gives the temperature dependence of the equilibrium constant. For a reaction in a gas or liquid mixture

$$d \ln K = -\frac{\Delta_r H^{\ominus}}{R} d \left(\frac{1}{T} \right) \tag{7.13}$$

The equilibrium constant can be obtained from pure component data. In order to calculate the driving force, we need data for the actual mixture.

Exercise 7.1.1 *Calculate the driving force for the esterification reaction at $T = 473K$ and $p = 2.5MPa$.*

$$\underbrace{CH_3COOH}_{acetic\ acid} + \underbrace{C_2H_5OH}_{ethanol} \rightleftharpoons \underbrace{CH_3COOC_2H_5}_{ethyl\ acetate} + H_2O$$

The composition is $x_{CH_3COOH} = 0.2$, $x_{C_2H_5OH} = 0.2$, $x_{CH_3COOC_2H_5} = 0.2$, and $x_{H_2O} = 0.4$, and the mixture is considered ideal. The Gibbs energies of formation at standard pressure and 298 K are given in the table

	$\Delta_f G^\ominus$ / kJ/mol	$\Delta_f H^\ominus$/ kJ/mol	ν_i	x_i
acetic acid	−374.3	-432.2	−1	0.2
ethanol	−167.7	-234.9	−1	0.2
ethyl acetate	−328.0	-444.5	1	0.2
water	−228.4	-241.8	1	0.4

- **Solution:** The standard reaction Gibbs energy calculated from the table is $(374.3 + 167.7 - 328.0 - 228.4) = -14.4$ kJ/mol. The corresponding value for $\Delta_r G^\ominus/RT = -5.8$ so the equilibrium constant at 298 K becomes $K_{298} = 0.003$.

  The standard reaction enthalpy according to the table is $\Delta_r H^\circ = (432 + 235 - 444 - 242) = -19.1$ kJ/mol. We assume that the enthalpy of reaction is constant with temperature, and calculate K for 473 K using Gibbs-Helmholtz equation (7.13). This gives $\ln K_{473} = 5.8 - 2.8 = 3.0$. The exothermal reaction is shifted to the left by raising the temperature, in agreement with Le Chaterlier's principle. The driving force for the reaction at this temperature becomes

$$\begin{aligned} -\frac{\Delta_r G_{473}}{T} &= R \ln K_{473} - R \ln \left(\prod_{i=1}^{n} (x_i)^{\nu_i} \right) \\ &= 8.314 \text{ J/(mol K)} \left(3.0 - \ln \left(\frac{0.1^1 0.7^1}{0.1^1 0.1^1} \right) \right) \\ &= 8.5 \text{ J/(mol K)} \end{aligned}$$

Exercise 7.1.2 *For the mixture specified in 7.1.1 calculate the equilibrium values of the mole fractions.*

- **Solution:** For equilibrium conditions in the ideal mixture (all $\gamma_i = 1$), we have from Eq. (7.9)

$$K = \frac{x_C x_D}{x_A x_B}$$

Consider one mole of the initial mixture, $N^* = 1$ mole. The initial amount of any substance N_i^* is then identical to the mole fraction, $N_i^* = x_i\ N^*$. At a given time, the extent of reaction is ξ. Any amount of substance is

$$N_i = N_i^* + \nu_i \xi$$

The total amount of substances is $N = \sum_{i=1}^{n} N_i = N^* + \xi \sum_{i=1}^{n} \nu_i$ and the mole fraction for any extent of reaction is

$$x_i = N_i^*/N + \nu_i\ \xi/N$$

In the considered case the amount of substance does not change, $N = N^* = 1$ mol. At equilibrium the extent of reaction is ξ_{eq}.

$$K = \frac{(0.1 + \xi_{eq}/\text{mol})(0.7 + \xi_{eq}/\text{mol})}{(0.1 - \xi_{eq}/\text{mol})(0.1 - \xi_{eq}/\text{mol})}$$

This quadratic equation in ξ_{eq} can be solved using $K = 19.4$, and gives $\xi_{eq} = 0.030$ mol. The mole fractions are then $x_{C_2H_5OH} = 0.07$, $x_{CH_3COOH} = 0.07$, $x_{CH_3COOC_2H_5} = 0.13$, and $x_{H_2O} = 0.73$.

7.2 The reaction path

For a given composition ξ there is a continuous sequence of states between the pure reactant state with $\gamma = 0$ and the pure product state with $\gamma = 1$. The probability to find the the reaction complex in the state γ between these two states is given by $c(\gamma)$. The reacting complex changes its energetic along the path. The left side of Fig. 7.2 shows the energy of the reacting complex, Φ, plotted versus γ. The picture shows that the reaction has an energy barrier, with a peak at a particular value of γ. The reaction must be activated to this level in order to proceed, even if the energy of the energy of the products are lower than that

of the reactants. The fact that there exists an energy barrier for conversion of reactants into products is not manifested in Fig. 7.1.

The coordinate γ is thus a *mesoscopic* measure for the progress of a reaction in any macroscopic state with a composition ξ. The mesoscopic state of the system is given by the probability density $c(\gamma)$ of a reacting complex to be in the state γ. This probability density is our internal variable.

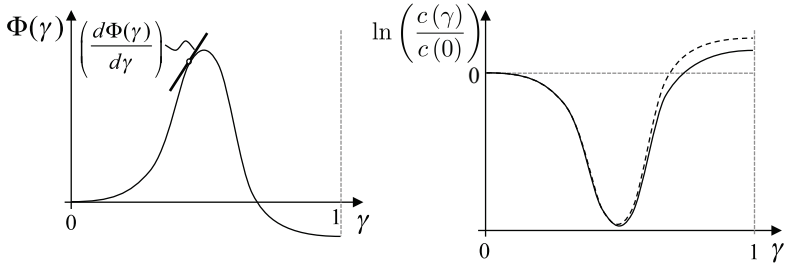

Figure 7.2: The two contributions to the chemical potential of the reacting mixture in internal coordinate space, cf. Eq. (7.14). The left diagram illustrates the energy barrier of a chemical reaction. The right diagram shows the logarithm of the probability density of having molecules in a state characterised by the coordinate γ (solid line). The dashed line is for chemical equilibrium.

7.2.1 The chemical potential

The logarithm of the probability for the reacting complex is illustrated in Fig. 7.2 (right). The probability of finding reacting complexes at the peak of the energy barrier in $\Phi(\gamma)$ (left) is low.

The chemical potential $\mu(\gamma)$ has an entropic part and an en-

thalpic part $\Phi(\gamma)$

$$\mu(\gamma) = \mu(0) + RT \ln \frac{c(\gamma)}{c(0)} + \Phi(\gamma) \tag{7.14}$$

where $\mu(0)$ is the reference chemical potential, see Fig. 7.2. The probability distribution of $c(\gamma)$ is here not normalized. Instead of such a normalization we choose $c(0)$ such that $\mu(0) = RT \ln c(0)$. This means that $\Phi(0) = 0$, as shown in the left side of Fig. 7.2 and $\Phi(1) = \mu(1) - RT \ln c(1)$. The activation energy for the forward reaction is measured with respect to $\Phi(0) = 0$.

In equilibrium, the chemical potential is constant along the reaction coordinate, $\mu_{eq} = \mu_{eq}(\gamma) = \mu_{eq}(0)$. Using Eq. (7.14) it then follows that

$$c_{eq}(\gamma) = c_{eq}(0) \exp\left(-\frac{\Phi(\gamma)}{RT}\right) \tag{7.15}$$

Equation (7.15) is used to illustrate the dashed line in Fig. 7.2 (right). In equilibrium only a few molecules reach the top of the barrier $\Phi(\gamma)$, so the probability of this state $c_{eq}(\gamma)$ is low. Also away from equilibrium (solid line in Fig. 7.2) the probability of a reacting complex $c(\gamma)$ is small at the high energy barrier. The potential profile $\Phi(\gamma)$ is the same for an equilibrium and a non-equilibrium system for all values of the composition ξ.

The value of $\mu(\gamma)$ at the boundaries is known. For a reaction $2A \rightleftharpoons B$, the reactants' chemical potential is $\mu(\gamma = 0) = |-2|\ \mu_A$ and the product $\mu(\gamma = 1) = +1\ \mu_B$. More general, the chemical potential $\mu(0)$ is

$$\begin{aligned} \mu(0) &= \sum_i^{\{\text{reactants}\}} |\nu_i|\ \mu_i = \sum_i^{\{\text{reactants}\}} |\nu_i|\ \left[\mu_i^{\ominus} + RT \ln f_i\right] \\ &= \sum_i^{\{\text{reactants}\}} |\nu_i|\ \left[\mu_i^{\ominus} + RT \ln (x_i \gamma_i)\right] \end{aligned} \tag{7.16}$$

Here the activity coefficients γ_i are defined by $f_i = x_i p^{\ominus} \gamma_i$ which reduces to $f_i = x_i \gamma_i$ for the standard state pressure $p^{\ominus} = 1$ bar. The chemical potential of the products is

$$\mu(1) = \sum_{i}^{\{\text{products}\}} \nu_i \left[\mu_i^{\ominus} + RT \ln (x_i \gamma_i)\right] \tag{7.17}$$

Together with Eq. (7.14) these two relations determine $c(0)$ and $c(1)$. The standard state of $\mu(0)$ and $\mu(1)$ is the same as the standard states of the reactants together and the products together, respectively, see also Eqs. (7.16) and (7.17).

7.2.2 The entropy production

The entropy production along the γ-coordinate is again the product of a flux $r(\gamma)$ and a driving force $-(1/T)(d\mu(\gamma)/d\gamma)$:

$$\sigma(\gamma) = -r(\gamma) \frac{1}{T} \frac{\partial \mu(\gamma)}{\partial \gamma} \tag{7.18}$$

This equation can be compared to Eq. (7.1). It has the same form, but is now written on a smaller scale, the mesoscale. The resulting flux-force relation is

$$r(\gamma) = -\frac{l(\gamma)}{T} \frac{\partial \mu(\gamma)}{\partial \gamma} \tag{7.19}$$

The variation in the chemical potential for a reaction complex is illustrated in Fig. 7.3. We see the reactant and product states for a reaction, say of $2\mathrm{A} \rightleftharpoons \mathrm{B}$, and the smooth transition between the states. The entropy production in γ-space is everywhere positive.

7.3 A rate equation with a thermodynamic basis

The large (compared to RT) energy barrier in Fig. 7.2 hinders the chemical reaction. The conditions at the barrier peak are

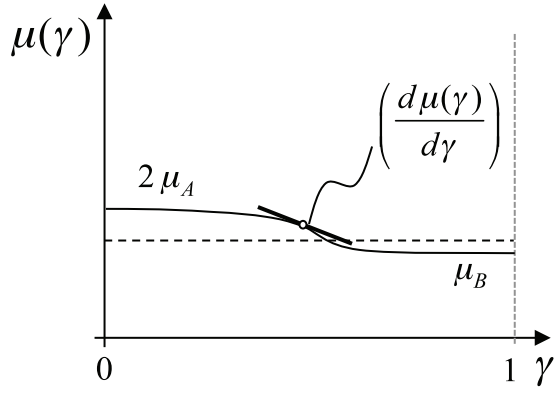

Figure 7.3: The variation in the chemical potential for a reaction ($2A \rightleftharpoons B$) along the mesoscopic reaction coordinate γ. The dashed line is for equilibrium.

decisive for the overall rate. A quasi-stationary state thus develops, making the reaction rate constant along the coordinate, $r(\gamma) = r$. Using this property and the boundary conditions of Eqs. (7.16) and (7.17), we can integrate Eq. (7.18) to

$$\sigma_r = -r\frac{\mu(1) - \mu(0)}{T} = r(-\frac{\Delta_r G}{T}) \tag{7.20}$$

which is equal to Eq. (7.1). The integrated entropy production along the γ-coordinate is equal to the macroscopic value, which it should be.

The chemical reaction can be seen as a diffusion process along the reaction coordinate over the activation energy barrier, see Fig. 7.2 (left). The conductivity $l(\gamma)$ in Eq. (7.19) is in good approximation proportional to the probability density $c(\gamma)$ [66], and we introduce a constant diffusion coefficient by

$$D_r \equiv \frac{Rl(\gamma)}{c(\gamma)} \tag{7.21}$$

Substituting this relation into Eq. (7.19), using Eq. (7.14) and that r is constant, we find

$$\begin{aligned} r &= -\frac{D_r c(\gamma)}{RT}\frac{\partial \mu(\gamma)}{\partial \gamma} \\ &= -\frac{D_r c(0)}{RT}\exp\left(-\frac{\Phi(\gamma)}{RT}\right)\exp\left(\frac{\mu(\gamma)-\mu\,(0)}{RT}\right)\frac{\partial \mu(\gamma)}{\partial \gamma} \\ &= -D_r c(0)\exp\left(-\frac{\Phi(\gamma)}{RT}\right)\frac{\partial}{\partial \gamma}\exp\left(\frac{\mu(\gamma)-\mu\,(0)}{RT}\right) \end{aligned} \tag{7.22}$$

After multiplying this equation with $\exp\left(\Phi(\gamma)/RT\right)$, it can be integrated and we obtain

$$r = l_{rr}\left(1-\exp\frac{\Delta_r G}{RT}\right) \tag{7.23}$$

where l_{rr} is given in the next Section. The flux-force relation becomes a non-linear one after integration over the internal coordinate. This is the preferred expression for the reaction rate to be used in the entropy production of Chapters 3, 6 and 10. The coefficient l_{rr} is the macroscopic conductivity which does not explicitly depend on γ.

We see that the expression gives $r = 0$ for the equilibrium condition $\Delta_r G = 0$, and that a Taylor expansion of the exponential gives the linear relation (7.3) close to equilibrium, when $\Delta_r G << RT$. The coefficient l_{rr} must be determined from experiments.

We shall next see that the thermodynamic rate equation contains the law of mass action, which has been documented by numerous observations since its discovery in 1864 [67].

7.4 The law of mass action

The law of mass action can be derived from the thermodynamic description given in the previous Section. This was first done by Prigogine and Mazur for ideal mixtures, see [12, 65]. The macroscopic conductivity coefficient is

$$\begin{aligned} l_{rr} =& \frac{1}{r_{rr}} = D_r c(0) \left[\int_0^1 \exp \frac{\Phi(\gamma)}{RT} d\gamma \right]^{-1} \\ =& D_r \exp \frac{\mu(0)}{RT} \left[\int_0^1 \exp \frac{\Phi(\gamma)}{RT} \right]^{-1} \\ =& D_r \left[\int_0^1 \exp \frac{\Phi(\gamma)}{RT} d\gamma \right]^{-1} \prod_i^{\{\text{reactants}\}} \exp \frac{|\nu_i| \, \mu_i}{RT} \\ =& D_r \left[\int_0^1 \exp \frac{\Phi(\gamma)}{RT} d\gamma \right]^{-1} \prod_i^{\{\text{reactants}\}} f_i^{|\nu_i|} \exp \frac{|\nu_i| \mu_i^\circ}{RT} \end{aligned} \tag{7.24}$$

Here we used Eq. (7.16).

In the field of reaction kinetics [63], the rate has two contributions. The forward reaction rate is according to collision theory proportional to a kinetic coefficient and the concentrations of the reactants. The reverse reaction is proportional to a kinetic coefficient and the concentrations of the products.

By introducing Eqs. (7.16) and (7.17), the reaction rate becomes

$$\begin{aligned} r =& D_r \left[\int_0^1 \exp \frac{\Phi(\gamma)}{RT} d\gamma \right]^{-1} \\ & \times \left\{ \prod_i^{\{\text{reactants}\}} f_i^{|\nu_i|} \exp \frac{|\nu_i| \mu_i^\circ}{RT} - \prod_i^{\{\text{products}\}} f_i^{\nu_i} \exp \frac{\nu_i \mu_i^\circ}{RT} \right\} \end{aligned}$$

or

$$r = \underbrace{D_r \frac{\exp\left(\sum_i^{\{\text{reactants}\}} \frac{|\nu_i|\mu_i^\circ}{RT}\right)}{\left[\int_0^1 \exp\frac{\Phi(\gamma)}{RT} d\gamma\right]}}_{k_f}$$

$$\times \left\{ \prod_i^{\{\text{reactants}\}} f_i^{|\nu_i|} - \underbrace{\exp\left(\sum_{i=1}^{n} \frac{\nu_i \mu_i^\circ}{RT}\right)}_{1/K} \prod_i^{\{\text{products}\}} f_i^{\nu_i} \right\}$$

which gives

$$r = k_f \prod_i^{\{\text{reactants}\}} (f_i)^{|\nu_i|} - k_r \prod_i^{\{\text{products}\}} (f_i)^{\nu_i} \tag{7.25}$$

Values of the kinetic coefficients vary by many orders of magnitude for various systems, mainly due to different heights of the energy barrier. The energy barrier typically has a narrow maximum which is large compared to RT at the so-called transition state γ_0. We may therefore write

$$\int_0^1 \exp\frac{\Phi(\gamma)}{RT} d\gamma = A \exp\frac{\Phi(\gamma_0)}{RT} \tag{7.26}$$

This factor leads to the well known Arrhenius behavior of the kinetic coefficients.

The forward and reverse kinetic coefficients are related by

$$k_r = k_f / K \tag{7.27}$$

This relation between the kinetic coefficients ensures that the reaction rate vanishes in the equilibrium state. Only one kinetic coefficient is independent in Eq. (7.25).

For ideal mixtures with $\gamma_i = 1$, Eq. (7.25) can be written in the form familiar from reaction kinetics

$$r = k_f \prod_i^{\{\text{reactants}\}} c_i^{|\nu_i|} - k_r \prod_i^{\{\text{products}\}} c_i^{\nu_i} \tag{7.28}$$

This shows how the thermodynamic equation for r can be reduced to the law of mass action for ideal mixtures.

7.5 The entropy production on the mesoscopic scale

We have postulated the local entropy production $\sigma(\gamma)$ as a product of a flux and the driving force along the γ-coordinate. We can substantiate this by analyzing the entropy production. We study the properties of the mixture at one point in Fig. 7.1 and along the coordinate. We assume local equilibrium for any mesoscopic state γ, so that the Gibbs equation is valid locally. The differential of the entropy due to a change $\delta c(\gamma)$ in the probability distribution is given by

$$\delta s = -\frac{1}{T} \int_0^1 \mu(\gamma) \delta c(\gamma) d\gamma \tag{7.29}$$

We did not consider changes in internal energy or volume in this expression, and we do not indicate the time dependence explicitly, to simplify notation. When the mixture is in chemical equilibrium,

$$\delta s = -\frac{1}{T} \int_0^1 \mu_{eq}(\gamma) \delta c(\gamma) d\gamma = 0 \tag{7.30}$$

Mass is conserved, so

$$\int_0^1 \delta c(\gamma) d\gamma = 0 \tag{7.31}$$

It follows from Eqs. (7.30) and (7.31) that the equilibrium chemical potential is independent of γ in equilibrium. It is constant, as illustrated in Fig. 7.3.

The entropy change which follows from Eq. (7.29) is

$$\frac{\partial s}{\partial t} = -\frac{1}{T}\int_0^1 \mu(\gamma)\frac{\partial c(\gamma)}{\partial t}d\gamma \tag{7.32}$$

The number of reaction complexes are constant, so the time rate of change of the probability can be written as

$$\frac{\partial c(\gamma)}{\partial t} = -\frac{\partial r(\gamma)}{\partial \gamma} \tag{7.33}$$

By substituting this equation into Eq. (7.32) we obtain the entropy production integrated over the mesoscopic scale

$$\frac{\partial s}{\partial t} = \frac{1}{T}\int_0^1 \mu(\gamma)\frac{\partial r(\gamma)}{\partial \gamma}d\gamma \tag{7.34}$$

Partial integration then gives

$$\begin{aligned}\frac{\partial s}{\partial t} =& \frac{1}{T}\int_0^1 \frac{\partial \mu(\gamma) r(\gamma)}{\partial \gamma}d\gamma - \frac{1}{T}\int_0^1 r(\gamma)\frac{\partial \mu(\gamma)}{\partial \gamma}d\gamma \\ =& -\frac{\mu(0)}{T}r(0) + \frac{\mu(1)}{T}r(1) \\ & -\frac{1}{T}\int_0^1 r(\gamma)\frac{\partial \mu(\gamma)}{\partial \gamma}d\gamma\end{aligned} \tag{7.35}$$

The entropy flux along the γ-coordinate is given by

$$J_s(\gamma) = -\frac{\mu(\gamma) r(\gamma)}{T} \tag{7.36}$$

We see in Eq. (7.35) that the integral of the divergence of this flux along the γ-coordinate gives the difference of the entropy flux into the γ-coordinate at $\gamma = 0$ minus the flux out of the coordinate at $\gamma = 1$. The last term of Eq. (7.35) gives the local entropy production along the γ-coordinate, it is Eq. (7.18).

Exercise 7.5.1 *The potential $\Phi(\gamma)$ can in principle depend on the temperature and the pressure in the system. When $\Phi(\gamma)$ is assumed independent of both, show that the second and third terms in Eq. (7.14) are entropic and enthalpic contributions to the chemical potential, respectively.*

- **Solution:** When $\Phi(\gamma)$ is not a function of temperature and pressure, the entropy difference of a reaction complex in state γ and state $\gamma = 0$ becomes

$$s(\gamma) - s(0) = -\frac{\partial(\mu(\gamma) - \mu(0))}{\partial T} = -R \ln \frac{c(\gamma)}{c(0)} \qquad (7.37)$$

  It follows that the enthalpy difference along the reaction coordinate is given by

$$h(\gamma) - h(0) = \mu(\gamma) - \mu\,(0) + T\,(s(\gamma) - s(0)) = \Phi(\gamma) \quad (7.38)$$

  The reaction enthalpy is therefore $\Delta_r H = \Phi(1) - \Phi(0) = \Phi(1)$ with the reference chosen.

7.6 Concluding remarks

We have shown that chemical reactions can be given a thermodynamic basis through mesoscopic non-equilibrium thermodynamics. The chemical reaction can then be dealt with in the same systematic way as we can deal with other transport processes. All transport laws can then be derived from the entropy production in the system. This is an advantage when we want to minimize the entropy production in process equipments, see Chapter 10.

In this derivation, the reacting mixture has been characterized by a probability distribution over the available states along the reaction coordinate γ. The reaction proceeds by diffusion of the

reaction complex over an activation energy barrier. The rate is an explicit non-linear function of the driving force. When derived from this thermodynamic basis, the law of mass action contains fugacities rather than concentrations as variables.

This page intentionally left blank

Chapter 8

The lost work in the aluminum electrolysis

The purpose of this chapter is to map the entropy production in an industrial process and to discuss the information in such a map. The lost work in a 230 kA aluminum electrolysis cell is calculated from the entropy production in the various parts of the cell. The thermodynamic efficiency is calculated. The entropy production due to charge transfer and heat exchange are both large. The first can be changed by changing materials and electrode distances. The second can be changed by increasing the cell dimensions.

The energy balance is central for the aluminum electrolysis industry, because energy prices are central. An accurate control of the heat production is also crucial, to avoid cell disruption by metal leakage through the frozen crust. Much work has therefore been spent to determine the energy balance [68].

A good electrolysis cell in the 1980-90's used about 13 kWh of electric energy per kg aluminum produced [69]. Values be-

tween 14 and 18 kWh/kg_{Al} are normal [70]. The minimum energy needed for the electrolysis at room temperature is only 5.4 kWh/kg_{Al}. The lost work is the difference between these numbers. In this chapter we study the reasons for lost work, and discuss the possibilities for a reduction. Insight into this can be useful for cell design.

8.1 The aluminum electrolysis cell

Aluminum is produced from alumina, $Al_2O_3(s)$. Alumina is dissolved in molten cryolite, $Na_3AlF_6(l)$ before electrolysis. An oxygen-containing complex, probably $Al_2O_2F_6^{4-}$, reacts with the anode carbon (C) to give CO_2 (g), and to some degree also CO [71, 72]. The overall reaction is:

$$\frac{1}{6}Al_2O_3(s) + \frac{1}{4}C(s) \rightarrow \frac{1}{3}Al(l) + \frac{1}{4}CO_2(g) \qquad (8.1)$$

Since the bulk anode is in contact with air, there is also some excess carbon consumption:

$$C(s) + \frac{1}{2}O_2(g) \rightarrow CO(g) \qquad (8.2)$$

Carbon monoxide is thermodynamically more stable at the cell temperature and pressure than carbon dioxide. The gas stirs the bulk melt as it escapes and is collected at the top of the cell. The cell is illustrated schematically in Fig. 8.1. Aluminum is formed in the bottom of the cell. The metal layer on top of the carbon block forms the bulk cathode. The product is collected at regular intervals, typically once a day. While the feeding of alumina is nearly continuous, the tapping of aluminum and the replenishing of the anode carbon, are not, so the cell does not operate under steady state conditions. An operation close to such conditions is an aim, however.

The electrolyte is contained in the central part of the cell, on top

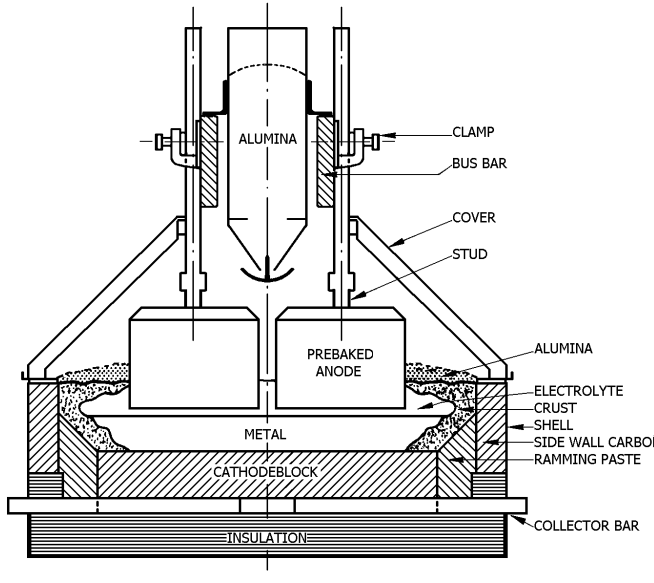

Figure 8.1: Cross section of the aluminum electrolysis cell. The metal is formed between the carbon anode and carbon bottom. Frozen electrolyte (crust) insulates the melt from the side walls. (Courtesy of K. Grjotheim)

of the aluminum pool. The bulk anode consists of several carbon blocks and steel connectors. Insulating material (alumina) covers the anode. The electrodes are prebaked (pre-made), and the anode is replaced as it is used. The cathode carbon conducts electric current from the metal to steel collector bars in the bottom of the cell. Many such cells are sequenced and the electric current goes from one cell via the electric connectors to the next. The insulation in the bottom and on the sides consists of refractories, which are heat-resistant bricks.

The electrolyte has an average temperature of 960 °C, and starts to freeze at 949^{o}C. The cell potential, measured between the anode beams of two neigbouring cells, is 4.1 V. The anode - cathode

distance is 4.50 cm. The anode surface area is 30 m^2, while the cathode surface area is 50 m^2 giving an anodic and cathodic current densities of $j_a = 7.7\text{x}10^3$ and $4.6\text{x}10^3$ A/m^2, respectively. A current efficiency of $y = 0.95$ can be obtained, giving 73.3 kg aluminum produced per hour. The current efficiency is defined as the fraction of the electrons which reduce Al^{3+}. These data are typical of a 230 kA cell of Hydro Aluminum in Øvre Årdal, Norway. Aluminum electrolysis cells draw typically between 100 and 310 kA.

The frozen side ledge prevents contact between the molten corrosive melt and the side lining (that consists of carbon, refractories and steel). It is imperative that the side ledge remains frozen for all conditions. This means that a careful control of the heat fluxes out of the cell is necessary. The heat fluxes through the cell surfaces have been measured. The heat flux through surface number k is $J'_{q,k}$ (in kW/m^2) and the surface area is A_k (in m^2). The heat loss through one surface is then $q_k = J'_{q,k}A_k$, see Table 8.1, and the total heat loss per kg of aluminum is

$$|q| = \sum_k q_k = \sum_k J'_{q,k}A_k = 6.5 \text{ kWh/kg}_{\text{Al}} \tag{8.3}$$

In order to be able to compare different factories, it is customary to give all quantities per kg of aluminum produced.

8.2 The thermodynamic efficiency

The thermodynamic efficiency gives an overall perspective on the energy transformation in the cell. Reactants enter and products leave the factory at temperature T_0 and pressure p_0, and these variables define the environment (compare Section 2.3). Electric work, w_{el}, is used to accomplish the cell reaction. The reactants are in practice heated to the temperature of the bath, where the reaction takes place, and the products are subsequently cooled to the temperature of the environment. The change in inter-

Table 8.1: Measured heat flows through the external surfaces of the electrolysis cell. The absolute values of the heat flows are given per kg aluminum produced. The current efficiency was 0.95.

External surface	**Absolute heat flow** / [$\mathrm{kWh/kg_{Al}}$]
Electrolyte cover	0.37
Cell sides	2.42
Cell ends	0.48
Cell bottom	0.71
Anode top	2.14
Iron conductors	0.35
Sum, $\|q\|$, Eq. (8.4)	6.5

nal energy between products and reactants at T_0 and p_0 is ΔU. Some energy is also used to do mechanical work on the surroundings, $p_0\Delta V$. A large amount of heat, q, (cf. Table 8.1) is given off to the surroundings. The first law of thermodynamics gives:

$$\Delta U = q - p_0\Delta V + w_{\mathrm{el}} \tag{8.4}$$

where $q < 0$. The electric work added per kg of aluminum is:

$$w_{\mathrm{el}} = I\Delta\phi = 12.9 \ \mathrm{kWh/kg_{Al}} \tag{8.5}$$

where I is the electric current (here 230 kA) and $\Delta\phi$ is the cell potential (here 4.1 V).

The second law of thermodynamics distinguishes between the minimum work needed to do the process, and the work that is actually used. The difference is the lost work :

$$w_{\mathrm{el}} - w_{\mathrm{el,min}} = w_{\mathrm{lost}} \tag{8.6}$$

The minimum work that is needed to perform the process at T_0 and p_0 is the reaction Gibbs energy. This quantity is found from

the reversible cell potential at these conditions, $\Delta\phi_{\text{rev}} = -1.73$ V [68], giving $w_{\text{el,min}} = 5.4$ kWh/kg$_{\text{Al}}$. The thermodynamic efficiency is therefore

$$\eta_{II} = \frac{w_{\text{el}} - w_{\text{lost}}}{w_{\text{el}}} = \frac{w_{\text{el,min}}}{w_{\text{el}}} = 0.42 \tag{8.7}$$

The second law of thermodynamics makes a distinction between energy forms, by ranging their potential to do work. Heat production at high temperature is more valuable than heat production at the temperature of the surroundings, because the former energy can be used to extract work. The difference between the first and the second law efficiencies is their way of dealing with the reaction entropy. The entropy change is included in $w_{\text{el,min}} = -\Delta_1 G$ in Eq. (8.7).

The difference between the real work input and the minimum requirement is 7.5 kWh/kg$_{\text{Al}}$. This is the total lost work in the electrolysis cell (see Section 2.3):

$$w_{\text{lost}} = T_0 \frac{dS_{\text{irr}}}{dt} \tag{8.8}$$

In order to find the origin of the losses, we shall calculate dS_{irr}/dt for all parts of the cell. A first step toward a possible reduction of losses is knowledge about where and how work is lost in the cell.

Remark 8.1 *The first law of thermodynamics places all forms of energy changes on an equal footing; that is, all forms are equivalent in the energy balance. Heat leaving the electrolyte at $T_c = 960\ ^oC$ is then equivalent to heat given to the surroundings at the lower temperature $T_0 = 25\ ^oC$.*

The enthalpy, $\Delta_1 H$, as well as the entropy, $\Delta_1 S$, of reaction (8.1) are positive. The reaction Gibbs energy, $\Delta_1 G$, is accordingly smaller than $\Delta_1 H$. Part of the ohmic heat that is produced in the cell, is used to compensate the heating need equal

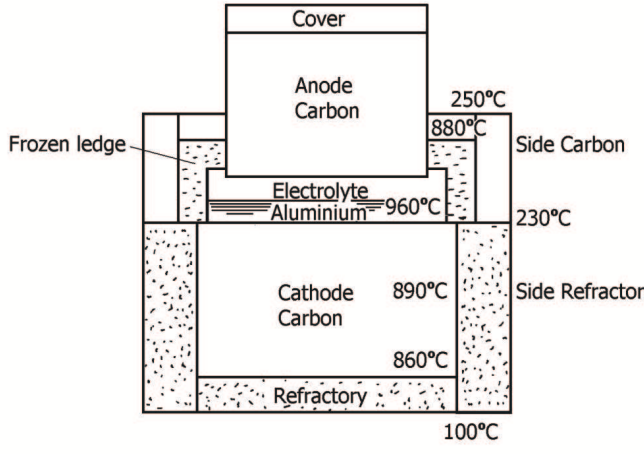

Figure 8.2: Schematic illustration of the cell showing typical temperatures.

to $T_c\Delta_1 S$. Heat produced in excess of this is given off to the surroundings, leading to the values in in Table 8.1, where $|q| = 6.5\ kWh/kg_{Al}$. For this work consuming process, the first law efficiency is the ratio of energy gained by the process and the energy (work) that is actually used, compare Section 2.3. We obtain

$$\eta_I = \frac{\Delta U(T_0) + p_0 \Delta V}{w_{el}} = \frac{\Delta H(p_0, T_0)}{w_{el}} = \frac{w_{el} + q}{w_{el}} = 0.50 \quad (8.9)$$

This equation says that a small $|q|$ is favorable, but does not instruct us on where it is beneficial to reduce $|q|$.

8.3 A simplified cell model

In order to make a first estimate, we simplify the cell geometry. A cross-section of the cell in Fig. 8.1 is presented in Fig. 8.2. The entropy production for coupled transport of heat, mass and

charge was given in Chapter 3. We assume constant fluxes perpendicular to cross-sectional areas Ω_j in the cell, and obtain for all bulk materials

$$\begin{aligned}\frac{dS_{\text{irr}}}{dt} &= \int\int \sigma d\Omega dx \\ &= \sum_j q_j \Delta\left(\frac{1}{T_j}\right) + \sum_i J_i \Omega_i \left(-\frac{\Delta\mu_{i,T}}{T}\right) + I\left(-\frac{\Delta\phi_j}{T}\right)\end{aligned} \tag{8.10}$$

Here q_j is the total heat flow through an area, and I is the electric current. The conjugate forces are given by the parentheses.

The entropy production of a reaction is:

$$\frac{dS^{\text{r}}_{\text{irr}}}{dt} = r\left(-\frac{\Delta G}{T_c}\right)V \tag{8.11}$$

The reaction rate r of Eq. (8.2) is related to the number of faradays transferred through the cell. The value is calculated for the process volume.

In the electrode surfaces, the entropy production is [73, 74]

$$\begin{aligned}\frac{dS^{\text{s}}_{\text{irr}}}{dt} &= q^{\text{i}}\Delta_{\text{i,s}}\left(\frac{1}{T}\right) + q^{\text{o}}\Delta_{\text{s,o}}\left(\frac{1}{T}\right) - I\frac{\Delta_{\text{i,o}}\phi}{T} \\ &\quad - \sum_i J^{\text{i}}_i \Omega_{\text{i}} \frac{\Delta_{\text{i,s}}\mu_{i,T}}{T} - \sum_i J^{\text{o}}_i \Omega_{\text{o}} \frac{\Delta_{\text{s,o}}\mu_{i,T}}{T}\end{aligned} \tag{8.12}$$

The heat flow into the surface is q^{i}, and out of the surface is q^{o}. The mass fluxes J^{i}_i are directed into the surface, and J^{o}_i are directed out of the surface. The potential difference $\Delta_{\text{i,o}}\phi$ is the surface potential drop. Details on the construction of the excess entropy production of the surface are given by Hansen and Kjelstrup [73].

The total entropy production shall be obtained by adding the results using these equations in the different parts of the cell. We

distinguish between entropy production due to charge transfer, due to excess carbon consumption (reaction (8.2)), and due to heat conduction through the walls. We shall estimate $dS_{\rm irr}/dt$, $dS^{\rm s}_{\rm irr}/dt$ and $dS^{\rm r}_{\rm irr}/dt$ using the simplified cell geometry and the temperatures shown in Fig. 8.2. The temperatures are given in Celsius in the figures and tables.

More accurate calculations can be done with better geometries using transport properties that are functions of temperature and composition.

8.4 Lost work due to charge transfer

Consider first the losses connected with the electric circuit. We shall see below that these can be estimated to 2.4 $\rm kWh/kg_{Al}$. The losses in the iron bars that connect the series of single cells, are small in this context.

8.4.1 The bulk electrolyte

There are losses related to the potential drop across the electrolyte. These losses are mainly ohmic, due to good stirring of the electrolyte when CO_2(g) escapes the electrolyte, and due to a circular movement of the metal in the very strong magnetic field due to the electric current. An electric potential drop of -1.7 V is normal, where -1.5 V is due to the main part of the electrolyte and -0.2 V is assumed for the bulk part of the melt that contains gas bubbles. The last term of Eq. (8.10) gives

$$w_{\rm lost,1} = T_0 \left(\frac{dS_{\rm irr}}{dt} \right)_1 = \frac{T_0}{T_c} I(-\Delta\phi_1) = 1.30 \ \rm kW/kg_{Al} \qquad (8.13)$$

8.4.2 The diffusion layer at the cathode

The main charge carrier in the melt is Na^+. Close to the cathode Na^+ accumulates, and diffuses back. The diffusion layer

with gradients in chemical potential and in electric potential, is approximately 1 mm thick (= Δx). We neglect temperature gradients in the layer. With the electrode surface as a frame of reference for transport, 3 Na^+ ions move away from the surface in exchange for one Al^{3+} ion. The steady state flux of AlF_3 into the surface is therefore $J_{AlF_3} = j/3F$, while the net flux of NaF is zero. The entropy production for the layer is

$$\left(\frac{dS_{\text{irr}}}{dt}\right)_2 = -\frac{I}{T_c}\left(\frac{\Delta\mu_{AlF_3}}{3F} + \Delta\phi_2\right) \tag{8.14}$$

The current density at stationary state is therefore

$$\frac{I}{\Omega} = -\frac{\kappa}{\Delta x}\left(\frac{\Delta\mu_{AlF_3}}{3F} + \Delta\phi_2\right) \tag{8.15}$$

where κ is the conductivity of the stationary state boundary layer, 19 kohm m^{-1} [75]. The lost work is

$$w_{\text{lost},2} = T_0\left(\frac{dS_{\text{irr}}}{dt}\right)_2 = \frac{T_0}{T_c\kappa}\frac{I^2}{\Omega}\Delta x = 0.05 \text{ kW/kg}_{\text{Al}} \tag{8.16}$$

8.4.3 The electrode surfaces

The anode overpotential gives the major lost work at the electrode surfaces. A typical overpotential, η, is 0.50 V [68]. Hansen [73, 74] estimated thermal and chemical forces as well as transport coefficients consistent with this value. Small forces (< 5 K^{-1}, and < 1 J/K mol) were obtained. In the stationary state, the mass fluxes relative to the fluoride ion frame of reference (or the surface frame of reference) is zero. The lost work from Eq. (8.12) was therefore essentially given by the thermal and electrical forces, which add to

$$w_{\text{lost,s}} = 0.48 \text{ kW/kg}_{\text{Al}} \tag{8.17}$$

The entropy production at the cathode was negligible [73, 74], consistent with a small overpotential at this electrode.

8.4.4 The bulk anode and cathode

The carbon parts of the anode and cathode conduct heat and charge. From Eq. (8.10) we obtain (see Refs. [76, 77] for more details):

$$\left(\frac{dS_{\text{irr}}}{dt}\right)_j = q_j \Delta\left(\frac{1}{T_j}\right) + \frac{I}{T}(-\Delta\phi_j) \tag{8.18}$$

The constitutive relations are

$$q_j = -\lambda_j \Omega_j \frac{\Delta T_j}{\Delta x_j} + \pi_j \frac{I}{F} \tag{8.19}$$

$$\Delta\phi_j = -\frac{\pi_j}{FT}\Delta T - \frac{\Delta x_j}{\Omega_j \kappa_j} I \tag{8.20}$$

When these equations are introduced into Eq. (8.18), we obtain for both electrodes:

$$\left(\frac{dS_{\text{irr}}}{dt}\right)_j = -\lambda_j \Omega_j \frac{\Delta T_j}{\Delta x_j}\Delta\left(\frac{1}{T_j}\right) + \frac{I^2}{\Omega_j}\frac{\Delta x_j}{\kappa_j T} \tag{8.21}$$

The input data for each electrode and results of these calculations are given in Table 8.2. The thermal conductivities are little influenced by charge transfer [68]. The heat is transferred in the bulk anode from 960 °C to an estimated 785 °C, and in the bulk cathode from 960 °C to an estimated 860 °C. The table shows that the lost work in the two electrodes are the same, 0.33 kW/kg_{Al}.

8.5 Lost work by excess carbon consumption

By excess carbon consumption, we mean carbon that disappear from the cell in excess of what is used by reaction (8.1). The carbon disappears as CO. The reaction (8.2) describes the production of CO. The rate of the consumption of carbon was estimated from excess weight loss of anode material. The minimum amount of carbon needed for production of one ton of aluminum

Table 8.2: The lost work in the bulk anode and cathode,

	Anode	**Cathode**
λ/ $\mathrm{W(Km)^{-1}}$	10	13
$T_h - T_l$/ K	960-785	960-860
Δx_j/ m	0.35	0.44
Ω_j/ $\mathrm{m^2}$	30	50
κ/ $\mathrm{ohm^{-1}m^{-1}}$	19 000	40000
π/ $\mathrm{J(Kmol)^{-1}}$	1520	2446
w_{lost}/ $\mathrm{kWh/kg_{Al}}$	0.33	0.33

is 350 kg. The real consumption is typically 400 kg. This gives the rate of excess carbon consumption as 14% of the rate of reaction (8.1). The Gibbs energy change of reaction (8.1) is −219.5 kJ/mol CO produced [68]. This gives

$$w_{\mathrm{lost,r}} = T_0 \left(\frac{dS^{\mathrm{r}}_{\mathrm{irr}}}{dt} \right) = 0.10 \ \mathrm{kWh/kg_{Al}} \tag{8.22}$$

The work lost by the excess carbon consumption is small compared to other losses.

8.6 Lost work due to heat transport through the walls

The work that is lost by heat conduction through the walls of the container, can be calculated from the two temperatures that bound the walls and the total heat flow, $q = 6.5$ $\mathrm{kWh/kg_{Al}}$, see Table 8.1. Grossly speaking we can use $T_0 = 25$ °C (the temperature in the hall) and $T_c = 860$ °C (see Figure 8.2). This gives:

$$w_{\mathrm{lost}} = T_0 q \left(\frac{1}{T_0} - \frac{1}{T_c} \right) = 4.80 \ \mathrm{kWh/kg_{Al}} \tag{8.23}$$

This calculation of the lost work is not specific. It does not address the different modes of heat transfer. Heat transferred by

conduction across the cell walls, but by convection from the cell surface to the room. There is also black body radiation from the cell surface. We would like to know more about the specific contributions, and proceed to estimate the separate contributions.

8.6.1 Conduction across the walls

Wall number j has a thickness Δx_{wj} and a cross-sectional area for heat transfer equal to Ω_{wj}. The temperature difference across Δx_j is ΔT_j, and the thermal conductivity is λ_j. The entropy production in the wall materials is then

$$\left(\frac{dS_{\text{irr}}}{dt}\right)_j = -\lambda_j \frac{\Delta T_j}{\Delta x_{wj}} \Omega_{wj} \Delta \left(\frac{1}{T_j}\right) \tag{8.24}$$

Material data, temperatures and geometries are given in Table 8.2 and in Fig. 8.2. The temperature of the solid material on the electrolyte side, is the temperature of the electrolyte, 960 °C. The surface temperature of the container side is 230 °C, of the top crust it is 250 °C and in the bottom of the pot, it is 100 °C. Between the side ledge and the side wall it is 450 °C. Below the cathode carbon it is 860 °C[1]. The temperature T_h is the temperature of the surface facing the electrolyte, while T_l is the temperature of the surface facing the outside of the container. Surface temperatures are given in Table 8.3. The values of the high and low temperature in each layer are given in Celsius.

The sum of lost work from the container walls (sum of the bottom line of Table 8.3) is $w_{\text{lost},4} = 1.4$ kWh/kg$_{\text{Al}}$. There is a difference in lost work between the sides and the ends of the cell. This reflects, on one hand, the difference in area of these surfaces (the area ratio is 1:3), and on the other hand, the fact that relatively more entropy production takes place at the sides,

[1]The isotherms, from which these average temperatures were taken, were all generated for the accurate geometry in a numerical model of Hydro Aluminum ASA

Table 8.3: Contributions to lost work from the sides of the container walls in Fig. 8.2. Symbol C means that the walls are lined with carbon, while R means refractory lining.

	Top layer	**Side R**	**Side C**
λ/ W(Km)$^{-1}$	0.34	3.1	5.0
$T_h - T_l$/ ^oC	880-250	865-190	450-250
Δx_w/ m	0.12	0.42	0.15
Ω_w/ m^2	15	18	13
w_{lost}/ kWh/kg$_{\text{Al}}$	0.11	0.46	0.19
	End R	**End C**	**Bottom**
λ/ W(Km)$^{-1}$	0.76	4.4	0.4
$T_h - T_l$/ ^oC	880-110	470-255	860-90
Δx_w/ m	0.35	0.15	0.29
Ω_w/ m^2	6	4	50
w_{lost}/ kWh/kg$_{\text{Al}}$	0.07	0.05	0.40

because the current collector bars are located there. The lost work in the frozen side ledges was estimated by Hansen [74] to be 0.2 kWh/kg$_{\text{Al}}$. The losses together account for 1.6 kWh/kg$_{\text{Al}}$.

8.6.2 Surface radiation and convection

The sum of all calculated losses in the walls so far do not explain a total loss of 4.8 kWh/kg$_{\text{Al}}$. The outer walls of the container are cooled by radiation, convection and conduction. The energy flux by black body radiation from is

$$J_q = \frac{cu}{4\pi} \tag{8.25}$$

where c is the velocity of light and u is the energy density $u = \beta T^4$. With $\beta = 7.56 \times 10^{-16}$J/m^{3}K^4, $c = 3 \times 10^8$m/s, and using an estimated surface temperature of 390 K, we obtain $J_q = 23.4$ W/m^2.

The entropy production due to radiation is obtained by multiplying this energy flux with the thermal driving force and the surface area (about 160 m^2). In this case there is no linear relation between the flux and the driving force, but the expression for the entropy production is the same.

The lost work by radiation is accordingly 67 kW or 0.9 kWh/kg_{Al} for the present example. The estimate is uncertain because of the T^4-dependence. A 10% increase of the temperature of the surface gives about a 50% increase in the entropy production. It is also difficult to estimate the air circulation around the cell which takes heat away by convection.

Lost work from radiation form the cell and convection between the wall surface and the surroundings, can therefore be significant.

8.7 A map of the lost work

The lost work in all the different parts of the electrolysis cell can now be summarized. This is done in Table 8.4. As lost work from heat transport through the walls is taken the value calculated in Section 8.6. We see then that the total loss, 7.7 kWh/kg_{Al} , is close to the difference between the real work and the minimum work (12.9-5.4) $kWh/kg_{Al} = 7.5$ kWh/kg. A simplified geometry was, however, chosen for the model, so uncertainties are large.

The table gives a map of where and why the losses occur, and this can point to directions for further efforts.

The accumulated lost work in the charge conducting pathways is 2.5 kW/kg_{Al}. The ohmic losses in the bath gives the largest contribution to this type of lost work. The other major loss occurs at the anode surface. Around 72% of the lost work in the charge conducting pathways can be explained by these process steps.

Table 8.4: **The lost work in the total cell.** All contributions are in kWh/kg_{Al}. The sum is the accumulated loss.

Loss type	Loss location	Amount lost	Sum
Charge transfer	electrolyte resistance	1.3	
	diffusional layers	0.1	
	electrode surfaces	0.5	
	bulk cathode	0.3	
	bulk anode	0.3	2.5
Hot reactants	Al and CO_2	0.3	2.8
Reaction 5.2	anode	0.1	2.9
Thermal	walls, surroundings	4.8	7.7

Efforts that lower the electrolyte resistance have therefore been many. The ohmic losses in the electrolyte could be reduced by reducing the distance between the anode and the surface of the aluminum further. In practice this is very difficult, however, due to the large magnetic fields that rotate the metal. The substantial entropy production in the anode surface has also made the anode a target of further attention. The electrode mechanism for the reaction is still largely unknown. The lost work connected to the electrode reaction cannot be avoided, but it can be changed. Inert anodes, that liberate oxygen in stead of carbon dioxide, have not yet been made.

The energy content in the hot products (0.3 kWh/kg_{Al}) can be regained by heat exchange. The excess loss of carbon to the air in the electrolysis hall, cf. Eq. (8.2), is difficult to reduce.

The thermal losses by conduction and convection are by far the most substantial losses. The losses at low temperature dominate. The losses depend largely on the location. For instance, without an extra alumina layer on top of the crust, there is an extra energy need of 0.3 kWh/kg_{Al} to maintain the electrolyte

temperature. But an (excess) heat leak at the top, reduces the heat flux through the cell sides. As a consequence, the side ledge crusts may grow in thickness, and lead to more lost work.

The relatively large entropy production in the carbon parts of the electrodes can also be reduced, but this may also increase losses in other parts. A good cell design therefore means that the heat fluxes are distributed in a manner that gives minimum total lost work (see Chapter 9). The requirement that there is a side ledge of frozen melt to prevent the molten electrolyte from attacking the outer steel walls, limits the possibilities for a reduction.

8.8 Concluding remarks

We have seen above how a map for lost work in a process immediately can point to directions for further work, even different ways to operate the process with present days materials.

The losses listed in Table 8.4 are of two types. One type, i.e. losses connected with charge conduction, is (nearly) proportional to the electric current. The thermal type losses are not proportional to the electric current. These losses are mainly given by the heat flux and the temperature difference between the bath and the surroundings.

So how can this knowledge be used to improve the design? The electric current must run and the temperature difference cannot be changed. But the total heat transferred to the surroundings will depend on the surface area of the container. Here lies a possibility for reduction of the lost work per kg Al produced. The lost work in the charge conducting circuit is largely proportional to the amount of aluminum produced, but the lost work in the container walls is not so. By making the cells larger, the lost work from heat transport in the walls can be reduced per kg Al produced. An argument in favor of larger production cells, see

Grjotheim and Kvande [77], is therefore also an argument about reductions of lost work.

Since so much of the lost work can be related to heat transfer from the cell walls to the surroundings, methods to recover this waste heat may be beneficial, cf. Section 4.3. Large low-temperature thermal losses are typical in many industries.

Chapter 9

The state of minimum entropy production and optimal control theory

We present a procedure to minimize the entropy production in a process where defined output conditions are maintained. The procedure is demonstrated for ideal gas expansion and single plate heat exchange. We show that a process with minimum total entropy production can be characterized by uniform local entropy production.

It is an aim of the process engineer to reduce the lost work in industrial processes. According to Chapter 2, this means that of the total entropy production in the process should be made as small as possible. While we seek to minimize the entropy production, the production in the plant must be maintained, however. This puts at least one constraint on the minimization procedure. In this Chapter we demonstrate for two simple cases, that the path of minimum total entropy production, has

constant local entropy production. Optimal control theory can be used to calculate the path of minimum entropy production.

This Chapter concerns entropy production minimization in gas expansion and in heat exchange [78, 79]. In these cases we can find analytic results. Chemical reactors [47, 80–83] and distillation columns [84–90] are discussed in the next Chapter. These examples can only be solved with numerical procedures. The processes are all very common in industry.

We start by explaining the isothermal expansion of an ideal gas, so we can give some exact results. We find the work, the ideal work, the lost work, the entropy production and the minimum entropy production, given certain constraints. We then introduce optimal control theory and explain how this mathematical framework can be used to find the state of minimum entropy production, using the isothermal expansion as an example. We find that the local entropy production is constant throughout the optimal expansion process. This is an example of the theorem of equipartition of entropy production (EoEP) [80, 91–95]. It says that the entropy production should be constant throughout the process.

9.1 Isothermal expansion of an ideal gas

A schematic picture of a container filled with an ideal gas is given in Fig. 9.1. The container is equipped with a piston so that work can be extracted by expanding the gas. Heat is transferred to the gas from the surroundings in order to keep the temperature constant. The temperature of the surroundings and the system is T_0 (reversible heat transfer). We consider the expansion of the gas from an initial pressure p_1 to a final pressure p_2. The corresponding volumes are V_1 and V_2, respectively. Elementary textbooks are mainly dealing with the reversible ver-

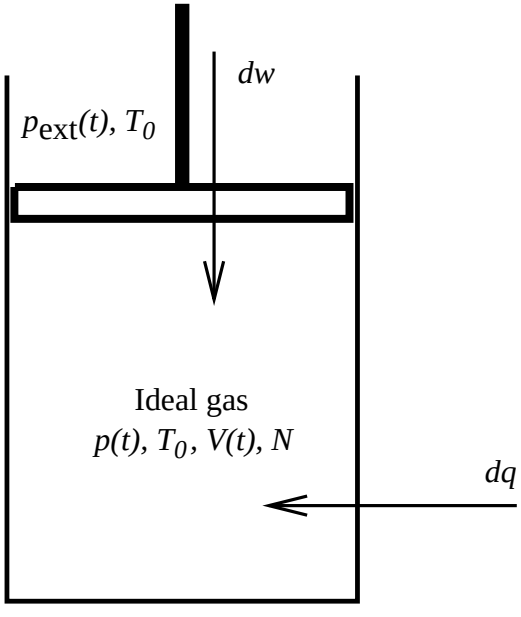

Figure 9.1: A container filled with N mol of an ideal gas with pressure $p(t)$, temperature T_0, and volume $V(t)$. The heat dq is added to the gas and work dw is done in a small time interval dt. The container is equipped with a piston. The gas expands isothermally against an external pressure $p_{\rm ext}(t)$. The temperature of the environment is T_0.

sion of the process. Only simple irreversible examples, without any constraint on the process duration, are discussed (see for instance [96]). For such simple processes, a complete thermodynamic treatment is possible without introducing any details about time and the dynamics of the process.

Most processes, both in nature and in industry, proceed in a finite period of time, however. We fix the duration of the expansion, Θ, and assume that the movement of the piston can be

described by the differential equations

$$\frac{dV(t)}{dt} = -\frac{f}{p(t)^2}\ (p_{\rm ext}(t) - p(t))$$
$$\Leftrightarrow \qquad \frac{dp(t)}{dt} = \frac{f}{N\ R\ T_0}\ (p_{\rm ext}(t) - p(t)) \qquad (9.1)$$

where f is a constant describing the friction between the piston and the container wall. For the limiting case $f \to \infty$ the system is free of friction. The other symbols are explained in Fig. 9.1. We used the ideal gas law to relate $dV(t)/dt$ and $dp(t)/dt$, and we added the factor $1/p(t)^2$ in $dV(t)/dt$ to simplify the mathematical treatment (see Exercises 9.1.1 and 9.2.1

9.1.1 Expansion work

Expansion produces work. The work that is done *on* the gas is [96]

$$w = -\int_{V_1}^{V_2} p_{\rm ext}(t)\ dV \qquad (9.2)$$

In the ideal limit, the expansion is a reversible process. In this limit, the external pressure equals the pressure of the gas at all times, and the expansion proceeds infinitely slowly. The ideal work is

$$w_{\rm ideal} = -\int_{V_1}^{V_2} p\ dV = N\ R\ T_0\ \ln\frac{p_2}{p_1} \qquad (9.3)$$

The work is called ideal since the extracted work $(-w)$ in any other version of the expansion is smaller than $-w_{\rm ideal}$. An irreversible version of the process has lost work, $w_{\rm lost} = w - w_{\rm ideal}$, which is always positive. The name "lost work" reflects that there is potential work which we are not able to extract. The ideal work gives a yardstick, which all other expansions can be compared to. This is the idea behind the second law efficiency (see Chapter 2).

In a K-step expansion process against a constant external pressure, the pressure is decreased in K steps to a constant value in each step. The work from Eq. (9.2) becomes

$$w = -N\,R\,T_0 \sum_{i=1}^{K} p_{\text{ext},i} \left(\frac{1}{p_{2,i}} - \frac{1}{p_{1,i}} \right) \tag{9.4}$$

where $p_{\text{ext},i}$, $p_{1,i}$, and $p_{2,i}$ are the external pressure, the initial pressure of the gas and the final pressure of the gas in step number i, respectively. Given the values of $p_{\text{ext},i}$ and $p_{1,i}$, one can find $p_{2,i}$ by integrating Eq. (9.1), see Exercise 9.1.1. The corresponding lost work is

$$\begin{aligned} w_{\text{lost}} =& w - w_{\text{ideal}} \\ =& -N\,R\,T_0 \left[\sum_{i=1}^{K} p_{\text{ext},i} \left(\frac{1}{p_{2,i}} - \frac{1}{p_{1,i}} \right) + \ln \frac{p_2}{p_1} \right] \end{aligned} \tag{9.5}$$

The work in an isothermal expansion (or compression) is often illustrated in a pV-diagram. Examples of such diagrams are given in Fig. 9.2. The ideal work of the expansion, Eq. (9.3), is minus the area below the isotherm in these diagrams. The work in a $K = 1$ step expansion, Eq. (9.4), is minus the area of the shaded rectangle in Fig. 9.2(a). The lost work of the same process, Eq. (9.5), is the area between the isotherm and the rectangle in the same figure. Figures 9.2(b)-(d) show expansions with 3, 5 and 15 steps, respectively. We return to this figure when we discuss the entropy production minimization problem later.

9.1.2 The entropy production

The entropies of the gas and the surroundings change during the expansion, and the local entropy production is

$$\sigma(t) = \frac{dS^{\text{system}}(t)}{dt} + \frac{dS^{\text{surroundings}}(t)}{dt}$$

$$\sigma(t) = \frac{1}{T_0}\,\frac{dq_{\rm rev}}{dt} + \frac{1}{T_0}\,\left(-\frac{dq}{dt}\right) \tag{9.6}$$

Here, $dq_{\rm rev}/dt$ is the rate of heat transfer in a reversible expansion between the same initial and final states of the gas. We have taken advantage of entropy being a state function in this calculation. Furthermore, $-dq/dt$ is the rate at which heat is transferred (reversibly) to the surroundings in the irreversible expansion.

Since the expansion is isothermal, the internal energy of the ideal gas, U, is constant and the first law gives $dq = -dw$. By using this identity, Eqs. (9.1) and (9.2) in differential form, we can write the local entropy production as

$$\begin{aligned}\sigma(t) =& \frac{1}{T_0}\,\left(p_{\rm ext}(t) - p(t)\right)\,\left(-\frac{dV(t)}{dt}\right)\\ =& \frac{1}{T_0}\,\frac{f}{p(t)^2}\,\left[p_{\rm ext}(t) - p(t)\right]^2\end{aligned} \tag{9.7}$$

The total entropy production of the expansion is found by integration of the local entropy production over the process duration. With $K \geq 1$ steps, the total entropy production is

$$\begin{aligned}\frac{dS_{\rm irr}}{dt} &= \sum_{i=1}^{K}\int_{t_{1,i}}^{t_{2,i}} \frac{1}{T_0}\,\left(p_{{\rm ext},i} - p(t)\right)\,\left(-\frac{dV(t)}{dt}\right)dt\\ &= -N\,R\,\left[\sum_{i=1}^{K} p_{{\rm ext},i}\left(\frac{1}{p_{2,i}} - \frac{1}{p_{1,i}}\right) + \ln\frac{p_2}{p_1}\right]\end{aligned} \tag{9.8}$$

By comparing this result with the lost work, Eq. (9.5), we see that the Gouy-Stodola theorem, Eq. (2.17), applies. The Gouy-Stodola theorem is generally valid (see e.g. [43] and Section 2.3 for details). In the proof, an important assumption is that all heat is discarded or extracted from a reservoir at the reference temperature T_0. We made things simple in this example by assuming that the system and the surroundings are both at

T_0. Given that they were at another temperature, the Gouy-Stodola theorem would not apply directly. In that case, the Gouy-Stodola theorem applies if an imaginary Carnot machine is used in order to discard or extract the heat from a reservoir at T_0 (see Section 9.3.2).

9.1.3 The optimization idea

We are interested in the path that gives minimum entropy production during expansion from a fixed initial to a fixed final state of the gas. The ideal work is then also fixed, cf. Eq. (9.3). Maximizing the work output $(-w)$ and maximizing the second law efficiency are equivalent optimization problems. It makes no sense to for instance maximize the work output or minimize the entropy production of this process without fixing the ideal work: Given that the process duration is fixed, maximum work would give an infinite pressure ratio p_2/p_1, and minimum entropy production would give $p_2/p_1 = 1$ (no expansion at all).

Without constraints on the duration of the expansion, the minimum entropy production would be a trivial zero, and the maximum work output would be $-w_{\text{ideal}}$, as pointed out above. Since we have a fixed and finite process duration, Θ, the entropy production is not zero and the maximum work output will be lower than $-w_{\text{ideal}}$. For a $K = 1$ step expansion, there is only one external pressure which takes the pressure of the gas from p_1 at time 0 to p_2 at time Θ. The work and the lost work of this process is illustrated in Fig. 9.2(a). For $K > 1$, there are infinitely many feasible choices of external pressures. This freedom can be used to minimize the entropy production (maximize the work output) of the expansion. The details of this optimization problem are left as an exercise (see Exercise 9.1.1). Figs. 9.2(b)-(d) show the work and the lost work for the optimal processes with 3, 5 and 15 steps, respectively.

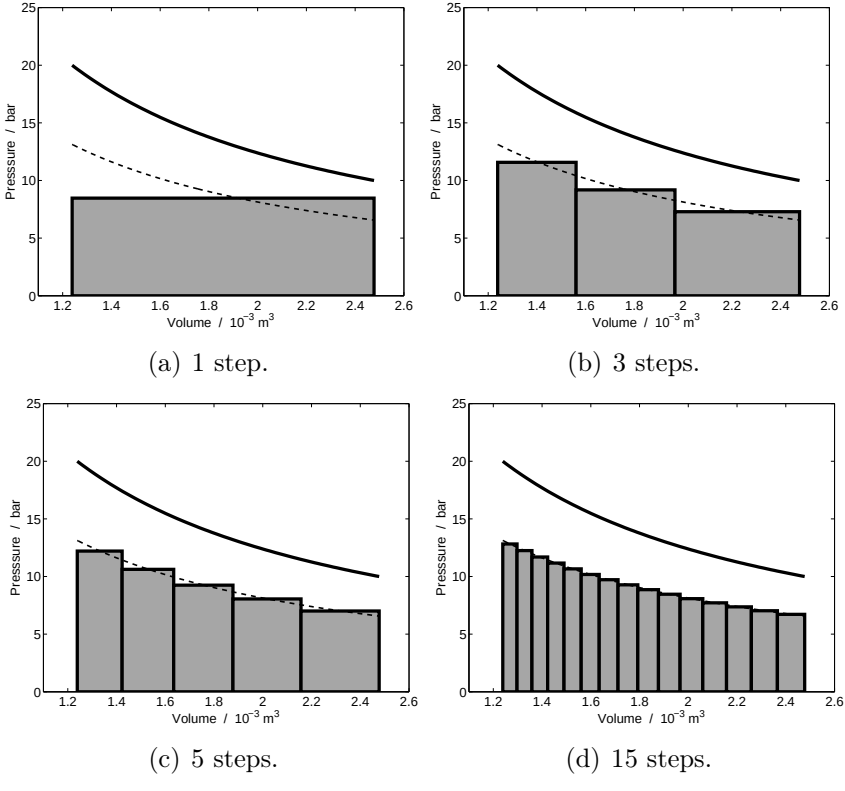

(a) 1 step. (b) 3 steps.

(c) 5 steps. (d) 15 steps.

Figure 9.2: Optimal external pressure vs. volume of the ideal gas. The gray areas are the work output in each expansion step. The lost work is the area between the rectangle(s) and the isotherm (the solid line). The dashed line corresponds to the expansion that produce minimum entropy for the given process duration. ($N = 1$ mol, $T = 298$ K, $p_1 = 20$ bar, $p_2 = 10$ bar, $f = 500\,\mathrm{m^3\,Pa/s}$, $\Theta = 10$ s).

We are now in a position where we can present the kind of entropy production minimization problems that are central for development of energy efficient processes. By comparing the sub-figures in Fig. 9.2, we see that the work output (the total area of the rectangles) increases, and the entropy production decreases, as K increases. Furthermore, the external pressure of the process (the upper edge of the rectangles) approximates the dashed line in the figures better and better, as K increases. The dashed line, characterized by infinitely many steps and a continuously changing external pressure, is a limit for the performance of the process, given that the process duration is fixed.

As a limiting process, it can also be used as a yardstick, much like the reversible process is used when the process is allowed to take infinitely long time. The limiting process in Fig 9.2 is not as general as the reversible limit; it depends on the piston/container used and the dynamics of the system (Eq. (9.1)). In this manner it is a yardstick that can be used in practice to measure the performance [45]. We show in Section 9.2 that the two limiting processes become the same as Θ goes to infinity.

We say that the system is in the state of minimum entropy production when the expansion proceeds along the dashed line that is given in all the sub-figures of Fig. 9.2. We show in Section 9.2 that this expansion has constant local entropy production throughout. This is one example of the theorem of equipartition of entropy production (EoEP); a result describing the characteristics of the state of minimum entropy production. In the next Chapter, we shall study the state of minimum entropy production for processes of more practical interest.

Exercise 9.1.1 *Solve the following optimization problem: Minimize the total entropy production of the K-step expansion Eq.* (9.8)*. In each step, the time variation of the gas pressure*

is given by Eq. (9.1)*. The initial and final gas pressures of the overall process are* p_1 *and* p_2*, respectively. Give the total entropy production, the work and the lost work of the optimum.*

Solution: By integrating Eq. (9.1) over step i, we obtain

$$p_{\text{ext},i} = \frac{1}{\alpha - 1} \left(\alpha\, p_{1,i} - p_{1,i+1}\right), \qquad i \in [1, K]$$

where $\alpha = \exp\left(-\frac{f}{N\,R\,T_0}\frac{\Theta}{K}\right)$. We used here that $p_{\text{ext},i}$ is constant, but different from $p_{2,i} = p_{1,i+1}$ in each step. By introducing this result into Eq. (9.8), we obtain

$$\frac{dS_{\text{irr}}}{dt} = -N\,R\,\ln\left(\frac{p_2}{p_1}\right) - \frac{NR}{\alpha - 1}\sum_{i=1}^{K}\left(\alpha\,\frac{p_{1,i}}{p_{1,i+1}} - \alpha - 1 + \frac{p_{1,i+1}}{p_{1,i}}\right)$$

We minimize the total entropy production subject to $p_{1,1} = p_1$ and $p_{1,K+1} = p_2$, and construct therefore the Euler-Lagrange function

$$\begin{aligned}\mathcal{L} = &- N\,R\,\ln\left(\frac{P_2}{P_1}\right) - \frac{NR}{\alpha - 1}\sum_{i=1}^{K}\left(\alpha\,\frac{p_{1,i}}{p_{1,i+1}} - \alpha - 1 + \frac{p_{1,i+1}}{p_{1,i}}\right) \\ &+ \lambda_1\,(p_{1,1} - p_1) + \lambda_2\,(p_{1,K+1} - p_2)\end{aligned}$$

from which we derive the necessary conditions for the optimum:

$$0 = \frac{\partial \mathcal{L}}{\partial p_{1,i}} = \begin{cases} -\frac{N\,R}{\alpha-1}\left(\alpha\,\frac{1}{p_{1,2}} - \frac{p_{1,2}}{p_{1,1}^2}\right) + \lambda_1, \\ i = 1 \\ -\frac{N\,R}{\alpha-1}\left(\alpha\,\frac{1}{p_{1,i+1}} - \frac{p_{1,i+1}}{p_{1,i}^2} - \alpha\,\frac{p_{1,i-1}}{p_{1,i}^2} + \frac{1}{p_{1,i-1}}\right), \\ i \in [2, K] \\ -\frac{N\,R}{\alpha-1}\left(-\alpha\,\frac{p_{1,K}}{p_{1,K+1}^2} + \frac{1}{p_{1,K}}\right) + \lambda_2, \\ i = K + 1 \end{cases}$$

By solving these conditions, we find the optimal initial pressure of the gas and the optimal external pressure in each step:

$$p_{1,i} = p_1 \left(\frac{p_2}{p_1}\right)^{(i-1)/K}, \qquad i \in [1, K+1]$$

$$p_{\text{ext},i} = p_1 \left(\frac{p_2}{p_1}\right)^{(i-1)/K} \left(\frac{\alpha - (p_2/p_1)^{1/K}}{\alpha - 1}\right), \qquad i \in [1, K]$$

The corresponding total entropy production is

$$\frac{dS_{\text{irr}}}{dt} = -N\,R \times \left[\ln\left(\frac{p_2}{p_1}\right) + \frac{K}{\alpha - 1}\left(\alpha\left(\frac{p_2}{p_1}\right)^{-\frac{1}{K}} - \alpha - 1 + \left(\frac{p_2}{p_1}\right)^{\frac{1}{K}}\right)\right]$$

and the corresponding work and lost work are:

$$w = -N\,R\,T_0\,\frac{K}{\alpha - 1}\left(\alpha\left(\frac{p_2}{p_1}\right)^{-\frac{1}{K}} - \alpha - 1 + \left(\frac{p_2}{p_1}\right)^{\frac{1}{K}}\right)$$

$$w_{\text{lost}} = -N\,R\,T_0 \times \left[\ln\left(\frac{p_2}{p_1}\right) + \frac{K}{\alpha - 1}\left(\alpha\left(\frac{p_2}{p_1}\right)^{-\frac{1}{K}} - \alpha - 1 + \left(\frac{p_2}{p_1}\right)^{\frac{1}{K}}\right)\right]$$

The fomulae are illustrated in Examples in Fig. 9.2.

Remark 9.1 *The optimization problem above was well solved with the standard Euler-Lagrange method. In the next subsection, we introduce optimal control theory, which is built on some of the same ideas. Optimal control theory can also handle inequality constraints.*

9.2 Optimal control theory

Consider again the search for the state of minimum entropy production, using the expansion of a piston as example. The dashed lines in Fig. 9.2 are the solutions of the following optimization problem: Minimize the total entropy production

$$\frac{dS_{\text{irr}}}{dt} = \int_0^\Theta \sigma(t)\, dt = \int_0^\Theta \frac{1}{T_0}\, \frac{f}{p(t)^2}\, \left(p_{\text{ext}}(t) - p(t)\right)^2 dt \qquad (9.9)$$

subject to the governing equation for the pressure of the gas

$$\frac{dp(t)}{dt} = \frac{f}{N\, R\, T_0}\, \left(p_{\text{ext}}(t) - p(t)\right) \qquad (9.10)$$

We have also required that the process duration, Θ, is fixed, and that the initial and final pressures of the gas are p_1 and p_2, respectively. The optimal profile of the external pressure throughout the process is of interest (dashed line in Fig. 9.2).

This optimization problem can be solved using optimal control theory ([97], see also [98]). In optimal control theory, the variables of the system are divided in two groups; state variables and control variables:

- The state variables are the variables which are governed by differential equations. The pressure of the gas (or alternatively its volume) is thus a state variable in the present example since it is governed by Eq. (9.10).
- The control variables are our handles on the system, or the means with which we control it. In the present example, the external pressure is the control variable. We assume that we have full control over it, and that it can take any positive value.

Optimal control theory gives a set of necessary conditions for minimum entropy production, much like setting derivatives equal

to zero in ordinary calculus. The first step is to construct the Hamiltonian of the optimal control problem. In our example, the Hamiltonian is

$$\mathcal{H} = \frac{1}{T_0}\,\frac{f}{p(t)^2}\,\left(p_{\text{ext}}(t) - p(t)\right)^2 + \lambda(t)\,\frac{f}{N\,R\,T_0}\,\left(p_{\text{ext}}(t) - p(t)\right) \tag{9.11}$$

The Hamiltonian has two parts. The first part is the local entropy production, the integrand in the total entropy production. The second part contains the functional constraints, as products of multiplier functions ($\lambda(t)$'s) and the right hand sides of the governing equations. In this problem, there is only one governing equation, meaning that the second part of the Hamiltonian consists of one term only.

We can benefit from a special property of the Hamiltonian: A general result in optimal control theory is that the Hamiltonian is constant along the coordinate of the system, time in this case, when it is autonomous [97]. The Hamiltonian is autonomous when it does not depend explicitly on the coordinate of the system (here time), but only implicitly through the state variables (here pressure), the control variables (here external pressure), and the multiplier functions. This is the case for the optimization problems studied in Chapter 10.

The necessary conditions for minimum entropy production can thus be derived from the Hamiltonian and consist of differential and algebraic equations. There are two differential equations for each state variable, and one algebraic equation for each control variable. In the present problem the differential equations are

$$\frac{dp(t)}{dt} = \frac{\partial \mathcal{H}}{\partial \lambda} = \frac{f}{NRT_0}\left(p_{\text{ext}}(t) - p(t)\right) \tag{9.12}$$

$$\frac{d\lambda(t)}{dt} = -\frac{\partial \mathcal{H}}{\partial p} = 2\,\frac{1}{T_0}\,\frac{f}{p(t)^2}\,\left(p_{\text{ext}}(t) - p(t)\right)\,\frac{p_{\text{ext}}(t)}{p(t)} + \lambda(t)\,\frac{f}{NRT_0} \tag{9.13}$$

In addition, the algebraic equation says that the external pressure should be chosen such that the Hamiltonian is minimized at every instant of time:

$$p_{\text{ext}}(t) = \underset{p_{\text{ext}}(t)>0}{\operatorname{argmin}}\, \mathcal{H} \tag{9.14}$$

The first differential equation is the governing equation for the pressure, and it is thus not "new". The second differential equation is new and describes the time variation of the multiplier function. In the expansion example, the optimal external pressure is always positive. Equation (9.14) reduces therefore to

$$\frac{\partial \mathcal{H}}{\partial p_{\text{ext}}} = 2\,\frac{1}{T_0}\,\frac{f}{p(t)^2}\,\left(p(t)_{\text{ext}} - p(t)\right) + \lambda(t)\,\frac{f}{N\,R\,T_0} = 0 \tag{9.15}$$

The first form of the algebraic equation (9.14) should be used when there are significant upper and lower bounds on the value of the external pressure.

We have to solve equations equivalent to Eqs. (9.12) to (9.15) in order to find the optimal solution in a given case. Together with appropriate boundary conditions, this is a two point boundary value problem. The problem is usually highly nonlinear and must be solved numerically.

The present problem is simple enough to be solved analytically. We do not use Eq. (9.13), but rather the fact that the Hamiltonian is constant in time. We solve Eq. (9.15) for λ, introduce the result in the Hamiltonian, and obtain

$$\begin{aligned}\mathcal{H}^{\min} &= \frac{1}{T_0}\,\frac{f}{p(t)^2}\,\left(p_{\text{ext}}(t) - p(t)\right)^2 - 2\,\frac{1}{T_0}\,\frac{f}{p(t)^2}\,\left(p_{\text{ext}}(t) - p(t)\right)^2 \\ &= -\sigma(t)\end{aligned} \tag{9.16}$$

The Hamiltonian reduces to the local entropy production, $\sigma(t)$. The state of minimum entropy production is thus characterized by constant local entropy production, since the Hamiltonian is no function of time. This is an example of the theorem of equipartition of entropy production (EoEP).

The fact that the local entropy production is constant, can be used to work out all details of the optimal solution analytically, see Exercise 9.2.1. The total entropy production of the optimal solution is

$$\frac{dS_{\mathrm{irr}}}{dt} = \frac{1}{f\,T_0\,\Theta}\left(N\,R\,T_0\,\ln\left(\frac{p_2}{p_1}\right)\right)^2 \tag{9.17}$$

This result fits well with intuition. The total entropy production increases when the process duration decreases, when the factor f decreases (more friction), and when p_2/p_1 increases. Moreover, the entropy production approaches zero when the process duration goes to infinity, which is in agreement with the reversible process being the ideal limiting process.

Control theory is a general tool to study the state of minimum entropy production and can be applied for example to heat exchange, chemical reactors and distillation columns.

Exercise 9.2.1 *Start with the fact that the state of minimum entropy production for expansion is characterized by constant local entropy production. Derive how the pressure of the gas and the external pressure vary with time in the optimal state.*

- **Solution:** We express the pressure difference by the local entropy production and obtain

$$(p_{\mathrm{ext}}(t) - p(t)) = -p(t)\,\sqrt{\frac{T_0\,\sigma_{\mathrm{opt}}}{f}}$$

where σ_{opt} is the constant and optimal entropy production throughout the process. The governing equation for the pressure becomes from (9.10)

$$\frac{dp(t)}{dt} = -\frac{1}{N\,R\,T_0}\,\sqrt{T_0\,\sigma_{\mathrm{opt}}\,f}\,p(t)$$

This is a separable differential equation which can be solved to find the pressure of the gas

$$p(t) = p_1 \, \exp\left(-\frac{1}{N\,R\,T_0}\,\sqrt{T_0\,\sigma_{\rm opt}\,f}\,t\right) = p_1\,\left(\frac{p_2}{p_1}\right)^{t/\Theta}$$

and the corresponding external pressure

$$\begin{aligned} p_{\rm ext}(t) &= p(t)\left(1-\sqrt{\frac{T_0\,\sigma_{\rm opt}}{f}}\right) \\ &= p_1\left(1+\frac{N\,R\,T_0}{f\,\Theta}\,\ln\left(\frac{p_2}{p_1}\right)\right)\,\left(\frac{p_2}{p_1}\right)^{t/\Theta} \end{aligned}$$

The total entropy production was given in Eq. (9.17). The factor $1/p(t)^2$ in $dV(t)/dt$, cf. Eq. (9.1), was introduced in order to simplify the algebra in this exercise and in Exercise 9.1.1.

Exercise 9.2.2 *Cost-benefit analysis is used in economic theory to help decide among production lines. In analogy with this analysis, consider the entropy production of a system as the "cost" we want to minimize. Consider a system with n independent production lines, and a total demand J. Find the conditions that give minimum total costs.*

- **Solution:** The production from one production line is

$$J_n = L_n X_n$$

where X_n is the driving force for production, and L_n a proportionality constant. The total production is

$$J_n = \sum_n J_n$$

and the cost of the production is

$$\frac{dS_{irr}}{dt} = \sum_n J_n X_n = \sum_n L_n X_n^2$$

The minimum of this cost at constant J is

$$\frac{\partial S_{irr}}{\partial X_n} = 0 = \frac{\partial}{\partial X_n}\left(\sum_n L_n X_n^2 + \lambda \sum_n J_n\right)$$

This gives

$$X_n = -\frac{1}{2}\lambda \tag{9.18}$$

Minimum costs are obtained when the driving force across all production lines is uniform. Paths leading to production are usually not independent in real processes.

9.3 Heat exchange

Heat exchangers operate with considerable entropy production (cf. Exercise 3.3.6 and 3.3.7) and are thus important targets for optimizations. Consider heat exchange across a metal plate that separates a warm and a cold fluid, see Fig. 9.3 [78, 79]. The fluids exchange heat in the $x-$direction. They are transported along the plate in the $z-$direction.

Bejan [43] describes how the various parts of the process, the pump work, the geometry, etc. must be taken into account in a minimization of the entropy production of the total system. We consider only one aspect here, namely the heat exchange, and neglect the other contributions to the entropy production, for instance from pressure drops.

Assume that the hot fluid and the cold fluid are perfectly mixed in the y-direction, normal to the paper in Fig. 9.3. Consider a length Δy in the y-direction. In the x-direction, there is a

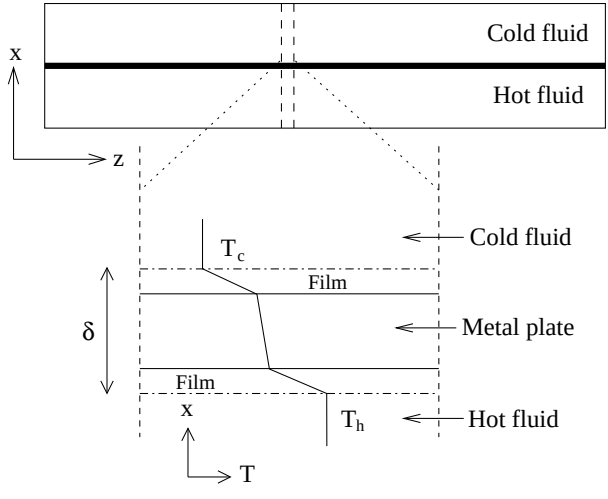

Figure 9.3: Schematic illustration of a heat exchanger. The thermal driving force is taken across δ, the thickness of the metal plate and adjacent film layers.

temperature gradient in the metal plate and in the fluid films next to the plate as shown in the lower part of Fig. 9.3. In the bulk of both fluids, there are only gradients in the z-direction. Heat is conducted through the metal plate in the x-direction. The conduction of heat in other directions is neglected. The system has length L, so $0 < z < L$.

The hot fluid flows from left to right. It enters at temperature $T_{h,\text{in}}$ and leaves at $T_{h,\text{out}}$. The flow rate, F, and the heat capacity, $C_p\,(T_h(z))$, are known. The governing equations are given in Table 9.1. The temperature profile of the hot fluid, $T_h(z)$, is then given by conservation of energy:

$$\begin{aligned} F\,C_p\,(T_h(z))\;dT_h(z) &= J_q'(z)\,\Delta y\,dz \\ \Rightarrow \quad \frac{dT_h(z)}{dz} &= \frac{\Delta y\;J_q'(z)}{F\,C_p\,(T_h(z))} \end{aligned} \tag{9.19}$$

Table 9.1: Governing equations for stationary state heat exchange.

Balance equation for internal energy:

$$\frac{dT_h}{dz} = \frac{\Delta y\, J_q'}{F\, C_p}$$

Balance equation for entropy:

$$\frac{dS_{\text{irr}}}{dt} = F\, S_{\text{out}} - F\, S_{\text{in}} - \Delta y \int_0^L \frac{J_q'}{T_c}\, dz$$

$$= \Delta y \int_0^L l_{qq} \left[\Delta\left(\frac{1}{T}\right)\right]^2 dz$$

where $J_q^{'}$ is the z-dependent measurable heat flux across the metal plate.

None of the properties of the cold fluid (fluid flow, flow direction, heat capacity, etc) are specified yet. We assume that we are able to control the temperature of the cold fluid at every position z in some way. This temperature is our control variable.

9.3.1 The entropy production

Heat is transported by conduction through the metal plate and the two adjacent stagnant film layers in the x-direction in the system illustrated by Fig. 9.3. The local entropy production is

$$\sigma(x,z) = J_q'(x,z)\, \frac{d}{dx}\left(\frac{1}{T(x,z)}\right) \tag{9.20}$$

We deal with stationary states only. In the $x-$direction, this gives

$$\frac{d}{dx} J_q'(x,z) = 0 \quad \Rightarrow \quad J_q'(x,z) = J_q'(z) \tag{9.21}$$

which means that the measurable heat flux across the metal is independent of x. It varies with position z, however. We integrate over the x-direction and find the entropy production in the plate as a function z:

$$\begin{aligned}\sigma'(z) &\equiv \Delta y \int_0^{\delta} \sigma(x,z)\, dx = \Delta y\, J'_q(z) \left(\frac{1}{T_h(z)} - \frac{1}{T_c(z)}\right) \\ &\equiv \Delta y\, J'_q(z)\, \Delta \left(\frac{1}{T}\right)\end{aligned} \tag{9.22}$$

where $\sigma'(z)$ denotes the entropy production per unit length in the z-direction and where δ includes the metal plate and its two adjacent stagnant film layers. On the basis of the integrated form, we write the heat flux proportional to its conjugate force

$$J'_q(z) = l_{qq}(z)\, \Delta \left(\frac{1}{T}\right) \tag{9.23}$$

where the thermal conductivity $l_{qq}(z)$ is the inverse of the integrated thermal resistivity in the $x-$direction:

$$l_{qq}(z) = \left[\int_0^{\delta} l_{qq}^{-1}(x,z)\, dx\right]^{-1} \tag{9.24}$$

The coefficient $l_{qq}(z)$ is independent of the thermodynamic force. It can depend on the temperature of either the hot or the cold fluid, but not on both. We take $l_{qq}(z)$ to depend on the temperature of the hot fluid, $T_h(z)$. The total entropy production of the heat exchanger is therefore:

$$\begin{aligned}\frac{dS_{\text{irr}}}{dt} &= \Delta y \int_0^{L}\int_0^{\delta} \sigma(x,z)\, dx\, dz = \int_0^{L} \sigma(z)'\, dz \\ &= \Delta y \int_0^{L} l_{qq}\left(T_h(z)\right) \left[\Delta\left(\frac{1}{T}\right)\right]^2 dz.\end{aligned} \tag{9.25}$$

The entropy production can also be derived from the entropy balance of the hot fluid. The entropy balance has three contributions in addition to the entropy production: Entropy of the

hot fluid in, $F\,S_{\rm in}$, and out, $F\,S_{\rm out}$ and entropy exchanged with the cold fluid. The entropy balance gives therefore

$$\frac{dS_{\rm irr}}{dt} = F\,S_{\rm out} - F\,S_{\rm in} + \Delta S_{\rm c} \tag{9.26}$$

where $\Delta S_{\rm c}$ is the change of the entropy of the cold fluid caused by transfer of heat from it. In a small element dz, this change is $-\Delta y\; J_q'(z)/T_c(z)\; dz$. The final expression for the total entropy production, derived from the entropy balance, is therefore

$$\frac{dS_{\rm irr}}{dt} = F\,S_{\rm out} - F\,S_{\rm in} - \Delta y \int_0^L \frac{J_q'(z)}{T_c(z)}\,dz \tag{9.27}$$

The total entropy productions in Eqs. (9.25) and (9.27) are consistent with each other. The proof of this is given as Exercise 9.3.1.

Exercise 9.3.1 *Show that Eqs.* (9.25) *and* (9.27) *are consistent with each other. Hint:* $\left[\partial S/\partial T\right]_p = C_p/T$

- **Solution:** Equation (9.27) can be rewritten as

$$\frac{dS_{\rm irr}}{dt} = \int_0^L \left[F\,\frac{dS_h\left(T_h(z)\right)}{dz} - \Delta y\,\frac{J_q'(z)}{T_c(z)}\right]\,dz$$

where we used that the difference between the state functions $S_{\rm out}$ and $S_{\rm in}$ can be calculated using any path. In our model we neglect the effects of pressure drop, so $\frac{dS_h(T_h(z))}{dT_h(z)} = \frac{C_p(T_h(z))}{T_h(z)}$. By using Eq. (9.19) we obtain

$$\begin{aligned}\frac{dS_h\left(T_h(z)\right)}{dz} =& \frac{dS_h\left(T_h(z)\right)}{dT_h(z)}\,\frac{dT_h(z)}{dz}\\ =& \frac{C_p\left(T_h(z)\right)}{T_h(z)}\,\frac{\Delta y\; J_q'(z)}{F\;C_p\left(T_h(z)\right)} = \frac{\Delta y}{F}\,\frac{J_q'(z)}{T_h(z)}\end{aligned}$$

which gives

$$\begin{aligned}\frac{dS_{\rm irr}}{dt} =& \Delta y \int_0^L J_q'(z) \left(\frac{1}{T_h(z)} - \frac{1}{T_c(z)}\right) dz \\ =& \Delta y \int_0^L l_{qq}\left(T_h(z)\right) \left[\Delta\left(\frac{1}{T}\right)\right]^2 dz\end{aligned}$$

This is Eq. (9.25). We have thus two ways to find $dS_{\rm irr}/dt$; from l_{qq}, $T_h(z)$ and $T_c(z)$ and from Eq. (9.27). This is an example of how the consistency of a model can be verified, as discussed in Section 2.5.

9.3.2 The work production by a heat exchanger

Concepts like work, ideal work and lost work are not as obvious for heat exchange as they are for the expansion in Section 9.1. We shall therefore explain that by cooling a hot fluid stream, the heat exchange process produces work. Likewise, by heating a cold fluid stream, the heat exchange process consumes work. A heat exchanger is thus a work producing or work consuming apparatus. By convention, we define work done and heat added as positive when they increase the internal energy of a system.

Figure 9.4 shows how the work production by heat exchange can be seen conceptually. At each position z, the cold fluid, with temperature $T_c(z)$, is connected to a reservoir at T_0 through a Carnot machine. In the small element dz, the heat which is transferred from the cold fluid to the hot fluid, is $dq = \Delta y J_q'(z) dz$. This heat is supplied to the cold stream by taking the heat $dq_0 = \frac{T_0}{T_c(z)}\, dq$ from the environment using the Carnot machine. The work needed to do this is

$$dw = \eta_C \left(\Delta y\, J_q'(z)\, dz\right) = \Delta y \left(1 - \frac{T_0}{T_c(z)}\right) J_q'(z)\, dz \quad (9.28)$$

where $\eta_C = 1 - T_0/T_c(z)$ is the Carnot efficiency[1]. The total work requirement of the heat exchange process is therefore

$$\begin{aligned} w &= \Delta y \int_0^L \left(1 - \frac{T_0}{T_c(z)}\right) J'_q(z)\, dz \\ &= q - \Delta y\, T_0 \int_0^L \frac{J'_q(z)}{T_c(z)}\, dz \\ &= F_{\text{out}}\, H_{\text{out}} - F_{\text{in}}\, H_{\text{in}} - \Delta y\, T_0 \int_0^L \frac{J'_q(z)}{T_c(z)}\, dz \end{aligned} \tag{9.29}$$

In the last equality, we used the first law which gives

$$F_{\text{out}}\, H_{\text{out}} - F_{\text{in}}\, H_{\text{in}} = q \tag{9.30}$$

where H_{out} and H_{in} are the molar enthalpy of the hot fluid out and in, respectively, and q is the total heat transferred to the hot fluid:

$$q = \Delta y \int_0^L J'_q(z)\, dz \tag{9.31}$$

Equation (9.29) shows that the work requirement is negative when we cool the hot fluid stream. This means that work can in fact be extracted from the process. The opposite is true when we consider heating a cold stream.

Remark 9.2 *Compare now Eqs.* (9.27) *and* (9.29). *We see again (cf. Section 9.1.3) that to minimize the total entropy production and to minimize the work requirement (maximize the work output) are equivalent problems when the inlet and outlet states of the hot fluid stream are fixed (S_{in}, S_{out}, H_{in} and H_{out} are fixed). Both optimization problems reduce to*

$$\min \qquad \left(-\int_0^L \frac{J'_q(z)}{T_c(z)}\, dz\right) \tag{9.32}$$

[1]The heat dq is the sum of the work needed in the Carnot machine and the heat extracted from the environment, that is $dq = \frac{T_0}{T_c(z)}\, dq + \eta_C\, dq$.

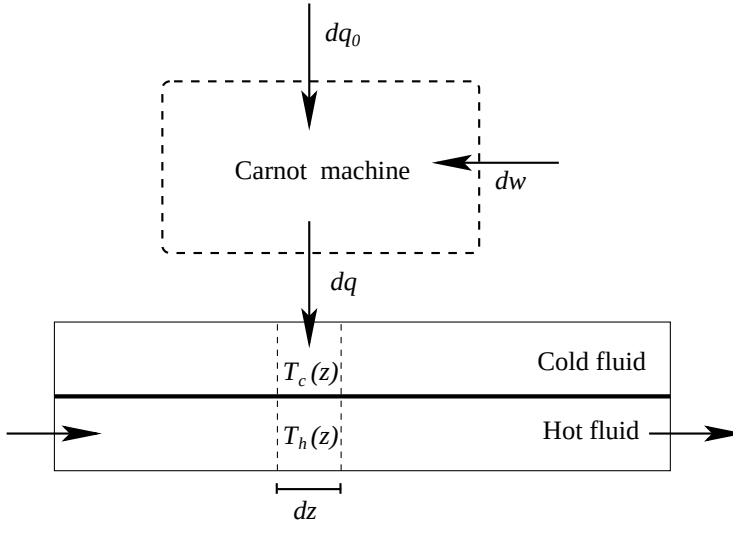

Figure 9.4: The heat exchanger as a work producing or work consuming machine.

The outcome of both optimization problems is to take heat out ($J'_q(z) < 0$) at as high temperatures as possible, and to supply heat ($J'_q(z) > 0$) at as low temperatures as possible. In other words, we should use low quality heat for heating and extract heat with high quality, a well known strategy in process integration. When the inlet and/or the outlet states are not fixed, the optimization problems are not equivalent. We study entropy production minimization because the entropy production is the most fundamental measure of energy dissipation.

We do not propose that a heat exchanger should be operated as a work-producing or work-consuming machine. In reality, heat extracted from a hot fluid stream is used for other purposes elsewhere in the plant. The same goes for the heat required to heat a cold fluid stream.

9.3.3 Optimal control theory and heat exchange

Optimal control theory can be applied to find the properties of the state of minimum entropy production in heat exchange. We want to minimize the total entropy production, Eq. (9.25), subject to Eq. (9.19) at every position z. In addition, we fix the total heat transported across the metal plate by fixing $T_{h,\mathrm{in}}$ and $T_{h,\mathrm{out}}$. The Hamiltonian of the optimal control problem is

$$\mathcal{H} = \Delta y \, l_{qq}\left(T_h(z)\right) \left[\Delta\left(\frac{1}{T}\right)\right]^2 + \lambda(z) \, \frac{\Delta y \, J_q'(z)}{F \, C_p\left(T_h(z)\right)} = \text{constant} \tag{9.33}$$

where $\lambda(z)$ is a multiplier function. The first term in the Hamiltonian is the local entropy production in Eq. (9.25) and second term is the product of the multiplier function and the right hand side of Eq. (9.19). The Hamiltonian is constant, because it does not depend explicitly on z.

The necessary conditions for minimum entropy production are then the differential equations

$$\frac{dT_h(z)}{dz} = \frac{\partial \mathcal{H}}{\partial \lambda} \qquad\qquad \frac{d\lambda(z)}{dz} = -\frac{\partial \mathcal{H}}{\partial T_h} \tag{9.34}$$

and the algebraic equation

$$\frac{\partial \mathcal{H}}{\partial T_c} = \Delta y \, l_{qq}\left(T_h(z)\right) \left[2\,\Delta\left(\frac{1}{T}\right) + \frac{\lambda(z)}{F \, C_p\left(T_h(z)\right)}\right] \frac{1}{T_c(x)^2} = 0 \tag{9.35}$$

The left part of Eq (9.34) reduces directly to Eq. (9.19), whereas the right part is a new differential equation which gives the position dependence of the multiplier function. The boundary conditions for these differential equations are the fixed values of $T_{h,\mathrm{in}}$ and $T_{h,\mathrm{out}}$. We have only given the weak form of the necessary condition for $T_c(z)$, Eq. (9.35), because we assume that the cold fluid can have any temperature at every position z. Optimal

control theory gives a stronger condition when there are significant upper and/or lower bounds on $T_c(z)$ (cf. Section 9.1), and is well suited to handle more complicated cases than here.

We solve the optimization problem in the same way as we solved the expansion problem in Section 9.1. The new differential equation for the multiplier function is not used. Instead, we solve Eq. (9.35) for $\lambda(z)$ and introduce the result in the Hamiltonian, Eq. (9.33). After some rearrangements we obtain

$$\begin{aligned}\mathcal{H} =& \Delta y \, l_{qq}\left(T_h(z)\right) \left[\Delta\left(\frac{1}{T}\right)\right]^2 - 2\,\Delta y \, J_q'(z)\,\Delta\left(\frac{1}{T}\right) \\ =& -\sigma(z) = \text{constant}\end{aligned} \tag{9.36}$$

This means that the state of minimum entropy production is again characterized by constant local entropy production (EoEP).

An interesting question is whether equipartition of the thermal driving force (EoF) gives a good approximation to the real optimum. The two equipartition results are trivially equivalent when $l_{qq}(z)$ is constant. When this is not the case, EoEP gives always the lower total entropy production, but the difference is negligible if the heat transfer duty is reasonably high [79]. This is illustrated in Exercise 9.3.2.

Exercise 9.3.2 *A hot stream needs to be cooled from 450 K ($T_{h,in}$) to 400 K ($T_{h,out}$). The heat exchanger has a heat transfer coefficient $l_{qq} = U\,T_h(z)^2$, and the heat capacity of the hot stream is taken to be constant.*

a) *Derive the temperature profile, the thermal driving force and the local and total entropy production for the EoEP case.*

b) *Repeat the derivations in* ***a)*** *for the EoF case.*

c) *Use $U = 340\ W/K\ m^2$, $\Delta y = 1\ m$, $L = 10\ m$ and $F\,C_p = 1200\ J/K$. Compare the total entropy productions of the EoEP and EoF cases.*

Solution:

a) From Eq. (9.22) it follows for the EoEP case that

$$\sigma_{\text{EoEP}} = \Delta y\, U\, T_h(z)^2 \left(\Delta\left(\frac{1}{T}\right)\right)^2$$

$$\Rightarrow \quad \Delta\left(\frac{1}{T}\right) = -\sqrt{\frac{\sigma_{\text{EoEP}}}{\Delta y\, U}}\,\frac{1}{T_h(z)}$$

By introducing this in Eq. (9.19) we find

$$\frac{1}{T_h(z)}\,\frac{dT_h(z)}{dz} = \frac{d\ln T_h(z)}{dz} \quad \text{is constant}$$

$$\Rightarrow \quad T_h(z) = T_{h,\text{in}} \left(\frac{T_{h,\text{out}}}{T_{h,\text{in}}}\right)^{z/L}$$

We then find the thermal driving force by rearranging Eq. (9.19) and introducing this temperature profile. The thermal driving force is

$$\Delta\left(\frac{1}{T}\right)_{\text{EoEP}} = \frac{F\,C_p}{\Delta y\, U}\,\frac{1}{T_h(z)^2}\,\frac{dT_h(z)}{dz}$$

$$= \frac{F\,C_p}{\Delta y\, U\, L}\,\ln\left(\frac{T_{h,\text{out}}}{T_{h,\text{in}}}\right)\,\frac{1}{T_h(z)}$$

The resulting local entropy production is

$$\sigma_{\text{EoEP}} = \frac{1}{\Delta y\, U}\left[\frac{F\,C_p}{L}\,\ln\left(\frac{T_{h,\text{out}}}{T_{h,\text{in}}}\right)\right]^2$$

and the total entropy production is

$$\left(\frac{dS_{\text{irr}}}{dt}\right)_{\text{EoEP}} = \frac{1}{\Delta y\, L\, U}\left[F\,C_p\,\ln\left(\frac{T_{h,\text{out}}}{T_{h,\text{in}}}\right)\right]^2.$$

b) When the thermal driving force is constant, we find from Eq. (9.19) that

$$\frac{1}{T_h(z)^2}\,\frac{dT_h(z)}{dz} \quad \text{is constant}$$

$$\Rightarrow \quad \frac{1}{T_h(z)} = \frac{1}{T_{h,\text{in}}} + \left(\frac{1}{T_{h,\text{out}}} - \frac{1}{T_{h,\text{in}}}\right)\,\frac{z}{L}$$

By rearranging Eq. (9.19) and introducing this temperature profile, we find the thermal driving force:

$$\begin{aligned}\Delta\left(\frac{1}{T}\right)_{\text{EoF}} =& \frac{F\,C_p}{\Delta y\,U}\,\frac{1}{T_h(z)^2}\,\frac{dT_h(z)}{dz}\\ =& -\frac{F\,C_p}{\Delta y\,U\,L}\,\left(\frac{1}{T_{h,\text{out}}} - \frac{1}{T_{h,\text{in}}}\right)\end{aligned}$$

which means that the local and the total entropy productions are

$$\sigma_{\text{EoF}} = \frac{1}{\Delta y\,U}\,\left[\frac{F\,C_p}{L}\,\left(\frac{1}{T_{h,\text{out}}} - \frac{1}{T_{h,\text{in}}}\right)\right]^2\,T_h(z)^2$$

and

$$\begin{aligned}&\left(\frac{dS_{\text{irr}}}{dt}\right)_{\text{EoF}}\\ &= \frac{1}{\Delta y\,U}\,\left[\frac{F\,C_p}{L}\,\left(\frac{1}{T_{h,\text{out}}} - \frac{1}{T_{h,\text{in}}}\right)\right]^2\,\int_0^L T_h(z)^2\,dz\\ &= \frac{1}{\Delta y\,L\,U}\,\left[F\,C_p\,\left(\frac{1}{T_{h,\text{out}}} - \frac{1}{T_{h,\text{in}}}\right)\right]^2\,T_{h,\text{out}}\,T_{h,\text{in}},\end{aligned}$$

respectively

c) When we introduce the numerical values the parameters, we find $(dS_{\text{irr}}/dt)_{\text{EoEP}} = 5.8756$ J/K s and $(dS_{\text{irr}}/dt)_{\text{EoF}} = 5.8824$ J/K s. The EoF-value is indeed larger than the

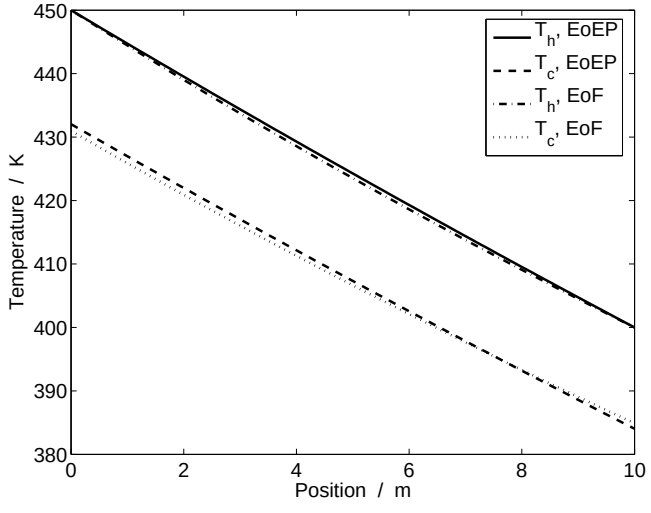

Figure 9.5: The temperature profiles of the EoEP- and EoF-solutions in Exercise 9.3.2c.

EoEP-value, which is the real optimum solution. The difference is only 1% and one may therefore conclude the also the use of the theorem of equipartition of the thermodynamic force leads to a very good approximation of the state of minimum entropy production. The temperature profiles of the EoEP- and EoF-solutions are shown in Fig. 9.5.

The temperature profiles of the hot and the cold fluid are approximately parallel when the production of entropy is minimum (see Fig. 9.5). How can this be achieved in a real heat exchanger? The heat capacity of the cold fluid is a central variable in this context. The heat capacity may be included as a variable in the optimization, and matched with a medium afterward. Full agreement with the optimum can be impractical or not economically feasible. It is therefore good to be able to approximate optimal heat exchange conditions.

For simple heat exchange processes, i.e. processes without phase change and small / moderate temperature change in each stream, counter-current heat exchange with a properly adjusted flow rate of the utility is probably the best approximation. For more complex situations, a series of counter-current, and/or cross-current heat exchangers might be needed to achieve a good approximation.

9.4 Concluding remarks

In this Chapter, we have explained concepts like work, ideal work, and lost work and their connection to the entropy production. We have also explained when different optimization problems, like maximum work output and minimum entropy production, are equivalent.

Optimal control theory was introduced in order to solve the entropy production minimization problems using a local description of the entropy production. This robust framework was used to reveal properties of the state of minimum entropy production. Specifically this theory gives optimal time-trajectories of batch processes and optimal process-conditions for stationary state processes. Whereas parameter-optimizations are core activities of process engineers, functional optimizations are relatively new for practical applications and have at the time of writing yet to be explored in many practical areas.

We derived the theorem of equipartition of entropy production for the simple processes; isothermal expansion and heat exchange.

Chapter 10

The state of minimum entropy production in selected process units

We shall see how control theory can be used in order to find paths of operation with minimum entropy production in two typical process units, the chemical reactor and the distillation tower. Some typical results are presented and concluded with practical guidelines for second law efficient design.

Chemical reactors and distillation towers are central units in chemical process plants. According to Humphrey and Siebert [99], the chemical industry accounts for 27 % of the industrial energy demand in the USA in 1991. The process of distillation was using 40 % of that. The chemical reactor has so far not been considered as a work producing or consuming system, as its main purpose is different; to produce chemicals. With increasing demands on available energy, and boundaries on the earth's ability to deal with entropy production, this may have

to change.

The chemical reactor and the distillation towers do not operate isolated, but heavily connected to other process equipments. Minimization of the entropy production in a single process unit alone, may thus lead to increases in other parts of the process. In this Chapter we study the optimal path of the single units. Steps toward a higher energy efficiency can thus only be anticipated when these units can be put in a proper perspective. Systematic efforts in this direction remain to be done, for a start see [100].

In the previous Chapter, we found that the optimal solution for a simple process unit (of gas expansion and heat exchange) gave uniform entropy production (EoEP). This equipartition result does not necessarily apply directly to more complicated units like a chemical reactor or a distillation column, because these units are often too constrained. But we shall see that parts of these units can have (approximately) uniform entropy production. This leads us to a hypothesis for the state of minimum entropy production in an optimally controlled system. The hypothesis explains when EoEP is a good approximations to the optimal state [80]. This can be used for apparatus design in chemical industry.

Knowledge of the present and previous Chapters shall be used in the end to formulate rules of thumb for some energy efficient process units.

10.1 The plug flow reactor

Consider a tubular reactor with diameter D and length L as sketched in Fig. 10.1. The reactor is filled with catalyst pellets with diameter D_{p} and density (per unit volume of reactor) ρ_{B}. The void fraction of the catalyst bed is ϵ. In the plug flow reactor model the gas velocity profile is flat, and that there are

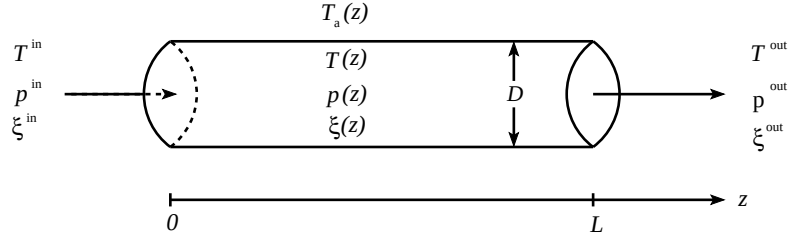

Figure 10.1: A tubular reactor.

no radial gradients inside the reactor. Heterogeneous effects due to diffusion and reaction inside and around the catalyst pellets are averaged out (a pseudo homogeneous model). Transport in the z-direction is only by convection. A cooling/heating medium with temperature $T_a(z)$ is placed on the outside of the reactor wall in order to remove/supply heat.

We consider a mixture of reacting gases with n components. At the catalyst surface m reactions take place. The reacting mixture is specified by state variables; temperature $T(z)$, pressure $p(z)$ and degrees of reactions $(\xi_j(z), j = 1, ..., m)$. The variables are governed by the balance equation for energy, momentum (Ergun's equation) and mass, see Table 10.1.

We shall find the T_a-profile that minimizes the entropy production of the reactor for a given chemical conversion. In other words, we are looking for the optimal heating/cooling strategy of the reactor, with $T_a(z)$ as the control variable.

10.1.1 The entropy production

The entropy production of the reactor can be found in two ways. At stationary states, the entropy balance has three contributions in addition to the entropy production. Entropy follows the flows in, $\left(\sum_i F_i\, S_i\right)_{\text{in}}$, and out, $\left(\sum_i F_i\, S_i\right)_{\text{out}}$. In addition, heat is exchanged with the utility. The entropy balance gives therefore

Table 10.1: Governing equations for the stationary state plug flow reactor.

Balance equation for internal energy:

$$\frac{dT}{dz} = f_T = \frac{\pi\, D\, J'_q + \Omega\, \rho_{\rm B}\, \sum_j [\, r_j\, (-\Delta_{\rm r} H_j)]}{\sum_i [\, F_i\, C_{p,i}\,]}$$

Momentum balance (Ergun's equation):

$$\frac{dp}{dz} = f_p = -\left(\frac{150\,\mu}{D_{\rm p}^2}\, \frac{(1-\epsilon)^2}{\epsilon^3} + \frac{1.75\,\rho^0\, v^0}{D_{\rm p}}\, \frac{1-\epsilon}{\epsilon^3} \right) v$$

Mole balances:

$$\frac{d\xi_j}{dz} = f_{\xi_j} = \frac{\Omega\, \rho_{\rm B}}{F_{\rm A}^0}\, r_j \qquad j = 1, ..., m$$

Balance equation for entropy:

$$\frac{dS_{\rm irr}}{dt} = S_{\rm out} - S_{\rm in} - \pi\, D\, \int_0^L \frac{J'_q}{T_{\rm a}}\, dz$$

$$= \int_0^L \left[\Omega\, \rho_{\rm B}\, \sum_j \left[r_j\, \left(-\frac{\Delta_{\rm r} G_j}{T} \right) \right] + \pi\, D\, J'_q\, \Delta \frac{1}{T} - \Omega\, \frac{v}{T}\, \frac{dp}{dz} \right] dz$$

$$\frac{dS_{\rm irr}}{dt} = \left(\sum_i F_i\, S_i \right)_{\rm out} - \left(\sum_i F_i\, S_i \right)_{\rm in} + \Delta S_{\rm u} \qquad (10.1)$$

where $\Delta S_{\rm u}$ is the change of the entropy of the utility caused by transfer of heat to or from it. In a small element dz, this change is $-\pi\, D\, J'_q(z)/T_{\rm a}(z)\, dz$, where $J'_q(z)$ is the heat flux from the utility to the reacting stream at z. The final expression for the total entropy production, derived from the entropy balance, is

therefore

$$\frac{dS_{\text{irr}}}{dt} = \left(\sum_i F_i\, S_i\right)_{\text{out}} - \left(\sum_i F_i\, S_i\right)_{\text{in}} - \pi\, D \int_0^L \frac{J'_q(z)}{T_{\text{a}}(z)}\, dz \tag{10.2}$$

The entropy production can also be calculated from the fluxes and forces. We saw in Chapter 6 that there are three phenomena that produce entropy in a plug flow reactor: Reactions, heat transport through the reactor wall and frictional flow (pressure drop). The local entropy production (on a unit length basis) was from Eq.(6.41)

$$\sigma' = \Omega\, \rho_{\text{B}} \sum_j \left[r_j \left(-\frac{\Delta_{\text{r}} G_j}{T}\right)\right] + \pi\, D\, J'_q\, \Delta\frac{1}{T} + \Omega\, v \left(-\frac{1}{T}\,\frac{dp}{dz}\right) \tag{10.3}$$

Each term in Eq. (10.3) is a product of a flux and its conjugate force. The first term is sum over all reactions; the flux is the reaction rate, r_j, and the chemical force is $-\Delta_{\text{r}} G_j/T$. This term was discussed in depth in Chapter 7.

The second term is due to heat transfer; the flux is the heat flux, J'_q, and the thermal force is $\Delta 1/T = 1/T - 1/T_{\text{a}}$. The last term is due to frictional flow; the flux is the gas velocity, v, and the force is $(-1/T)\ (dp/dz)$.

The total entropy production is the integral of σ over the reactor coordinate z

$$\frac{dS_{\text{irr}}}{dt} = \int_0^L \sigma'\, dz \tag{10.4}$$

The two expressions for the total entropy production, Eqs. (10.2) and (10.4), are equivalent. The proof of this is given in Exercise 10.1.1. We continue to use Eq. (10.4), because it enables us to connect with local variables.

It can be shown that the reactor produces or consumes work

in the same way as the heat exchanger, see Section 9.3.2. More precisely, an endothermic reactor is a work consuming apparatus and an exothermic reactor is a work producing apparatus. This means that to minimize the entropy production and to minimize the work requirement of the reactor are equivalent problems when the state of the reacting mixture is fixed at the inlet and at the outlet.

Exercise 10.1.1 *Show that Eqs.* (10.2) *and* (10.4) *are equivalent. Assume that the reacting stream is a mixture of ideal gases.*

Solution: The starting point is the total entropy balance Eq (10.2), which we rewrite as:

$$\frac{dS_{\rm irr}}{dt} = \int_0^L \left(\frac{d\sum_i F_i\, S_i}{dz} - \pi\, D\, \frac{J'_q}{T_{\rm a}} \right)\, dz$$

from which we recognize the local entropy production as

$$\sigma' = \frac{d\sum_i F_i\, S_i}{dz} - \pi\, D\, \frac{J'_q}{T_{\rm a}} = \sum_i$$

$$[5pt] \left[F_i\, \left(\frac{\partial S}{\partial T} \right)_{p,F_i} \frac{dT}{dz} + F_i\, \left(\frac{\partial S}{\partial p} \right)_{T,F_i} \frac{dp}{dz} + \left(\frac{\partial F_i\, S_i}{\partial F_i} \right)_{T,p} \frac{dF_i}{dz} \right]$$

$$- \pi\, D\, \frac{J'_q}{T_{\rm a}}$$

with one paranthesis $[]_i$ for each component. The temperature, the pressure and the flow rates describe now the reacting mixture. In order to derive the local entropy production we need the governing equations (Table 10.1) and the derivatives of the entropy with respect to temperature, pressure and flow rates. We use another form of the mole balances here:

$$\frac{dF_i}{dz} = \Omega\, \rho_{\rm B} \sum_{j=1}^{m} \nu_{j,i} r_j \qquad i = 1, ..., n$$

The partial molar entropy of component i for an ideal gas is:

$$S_i = S_i^{\ominus} - R \, \ln \frac{p \, x_i}{p^{\ominus}}$$

The derivatives of the entropy with respect to temperature, pressure and flow rates become:

$$\begin{aligned}
\sum_i F_i \left(\frac{\partial S_i}{\partial T}\right)_{p,F_i} &= \frac{1}{T} \sum_i \left[F_i \, C_{p,i}\right], \\
\sum_i F_i \left(\frac{\partial S}{\partial p}\right)_{T,F_i} &= -\frac{R}{p} \sum_i F_i = -\frac{\Omega \, v}{T}, \\
\left(\frac{\partial \sum_i F_i \, S_i}{\partial x_i}\right)_{T,p} &= S_i = S_i^{\ominus} - R \, \ln \frac{p \, x_i}{p^{\ominus}},
\end{aligned}$$

By introducing the balance equations and the derivatives of the entropy in the local entropy production, we obtain

$$\begin{aligned}
\sigma &= \pi \, D \, \frac{J_q'}{T} + \Omega \, \rho_{\mathrm{B}} \sum_{j=1}^{m} \left[r_j \, \frac{\Delta_{\mathrm{r}} H_j}{T} \right] + \Omega \, v \, \left(-\frac{1}{T} \, \frac{dp}{dz} \right) \\
&\quad + \Omega \, \rho_{\mathrm{B}} \sum_{i=1}^{n} \sum_{j=1}^{m} \left[\nu_{j,i} \, r_j \, S_i \right] - \pi \, D \, \frac{J_q'}{T_{\mathrm{a}}} \\
&= \Omega \, \rho_{\mathrm{B}} \sum_{j=1}^{m} \left[r_j \, \left(-\frac{\Delta_{\mathrm{r}} G_j}{T} \right) \right] + \pi \, D \, J_q' \, \Delta \frac{1}{T} + \Omega \, v \, \left(-\frac{1}{T} \, \frac{dp}{dz} \right)
\end{aligned}$$

which is the local entropy production as given in Eq. (10.3). In the last equality, we used $\sum_{i=1}^{n} \sum_{j=1}^{m} \left[\nu_{j,i} \, r_j \, S_i \right] = \sum_{j=1}^{m} \left[r_j \, \Delta_{\mathrm{r}} S_j \right]$. The derivation is similar for a nonideal gas mixture. We then have to change the balance equation for the internal energy to

$$C_p \frac{dT}{dz} = \pi \, D \, J_q' + \Omega \, \rho_{\mathrm{B}} \sum_j \left[\, r_j \, \left(-\Delta_{\mathrm{r}} H_j \right) \right] - \left(\frac{\partial H}{\partial p} \right)_{T,F_i} \frac{dp}{dz}$$

in order to account for the change of enthalpy caused by change of pressure.

10.1.2 Optimal control theory and plug flow reactors

We find necessary conditions for minimum entropy production using optimal control theory [97] in the same way as for the expansion and the heat exchanger, see Sections 9.1 and 9.3. The Hamiltonian for the present problem is

$$\mathcal{H} = \sigma + \lambda_{\mathrm{T}} f_{\mathrm{T}} + \lambda_{\mathrm{p}} f_{\mathrm{p}} + \sum_j \left[\lambda_{\xi_j} f_{\xi_j} \right] \tag{10.5}$$

The Hamiltonian contains the local entropy production Eq. (10.3), and products of multiplier functions, λ's, and the right hand sides of the conservation equations in Table 10.1. The Hamiltonian does not depend explicitly on z and is thus constant along the z-coordinate in the state of minimum entropy production [97].

The necessary conditions for minimum entropy production are the following $2m + 4$ differential equations

$$\begin{aligned}
\frac{dT}{dz} &= \frac{\partial \mathcal{H}}{\partial \lambda_{\mathrm{T}}} & \qquad \frac{d\lambda_{\mathrm{T}}}{dz} &= -\frac{\partial \mathcal{H}}{\partial T} \\
\frac{dP}{dz} &= \frac{\partial \mathcal{H}}{\partial \lambda_{\mathrm{P}}} & \qquad \frac{d\lambda_{\mathrm{p}}}{dz} &= -\frac{\partial \mathcal{H}}{\partial p} \\
\frac{d\xi_j}{dz} &= \frac{\partial \mathcal{H}}{\partial \lambda_{\xi_j}} & \qquad \frac{d\lambda_{\xi_j}}{dz} &= -\frac{\partial \mathcal{H}}{\partial \xi_j}
\end{aligned} \tag{10.6}$$

where $j = 1, ..., m$, and the algebraic equation

$$\frac{\partial \mathcal{H}}{\partial T_{\mathrm{a}}} = 0 \qquad \text{for all } z \in [0, L] \tag{10.7}$$

The left column in Eq. (10.6) reduces to the balance equations, see Table 10.1.

It is impossible to eliminate all the multiplier functions from the Hamiltonian in the same way as we did in Sections 9.2 and 9.3.3.

The reason is that there are less control variables than there are thermodynamic forces in the system (one control variable and $m + 2$ forces). This property of the problem has also consequences for the validity of the equipartition results (EoEP and EoF). Johannessen and Kjelstrup [80] showed that EoEP and EoF can be proved rigorously only when the number of control variables is equal to or larger than the number of thermodynamic forces in the system. This means that EoEP and EoF do not describe the state of minimum entropy production in the entire reactor. Equipartition may describe the optimal state in parts of the reactor, though.

10.1.3 A highway in state space

The necessary conditions, Eqs. (10.6)-(10.7), have to be solved numerically. Boundary conditions are needed together with the differential equations in Eq. (10.6). For a fixed chemical conversion (ξ_j fixed at the inlet and the outlet), the optimal state depends on the temperatures and the pressures at the inlet and the outlet. By studying all possible combinations of temperatures and pressures, an enormous collection of optimal states is obtained. The collection becomes even larger when we study the effect of varying the composition at both boundaries. We focus on a set of solutions crowding in on what seems to be a *highway in state space* [80]. This is a general property of the states of minimum entropy production in plug flow reactors. We use the oxidation of SO_2 to SO_3 as an example reaction, and neglect pressure gradients. The reaction is exothermic. Thermodynamic and kinetic data and other model parameters for the reactor can be found in Ref. [47].

The state of the reaction mixture in the SO_2 oxidation reactor is specified by the degree of reaction and the temperature of the mixture. Figure 10.2(a), which gives $T(z)$ as a function of $\xi(z)$, is a dynamic state diagram for the reactor. There are several

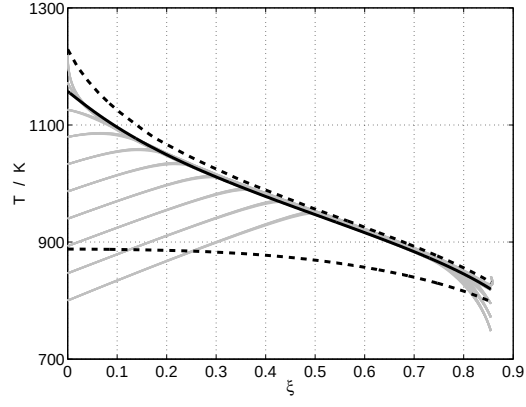

(a) State diagram for minimum entropy production for the SO_2 oxidation reactor. Printed with permission of Chemical Engineering Science

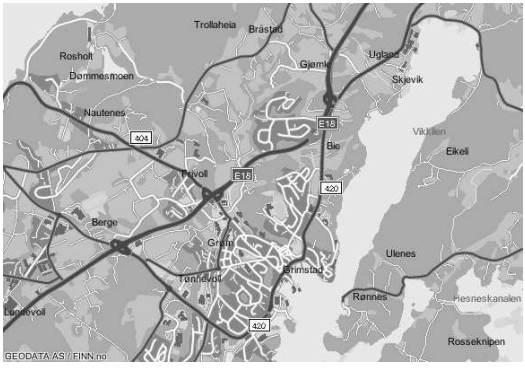

(b) A road map. Printed with permission of Geodata AS, Norway.

Figure 10.2: Solutions of the optimization problem for 50 combinations of inlet and outlet temperatures (10 gray solid lines can be seen) are shown in Fig. (a). The equilibrium line (upper dashed line) and the maximum reaction rate line (lower dashed line) are shown for $L = 6.096$ m, $\xi^{\text{in}} = 0$, $\xi^{\text{in}} = 0.8547$, $dP/dx = 0$. The highway in state space and its connecting paths, can be compared to the highway E18 with its connecting roads to the surroundings, as pictured in Fig. (b).

lines in Fig. 10.2(a). The upper dashed line is the equilibrium line. Along this line, $\Delta_r G$ and the reaction rate are both zero. The lower dashed line is the maximum reaction rate line. For any value of the conversion, the temperature given by this line corresponds to maximum reaction rate. Furthermore, we have plotted the optimal solutions for fifty combinations of ten inlet temperatures and five outlet temperatures (gray solid lines). Only ten gray lines can be distinguished in the figure. The solutions reveal an interesting property: The central parts of the solutions fall more or less on the same line. This line extends from the inlet on the left hand side to the outlet on the right hand side. The individual solutions enter and leave this line at different positions depending on where their initial and final destinations are. The collection of solutions in Fig. 10.2(a) looks like a highway with its connecting roads, cf. Fig. 10.2(b). Johannessen and Kjelstrup [80] adopted the highway picture and called the band, which all solutions enter, a "reaction highway".

The reaction highway is a path in state space which is especially crowded by solutions, just like a real highway is crowded by cars. A solution does not enter the highway if its initial and final points are close in state space. The exception is if both points are on or near the reaction highway. The reaction highway is primarily used in order to travel "far" in state space. This is another analogy with the real highway. The meaning of "far" and "short" is case dependent.

A real highway makes it possible to get from one place to another very quickly; using the highway is time efficient because we are able to drive at high speed. This property of a real highway is not immediately transferable since the reaction highway is an energy efficient path. Time efficiency, or high speed, corresponds to a different optimization problem: maximum chemical conversion (see for instance [101–103]). Large parts of the solu-

tions of this optimization problem lie on the maximum reaction rate line. The maximum reaction rate line is therefore the time efficient highway in state space. One might also say that the maximum reaction rate line is the fast lane on the real highway. The highway for the minimum entropy production problem corresponds then to the other lane - the lane for those who want to arrive in reasonable time with minimum use of fuel.

The highway coincides with the black solid line in Fig. 10.2(a). This is the solution of the same optimization problem when there is no resistance to heat transfer, when $U = \infty$. The reaction is then the only entropy producing process in the reactor, because we neglected the pressure drop here. The position of the pure reaction solution in state space, and thus the highway, is dictated by the process intensity (chemical conversion per meter reactor). For an infinitely long reactor, the highway coincides with the equilibrium line. As the process intensity increases, the highway shifts toward the maximum reaction line. The highway in Fig. 10.2(a) corresponds to a process intensity of technical relevance. Johannessen and Kjelstrup [47] showed that there exists an optimal reactor length which gives the best trade off between low entropy production of heat transfer and reactions (long reactors are favorable) and low entropy production of frictional flow or pressure drop (short reactors are favorable).

The nature of the highway is further presented in Fig. 10.3. The figure shows the local entropy production as a function of the conversion for one solution (solid line). The part of the solution with approximately constant local entropy production is on the highway. The contributions from the reaction (dashed line) and the heat transfer term (dash-dot line) are also included. The entropy production is not constant in the beginning and in the end of the reactor because the reactor has to accommodate certain boundary conditions. These parts of the solution are off the highway. The figure shows that there is a shift of operation

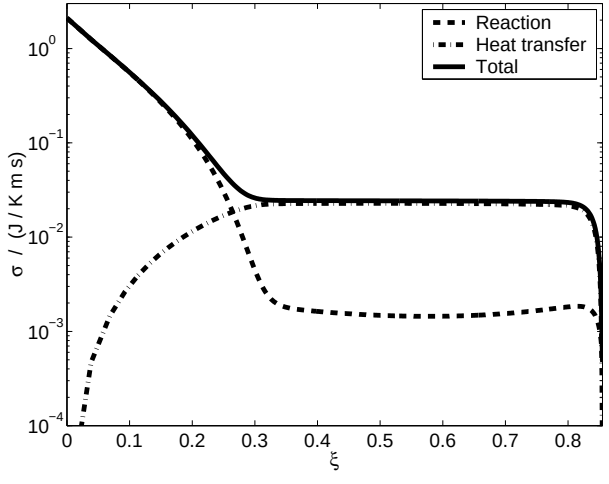

Figure 10.3: Local entropy production as a function of conversion for one solution of the optimization problem when we neglect the pressure drop. Printed with permission of Chemical Engineering Science (publication CES5877).

mode as the solution enters the highway. Up to this point the entropy production due to the reaction is much larger than the heat transfer term. We say that the reactor operates in a *reaction mode*. The reactor operates with low heat transfer duty in this region. It is basically the enthalpy of reaction that heats the reaction mixture until it reaches the highway. Once on the highway, the heat transfer term dominates the entropy production. It is the heat transfer that drives the solution along the highway, and we can say that the reactor is in a *heat transfer mode* of operation. There is a fine balance between the heat produced by the reaction and the rate of heat transfer. This fine balance prevents the reaction from reaching equilibrium and is therefore essential for the chemical production on the highway.

There is also a highway in state space when we include the pressure drop in the optimization. It exists for other reactors too,

with one or more reactions which might be exothermic or endothermic. When the process intensity is not too high, EoEP and EoF are good approximations to the optimal states on the highway. EoEP is slightly better than EoF. For high process intensities, the highway is shifted far away from the equilibrium line. The nonlinearities in the reaction rate expressions are then substantial, and EoEP and EoF do not approximate the highway any more. The process intensity in typical industrial reactors is usually in the range where EoEP and EoF approximate the highway well.

It is interesting that the highway can be characterized by almost constant entropy production and forces. These properties have been proved when there are enough control variables and the flux-force relations are linear [80, 92, 93]. But they are more general than that: The system adjusts to some kind of optimal behavior, if it is given enough freedom to do so, also when the flux is a nonlinear function of the force as in chemical reactors. It is clear, that there is enough freedom to adjust in the central part of the reactors. These findings were summarized as a hypothesis for the state of minimum entropy production in an optimally controlled system by Johannessen and Kjelstrup [80]:

> *EoEP, but also EoF are good approximations to the state of minimum entropy production in the parts of an optimally controlled system that have sufficient freedom to equilibrate internally.*

The concept of 'sufficient freedom" needs some explanation. A system where the number of control variables is at least as high as the number of forces has sufficient freedom throughout to equilibrate internally provided that it is not too far from equilibrium. A system with too few control variables has generally not enough freedom in the whole system. Boundary conditions

as well as the compromise that must take place between the dissipative phenomena, will restrict the solution. The central part of the system is relatively more free from these restrictions. Freedom is thus not only related to the number of control variables, but also to the number and type of constraints on the system. The sufficient freedom is then necessarily system specific.

10.1.4 Reactor design

In order to design a reactor that operates in the state of minimum entropy production, one would have to tailor the exact heating or cooling strategy along the reactor. As for the heat exchanger in Section 9.3.3, this is often too expensive and/or impractical.

We saw in the last Section that the optimal reactor is characterized by what we called a reaction mode and a heat transfer mode. This result and the result on the reactor length are important, when it comes to taking the results from theory to practice. We find that the reaction is best accomplished by an adiabatic reactor inlet and a counter-currently cooled subsequent part. It is only from a resolution of the local entropy production that this insight can be obtained.

We can draw some conclusions from the design of the SO_2-reactor, which turn out to be general:

1. A tubular chemical reactor of length L, operating in an energy efficient way, should have an inlet section, of length L_1, that is (close to) adiabatic. The heat of the reactions moves the reacting mixture toward chemical equilibrium, i.e. the reactor operates in the reaction mode.

2. A tubular chemical reactor of length L, operating in an energy efficient way, should have a central section, L_2, characterized by a fine balance between heat transfer and

reaction rate(s), so that the temperature of the reacting mixture is (approximately) at constant distance from the temperature at which the mixture is in equilibrium. This can be achieved by counter-current heat-exchange. We say that the reactor should operate in a heat transfer mode in L_2.

3. A tubular chemical reactor operating in an energy efficient way, should have a total reactor length $L \geq L_1 + L_2$, that gives the best trade off between low entropy production of heat transfer and reactions (long reactors are favorable) and low entropy production due to pressure drop (short reactors are favorable).

Similar statements can be made for other reactors. Examples of good engineering practices support these guidelines, i.e. state-of-the-art tubular steam reformers, see e.g. [104].

10.2 Distillation columns

Mixtures of chemicals are often separated by distillation. Distillation requires addition and withdrawal of heat. This is connected with a large entropy production. Distillation columns are therefore targets for optimization.

A sketch of a tray distillation column is shown in Fig. 10.4. The column has N trays which bring a rising stream of vapor in close contact with a descending stream of liquid. The feed stream, F, is separated into two fractions with different boiling temperatures and compositions. The low-boiling fraction is called the distillate, D, and is taken out at the top of the column. The high-boiling fraction is obtained as the bottom stream, B. In a conventional column, heat is only added in a reboiler and only withdrawn in a condenser, Q_{N+1} and Q_0 in Fig. 10.4. No heat is added on the trays, meaning that Q_1 to Q_N in Fig. 10.4 are zero. This is an *adiabatic* column.

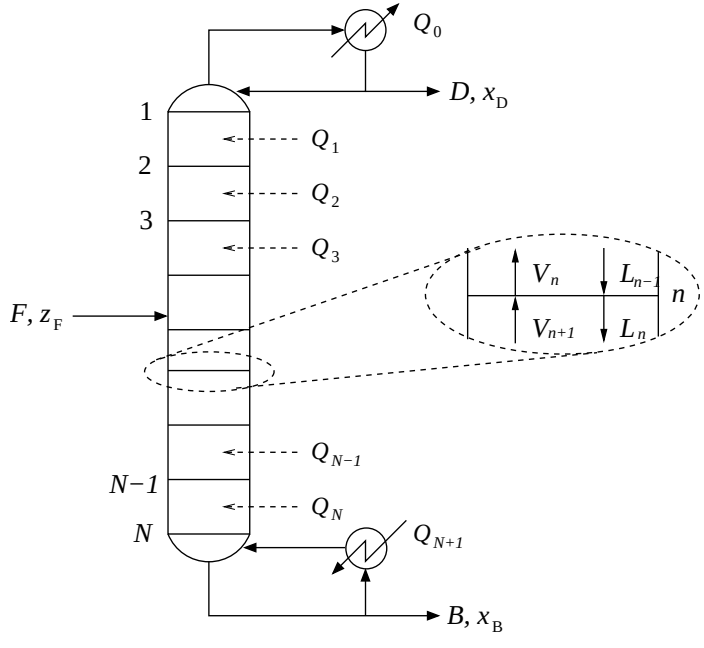

Figure 10.4: A tray distillation column with heat exchange on all trays. Q_1,...,Q_N are zero in an adiabatic column. All Q's are in general nonzero in a diabatic column.

In a *diabatic* column, heat may also be added/withdrawn by means of heat exchangers on every tray (cf. Fig. 10.4). We shall see that diabatic columns have better thermodynamic efficiencies than adiabatic ones [84, 105–107]. The total apparatus becomes more complicated, but there are still indications that diabatic distillation may be economically feasible [91, 108].

It is common to illustrate the properties of distillation columns with McCabe-Thiele diagrams [109]. The McCabe-Thiele diagrams for the adiabatic and diabatic columns are given in Figs. 10.5 and 10.6, respectively. The equilibrium line in the upper part of the diagrams give the compositions of co-existing liquid and gas. The *operating line* is the line that connects the distillate -, the feed stream - and the bottom stream composi-

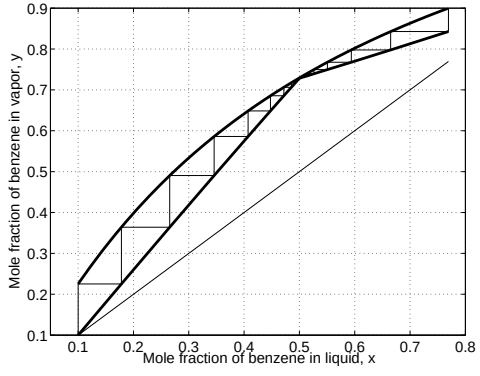

Figure 10.5: The McCabe-Thiele diagram for adiabatic distillation. The upper line gives vapor and liquid equilibrium compositions. The operating line (the lower line) gives corresponding compositions at the inlet of a tray. ($A_{\text{total}} = \infty$, $N = 20$, $x_D = 0.9$, $x_B = 0.1$)

tions. In the adiabatic column, the operating line has a bend; in the diabatic column it is continuous. The two lines are almost parallel in the diabatic column, see also [110]. On average, the operating line is closer to the equilibrium line in the diabatic column, than in the adiabatic column. The diabatic column operates thus closer to equilibrium and produces less entropy.

We want to find the column with minimum entropy production, and compare it to an adiabatic column. The question is how the entropy production can be minimized by distributing the heating/cooling capacity over the column in a different way than is done in the adiabatic column. More precisely, we want to find the optimal distributions of heat exchanged and heat transfer area on each tray, Q_n and A_n for $n = 0, 1, ..N + 1$, when the temperatures/compositions of the feed, distillate and bottom streams and the total heat transfer area, A_{total}, are fixed. We shall assume here that the heating/cooling utility in the heat exchangers can have any temperature.

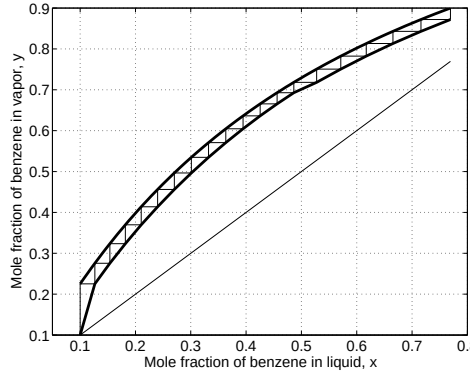

Figure 10.6: McCabe-Thiele diagram for the diabatic column. ($A_{\text{total}} = \infty$, $N = 20$, $x_D = 0.9$, $x_B = 0.1$)

We shall study binary distillation and use a standard model for the distillation column [109]. The governing equations are given in Table 10.3 [89]. The table gives the total mole balance, the mole balance for the light component and the balance equation for the internal energy at each tray. Two major assumptions in the model are

- The total pressure is constant throughout the column, $P =$ 1 bar.
- The liquid and the vapor that leave a tray, see the small frame in Fig. 10.4, are in equilibrium with each other at the temperature of the tray, T_n.

10.2.1 The entropy production

The entropy production of the column has separate contributions from all trays. On tray number n there is transport of heat and mass between the liquid and vapor phases. The model contains no details of these processes, and we find the entropy production due to heat and mass transfer across the phase boundary

Table 10.2: Physical chemical properties of benzene and toluene.

Component:	Benzene	Toluene
T^{boil}/K	353.25	383.78
C_P^{vap}/ J/mol K	81.63	106.01
C_P^{liq}/ J/mol K	133.50	156.95
$\Delta_{vap}H$/ J/mol	33600	38000
s_0^{liq}/ J/mol K	269.20	319.74

from the entropy balance equation only

$$\left(\frac{dS_{irr}}{dt}\right)_{\mathrm{col},n} = V_n\, S_n^{\mathrm{V}} + L_n\, S_n^{\mathrm{L}} - V_{n+1}\, S_{n+1}^{\mathrm{V}} - L_{n-1}\, S_{n-1}^{\mathrm{L}} - \frac{Q_n}{T_n} \tag{10.8}$$

The first four terms on the right hand side represent entropy carried in and out with the streams entering and leaving tray n. The last term is due to the heat exchanged in the heat exchanger.

There are also contributions to the entropy production from the heat exchangers. We use an average heat transfer force as described in Table 10.3. The contribution from the heat exchanger on tray n is therefore [86, 111].

$$\left(\frac{dS_{irr}}{dt}\right)_{\mathrm{hx},n} = Q_n\, X_n \tag{10.9}$$

The entropy production on tray n is the sum of Eqs. (10.8) and (10.9). We want to minimize the total entropy production in the column, which is found by summing over all trays, including the condenser ($n = 0$) and the reboiler ($n = N + 1$).

Take the separation of benzene (light component) and toluene as an example [85]. The feed, F=1.00 mol/s, is an equimolar liquid mixture at its boiling point ($z_F = 0.5$, $q = 1$). The distillate and the bottom streams are also liquids at their boiling points.

Table 10.3: Governing equations for stationary state binary tray distillation.

Total mole balance:

$$V_{n+1} - L_n = \begin{cases} D, & n \in [0, N_{\mathrm{F}} - 2] \\ D - (1-q)\, F, & n = N_{\mathrm{F}} - 1 \\ D - F, & n \in [N_{\mathrm{F}}, N+1] \end{cases}$$

Mole balance for light component:

$$V_{n+1}\, y_{n+1} - L_n\, x_n = \begin{cases} D\, x_{\mathrm{D}}, & n \in [0, N_{\mathrm{F}} - 2] \\ D\, x_{\mathrm{D}} - (1-q)\, F z_{\mathrm{F}}, & n = N_{\mathrm{F}} - 1, \\ D\, x_{\mathrm{D}} - F\, z_{\mathrm{F}}, & n \in [N_{\mathrm{F}}, N+1]. \end{cases}$$

Balance equation for internal energy:

$$Q_n = V_n\, H_n^{\mathrm{V}} + L_n\, H_n^{\mathrm{L}} - V_{n+1}\, H_{n+1}^{\mathrm{V}} - L_{n+1}\, H_{n+1}^{\mathrm{L}} - \kappa$$

$$\text{where } \kappa = \begin{cases} (1-q)\, F\, H_{\mathrm{F}}^{\mathrm{V}}, & n = N_{\mathrm{F}} - 1, \\ q\, F\, H_{\mathrm{F}}^{\mathrm{L}}, & n = N_{\mathrm{F}}, \\ 0, & \text{otherwise.} \end{cases}$$

Average force for heat exchange:

$$X_n = (\delta / \lambda_n\, T_n^2)\ (Q_n / A_n)$$

Balance equation for entropy:

$$\frac{dS_{\mathrm{irr}}}{dt} = B\, S^{\mathrm{B}} + D\, S^{\mathrm{D}} - F\, S^{\mathrm{F}} + \sum_{n=0}^{N+1} \left(-\frac{Q_n}{T_n} + Q_n\, X_n \right)$$

Some physical chemical properties for the mixture are given in Table 10.2.

The reference case is a column with $N = 20$ trays, where the mole fractions of benzene in the product streams are $x_D = 0.9$ and $x_B = 0.1$. The presented results are obtained with the numerical optimization method described by Røsjorde and Kjelstrup [89].

Consider the adiabatic column and the optimal diabatic column when the total heat transfer area, A_{total}, is infinitely large [84,

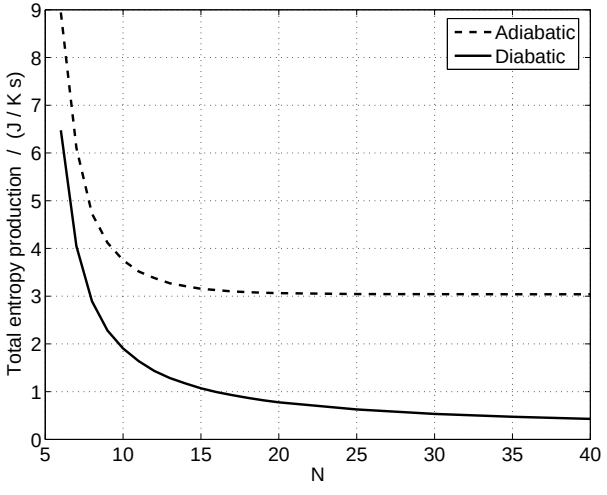

Figure 10.7: The total entropy productions of the adiabatic and the diabatic columns as a function of the number of trays. ($A_{\text{total}} = \infty$, $x_D = 0.9$, $x_B = 0.1$)

85, 87]. This corresponds to $X_n = 0$, meaning that the heat exchangers do not contribute to the entropy production. The characteristics of the optimal diabatic column when $X_n = 0$ is thus due to the heat and mass transfer processes at the phase boundary.

Figure 10.7 shows the total entropy production of the adiabatic column and the optimal diabatic column as a function of the number of trays for $A_{\text{total}} = \infty$, $x_D = 0.9$ and $x_B = 0.1$. The total entropy productions in both columns change rapidly when $N < 15$. In longer columns the entropy production changes slower. It approaches zero when N goes to infinity (not shown). The diabatic column produces less entropy for all values of N, as expected from the McCabe-Thiele diagrams. The reduction increases when N increases. It is between 28% and 86% in the N-range shown in the figure. The total entropy production in the adiabatic column and in the diabatic column with $N = 20$

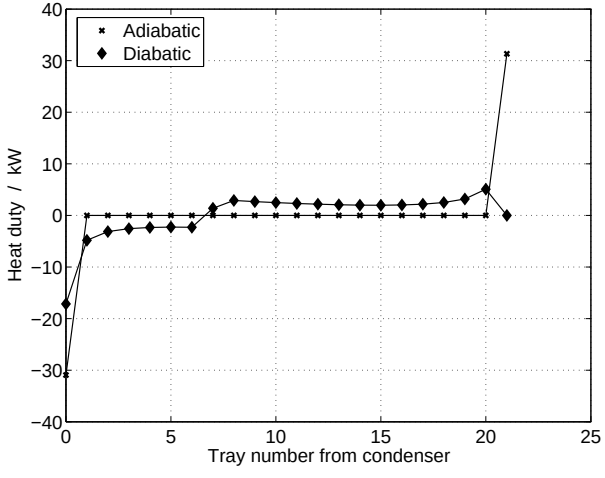

Figure 10.8: The heat duties along the adiabatic and the diabatic columns. ($A_{\text{total}} = \infty$, $N = 20$, $x_D = 0.9$, $x_B = 0.1$)

are 3.06 J/K s and 0.78 J/K s, respectively (75% reduction). Figure 10.8 shows why the entropy production is reduced. In the diabatic column, heat is withdrawn on each tray above the feed and added on all trays below the feed. The diabatic column has $Q_{21} = 0$, meaning that the reboiler is not operative; it can be omitted. In general, heat is added at a lower temperature and withdrawn at a higher temperature in the diabatic column than in the adiabatic column, where heat is added only at the reboiler and withdrawn only at the condenser.

Figure 10.9 shows how the total entropy production (with $N = 20$, $x_D = 0.9$, $x_B = 0.1$) vary when the total heat exchanger area, A_{total}, varies. The behavior is qualitatively the same as the behavior when the number of trays varies (cf. Fig. 10.7). For large transfer areas, the entropy production approaches the values for $A_{\text{total}} = \infty$, which are given by vertical lines in Fig. 10.9. For the range of A_{total}-values in the figure, the entropy production of the diabatic column is between 38% and 73% less than the

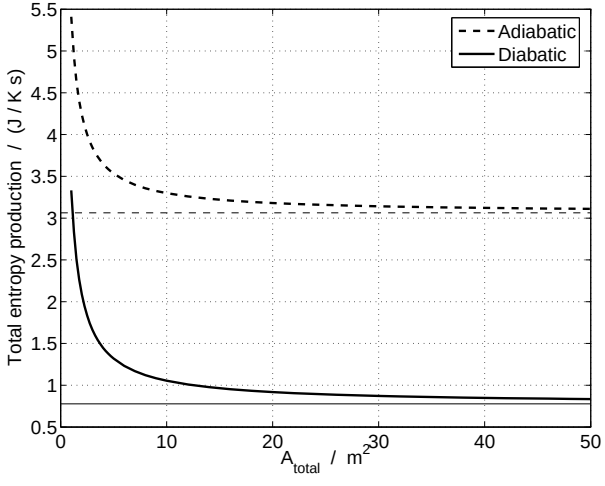

Figure 10.9: The total entropy productions of the adiabatic and the diabatic columns as a function of the total heat transfer area. ($N = 20$, $x_D = 0.9$, $x_B = 0.1$)

entropy production of the corresponding adiabatic column.

The value of the heat-exchanger area affects the profile of the diabatic column. With a realistic total heat transfer area, most of the area is placed close to the ends of the column. The same is true for the heat added/withdrawn on the trays. Actually, most of the heat exchangers are not operative if the column is long [89]. This means that the profiles of diabatic and adiabatic columns become more similar when the total heat exchanger area decreases. The profiles and the total entropy production, of the two columns are significantly different for realistic values of the total heat exchanger area, though.

The purities of the distillate and the bottom stream are other important parameters. At least one of these streams has a purity of 99% or better in most industrial columns. The difference between the entropy productions of the adiabatic and the dia-

batic columns decreases as the purity increases when all other parameters are fixed, but there is still a significant potential for improvement by making the column diabatic for high purities. By increasing the number of trays as the purity increases, the gain is much less sensitive to the product purity [85]. In general, proper choices of the number of trays and the total heat transfer area are important for both the adiabatic and the diabatic column, regardless of the product purities.

We have discussed equipartition results like EoEP and EoF for other processes earlier in this Chapter. The distillation column is different for two reasons. The other examples were continuous processes, whereas the tray distillation column was treated as a staged process. Furthermore, the local entropy production was a sum of fluxes times forces in the other examples. The model we have used for the distillation column is very simple. It contains no details of the processes at the liquid-vapor interface. It was therefore not possible to write the local entropy production as a sum of fluxes times forces. We had to use entropy balances instead, see Section 10.2.1. Despite these differences, EoEP and EoF are also important for the understanding of the optimal diabatic distillation column.

Figure 10.10 shows the heat exchanger force (squares) on each tray in the diabatic column for our base case ($N = 20$, $x_D = 0.9$, $x_B = 0.1$, $A_{\text{total}} = 20$ m^2). The figure shows clearly that the force is approximately constant in each section of the column and that the absolute value is approximately constant throughout the column. This property of the optimal diabatic column was first found by De Koeijer et al. [86]. They studied four different ways to distribute the total heat transfer area in the diabatic distillation column. The best area distribution rule was to keep the absolute value of the heat exchanger force constant, Røsjorde and Kjelstrup [89].

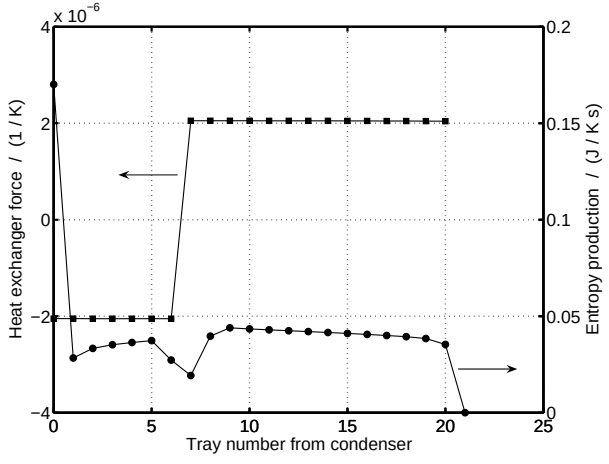

Figure 10.10: The heat exchanger force (squares) and the entropy production (circles) on each tray in the diabatic column. ($N = 20$, $x_D = 0.9$, $x_B = 0.1$, $A_{\text{total}} = 20$ m^2)

Johannessen and Røsjorde [90] studied a dynamic model of the distillation column using the hypothesis for the state of minimum entropy production (see Section 10.1.3). According to this hypothesis, a column with constant entropy production in the rectifying and the stripping sections (EoEP) is a good approximation to the optimal diabatic column, except when there is little freedom to adjust the path (small N and/or small A_{total} and/or high purity). The values of the tray entropy production in the two sections should in general be different because different duties are assigned to the two sections. The condenser, the reboiler and the trays that are directly affected by the feed should not be included in the equipartitioning. Johannessen and Røsjorde [90] compared the optimal diabatic column and the EoEP-column. They found that the predictions based on the hypothesis were correct. Figure 10.10 shows the entropy production (circles) on each tray in the diabatic column for our base case ($N = 20$, $x_D = 0.9$, $x_B = 0.1$, $A_{\text{total}} = 20$ m^2). The

figure shows clearly that the tray entropy production is approximately constant in each section, when the condenser ($n = 0$), the feed tray ($n = 7$) and the reboiler ($n = 21$) are not considered.

10.2.2 Column design

There are two major engineering challenges with making a distillation column fully diabatic. Firstly, the vapor and liquid flows vary through the column. This has important implications for the fluid dynamics in the column. To address this, the column can be designed with a varying diameter from top to bottom [112, 113]. The diameter should be roughly proportional with the vapor flow for low-pressure operations. Such a column could be expensive in combination with the costs of extra pumps, extra heat exchangers with tubing, etc. An alternative has been proposed by Olujic and coworkers [114,115]; the diameter is maintained, while the internal area is varied.

The second important challenge is the range of temperatures needed for the utilities. In the optimization, it was assumed that utilities at all temperatures are available in the plant. This is usually not the case in practice. The limited number of available utilities means that one has to approximate the fully diabatic column. One possibility is to use a single heating fluid circulating in series from one tray to the next below the feed tray and a single cooling fluid circulating in series above the feed tray [116]. The fluid dynamical problem was already mentioned.

One observation for the diabatic column is that the most important heat exchangers are close to the two ends of the column, especially when the column is long [89]. A practical alternative is therefore to only put heat exchangers on trays 1 and N. The hydrodynamics will not be affected too much and the additional capital costs are probably reasonable. Further improvements

can be achieved by integrating the two heat exchangers so that the heat added on tray N is taken from tray 1. This can be done with a heat pump [117], or by elevating the pressure in the rectifying section (above the feed tray) in order to shift the phase equilibrium to higher temperatures there [118]. The latter alternative is used in the state-of-the-art technology for air separation [119].

In summary, there are many ways to approach a completely diabatic column. All the options have common characteristics. An energy efficient distillation column allows for heat exchange along the column, facilitated by a distribution of the available heat transfer area. The heat may be exchanged through means of heating/cooling media, or by direct interaction with other columns matching the required heating/cooling duty.

10.3 Concluding remarks

In this Chapter, we have studied models of real process units. We have seen that the equipartition results from the previous Chapter do not apply to the entire reactor or distillation column. But, there are parts of these systems which have approximately constant local entropy production and / or thermodynamic forces when the system is in the state of minimum entropy production. The hypothesis for the state of minimum entropy production in an optimally controlled system, explains that we can expect such behavior in (a part of) a system if there is sufficient freedom. Tight constraints leads to deviations from the equipartition principle, however.

We presented the highway in state space for chemical reactors with minimum entropy production. This is a path in the reactor's state space which is crowded by solutions of the optimization problem; in the same way as a real highway is crowded by cars. A highway exists also for distillation columns.

The local expression for the entropy production enables a functional constrained optimization, where optimal profiles of the control variables can be identified. This adds insight to process operation, as the entropy production is obtainable from molecular properties. It also enables conceptual equipment design. We saw for the SO_2-reactor that quantitative information can be obtained about reactor length and operating conditions (adiabatic / non-adiabatic). Trade-offs of different transport processes can be handled, and local optimizations of operating variables can be included.

From the optimization results, we concluded on a set of guidelines or energy efficient operation of process units. Procedures should be found to design whole plants, not only process units. It has been proposed that process control can benefit from non-equilibrium thermodynamics [39]. Process control can be used to keep systems on their path of minimum entropy production.

This page intentionally left blank

Appendix A

A.1 Balance equations for mass, charge, momentum and energy

Balance equations are used in the Gibbs equation in this book, cf. 3, 6 and (A.39) below, to find the entropy production in terms of the conjugate fluxes and forces. It is the purpose of this Section to give the balance equations in a form that can be used in the Gibbs equation. Balance equations have the general form

$$\text{Accumulation} = \text{Influx} - \text{Outflux} + \text{Production} \qquad \text{(A.1)}$$

Compare this with Eqs. (3.1) and (3.2)! Prominent balance equations are conservation laws of mass, total energy and momentum. These laws have a zero production term. When the balance equation is formulated for non-conserved properties, like component mass, internal energy or entropy, Eq. (A.1) has a non-zero production term, which may be positive or negative, except for the entropy production which is always positive or zero. Momentum changes are best described when material densities are given in units of $\mathrm{kg/m^3}$, while chemical and elec-

trochemical reactions are best described when we used units of mol/m^3. Conversions between the two units are therefore often required in the balance equations.

Balance equations for mass and internal energy can be used directly in the Gibbs equation. The momentum balance affects the total energy, however, and enters Gibbs'equation via the internal energy balance. We start with a formulation of the mass balance of integral form, and continue to find the corresponding differential form. We consider only homogeneous systems without relativistic or radiative effects. We do not consider complex fluids, in which there are elastic contributions to the pressure tensor. We shall deal with systems away from mechanical equilibrium and include the effect of electric fields needed for descriptions of electrochemical systems in flow fields, even if this is not elaborated on in this book. Kjelstrup and Bedeaux described heterogeneous systems [29] in mechanical equilibrium.

A.1.1 Mass balance

The total mass balance is composed of component balances. The balance equation for the mass density ρ_i of component i in a time-independent volume, V, is[1]

$$\frac{d}{dt}\int_V \rho_i \, dV = -\int_A \rho_i \mathbf{v}_i \cdot \mathbf{n}_A \, dA + \int_V \nu_i M_i r \, dV \qquad \text{(A.2)}$$

where r is the reaction rate in units mol/(m^{3}s), M_i the molecular mass in kg/mol, and ν_i the stoichiometric coefficient. Furthermore $\mathbf{v}_i$ is the velocity of component i. The left-hand side of Eq. (A.2) represents accumulation of mass of component i in

[1]Throughout this appendix we indicate vectors by boldface letters, e.g. the velocity $\mathbf{v}$. The internal product $\mathbf{a}\cdot\mathbf{b} = \sum a_\alpha b_\alpha$,where α is x, y, z, leads to a scalar. Analogously, $\nabla\cdot\mathbf{a}$ is the divergence of the vector field $\mathbf{a}$ (and is thus a scalar).

volume V. The first term on the right-hand side accounts for the net flux of the component through the surface A. The vector $\mathbf{n}_A$ in Eq. (A.2) is the normal on the surface. It has a unit length, is orthogonal to the surface, and is pointed outward. The mass-transfer across the surface is obtained using the interior product (or dot-product) of the velocity vector with the normal. The second term on the right-hand side accounts for the net production of the component in a reaction. We restrict ourselves to one reaction. When there are multiple independent reactions, we sum over these reactions. Applying Gauss' divergence theorem, $\int_A \mathbf{F}\cdot\mathbf{n}_A\, dA = \int_V \nabla\cdot\mathbf{F}\, dV$, to the surface integral in Eq. (A.2), using that this equation is valid for an arbitrary choice of the volume, we find the balance equation for i in differential form

$$\frac{\partial \rho_i}{\partial t} = -\nabla\cdot\rho_i\mathbf{v}_i + \nu_i M_i r \tag{A.3}$$

This equation is often referred to as the continuity equation.Upon summing Eq. (A.3) over all n components, we obtain

$$\frac{\partial \rho}{\partial t} = -\nabla\cdot(\rho\,\mathbf{v}) \tag{A.4}$$

where the total mass density of the mixture is given by

$$\rho \equiv \sum_{i=1}^{n} \rho_i \tag{A.5}$$

The barycentric (center of mass) velocity $\mathbf{v}$ is

$$\mathbf{v} \equiv \frac{1}{\rho}\sum_{i=1}^{n} \rho_i\mathbf{v}_i = \sum_{i=1}^{n} w_i\mathbf{v}_i \tag{A.6}$$

Here $w_i \equiv \rho_i/\rho$ denotes the mass fraction of component i. To obtain Eq. (A.4), we used that the total mass is conserved in the reaction

$$\sum_{i=1}^{n} \nu_i M_i = 0 \tag{A.7}$$

Equation (A.4) is the conservation law for the total mass. For the component density $c_i \equiv \rho_i/M_i$ (in mol/m^3) the balance equation equivalent to Eq. (A.3) is:

$$\frac{\partial c_i}{\partial t} = -\nabla\cdot(c_i\mathbf{v}_i) + \nu_i r \tag{A.8}$$

Summing Eq. (A.8) over all components, we obtain

$$\frac{\partial c}{\partial t} = -\nabla\cdot(c\,\mathbf{v}_{mol}) + r\sum_{i=1}^{n}\nu_i \tag{A.9}$$

for the total molar density of the mixture

$$c \equiv \sum_{i=1}^{n} c_i \tag{A.10}$$

The average molar velocity is defined as

$$\mathbf{v}_{mol} \equiv \frac{1}{c}\sum_{i=1}^{n} c_i\mathbf{v}_i = \sum_{i=1}^{n} x_i\mathbf{v}_i \tag{A.11}$$

Here $x_i \equiv c_i/c$ is the mole fraction of the component. Only Eq. (A.4) for the total mass density is a conservation law. None of the other quantities is conserved. They all satisfy a balance equation with a production term. The last term $r\sum\nu_i$ in Eq. (A.9),for example, is the production of moles in the reaction. Equation (A.9) shall be used in Eq. (A.39) below.

A.1.2 Momentum balance

The momentum balance is [2]

$$\frac{\partial\rho\mathbf{v}}{\partial t} = -\nabla\cdot(\rho\mathbf{v}\mathbf{v} + \mathbf{P}) + \sum_{i=1}^{n}\rho_i\mathbf{f}_i \tag{A.12}$$

[2]Throughout this appendix we indicate tensors by boldface capital letters,e.g. for the pressure tensor $\mathbf{P}$. The product **ab**of two vectors, with vector-components a_α and b_β, leads to a tensor with tensor-components $a_\alpha b_\beta$. $\nabla\mathbf{a}$ is the gradient of the vector (and is thus a tensor). The internal product of two tensors $\mathbf{A}:\mathbf{B} = \sum\sum A_{\alpha\beta}B_{\beta\alpha}$ is indicated by a double-dot and gives a scalar.

This equation is also called the equation of motion. The first term on the right hand side is minus the divergence of the convective momentum flux. Further acceleration of the medium is due either to the pressure tensor $\mathbf{P}$, or to external forces $\mathbf{f}_i$ (in units N/kg)acting on component i. The pressure tensor can for isotropic fluids be decomposed into the static pressure p and a shear contribution $\mathbf{\Pi}$, as

$$\mathbf{P} = p\mathbf{1} + \mathbf{\Pi} \tag{A.13}$$

where $\mathbf{1}$ is the unit matrix. The momentum balance then becomes

$$\frac{\partial \rho \mathbf{v}}{\partial t} = -\nabla\cdot(\rho \mathbf{v}\mathbf{v} + \mathbf{\Pi}) - \nabla p + \sum_{i=1}^{n} \rho_i \mathbf{f}_i \tag{A.14}$$

We do not consider complex fluids, in which there are elastic contributions to the pressure tensor. The most common forces $\mathbf{f}_i$ to be considered in Eq. A.14are forces due a gravitational field or an electric field. The gravitational field is a conservative field, which is given by

$$\mathbf{f}_i = \mathbf{g} = g(0,0,1) = -\nabla\psi_{grav} = -\nabla gz \tag{A.15}$$

We assumed the gravitational acceleration $\mathbf{g}$ to be constant and directed in the z-direction. By substituting Eq. (A.15) into Eq. (A.14), the equation of motion becomes:

$$\frac{\partial \rho \mathbf{v}}{\partial t} = -\nabla\cdot(\rho \mathbf{v}\mathbf{v}+\mathbf{\Pi}) - \nabla p + \rho\mathbf{g} = -\nabla\cdot(\rho \mathbf{v}\mathbf{v}+\mathbf{\Pi}) - \nabla p - \rho\nabla\psi_{grav} \tag{A.16}$$

The electric force on component i in the absence of a magnetic field is

$$\mathbf{f}_i = q_i\mathbf{E} = -\, q_i\nabla\psi \tag{A.17}$$

where q_i is the charge of ion i per unit of mass and ψ is the Maxwell potential. The total charge per unit of mass, q, is

$$\rho q = \sum_{i=1}^{n} \rho_i q_i \tag{A.18}$$

By substituting Eqs. (A.17) and (A.18) into Eq. (A.14), the equation of motion becomes:

$$\frac{\partial \rho \mathbf{v}}{\partial t} = -\nabla\cdot(\rho\mathbf{v}\mathbf{v}+\mathbf{\Pi})-\nabla p+\rho z\mathbf{E} = -\nabla\cdot(\rho\mathbf{v}\mathbf{v}+\mathbf{\Pi})-\nabla p-\rho q\nabla\psi \tag{A.19}$$

There is no magnetic contribution to this equation when the magnetic field is zero. A more detailed discussion was given by de Groot and Mazur [12] Chapter VIII. Most systems relax to an electroneutral state very quickly, in a few nanoseconds. The equation of motion does then no longer contain an electric force ($q = 0$), and the last term of Eq. (A.19) disappears. We are concerned with such systems in this book.It is then possible to describe the local thermodynamic state by densities of neutral components. For an electrolyte solution, for instance, salt concentrations are sufficient for a complete description. Concentrations of ions can all be given in terms of the salt concentrations. The gradient of the electric potential, $\nabla\phi$, drives the electric flux via the electrodes of the system (the entropy production in Chapter 3 contains the term $-(\mathbf{j}\cdot\nabla\phi)/T$). An electrolyte has an electric current when there is a relative motion of charged components (see e.g. Kjelstrup and Bedeaux [29] Chapters 10 and 17).

$$\frac{\mathrm{j}}{F} = \sum_i z_i \mathrm{J}_i \tag{A.20}$$

where the sum is over the ion fluxes. The charge number z_i is the positive valence number for cations and the negative valence number for anions. The ion flux J_i have contributions to from the electric current and from the appropriate salt flux J_j

$$\mathrm{J}_i = \frac{t_i}{z_i}\frac{\mathrm{j}}{F} + \Sigma_j \nu_{ij}\mathrm{J}_j \tag{A.21}$$

where the sum is over the salts and ν_{ij} is the number of ions of type i in salt j. The factor f_i depends on the electrode materials, see example below. We note that $\Sigma_i f_i = 1$ and $\Sigma_i \nu_{ij} z_i = 0$ (salts

are electroneutral). When ions are chosen as components, we introduce the Maxwell potential. The electric potential is related to the Maxwell potential ψ (see e.g. Kjelstrup and Bedeaux [29] Chapters 10 and 17) by

$$\phi \equiv \psi + \frac{1}{F}\sum_i \frac{f_i}{z_i} M_i \mu_i = \frac{1}{F}\sum_i \frac{f_i}{z_i} M_i \widetilde{\mu}_i \tag{A.22}$$

where the sum is over the ions. The electrochemical potential is defined by

$$\widetilde{\mu}_i \equiv \mu_i + \frac{z_i F}{M_i}\psi \tag{A.23}$$

The chemical and electrochemical potentials are given in J/kg, and M_i is the molar mass in kg/mol. The last identity in Eq. (A.22) gives ϕ in terms of electrochemical potentials. In a system with two identical electrodes, the ion involved in the electrode reaction has $f_i = 1$, while the other ions has $f_i = 0$. In a system with two different electrodes and a monovalent salt, $f_i = 1/2$ for each ion involved in the electrode reaction. With two chloride reversible electrodes, say, the electric potential is

$$\phi = \psi - \frac{1}{F}\mu_{\mathrm{Cl}^-} = -\frac{1}{F}\widetilde{\mu}_{\mathrm{Cl}^-}$$

In a formation cell, with a chloride and a sodium reversible electrode, the relation between ϕ and ψ is

$$\phi = \psi + \frac{1}{2F}\mu_{\mathrm{Na}^+} - \frac{1}{2F}\mu_{\mathrm{Cl}^-} = \frac{1}{2F}\widetilde{\mu}_{\mathrm{Na}^+} - \frac{1}{2F}\widetilde{\mu}_{\mathrm{Cl}^-}$$

Expressions like these can be used to replace ϕ in the energy balance (A.37), if a description in terms of ions is of interest.

A.1.3 Total energy balance

The total energy of a system is conserved. It can only change if energy is added or removed across the system boundary:

$$\frac{\partial \rho e}{\partial t} = -\nabla \cdot \mathbf{J}_e \tag{A.24}$$

where e is the specific total energy of a system in J/kg, and $\mathbf{J}_e$ is the energy flux in J/(m^{2}s). The total energy per unit ofvolume ρe has contributions from internal energy ρu, kinetic energy $\frac{1}{2}\rho \mathrm{v}^2$ (where $\mathrm{v} = |\mathbf{v}|$), gravitational energy $\rho\psi_{grav}$, and the energy density of the electric field $\frac{1}{2}\varepsilon_0 E^2$ (where $E = |\mathbf{E}|$)

$$\rho e = \rho u + \tfrac{1}{2}\rho \mathrm{v}^2 + \rho\psi_{grav} + \tfrac{1}{2}\varepsilon_0 E^2 \qquad \text{(A.25)}$$

Here ε_0 is the dielectric constant of vacuum. The energy flux can be decomposed as

$$\mathbf{J}_e = \rho\left(u + \tfrac{1}{2}\mathrm{v}^2 + \psi_{grav}\right)\mathbf{v} + \mathbf{P}\cdot\mathbf{v} + \frac{\mathbf{j}}{F}\sum_{i=1}^{n}\frac{f_i}{z_i}M_i\mu_i + \mathbf{J}_q \qquad \text{(A.26)}$$

The first term on the right hand side of Eq. (A.26) represents the convective energy flux, the second term is the contribution due to mechanical work done on the system, the third term represents the energy flux due to the relative motion of the charged particles. The last term defines the total heat flux.

A.1.4 Kinetic energy balance

The starting point for deriving a balance equation for the kinetic energy, $\rho \mathrm{v}^2/2 = \rho\mathbf{v}\cdot\mathbf{v}/2$, is the momentum balance,Eq. (A.16). Using also the continuity equation, Eq. (A.4), we obtain

$$\frac{\partial}{\partial t}\frac{1}{2}\rho \mathrm{v}^2 = \frac{\partial}{\partial t}\frac{1}{2}\rho\mathbf{v}\cdot\mathbf{v} = -\nabla\cdot\left(\tfrac{1}{2}\rho \mathrm{v}^2\mathbf{v}\right) - \mathbf{v}\cdot(\nabla\cdot\mathbf{P}) + \rho\mathbf{v}\cdot\mathbf{g} \qquad \text{(A.27)}$$

The second term on the right hand side of Eq. (A.27) can be rewritten as

$$\mathbf{v}\cdot(\nabla\cdot\mathbf{P}) = \nabla\cdot(\mathbf{P}\cdot\mathbf{v}) - \mathbf{P} : \nabla\mathbf{v} \qquad \text{(A.28)}$$

By introducing Eq. (A.28) into Eq. (A.27),we obtain a balance equation for the specific kinetic energy

$$\frac{\partial}{\partial t}\frac{1}{2}\rho \mathrm{v}^2 = -\nabla\cdot\left(\tfrac{1}{2}\rho \mathrm{v}^2\mathbf{v}\right) - \nabla\cdot(\mathbf{P}\cdot\mathbf{v}) + \mathbf{P} : \nabla\mathbf{v} + \rho\mathbf{v}\cdot\mathbf{g} \qquad \text{(A.29)}$$

A.1.5 Potential energy balance

The time rate of change of the potential energy density in Eq. (A.25) satisfies

$$\frac{\partial}{\partial t}\rho\psi_{grav} = \psi_{grav}\frac{\partial \rho}{\partial t} = -\psi_{grav}\nabla\cdot\rho\mathbf{v} = -\nabla\cdot\rho\psi_{grav}\mathbf{v} - \rho\mathbf{v}\cdot\mathbf{g} \tag{A.30}$$

where we used that the potential ψ_{grav} does not change with time,and Eqs. (A.4) and (A.15).

A.1.6 Balance of the electric field energy

To obtain a balance equation for the electric field energy, we need the third Maxwell equation for a zero magnetic field and a zero electric polarization:

$$\varepsilon_0\frac{\partial \mathbf{E}}{\partial t} = -\mathbf{j} \tag{A.31}$$

The balance equation then becomes

$$\frac{\partial}{\partial t}\tfrac{1}{2}\varepsilon_0 E^2 = \varepsilon_0\mathbf{E}\cdot\frac{\partial \mathbf{E}}{\partial t} = -\mathbf{E}\cdot\mathbf{j} \tag{A.32}$$

A.1.7 Internal energy balance

The balance equation for the internal energy, which we need for finding the entropy production from Eq. (A.39), is obtained by subtracting Eqs. (A.29), (A.30) and (A.32) from Eq. (A.24) and using Eq. (A.26). We obtain

$$\frac{\partial \rho u}{\partial t} = -\nabla\cdot(\rho u\mathbf{v} + \frac{\mathbf{j}}{F}\sum_{i=1}^{n}\frac{f_i}{z_i}M_i\mu_i + \mathbf{J_q}) - \mathbf{P}:\nabla\mathbf{v} + \mathbf{E}\cdot\mathbf{j} \tag{A.33}$$

Because the system is electroneutral, $\nabla\cdot\mathbf{j} = 0$. Equation (A.33) becomes:

$$\begin{aligned}\frac{\partial \rho u}{\partial t} &= -\nabla\cdot(\rho u\mathbf{v} + \mathbf{J}_q) - \mathbf{P} : \nabla\mathbf{v} \\ &\quad + \left(\mathbf{E} - \frac{1}{F}\nabla\sum_{i=1}^{n}\frac{f_i}{z_i}M_i\mu_i\right)\cdot\mathbf{j} \\ &= -\nabla\cdot(\rho u\mathbf{v} + \mathbf{J}_q) - \mathbf{P} : \nabla\mathbf{v} \\ &\quad - \left[\nabla\left(\psi + \frac{1}{F}\sum_{i=1}^{n}\frac{f_i}{z_i}M_i\mu_i\right)\right]\cdot\mathbf{j} \\ &= -\nabla\cdot(\rho u\mathbf{v} + \mathbf{J}_q) - \mathbf{P} : \nabla\mathbf{v} - (\nabla\phi)\cdot\mathbf{j} \end{aligned} \tag{A.34}$$

In many applications of the balance equation for internal energy, it is convenient to decompose the pressure tensor in the static pressure and the shear pressure tensor, according to Eq. (A.13). Considering only the term inEq. (A.34) containing the pressure tensor

$$\begin{aligned}-\mathbf{P} : \nabla\mathbf{v} &= -p\ \nabla\cdot\mathbf{v} - \mathbf{\Pi} : \nabla\mathbf{v} \\ &= -\nabla\cdot(p\mathbf{v}) + \mathbf{v}\cdot\nabla p - \mathbf{\Pi} : \nabla\mathbf{v}\end{aligned} \tag{A.35}$$

By introducing Eq. (A.35) into Eq. (A.34), we obtain

$$\frac{\partial \rho u}{\partial t} = -\nabla\cdot\left(\rho(u + \frac{p}{\rho})\mathbf{v} + \mathbf{J}_q\right) + \mathbf{v}\cdot\nabla p - \mathbf{\Pi} : \nabla\mathbf{v} - (\nabla\phi)\cdot\mathbf{j} \tag{A.36}$$

which gives the balance equation of internal energy written in terms of the enthalpy that is carried along, $\rho h = \rho u + p$, as

$$\frac{\partial \rho u}{\partial t} = -\nabla\cdot(\rho h\mathbf{v} + \mathbf{J}_q) + \mathbf{v}\cdot\nabla p - \mathbf{\Pi} : \nabla\mathbf{v} - (\nabla\phi)\cdot\mathbf{j} \tag{A.37}$$

The internal energy is not conserved, because the last three terms of Eq. (A.37) are source terms. The first is due to mechanical work, the second is due to viscous dissipation and the third

is an electric work term. The electric work has its source outside the local volume element. Equation (A.37) is the first law for the systems under consideration. Throughout the text the measurable heat flux $\mathbf{J}'_q$ has been used with $\mathbf{J}_q + \rho h \mathbf{v} = \mathbf{J}'_q + \sum H_i \mathbf{J}_i$.

A.1.8 Entropy balance

The entropy is not conserved, so the entropy balance is

$$\frac{\partial \rho s}{\partial t} = -\nabla \cdot (\rho s \mathbf{v} + \mathbf{J}_s) + \sigma \tag{A.38}$$

where $\mathbf{J}_s$ is the entropy flux relative to the barycentric frame of reference and σ is the entropy production. According to the second law σ is non-negative. In order to derive explicit expressions for the entropy flux and production, we use the Gibbs relation

$$\frac{\mathrm{d}s}{\mathrm{d}t} = \frac{1}{T}\frac{\mathrm{d}u}{\mathrm{d}t} + \frac{p}{T}\frac{\mathrm{d}v}{\mathrm{d}t} - \sum_{i=1}^{n} \frac{\mu_i}{T}\frac{\mathrm{d}w_i}{\mathrm{d}t} \tag{A.39}$$

where the specific volume is $v \equiv 1/\rho$ and where the comoving time derivative is defined by

$$\frac{\mathrm{d}}{\mathrm{d}t} \equiv \frac{\partial}{\partial t} + \mathbf{v} \cdot \nabla \tag{A.40}$$

By introducing the continuity equation (A.4) for the total mass density, we can write for any specific density a

$$\rho \frac{\mathrm{d}a}{\mathrm{d}t} = \frac{\partial \rho a}{\partial t} + \nabla \cdot \rho a \mathbf{v} \tag{A.41}$$

Equation (A.38) together with Eq. (A.41) then gives

$$\rho \frac{\mathrm{d}s}{\mathrm{d}t} = -\nabla \cdot \mathbf{J}_s + \sigma \tag{A.42}$$

From Eq. (A.34) we similarly obtain

$$\rho \frac{\mathrm{d}u}{\mathrm{d}t} = -\nabla \cdot \mathbf{J}_q - \mathbf{P} : \nabla \mathbf{v} - (\nabla \phi) \cdot \mathbf{j} \tag{A.43}$$

and using the continuity equation (A.4) we obtain

$$\rho\frac{\mathrm{d}v}{\mathrm{d}t} = \nabla\cdot\mathbf{v} \tag{A.44}$$

For the mass fractions we obtain, using Eqs. (A.41) and (A.3),

$$\begin{aligned}\rho\frac{\mathrm{d}w_i}{\mathrm{d}t} &= \frac{\partial\rho_i}{\partial t} + \nabla\cdot\rho_i\mathbf{v} \\ &= -\nabla\cdot\rho_i\left(\mathbf{v}_i - \mathbf{v}\right) + \nu_i M_i r\end{aligned} \tag{A.45}$$

Finally, by substituting Eqs. (A.43)-(A.45) into the Gibbs relation (A.39) we obtain

$$\begin{aligned}\rho\frac{\mathrm{d}s}{\mathrm{d}t} =& -\frac{1}{T}\nabla\cdot\mathbf{J}_q - \frac{1}{T}\boldsymbol{\Pi} : \nabla\mathbf{v} - \frac{1}{T}\left(\nabla\phi\right)\cdot\mathbf{j} \\ &+ \sum_{i=1}^{n}\frac{\mu_i}{T}\nabla\cdot\rho_i\left(\mathbf{v}_i - \mathbf{v}\right) - \frac{1}{T}\left(\sum_{i=1}^{n}\mu_i\nu_i M_i\right) r\end{aligned} \tag{A.46}$$

We define diffusion fluxes relative to the barycentric motion by

$$\mathbf{J}_{i,\mathrm{bar}} \equiv \rho_i\left(\mathbf{v}_i - \mathbf{v}\right) \tag{A.47}$$

and the Gibbs energy of the reaction (in J/mol) by

$$\Delta_r G \equiv \sum_{i=1}^{n}\mu_i\nu_i M_i \tag{A.48}$$

Equation (A.46) simplifies to

$$\rho\frac{\mathrm{d}s}{\mathrm{d}t} = -\frac{1}{T}\nabla\cdot\mathbf{J}_q - \frac{1}{T}\boldsymbol{\Pi} : \nabla\mathbf{v} - \mathbf{j}\cdot\frac{\nabla\phi}{T} + \sum_{i=1}^{n}\frac{\mu_i}{T}\nabla\cdot\mathbf{J}_{i,\mathrm{bar}} - \frac{\Delta_r G}{T}r \tag{A.49}$$

We rewrite this as

$$\begin{aligned}\rho\frac{\mathrm{d}s}{\mathrm{d}t} =& -\nabla\cdot\frac{\mathbf{J}_q - \sum_{i=1}^{n}\mu_i\mathbf{J}_{i,\mathrm{bar}}}{T} + \mathbf{J}_q\cdot\nabla\frac{1}{T} - \frac{1}{T}\boldsymbol{\Pi} : \nabla\mathbf{v} - \mathbf{j}\cdot\frac{\nabla\phi}{T} \\ &- \sum_{i=1}^{n}\mathbf{J}_{i,\mathrm{bar}}\cdot\nabla\frac{\mu_i}{T} - r\frac{\Delta_r G}{T}\end{aligned} \tag{A.50}$$

By comparing this equation with Eq. (A.42) we identify the entropy flux

$$\mathbf{J}_s = \frac{\mathbf{J}_q - \sum_{i=1}^{n} \mu_i \mathbf{J}_{i,\mathrm{bar}}}{T} = \frac{\mathbf{J}'_q}{T} + \sum_{i=1}^{n} S_i \mathbf{J}_{i,\mathrm{bar}} \tag{A.51}$$

where $\mathbf{J}'_q$ is the measurable heat flux. The comparison of (A.49) with (A.50) gives the entropy production

$$\sigma = \mathbf{J}_q \cdot \nabla \frac{1}{T} - \frac{1}{T} \boldsymbol{\Pi} : \nabla \mathbf{v} - \mathbf{j} \cdot \frac{\nabla \phi}{T} - \sum_{i=1}^{n} \mathbf{J}_{i,\mathrm{bar}} \cdot \nabla \frac{\mu_i}{T} - r \frac{\Delta_r G}{T} \tag{A.52}$$

It follows from the definition of the diffusion fluxes that they are not independent. Their sum is zero

$$\sum_{i=1}^{n} \mathbf{J}_{i,\mathrm{bar}} = 0 \tag{A.53}$$

We can therefore preferably write the entropy production in the form

$$\sigma = \mathbf{J}_q \cdot \nabla \frac{1}{T} - \frac{1}{T} \boldsymbol{\Pi} : \nabla \mathbf{v} - \mathbf{j} \cdot \frac{\nabla \phi}{T} - \sum_{i=1}^{n-1} \mathbf{J}_{i,\mathrm{bar}} \cdot \nabla \frac{\mu_i - \mu_n}{T} - r \frac{\Delta_r G}{T} \tag{A.54}$$

A.2 Partial molar thermodynamic properties

Definitions for partial molar properties derive from the Gibbs equation

$$dU = TdS - pdV + \sum_{j=1}^{n} \mu_j dN_j \tag{A.55}$$

and its integrated form:

$$U = TS - pV + \sum_{j=1}^{n} \mu_j N_j \tag{A.56}$$

The Gibbs-Duhem equation given in Eq. (3.16) is obtained by differentiating the last equation, using the first, and dividing by the volume. The enthalpy is defined as

$$H \equiv U + pV = TS + \sum_{j=1}^{n} \mu_j N_j \tag{A.57}$$

By using the Gibbs equation, this gives

$$dH = TdS + Vdp + \sum_{j=1}^{n} \mu_j dN_j \tag{A.58}$$

The Gibbs energy is defined by

$$G \equiv U - TS + pV = \sum_{j=1}^{n} \mu_j N_j \tag{A.59}$$

Again, by using the Gibbs equation, we obtain:

$$dG \equiv -SdT + Vdp + \sum_{j=1}^{n} \mu_j dN_j \tag{A.60}$$

The partial molar volume and the partial molar entropy are defined by:

$$V_j \equiv \left(\frac{\partial V}{\partial N_j}\right)_{p,T,N_k}, \qquad S_j \equiv \left(\frac{\partial S}{\partial N_j}\right)_{p,T,N_k} \tag{A.61}$$

The partial molar properties obey:

$$\sum_j N_j V_j = V, \qquad \sum_j N_j S_j = S \tag{A.62}$$

By dividing these relation by the volume, we obtain

$$\sum_j c_j V_j = 1, \qquad \sum_j c_j S_j = \frac{S}{V} = s \tag{A.63}$$

From the expression for dG we find alternative expressions for the partial molar quantities

$$V_j \equiv \left(\frac{\partial \mu_j}{\partial p}\right)_{T,N_k}, \qquad S_j \equiv -\left(\frac{\partial \mu_j}{\partial T}\right)_{p,N_k} \tag{A.64}$$

This results in the expression for a differential change in the chemical potential

$$\begin{aligned} d\mu_j &= -S_j dT + V_j dp + \sum_{k=1}^{n} \left(\frac{\partial \mu_j}{\partial N_k}\right)_{T,p,N_l,E_{\mathrm{eq}}} dN_k \\ &= -S_j dT + V_j dp + \sum_{k=1}^{n} \left(\frac{\partial \mu_j}{\partial c_k}\right)_{T,p,c_l,E_{\mathrm{eq}}} dc_k \\ &\equiv -S_j dT + V_j dp + d\mu_j^c \end{aligned} \tag{A.65}$$

The last line defines $d\mu_j^c$. A combination of terms frequently used in this book, for instance in Eq. (3.15), is

$$d\mu_{j,T} = d\mu_j + S_j dT = V_j dp + d\mu_j^c \tag{A.66}$$

where we used the partial molar entropy. From the partial molar quantities defined above we can also define the partial molar internal energy and enthalpy

$$\begin{aligned} U_j &= TS_j - pV_j + \mu_j \\ H_j &= TS_j + \mu_j \end{aligned} \tag{A.67}$$

These properties are, according to the construction, functions of p, T and c_k. The partial molar Gibbs energy is the chemical potential, $G_j = \mu_j$.

Exercise A.2.1 *Find a form of Gibbs-Duhem's equation* (3.16) *that containsd*$\mu_{i,T}$ *instead of* $d\mu_i$. *Assume that the polarization of the system is negligible.*

- **Solution**: The solution is found by substituting Eq. (A.66) into Eq. (3.16):

$$dp = sdT + \sum_{i=1}^{n} c_i d\mu_{i,T} - \sum_{i=1}^{n} c_i S_i dT$$

By using $\sum_{i=1}^{n} c_i S_i = s$, Gibbs-Duhem's equation reduces to

$$dp = \sum_{i=1}^{n} c_i d\mu_{i,T} \tag{A.68}$$

The equation applies also to a system in a temperature gradient.

A.3 The chemical potential and its reference states

The chemical potential is a function of temperature, pressure and composition. Like other energy variables, it is not absolute. Only differences in chemical potentials are absolute and can be measured.

The mass transport equations presented in chapter 5 require expressions for the gradient of the chemical potential. For an ideal gas we can calculate this gradient from gradients in temperature, pressure and concentrations, knowing in addition only the ideal gas molar enthalpy $H_i^{ig}(T)$, or heat capacity $c_{p,i}^{ig}(T)$. For real fluids and solids, experimental values or models are needed. There are three main approaches to obtain the chemical potential. We can use

- the equation of state
- the excess Gibbs energy, or
- Henry's law

The first approach is general and suited for any phase, while the last two approaches use additional *auxiliary reference points*: the pure liquid, the pure solvent or, for electrolyte solutions, a one-molar solution. These references are for liquid phases only.

All three approaches can be formulated with the ideal gas as a reference. The choice of the considered temperature and pressure of the reference chemical potential is irrelevant when gradients of the chemical potential are targeted and when phase equilibria are calculated. The reference chemical potential drops out of these calculation.

For chemical reactions the reference chemical potentials, however, are important. A *standard state* ($p^{\ominus} = 1$ bar) has been defined in order to allow tabulations of reference state values, usually at 298.15 K.

We summarize here how the three approaches are used to calculate the chemical potential of a single component, alone or in a mixture. Calculations for chemical reactions are summarized in Chapter A.4. Superscripts *ig* and *sat* are used as abbreviations for the ideal gas and the saturated pure component (i.e. at vapor-liquid equilibrium), respectively, while subscripts 'V' and 'L' are used to denote vapor and liquid phase. Subscript '$0i$' shall denote pure component i. A composition dependence is indicated with the symbol $\mathbf{x}$, with $\mathbf{x} = x_1, \ldots x_{n-1}$.

A.3.1 The equation of state as a basis

The chemical potential of a component i in a real mixture is given by

$$\mu_i(T, p, \mathbf{x}) = \mu_{0i}^{ig}(T, p^*) + RT \ln\left(\frac{f_i}{p^*}\right) \qquad \text{(A.69)}$$

This equation defines the fugacity of component i in the given state, $f_i(T, p, \mathbf{x})$. For a pure ideal gas, the fugacity is equal to the pressure. In a mixture of ideal gases, the fugacity of

component i is equal to the partial pressure $x_i p$. The pressure p^* can be chosen to be the standard state pressure, $p^* = p^\ominus$, or any pressure, when heat capacity data are available. The choice is irrelevant for phase equilibrium calculations or for chemical potential gradients.

From the fugacity we define the fugacity coefficient, ϕ_i, with $f_i = x_i \phi_i p$, so that

$$\mu_i(T, p, \mathbf{x}) = \mu_{0i}^{ig}(T, p^*) + RT \ln \left(\frac{x_i \phi_i p}{p^*} \right) \tag{A.70}$$

The fugacity coefficient $\phi_i(T, p, \mathbf{x})$ accounts for the deviation of the chemical potential from ideal gas behavior, with $\phi_i^{ig} = 1$ for ideal gases. It is always greater than zero. The fugacity coefficient is calculated with an equation of state [120]. Equations of state are nowadays used also for complex fluids, like polymers, associating substances and electrolyte solutions [121–126]. The equation of state approach can be applied to (coexisting) solid, liquid, and gaseous phases. It is most general, because auxiliary reference points, such as the pure component at vapor pressure or a substance infinitely dilute in a solvent, are not needed.

A.3.2 The excess Gibbs energy as a basis

The chemical potential of a component in a liquid mixture takes the form

$$\mu_i(T, p, \mathbf{x}) = \mu_i^\circ(T, p, \mathbf{x}^\circ) + RT \ln (x_i \gamma_i) \tag{A.71}$$

where the choice of the reference chemical potential μ_i° defines the activity coefficient γ_i. It is common to choose the reference chemical potential as the pure component chemical potential of the (hypothetical) liquid, $\mu_i^\circ(T, p, \mathbf{x}^\circ) = \mu_{0i}^L(T, p)$. The activity coefficient accounts then for the non-ideality of mixing at (T, p). The reference chemical potential is conveniently based on the

saturated liquid state as

$$\mu_{0i}^{L}(T,p) = \mu_{0i}^{L}(T,p_{0i}^{sat}(T)) + \int_{p_{0i}^{sat}}^{p} \frac{V_{0i}^{L}}{RT}\mathrm{d}p \tag{A.72}$$

The integral of V_{0i}^{L}/RT with p, is the Poynting correction to the auxiliary reference state (pure liquid at vapor-liquid equilibrium). If the the pure substance i is a vapor at (T,p), then the liquid molar volume V_{0i}^{L} is extrapolated down to p. That is practiced in the majority of all phase equilibrium calculation, because the light-boiler's vapor pressure is usually higher than the system pressure.

Often, it is necessary to consider the pure component in the ideal gas state as a reference. This is, for example, needed in order to make the approach compatible with Eq. (A.70) for phase equilibrium calculations, or because temperature variations have to be formulated using the ideal gas heat capacity (rather than the liquid state heat capacity). We obtain from Eqs. (A.70) and (A.72) that

$$\mu_{0i}^{L}(T,p) = \mu_{0i}^{ig}(T,p^*) + RT\ln\left(\frac{\phi_{0i}^{sat}p_{0i}^{sat}}{p^*}\right) + \int_{p_{0i}^{sat}}^{p} \frac{V_{0i}^{L}}{RT}\mathrm{d}p \tag{A.73}$$

With the ideal gas reference state, the chemical potential is

$$\mu_i(T,p) = \mu_{0i}^{ig}(T,p^*) + RT\ln\left(\frac{x_i\gamma_i\phi_{0i}^{sat}p_{0i}^{sat}\Pi_{0i}}{p^*}\right) \tag{A.74}$$

The Poynting correction has here been estimated with a constant pure component molar volume, giving

$$\Pi_{0i} = \exp\left(\frac{V_{0i}^{L}}{RT}\left(p - p_{0i}^{sat}\right)\right) \tag{A.75}$$

The Poynting correction is near unity at moderate pressure-differences. The fugacity coefficient of the pure saturated vapor

phase ϕ_{0i}^{sat} is approximately unity for low pressures. The activity coefficients are obtained from the excess Gibbs energy, G^E, from $(\partial G^E/\partial N_i)_{T,p,N_{j\neq i}} = RT\ln\gamma_i$. In practice, the models for G^E are expressed only in terms of temperature and composition as variables, $G^E(T,\mathbf{x})$. Neglect of the pressure leads to numerically simple models. This approach for the chemical potential requires a correlation of the vapor pressure $p_{0i}^{sat}(T)$ and the pure substance i needs to be below the critical point.

A.3.3 Henry's law as a basis

The solubility of solute i in a solvent s is described by Henry's law in the dilute limit

$$y_i\phi_i^V p = x_i k_{H,i} \tag{A.76}$$

where Henry's law constant is defined by $k_{H,i} \equiv \lim_{x_s\to 1}\phi_i^L p$. At finite solute concentration, Henry's law is corrected by an activity coefficient

$$y_i\phi_i^V p = x_i\hat{\gamma}_i\, k_{H,i}\,\Pi_i^{\infty} \tag{A.77}$$

The Henry constant in this form is only a function of temperature. The activity coefficient $\hat{\gamma}_i$ is related to the activity coefficient of Eq. (A.74), by $\hat{\gamma}_i = \gamma_i/\gamma_i^{\infty}$, with $\gamma_i^{\infty} \equiv \lim_{x_s\to 1}\gamma_i$. The factor $\Pi_i^{\infty} = \exp\left(\frac{V_i^{\infty}}{RT}\,(p - p_{0s}^{sat})\right)$ accounts for a deviation in the pressure from the solvent's vapor pressure. Here, the partial molar volume of component i at infinite dilution, V_i^{∞}, is used. By introducing Eq. (A.77) into (A.70), we obtain the chemical potential with respect to the ideal gas reference as

$$\mu_i = \mu_{0i}^{ig} + RT\ln\left(\frac{x_i\hat{\gamma}_i k_{H,i}\Pi_i^{\infty}}{p^*}\right) \tag{A.78}$$

A.4 Driving forces and equilibrium constants

For chemical reactions, the reference chemical potentials define the equilibrium constant. It is convention to define the equilibrium 'constant' $K(T)$ as a function of temperature, but at the standard pressure $p^{\ominus} = 1$ bar. Most tabulated values for the pure component chemical potential (also termed Gibbs energy of formation) are given for the temperature of $T_{298} = 298.15$ K, $\mu_i^{\ominus} = \mu_{0i}(T_{298}, p^{\ominus})$. These values are for a pure component either in *ideal gas state*, or in pure *liquid*, or pure *solid* states. Consistency in the reference state of all components involved is required. As we have seen above, the chemical potential can always be cast into the form

$$\mu_i = \mu_i^{\{\pi\}^{\ominus}} + RT \ln \left(\frac{f_i}{f_i^{\{\pi\}^{\ominus}}} \right) \tag{A.79}$$

where π is an index specifying the state, $\pi \in \{ig, L, S\}$ for the ideal gas, liquid or solid state. For the three states, the reference chemical potentials and the corresponding fugacities are

$$\begin{aligned} \mu_i^{\{ig\}^{\ominus}} &= \mu_{0i}^{ig}(T, p^{\ominus}) \\ f_i^{\{ig\}^{\ominus}} &= p^{\ominus} \end{aligned} \tag{A.80}$$

$$\begin{aligned} \mu_i^{\{L\}^{\ominus}} &= \mu_{0i}^{L}(T, p^{\ominus}) \\ f_i^{\{L\}^{\ominus}} &= \phi_{0i}^{sat} p_{0i}^{sat} \cdot \exp\left(\frac{V_{0i}^{L}}{RT} \left(p^{\ominus} - p_{0i}^{sat} \right) \right) \end{aligned} \tag{A.81}$$

$$\begin{aligned} \mu_i^{\{S\}^{\ominus}} &= \mu_{0i}^{S}(T, p^{\ominus}) \\ f_i^{\{S\}^{\ominus}} &= \phi_{0i}^{subl} p_{0i}^{subl} \cdot \exp\left(\frac{V_{0i}^{S}}{RT} \left(p^{\ominus} - p_{0i}^{subl} \right) \right) \end{aligned} \tag{A.82}$$

The driving force for a chemical reaction is then in general

$$\begin{aligned}\frac{\Delta_r G}{RT} &= \sum_{i=1}^{n} \nu_i \frac{\mu_i}{RT} \\ &= \underbrace{\sum_{i=1}^{n} \nu_i \frac{\mu_i^{\{\pi\}\ominus}}{RT}}_{\equiv -\ln K^{\{\pi\}}} + \ln\left(\prod_{i=1}^{n}\left(\frac{f_i}{f_i^{\{\pi\}\ominus}}\right)^{\nu_i}\right)\end{aligned} \tag{A.83}$$

The equilibrium constant depends thus on the choice of the reference chemical potentials. We give more details below for the case where the equilibrium constant is formulated in terms of ideal gas chemical potentials, and for the case where the equilibrium constant is written in terms of the liquid chemical potentials.

A.4.1 The ideal gas reference state

With the ideal gas as a reference state, the driving force for a chemical reaction becomes

$$\frac{\Delta_r G}{RT} = \underbrace{\sum_{i=1}^{n} \nu_i \frac{\mu_i^{\{ig\}\ominus}}{RT}}_{\equiv -\ln K^{\{ig\}}} + \ln\left(\prod_{i=1}^{n}\left(x_i \phi_i \frac{p}{p^{\ominus}}\right)^{\nu_i}\right) \tag{A.84}$$

This formulation is valid for reactions in any phase. The fugacity coefficient accounts for the deviations from ideal gas state. An equation of state can be used to calculate the fugacity coefficients. The equation shows that driving forces and equilibria of gas-phase reactions are strongly dependent on pressure. In order to calculate the equilibrium constant at system temperature from values at $T_{298} = 298.15\ K$, one uses the integrated

Gibbs-Helmholtz relation

$$\underbrace{\sum_{i=1}^{n}\nu_i\frac{\mu_i^{\{ig\}\ominus}(T)}{RT}}_{\equiv-\ln K^{\{ig\}}}=\underbrace{\sum_{i=1}^{n}\nu_i\frac{\mu_i^{\{ig\}\ominus}(T_{298})}{RT_{298}}}_{\equiv-\ln K_{298}^{\{ig\}}}+R^{-1}\int_{298.15\ K}^{T}\sum_{i=1}^{n}\nu_i H_i^{ig}(T)\,\mathrm{d}\left(\frac{1}{T}\right) \quad \text{(A.85)}$$

Equations (A.84) and (A.85) require that all the reference chemical potentials are for the ideal gas state. If the chemical potential of any constituent is tabulated for the liquid phase, it can be converted by

$$\mu_i^{\ominus\{ig\}}(T)=\mu_i^{\ominus\{L\}}(T)-RT\ln\left(\frac{1}{p^{\ominus}}p_{0i}^{sat}\phi_{0i}^{sat}\cdot\exp\left(\frac{V_{0i}^{L}}{RT}\left(p^{\ominus}-p_{0i}^{sat}\right)\right)\right) \quad \text{(A.86)}$$

For a low enough vapor pressure, p_{0i}^{sat}, the fugacity coefficient and the exponent are approximately unity. The argument in the last term in Eq. (A.86) then simplifies to the vapor-pressure divided by standard pressure only.

A.4.2 The pure liquid reference state

The equilibrium constant, formulated in terms of liquid phase reference potentials, gives

$$\frac{\Delta_r G}{RT}=\underbrace{\sum_{i=1}^{n}\nu_i\frac{\mu_i^{\{L\}\ominus}}{RT}}_{\equiv-\ln K^{\{L\}}}+\ln\left(\prod_{i=1}^{n}\left(x_i\gamma_i\Pi_{0i}^{\ominus}\right)^{\nu_i}\right) \quad \text{(A.87)}$$

The Poynting correction is modified, cf. the regular definition Eq. (A.75), with

$$\Pi_{0i}^{\ominus}=\exp\left(\frac{V_{0i}^{L}}{RT}\left(p^{\ominus}-p_{0i}^{sat}\right)\right) \quad \text{(A.88)}$$

The temperature integration is now carried out in the liquid phase, from tabulated values of the chemical potential at $T_{298} = 298.15\ K$, so that

$$\underbrace{\sum_{i=1}^{n} \nu_i \frac{\mu_i^{\{L\}\ominus}(T)}{RT}}_{\equiv -\ln K^{\{L\}}} = \underbrace{\sum_{i=1}^{n} \nu_i \frac{\mu_i^{\{L\}\ominus}(T_{298})}{RT_{298}}}_{\equiv -\ln K_{298}^{\{L\}}} + R^{-1} \int_{298.15\ K}^{T} \underbrace{\sum_{i=1}^{n} \nu_i H_{0i}^{L}(T, p^{\ominus})}_{\equiv \Delta_r H} \, \mathrm{d}\left(\frac{1}{T}\right) \tag{A.89}$$

where H_{0i}^{L} is the molar enthalpy of the pure liquid. Whenever reference chemical potentials are tabulated for the liquid, then usually the enthalpies are also listed for the liquid. We can also calculate a chemical potential in Eq. (A.89) using the ideal gas enthalpy. The calculation is done along the integration path: (1) integrate to the ideal gas state at $T_{298} = 298.15\ K$, then (2) integrate from T_{298} to system temperature, and (3) integrate back to the liquid state, so that

$$\frac{\mu_i^{\{L\}\ominus}(T)}{RT} = \frac{\mu_i^{\{L\}\ominus}(T_{298})}{RT_{298}} + R^{-1} \int_{298.15\ K}^{T} H_i^{ig}(T) \, \mathrm{d}\left(\frac{1}{T}\right) + \ln \left(\frac{p_{0i}^{sat}(T) \phi_{0i}^{sat}(T) \exp\left(\frac{V_{0i}^{L}}{RT}(p^{\ominus} - p_{0i}^{sat}(T))\right)}{p_{0i}^{sat}(T_{298}) \phi_{0i}^{sat}(T_{298}) \exp\left(\frac{V_{0i}^{L}}{RT_{298}}(p^{\ominus} - p_{0i}^{sat}(T_{298}))\right)} \right) \tag{A.90}$$

In many cases (i.e. at low enough vapor pressures), the exponents and the fugacity coefficients can be approximated as unity. The argument in the last term in Eq. (A.90) then simplifies to the vapor-pressure ratio.

Bibliography

[1] W. Thomson (Lord Kelvin). *Mathematical and Physical Papers. Collected from different Scientific Periodicals from May, 1841, to the Present Time*, volume II. Cambrigde University Press, London, 1884.

[2] L. Onsager. Reciprocal relations in irreversible processes. I. *Phys. Rev.*, 37:405–426, 1931.

[3] L. Onsager. Reciprocal relations in irreversible processes. II. *Phys. Rev.*, 38:2265–2279, 1931.

[4] H. Hemmer, H. Holden and S.K. Ratkje, editor. *The Collected Works of Lars Onsager*. World Scientific, Singapore, 1996.

[5] J. Meixner. Zur thermodynamik der thermodiffusion. *Ann. Physik 5. Folge*, 39:333–356, 1941.

[6] J. Meixner. Reversible bewegungen von flüssigkeiten und gasen. *Ann. Physik 5. Folge*, 41:409–425, 1942.

[7] J. Meixner. Zur Thermodynamik der irreversibelen Prozesse in Gasen mit chemisch reagierenden, dissozierenden und anregbaren Komponenten. *Ann. Physik 5. Folge*, 43:244–270, 1943.

[8] J. Meixner. Zur Thermodynamik der Irreversibelen Prozesse. *Zeitschr. Phys. Chem. B*, 53:235–263, 1943.

[9] I. Prigogine. *Etude thermodynamique des phenomenes irreversibles*. Desoer, Liege, 1947.

[10] P. Mitchell. Coupling of phosphorylation to electron and hydrogen transfer by a chemi-osmotic type of mechanism. *Nature (London)*, 191:144–148, 1961.

[11] S. R. de Groot and P. Mazur. *Non-Equilibrium Thermodynamics*. North-Holland, Amsterdam, 1962.

[12] S. R. de Groot and P. Mazur. *Non-Equilibrium Thermodynamics*. Dover, London, 1984.

[13] R. Haase. *Thermodynamics of Irreversible Processes*. Addison-Wesley, Reading, MA, 1969.

[14] R. Haase. *Thermodynamics of Irreversible Processes*. Dover, London, 1990.

[15] A. Katchalsky and P. Curran. *Nonequilibrium Thermodynamics in Biophysics*. Harvard University Press, Cambrigde, Massachusetts, 1975.

[16] S.R. Caplan and A. Essig. *Bioenergetics and linear nonequilibrium thermodynamics - The steady state*. Harvard University Press, Cambrigde, Massachusetts, 1983.

[17] K. S. Førland, T. Førland and S. Kjelstrup Ratkje. *Irreversible thermodynamics. Theory and application*. Wiley, Chichester, 1988.

[18] K. S. Førland, T. Førland and S. Kjelstrup. *Irreversible thermodynamics. Theory and application*. Tapir, Trondheim, 3rd. edition, 2001.

[19] V.P. Carey. *Statistical Thermodynamics and Microscale Thermophysics*. Cambrigde University Press, Cambrigde, 1999.

[20] D. Kondepudi and I. Prigogine. *Modern thermodyamics. From heat engines to dissipative structures*. Wiley, Chichester, 1998.

[21] D. Jou, J. Casas-Vásquez and G. Lebon. *Extended Irreversible Thermodynamics*. Springer, Berlin, 2 edition, 1996.

[22] H.C. Õttinger. *Beyond Equilibrium Thermodynamics*. Wiley-Interscience, Hoboken, 2005.

[23] D.D. Fitts. *Nonequilibrium Thermodynamics*. McGraw-Hill, New York, 1962.

[24] G.D.C. Kuiken. *Thermodynamics for irreversible processes*. Wiley, Chichester, 1994.

[25] A. Perez-Madrid I. Pagonabarraga and J.M. Rubi. Fluctuating hydrodynamics approach to chemical reactions. *Physica A*, 237:205–219, 1997.

[26] I. Pagonabarraga and J.M. Rubi. Derivation of the langmuir adsorption equation from non-equilibrium thermodynamics. *Physica A*, 188:553–567, 1992.

[27] D. Reguera and J.M. Rubi. Non-equilibrium translational-rotational effects in nucleation. *J. Chem. Phys.*, 115:7100–7106, 2001.

[28] D. Bedeaux and P. Mazur. Mesoscopic non-equilibrium thermodynamics for quantum systems. *Physica A*, 298:81–100, 2001.

[29] S. Kjelstrup and D. Bedeaux. *Non-equilibrium Thermodynamics of Heterogeneous Systems. Series on Advances in Statistical Mechanics. Vol.16.* World Scientific, Singapore, 2008.

[30] K.G. Denbigh. The second-law efficiency of chemical processes. *Chem. Eng. Sci.*, 6:1–9, 1956.

[31] R. B. Bird, W. E. Stewart and E. N. Lightfoot. *Transport Phenomena.* Wiley, 1960.

[32] R. Taylor and R. Krishna. *Multicomponent Mass Transfer.* Wiley, New York, 1993.

[33] E.L. Cussler. *Diffusion, Mass Transfer in Fluid Systems.* Cambridge, 2nd. edition, 1997.

[34] Y. Demirel. *Nonequilibrium thermodynamics.* Elsevier, Boston, 2002.

[35] R. Krishna and J.A. Wesselingh. The Maxwell-Stefan approach to mass transfer. *Chem. Eng. Sci.*, 52:861–911, 1997.

[36] A. Bejan. Entropy generation minimization: The new thermodynamics of finite-size devices and finite-time processes. *J. Appl. Phys.*, 79:1191–1218, 1996.

[37] J. Szargut, D.R. Morris and F. R. Steward. *Exergy Analysis of Thermal, Chemical and Metallurgical Processes.* Hemisphere, New York, 1988.

[38] R.S. Berry, V. Kazakov, S. Sieniutycz, Z. Szwast and A.M. Tsirlin. *Thermodynamic Optimization of Finite-Time Processes.* Wiley, Chichester, 2000.

[39] W.L. Luyben, B. Tyréus, and M.L. Luyben. *Plantwide Process Control.* McGraw-Hill, New York, 1998.

[40] D. Bedeaux and S. Kjelstrup. Impedance spectroscopy of surfaces described by irreversible thermodynamics. *J. Non-Equilib. Thermodyn.*, 24:80–96, 1999.

[41] G. Tsatsaronis. Definition and nomenclature in exergy analysis and exergoeconomics. In S. Kjelstrup, J. Hustad, T. Gundersen, A. Røsjorde and G. Tsatsaronis, editor, *Proceedings of ECOS 2005*, pages 321–326, Trondheim, Norway, June 20 - June 22 2005. Norwegian University of Science and Technology, Norway. ISBN 82-519-2041-8.

[42] J.W. Gibbs. *Collected Works, 2 vols.* Dover, London, 1961.

[43] A. Bejan. *Entropy Generation Minimization. The Method of Thermodynamic Optimization of Finite-Size Systems and Finite-Time Processes.* CRC Press, New York, 1996.

[44] M. J. Moran and H. N. Shapiro. *Fundamentals of Engineering Thermodynamics.* Wiley, New York, 2nd. edition, 1993.

[45] A. Zvolinschi and S. Kjelstrup. A process maturity indicator for industrial ecology. *J. Ind. Ecol.*, 12:159–172, 2008.

[46] P.W. Atkins. *Physical Chemistry.* Oxford, 6th. edition, 1998.

[47] E. Johannessen and S. Kjelstrup. Minimum entropy production in plug flow reactors: An optimal control problem solved for SO_2 oxidation. *Energy*, 29:2403–2423, 2004.

[48] A. Zvolinschi, E. Johannessen and S. Kjelstrup. The second-law optimal operation of a paper drying machine. *Chem. Eng. Sci.*, 61:3653–3662, 2006.

[49] B. Hafskjold and S. Kjelstrup Ratkje. Criteria for local equilibrium in a system with transport of heat and mass. *J. Stat. Phys.*, 78:463–494, 1995.

[50] T. Holt, E. Lindeberg and S. Kjelstrup Ratkje. The effect of gravity and temperature gradients on methane distribution in oil reservoirs. *SPE-paper no. 11761*, page 19, 1983.

[51] L.J.T.M. Kempers. A thermodynamic theory of the Soret effect in a multicomponent liquid. *J. Chem. Phys.*, 90:6541–6548, 1989.

[52] W.H. Furry, R.C. Jones and L. Onsager. On the theory of isotope separation by thermal diffusion. *Phys. Rev.*, 55:1083–1095, 1939.

[53] L.J.T.M. Kempers. A comprehensive thermodynamic theory of the Soret effect in a multicomponent gas, liquid or solid. *J. Chem. Phys.*, 115:6330–6341, 2001.

[54] V.E. Zinoviev. *Thermophysical properties of metals at high temperatures*. Metallurgiya, Moscov, 1989.

[55] H.S. Harned and B.B. Owen. *Physical Chemistry of Electrolytic Solutions*. Reinhold, New York, 3rd. edition, 1958.

[56] M. Ottøy. *Mass and Heat Transfer in Ion-Exchange Membranes, dr. ing. Thesis no. 50*. University of Trondheim, Norway, 1996.

[57] S. Kjelstrup and A. Røsjorde. Local and total entropy production and heat and water fluxes in a one-dimensional polymer electrolyte fuel cell. *J. Phys. Chem. B*, 109:9020–9033, 2005.

[58] J. Meixner. Strömungen von fluïden Medien mit inneren Umwandlungen und Druckviscosität. *Zeitschrift für Physik*, 131:456–469, 1952.

[59] S. Hess. Irreversible thermodynamics of nonequilibrium alignment phenomena in molecular liquids and in liquid crystals. I. *Z. Naturforschung*, 30a:728, 1975.

[60] S. Hess. Irreversible thermodynamics of nonequilibrium alignment phenomena in molecular liquids and in liquid crystals. II. viscous flow and flow alignment in the isotropic (stable ad metastable) and nematic phases. *Z. Naturforschung*, 30a:1224, 1975.

[61] D. Bedeaux and J.M. Rubi. Nonequilibrium thermodynamics of colloids. *Physica A*, 305:360–370, 2002.

[62] J. Xu, S. Kjelstrup, D. Bedeaux and J.-M. Simon. Transport properties of $2F = F_2$ in a temperature gradient as studied by molecular dynamics simulations. *Phys. Chem. Chem. Phys.*, 9:969–981, 2007.

[63] H. Eyring and E. Eyring. *Modern Chemical Kinetics*. Chapman & Hall, London, 1965.

[64] J.M. Rubi and S. Kjelstrup. Mesoscopic nonequilibrium thermodynamics gives the same thermodynamic basis to Butler-Volmer and Nernst equations. *J. Phys. Chem. B*, 107:13471–13477, 2003.

[65] S. Kjelstrup, J.M. Rubi and D. Bedeaux. Energy dissipation in slipping biological pumps. *Phys. Chem. Chem. Phys.*, 7:4009–4018, 2005.

[66] H.A. Kramers. Brownian motion in a field of force and the diffusion model of chemical reactions. *Physica*, 7:284–304, 1940.

[67] C.M. Guldberg and P. Waage. Studies concerning affinity. *Forhandlinger: Videnskabs-Selskabet i Christiania*, page 35, 1864.

[68] K. Grjotheim and B. Welch. *Aluminium Smelter Technology*. Aluminium-Verlag, Düsseldorf, 2nd. edition, 1988.

[69] B. Welch. Aluminum Production Paths in the New Millennium. *J. Metals*, pages 24–28, 1999.

[70] R. Huglen and H. Kvande. Global considerationf of aluminium electrolysis on energy and the environment. *Light Metals*, pages 373–380, 1994.

[71] T. S. Sørensen and S. Kjelstrup. Paralell Butler-Volmer reactions at the carbon anode in a laboratory cell for electrolytic reduction of aluminium, one producing CO and another producing CO_2. II. Effect of temperature and relations between current efficiency, carbon consumption and gas composition. *Aluminium Trans.*, 1:186–196, 1999.

[72] T. S. Sørensen and S. Kjelstrup. Paralell Butler-Volmer reactions at the carbon anode in a laboratory cell for electrolytic reduction of aluminium, one producing CO and another producing CO_2. I. Electrode kinetic model of the carbon anode and its application on current-voltage curves. *Aluminium Trans.*, 1:179–185, 1999.

[73] E. M. Hansen and S. Kjelstrup. Application of nonequilibrium thermodynamics to the electrode surfaces of aluminium electrolysis cells. *J. Electrochem. Soc.*, 143:3440, 1996.

[74] E. M. Hansen. *Modeling of Aluminium Electrolysis Cells Using Non-Equilibrium Thermodynamics.* PhD thesis, University of Leiden, 1997.

[75] J. Hives, J. Thonstad, Å. Sterten and P. Fellner. Electrical conductivity of molten cryolite-based mixtures obtained with a tube-type cell made of pyrolitic boron nitride. *Light Metals*, page 187, 1994.

[76] E. M. Hansen, E. Egner and S. Kjelstrup. Peltier effects in electrode carbon. *Metall. and Mater. Trans. B*, 29:69–76, 1997.

[77] K. Grjotheim and H. Kvande. *Understanding the Hall-Heroult Process for Production of Aluminium*. Aluminium-Verlag, Düsseldorf, 1986.

[78] L. Nummedal and S. Kjelstrup. Equipartition of forces as a lower bound on the entropy production in heat transfer. *Int. J. Heat Mass Transfer*, 44:2827–2833, 2000.

[79] E. Johannessen and L. Nummedal and S. Kjelstrup. Minimizing the entropy production in heat exchange. *Int. J. Heat Mass Transfer*, 45:2649–2654, 2002.

[80] E. Johannessen and S. Kjelstrup. A highway in state space for reactors with minimum entropy production. *Chem. Eng. Sci*, 60:3347–3361, 2005.

[81] L. Nummedal and M. Costea and S. Kjelstrup. Minimizing the entropy production rate of an exothermic reactor with constant heat transfer coefficient: The ammonia reaction. *Ind. Eng. Chem. Res.*, 42:1044–1056, 2003.

[82] L. Nummedal, A. Røsjorde, E. Johannessen, and S. Kjelstrup. Second law optimisation of a tubular steam reformer. *Chem. Eng. Process*, 44:429–440, 2005.

[83] A. Røsjorde and E. Johannessen and S. Kjelstrup. Minimising the entropy production rate in two heat exchangers and a reactor. In N. Houbak, B. Elmegaard, B. Qvale, and M.J. Moran, editors, *Proceedings of ECOS 2003*, pages 1297–1304, Copenhagen, Denmark, June 30 - July 2 2003. Department of Mechanical Engineering, Technical University of Denmark. ISBN 87-7475-297-9.

[84] G. M. de Koeijer and S. Kjelstrup. Minimizing entropy production in binary tray distillation. *Int. J. Appl. Thermodyn.*, 3:105–110, 2000.

[85] G.M. de Koeijer and S. Kjelstrup and P. Salamon and G. Siragusa and M. Schaller and K.H. Hoffmann. Comparison of entropy production rate minimization methods for binary diabatic tray distillation. *Ind. Eng. Chem. Res.*, 41:5826–5834, 2002.

[86] G.M. de Koeijer and A. Røsjorde and S. Kjelstrup. Distribution of heat exchange in optimum diabatic distillation columns. *Energy*, 29:2425–2440, 2004.

[87] M. Schaller and K. H. Hoffmann and G. Siragusa and P. Salamon and B. Andresen. Numerically optimized performance of diabatic distillation columns. *Comp. Chem. Eng.*, 25:1537–1548, 2001.

[88] M. Schaller and K. H. Hoffmann and R. Rivero and B. Andresen and P. Salamon. The influence of heat transfer irreversibilities on the optimal performance of diabatic distillation columns. *J. Non-Equilib. Thermodyn.*, 27:257–269, 2002.

[89] A. Røsjorde and S. Kjelstrup. The second law optimal state of a diabatic binary tray distillation column. *Chem. Eng. Sci.*, 60:1199–1210, 2005.

[90] E. Johannessen and A. Røsjorde. Equipartition of entropy production as an approximation to the state of minimum entropy production in a diabatic distillation column. *Energy*, 32:467–473, 2007.

[91] D. Tondeur and E. Kvaalen. Equipartition of entropy production. An optimality criterion for transfer and separation processes. *Ind. Eng. Chem. Res.*, 26:50–56, 1987.

[92] W. Spirkl and H. Ries. Optimal finite-time endoreversible processes. *Phys. Rev. E*, 52:3485–3489, 1995.

[93] L. Diosi and K. Kulacsy and B. Lukacs and A. Racz. Thermodynamic length, speed, and optimum path to minimize entropy production. *J. Chem. Phys.*, 105:11220–11225, 1996.

[94] D. Bedeaux, F. Standaert, K. Hemmes and S. Kjelstrup. Optimization of processes by equipartition. *J. Non-Equilib. Thermodyn.*, 24:242–259, 1999.

[95] E. Sauar, S. Kjelstrup and K. M. Lien. Equipartition of forces. A new principle for process design and operation. *Ind. Eng. Chem. Res.*, 35:4147–4153, 1996.

[96] P. W. Atkins. *Physical Chemistry.* Oxford, 5th. edition, 1994.

[97] A.E. Bryson and Y.C. Ho. *Applied Optimal Control. Optimization, estimation and control.* Wiley, New York, 1975.

[98] L.S. Pontryagin and V.G. Boltyanskii and R.V. Gamkrelidze and E.F. Mishchenko. *The Mathematical Theory of Optimal Processes.* Pergamon Press, Oxford, 1964.

[99] J. Humphrey and A. Siebert. Separation technologies: An opportunity for energy savings. *Chemical Engineering Progress*, 88:32–41, 1992.

[100] A. Røsjorde, S. Kjelstrup, E. Johannessen and R. Hansen. Minimizing the entropy production in a chemical process for dehydrogenation of propane. *Energy*, 32:335–343, 2007.

[101] R. Aris. *The Optimal Design of Chemical Reactors.* Academic Press, New York, 1961.

[102] B. Månsson and B. Andresen. Optimal Temperature Profile for an Ammonia Reactor. *Ind. Eng. Chem. Process Des. Dev.*, 25:59–65, 1986.

[103] C. Schön and B. Andresen. Finite-time optimization of chemical reactions: nA = mB. *J.Phys.Chem.*, 100:8843–8853, 1996.

[104] J. R. Rostrup-Nielsen, I. Dybkjaer, and L.J. Christiansen. *Chemical ReactorTechnology for Environmentally Safe Reactors and Products*, chapter Steam reforming opportunities and limits of the technology, pages 249–281. Kluwer Academic Publishers, 1993.

[105] R. Rivero. *L'analyse d'exergie: Application à la Distillation et aux Pompes à Pompes à Chaleur à Absorption.* PhD thesis, Institut National Polytechnique de Lorraine, Nancy, France, 1993.

[106] P. Le Goff, T. Cachot and R. Rivero. Exergy analysis of distillation processes. *Chem. Eng. Technol.*, 19:478–485, 1996.

[107] R. Agrawal and Z.T. Fidbowski. On the use of intermediate reboilers in the rectifying section and condensers in the stripping section of a distillation coulmn. *Ind. Eng. Chem. Res.*, 35(8):2801–2807, 1996.

[108] S. Kauchali, C. McGregor and D. Hildebrandt. Binary distillation re-visited using the attainable region theory. *Comp. Chem. Eng.*, 24:231–237, 2000.

[109] W. McCabe and J. Smith and P. Harriot. *Unit Operations of Chemical Engineering.* McGraw-Hill, New York, 5th. edition, 1993.

[110] E. Sauar, R. Rivero, S. Kjelstrup and K. M. Lien. Diabatic column optimization compared to isoforce columns. *Energy Convers. Mgmt.*, 38:1777–1783, 1997.

[111] G.M. de Koeijer and R. Rivero. Entropy production and exergy loss in experimental distillation columns. *Chem. Eng. Sci.*, 58:1587–1597, 2003.

[112] Z. Fonyo. Thermodynamic analysis of rectification. I. Reversible model of rectification. *Int. Chem. Eng.*, 14:18–27, 1974.

[113] G.M. De Koeijer. *Energy Efficient Operation of Distillation Columns and a Reactor Applying Irreversible Thermodynamics*. PhD thesis, Norwegian University of Science and Technology, Department of Chemistry, Trondheim, Norway, 2002. ISBN 82-471-5436-6, ISSN 0809-103x.

[114] J. de Graauw, A. de Rijke, Z. Olujic and P.J. Jansens. Distillation column with heat integration. *European Patent no.*, EP1332781:06–08, 2003.

[115] Z. Olujic, L. Sun, A. de Rijke and P.J. Jansens. Conceptual design of energy efficient propylene splitter. In R. Rivero, L. Monroy, R. Pulido and G. Tsatsaronis, editor, *Proceedings of ECOS 2004*. Instituto Mexicano del Petroleo, Mexico, 2004. ISBN 968-489-027, pages 61-78.

[116] E.S. Jimenez and P. Salamon and R. Rivero and C. Rendon and K.H. Hoffmann and M. Schaller and B. Andresen. Optimization of a Diabatic Distillation Column with Sequential Heat Exchangers. *Ind. Eng. Chem. Res.*, 43:7566–7571, 2004.

[117] H.R. Null. Heat pumps in distillation. *Chem. Eng. Prog.*, 78:58–64, 1976.

[118] M. Nakaiwa, K. Huang, T. Ohmori, T. Akiya, and T. Takamatsu. Internally heat-integrated distillation columns: A review. *Trans. I. Chem. E*, 81A:162–177, 2003.

[119] Ullmann's. *Encyclopedia of Industrial Chemistry*. Germany, 5th. edition, 1995.

[120] J.M. Smith, H.C. Van Ness, and M.M. Abbott. *Introduction to Chemical Engineering Thermodynamics*. McGraw-Hill, 7th. edition, 2005.

[121] J. Gross and G. Sadowski. Perturbed-chain saft: An equation of state based on a perturbation theory for chain molecules. *Ind. Eng. Chem. Res.*, 40(4):1244–1260, 2001.

[122] J. Gross and G. Sadowski. Application of the perturbed-chain saft equation of state to associating systems. *Ind. Eng. Chem. Res.*, 41(22):5510–5515, 2002.

[123] J. Gross and G. Sadowski. Modeling polymer systems using the perturbed-chain statistical associating fluid theory equation of state. *Ind. Eng. Chem. Res.*, 41(5):1084–1093, 2002.

[124] J. Gross. An equation-of-state contribution for polar components: Quadrupolar molecules. *AIChE J.*, 51(9):2556–2568, 2005.

[125] J. Gross and J. Vrabec. An equation-of-state contribution for polar components: Dipolar molecules. *AIChE J.*, 52(3):1194–1204, 2006.

[126] Sugata P. Tan, Hertanto Adidharma, and Maciej Radosz. Recent advances and applications of statistical associating fluid theory. *Ind. Eng. Chem. Res.*, 47(21):8063–8082, 2008.

List of Symbols

Latin symbols

A	m^2	heat exchange area
B	$\mathrm{mol\ s}^{-1}$	bottom stream flow
C_p	$\mathrm{J\ K}^{-1}$	heat capacity at constant pressure
$C_{p,i}$	$\mathrm{J\ K}^{-1}\ \mathrm{mol}^{-1}$	molar heat capacity, constant pressure
C_v	$\mathrm{J\ K}^{-1}$	heat capacity at constant volume
c_i	$\mathrm{mol\ m}^{-3}$	concentration or molar density
D	$\mathrm{m}^2\ \mathrm{s}^{-1}$	diffusion coefficient
D_p	m	catalyst pellet diameter
D_T	$\mathrm{m}^2\ \mathrm{s}^{-1}\ \mathrm{K}^{-1}$	thermal diffusion coefficient
D	$\mathrm{J\ s}^{-1}$	the dissipation function, space integral
D	m	diameter
D	$\mathrm{mol\ s}^{-1}$	distillate flow
E	$\mathrm{V\ m}^{-1}$	electric field
E_{eq}	$\mathrm{V\ m}^{-1}$	electric field of a system in equilibrium
F	$\mathrm{C\ mol}^{-1}$	Faraday's constant 96500 C mol^{-1}
F	$\mathrm{mol\ s}^{-1}$	feed flow
F_i	$\mathrm{mol\ s}^{-1}$	molar flow rate
f	$\mathrm{Pa\ s}^{-1}$	friction constant
f_i	bar	fugacity
G	J	Gibbs energy
$\Delta_r G$	$\mathrm{J\ mol}^{-1}$	reaction Gibbs energy
g_i	$\mathrm{J\ m}^{-3}\ \mathrm{mol}^{-1}$	partial molar Gibbs energy
g	$\mathrm{m\ s}^{-2}$	acceleration of gravity
H	J	enthalpy
H_i	$\mathrm{J\ mol}^{-1}$	partial molar enthalpy
$\mathcal{H}$	$\mathrm{J\ K}^{-1}\ \mathrm{s}^{-1}$	Hamiltonian in optimal control theory
	$\mathrm{J\ K}^{-1}\ \mathrm{m}^{-1}\ \mathrm{s}^{-1}$	- 1D, stationary system

$\Delta_r H$	J mol^{-1}	reaction enthalpy
$\Delta_{vap} H$	J mol^{-1}	enthalpy of evaporation
h	J m^{-3}	enthalpy per volume
h	m	height
j	A m^{-2}	electric current density
j_{displ}	A m^{-2}	displacement current density
J_q	J m^2 s^{-1}	flux of internal energy
$J_q^{'}$	J m^2 s^{-1}	flux of measurable heat
J_i	mol m^2 s^{-1}	flux of component i
J_s	J K^{-1} m^2 s^{-1}	flux of entropy
k_B	J K^{-1}	Boltzmann's constant 1.381 10^{-23}JK^{-1}
K		thermodynamic equilibrium constant
L_{ik}		phenomenological coefficient for coupling of fluxes i and k
$\mathcal{L}$	J K^{-1}	Euler-Lagrange function
L	m	system length
L	mol s^{-1}	vapor flow
l	m	length of box
l_{ik}		phenomenological coefficient for coupling of diffusional fluxes i and k
m_i	kg	mass of component i
N_i	mol	amount of component i
N	mol	number of moles
N		number of trays
n		number of independent components
P	C m^{-2}	polarization density in the bulk phase
p	bar (Pa)	pressure of the system
p_{ext}	bar (Pa)	external pressure
p_0	bar (Pa)	pressure of the surroundings
$p^{\ominus}$	bar	standard pressure (1 bar)
p^*	bar (Pa)	saturation pressure of pure gas

Q_n	W	heat transferred on tray n
q	J	heat delivered to the system
q_0	J	heat delivered to the surroundings
q^*	J mol^{-1}	heat of transfer
R	J K^{-1} mol^{-1}	gas constant 8.314 JK^{-1} mol^{-1})
R_{ik}		resistivity coefficient for coupling of fluxes i and k
r_{ik}		resistivity coefficient for coupling of diffusional fluxes i and k
r	mol m^{-3} s^{-1}	reaction rate
S	J K^{-1}	entropy of the system
s	J K^{-1} m^3	entropy per volume
S_0	J K^{-1}	entropy of the surroundings
S^*	J K^{-1} mol^{-1}	transported entropy (per mol)
S_i	J K^{-1} mol^{-1}	partial molar entropy
S	J K^{-1} mol^{-1}	molar entropy
dS_{irr}/dt	J K$^{-1}s^{-1}$	total entropy production
$\Delta_r S$	J K^{-1} mol^{-1}	reaction entropy
T	K	absolute temperature
T_0	K	temperature of the surroundings
t	s	time
t_{ion}		transference number of ion
t_i		transference coefficient of i
U	J	internal energy
U_i	J mol^{-1}	partial molar internal energy of i
u	J m^{-3}	internal energy per volume
u_{ion}	m^2 s^{-1} V^{-1}	mobility of ion in electric field
V	m^3	volume
V_i	m^3 mol^{-1}	partial molar volume of i
v_i	m s^{-1}	particle velocity
v	m s^{-1}	superficial gas velocity

X_i		general symbol, thermodynamic driving force
w	J	work done on the system
W	kg	weight
x, y, z	m	coordinates
x_i, y_i		mole fraction of i in liquid, and gas
y_i		activity coefficient for non-electrolyte
z	C m^{-3}	charge density

Greek and mathematical symbols

δ	m	film thickness
ϵ		catalyst bed porosity
φ	V	electric potential
φ_i		fugacity coefficient of i
η_C		Carnot efficiency
η_I		first law efficiency
η_{II}		second law efficiency
γ		internal coordinate, mesoscopic description
γ_i		activity coefficient of i in liquid mixture
κ	S m^{-1}	electrical conductivity
λ	W K^{-1} m $^{-1}$	thermal conductivity
λ		Lagrange multiplier function
μ_i	J mol^{-1}	chemical potential of i
$\mu_{i,T}$	J mol^{-1}	chemical potential of i at constant T
μ	kg m^{-1} s^{-1}	viscosity
$\nu_{j,i}$		stoichiometric coefficient of component i in reaction j
ξ		degree of conversion
π	J	Peltier heat
Π		Poynting correction
ρ	ohm m	specific resistivity

ρ	kg m^{-3}	density
ρ_B	kg m^{-3}	catalyst bed density
σ	J s^{-1} K^{-1} m^{-3}	local entropy production
τ	s	time lag
Θ	s	process duration
Ω	m^2	cross sectional area
d		differential
∂		partial derivative
Δ		change in a quantity
Σ		sum
$\equiv$		defined by
$\ominus$		denotes the standard state of 1 bar
∞		denotes an infinitely dilute solution

Superscripts and subscripts

a	super- or subscript meaning bulk anode
a	subscript which means heating/cooling medium
B	super- or subscript meaning bottom stream
c	super- or subscript meaning cathode
c	subscript meaning cold fluid
D	super- or subscript meaning distillate
eq	subscript meaning system in equilibrium
e^-	property of electron
F	super- or subscript meaning feed stream
g	super- or subscript meaning gas phase
h	subscript meaning hot fluid
ig	superscript meaning ideal gas
l or L	super- or subscript meaning liquid phase
i	subscript meaning component i
r	subscript meaning reaction
sat	superscript meaning saturated vapor phase

V superscipt meaning vapor phase
$0i$ subscript meaning pure component i

Index

About the authors

Signe Kjelstrup is a professor of physical chemistry since 1985 at the Norwegian University of Science and Technology, Trondheim. Since 2005, she holds a part time chair on irreversible thermodynamics and sustainable processes at the Technical University of Delft, The Netherlands. Her works in non-equilibrium thermodynamics concern electrochemical cells, membrane systems and entropy production minimization in process equipments. She is honorary doctor of the University of North East China, and has been a guest professor of Kyoto University. Her book on irreversible thermodynamics coauthored with K.S. Førland and T. Førland (Wiley, 1988 and1994, Tapir 2001) has been translated into Japanese and Chinese. Together with Dick Bedeaux she wrote the World-Scientific bestseller "Non-equilibrium Thermodynamics of Heterogeneous Systems" in 2008.

Dick Bedeaux is professor emeritus of physical chemistry at the University of Leiden, The Netherlands, and holds since 2002 a part time chair at the Norwegian University of Science and Technology, Trondheim. Bedeaux, together with Albano and Mazur, extended the theory of irreversible thermodynamics to surfaces. In the context of equilibrium thermodynamics he has worked on curved surfaces. Bedeaux is a fellow of the American Physical Society, and the recipient of the Onsager Medal from the Norwegian University of Science and Technology. Together with Jan Vlieger he wrote the book "Optical Properties of Surfaces" (Imperial College Press, 2002 and 2004). Together with Signe Kjelstrup he wrote the World-Scientific bestseller "Non-equilibrium Thermodynamics of Heterogeneous Systems" in 2008.

Eivind Johannessen is dr.ing. from the Norwegian University of Science and Technology (NTNU) and is presently a researcher at the Norwegian energy company, Statoil. His doctor thesis

on the state of systems with minimum entropy production was awarded Best doctor thesis defended at Norwegian University of Technology and Science in 2004.

Joachim Gross is professor of Thermodynamics and Thermal Process Engineering at the University of Stuttgart. His research interest is in Molecular Thermodynamics and the development of Fluid Theories. After receiving his PhD from the University of Berlin he worked in the Conceptual Process Design group of the BASF AG in Ludwigshafen for 4 years. In 2004 he became Associate Professor at the Delft University of Technology in the Separation Technology group. In 2005, he was appointed chair of Thermodynamics at the same university. In 2010 he moved to Stuttgart.